

**PRIMATE MOTOR CORTEX: INDIVIDUAL AND ENSEMBLE
NEURON-MUSCLE OUTPUT RELATIONSHIPS**

By

Darcy M. Griffin
B.S. (Biology), University of Kansas, 2000

Submitted to the graduate degree program in Molecular and Integrative
Physiology and the Graduate Faculty of the University of Kansas
In partial fulfillment of the requirements for the degree of
Doctor of Philosophy

Paul D. Cheney, Ph.D., Chairman

Committee members:

Dianne Durham, Ph.D.

Thomas J. Imig, Ph.D.

Randolph J. Nudo, Ph.D.

John A. Stanford, Ph.D.

Dissertation defended: July 11th, 2008

The Dissertation Committee for Darcy M. Griffin certifies
that this is the approved version of the following dissertation:

**PRIMATE MOTOR CORTEX: INDIVIDUAL AND ENSEMBLE
NEURON-MUSCLE OUTPUT RELATIONSHIPS**

Paul D. Cheney, Ph.D., Chairman

Committee members:

Dianne Durham, Ph.D.

Thomas J. Imig, Ph.D.

Randolph J. Nudo, Ph.D.

John A. Stanford, Ph.D.

Date approved: July 11th, 2008

ABSTRACT

The specific aims of this study were to: 1) investigate the encoding of forelimb muscle activity timing and magnitude by corticomotoneuronal (CM) cells, 2) test the stability of primary motor cortex (M1) output to forelimb muscles under different task conditions, and 3) characterize input/output relationships associated with different intracortical microstimulation (ICMS) methods.

Neuronal recording and stimulating methods were used in combination with electromyographic (EMG) recording of 24 forelimb muscles to investigate questions related to M1 control of forelimb muscles. Target muscles of CM neurons were identified by the presence of post-spike facilitation (PSpF) in spike-triggered averages (SpTA) of EMG activity. Post-stimulus output effects were obtained with three different ICMS methods; stimulus-triggered averaging (StTA) of EMG activity, repetitive short duration ICMS (RS-ICMS) and repetitive long duration ICMS (RL-ICMS).

Our results demonstrate that CM cells exhibit strong and consistent coactivation with their target muscles. Further, the summed activity of populations of identified CM cells was a better predictor of the common muscle's EMG activity than individual neurons. Our data support the view that M1 output encodes muscle activation related parameters.

Regarding stability, we found that output effects in StTAs of EMG activity are remarkably stable and largely independent of changes in joint

angle, or limb posture. This further validates the use of StTA for mapping and other studies of cortical motor output.

RL-ICMS evoked EMG activity was also stable in sign, strength and distribution independent of starting position of the hand. Our data support a model in which RL-ICMS produces sustained co-activation of multiple agonist and antagonist muscles which then generates joint movements according to the length-tension properties of the muscles until an equilibrium position is achieved. Further, RL-ICMS evoked EMG activity did not sum with the existing level of activity; rather the stimulus forced a new EMG level that was independent of existing voluntary background.

Our results further show that post-stimulus output effects on muscle activity obtained with StTA and RS-ICMS closely resemble one another. However, RL-ICMS produces effects that can deviate substantially from those observed with StTA.

ACKNOWLEDGEMENTS

Although this journey has been filled with struggle, it has more importantly given me confidence, happiness and a true sense of purpose in my life. I would like to first thank my husband Scott Miller, for being so understanding and supportive; no matter how many hours I spent in the lab. I also must thank my parents, Janice and Dennis Griffin, Florene Hart, sister, Amy Gillam and her wonderful family and my husband's family, the Millers, for their love and understanding. See mom and dad, my stubborn independent nature finally paid off.

This work came into existence with the help of many others. With much gratitude I acknowledge the hard work, long hours and patience of my mentor Dr. Paul Cheney. His financial support made all this possible and his intellectual contribution to my understanding of neurophysiology is immense.

In addition to Paul, I must thank all the members of the Cheney lab. Each of you has made the long hours of surgery, experimental recording and monkey wrestling not only a learning experience but also fun. Thank you, Heather Hudson for your sense of humor, camaraderie and moral support and Dr. Abdaraouf Belhaj-Saïf for your enthusiasm and guidance. I must also thank Ian Edwards for his mechanical, computer, electrical and technical knowledge and support.

There were many other people around the medical center that contributed to this work that I must thank. Thank you, Dr. Don Warn and Phil

Shafer for teaching me how to use the software programs needed for research presentations. And thank you to all of the past and present Hougland Brain Imaging Center personnel for their expertise in MRI and related software application programs, specifically Dr. Sang-Pil Lee and Allan Schmitt.

I would also like to thank each member of my committee: Randy Nudo, Tom Imig, John Stanford and Dianne Durham, who were not only sources of inspiration but also gave their valuable time and energy to advise my scientific endeavors.

There are other scientists who have not only inspired but taught me a great deal about biology and life before graduate school and I may not have ever gotten to graduate school if it had not been for them. As a high school student, I had the privilege of having a wonderful Biology teacher, Mike McRoberts. He was the first person I ever met who shared my excitement about insects, amphibians and reptiles. As a member of the Olathe North Student Naturalists, I learned that my curiosity and love of the natural world could become a career. I must also thank my undergraduate research advisor, Dr. Kenneth Mason, for being the first person to say, "Of course you should go to graduate school!" Lastly, I would like to thank Dr. Edward Stephens for being so supportive of my interests in neuroscience and help getting into graduate school here at KUMC.

TABLE OF CONTENTS

ACCEPTANCE PAGE.....	2
ABSTRACT.....	3
ACKNOWLEDGEMENTS.....	5
TABLE OF CONTENTS.....	7
LIST OF TABLES.....	11
LIST OF FIGURES.....	13
LIST OF ABBREVIATIONS.....	17
CHAPTER 1	
INTRODUCTION.....	18
REFERENCES.....	39
CHAPTER 2	
DO CORTICOMOTONEURONAL CELLS PREDICT TARGET MUSCLE EMG ACTIVITY?.....	43
ABSTRACT.....	44
INTRODUCTION.....	46
MATERIALS AND METHODS.....	49
RESULTS.....	60
DISCUSSION.....	77

REFERENCES.....	115
-----------------	-----

CHAPTER 3

STABILITY OF OUTPUT EFFECTS FROM MOTOR CORTEX TO FORELIMB MUSCLES IN PRIMATES.....	118
ABSTRACT.....	119
INTRODUCTION.....	120
MATERIALS AND METHODS.....	123
RESULTS.....	133
DISCUSSION.....	147
REFERENCES.....	172

CHAPTER 4

EMG ACTIVATION PATTERNS ASSOCIATED WITH LONG DURATION ICMS OF PRIMARY MOTOR CORTEX.....	178
ABSTRACT.....	179
INTRODUCTION.....	181
MATERIALS AND METHODS.....	184
RESULTS.....	193
DISCUSSION.....	206
REFERENCES.....	228

CHAPTER 5

INSIGHT INTO THE MECHANISM OF NEURAL CIRCUIT ACTIVATION WITH REPETITIVE INTRACORTICAL MICROSTIMULATION.....	235
ABSTRACT.....	236
INTRODUCTION.....	238
MATERIALS AND METHODS.....	240
RESULTS.....	249
DISCUSSION.....	254
REFERENCES.....	270

CHAPTER 6

COMPARISON OF OUTPUT EFFECTS ON EMG ACTIVITY OBTAINED WITH DIFFERENT METHODS OF MICROSTIMULATION.....	276
ABSTRACT.....	277
INTRODUCTION.....	279
MATERIALS AND METHODS.....	281
RESULTS.....	290
DISCUSSION.....	300
REFERENCES.....	328

CHAPTER 7

CONCLUSION.....333

REFERENCES.....341

LIST OF TABLES

TABLE	PAGE
Chapter 2	
2.1. Muscles recorded.....	90
2.2. Timing and percentage overlap of peaks in CM cell activity relative to matching peaks in facilitated target muscle EMGs.....	91
2.3. Analysis of CM cell populations for individual muscles.....	92
Chapter 3	
3.1. Joint angles achieved in the isometric push-pull task.....	154
3.2. Stability results from different tasks (15 μ A).....	155
Chapter 4	
4.1. Joint angles achieved with different hand starting positions.....	212
4.2. Stability of RL-ICMS evoked EMG activity.....	213
Chapter 5	
5.1. RL-ICMS evoked EMG activation levels in Figure 5.1.....	257

Chapter 6

6.1. Properties of post-stimulus facilitation (PStF) output effects.....	306
6.2. Properties of post-stimulus suppression (PStS) output effects.....	307

LIST OF FIGURES

FIGURE	PAGE
Chapter 1	
1.1. Cortical projections to motoneurons.....	34
1.2. Different forms of ICMS.....	36
1.3. Afferent feedback to motoneurons.....	38
Chapter 2	
2.1. Examples of SpTA of EMG activity.....	94
2.2. Segmentation of the reach-to-grasp task.....	96
2.3. Cortical locations of investigated CM cells.....	98
2.4. Examples of response averages.....	100
2.5. Distribution of firing rate peaks.....	102
2.6. Analysis of matching CM cell-target muscle activity peaks.....	104
2.7. Identification of matching CM cell-target muscle activity peaks.....	106
2.8. Timing between matching CM cell-target muscle activity peaks.....	108
2.9. Example response average and scatter plot for a CM cell-target muscle pair with strong PSpF.....	110
2.10. Distribution of Pearson Correlation Coefficients (r) for CM cell-target muscle pairs.....	112
2.11. CM cell populations sharing a common target muscle.....	114

Chapter 3

3.1. Illustrations depicting the tasks used to test the stability of output effects From motor cortex to forelimb muscles.....	157
3.2. Three dimensional reconstructions and muscle maps of subject's left hemispheres.....	159
3.3. Experimental sites used to test stability of StTAs of EMG activity.....	161
3.4. Typical layer V site with stable effects in all muscles during performance of the Isometric wrist task.....	163
3.5. Consistent PStEs relationships.....	165
3.6. All 18 inconsistent effects observed during performance of the isometric wrist task and the corresponding percentage of EMG activity level change.....	167
3.7. Typical layer V site with stable effects observed in all muscles during performance of the push-pull task at four different positions.....	169
3.8. Polar plots of the distributions of magnitudes (ppi) for each of 24 muscles at five different workspace locations	171

Chapter 4

4.1. Illustrations depicting the tasks used to study the EMG activation patterns associated with RL-ICMS of primary motor cortex... ..	215
4.2. Experimental sites used to study EMG activity patterns associated with	

RL-ICMS of primary motor cortex.....	217
4.3. Qualitative characterization of EMG activity patterns evoked with RL-ICMS and the percentage of their occurrence during performance of the tasks.....	219
4.4. RL-ICMS elicited EMG activation patterns associated with 7 starting hand positions at a layer V site.....	221
4.5. RL-ICMS evoked EMG activity magnitude relationships.....	223
4.6. RL-ICMS elicited EMG activation patterns associated with the wrist tasks.....	225
4.7. Illustration depicting how the length-tension relationships of biceps and triceps specify elbow joint angle.....	227
Chapter 5	
5.1. Examples of “opposite” muscle activation patterns elicited with RL-ICMS at a single cortical site	259
5.2. Superimposed examples of “opposite” muscle activation patterns elicited by RL-ICMS at a single cortical site	261
5.3. Relationship between RL-ICMS evoked mean EMG levels at different starting hand positions.....	263
5.4. A layer V site and the RL-ICMS elicited shoulder muscle EMG activation patterns associated with stimulus interrupted movement.....	265
5.5. Distribution of declining EMG onset latencies measured relative to	

stimulus train onset.....	267
5.6. Diagram of proposed RL-ICMS mechanism.....	269
Chapter 6	
6.1. Sites used to compare output effects with different ICMS methods.....	309
6.2. Effects produced with different microstimulation methods.....	311
6.3. Examples of RL-ICMS elicited long latency onset activity.....	313
6.4. Percent of matching output effects across ICMS methods.....	315
6.5. Distribution of matching output effects across ICMS methods.....	317
6.6. Percent of matching distal muscle output effects across ICMS methods.....	319
6.7. Distribution of matching distal muscle output effects across ICMS methods.....	321
6.8. Percent of matching output magnitudes across ICMS methods.....	323
6.9. Distribution of onset latencies with RL-ICMS.....	325
6.10. Distribution of median mpi values for all ICMS methods and median ppi values for StTA at four stimulus intensities.....	327

LIST OF ABBREVIATIONS

CM.....	Corticomotoneuronal
EMG.....	Electromyography
ICMS.....	Intracortical Microstimulation
M1.....	Primary Motor Cortex
MRI.....	Magnetic Resonance Imaging
PSpE.....	Post-spike Effect
PSpF.....	Post-spike Facilitation
PSpS.....	Post-spike Suppression
PStE.....	Post-stimulus Effect
PStF.....	Post-stimulus Facilitation
PStS.....	Post-stimulus Suppression
RL-ICMS.....	Repetitive Long Duration ICMS
RS-ICMS.....	Repetitive Short Duration ICMS
SD.....	Standard Deviation
SpTA.....	Spike-triggered Averaging
StTA.....	Stimulus-triggered Averaging
TMS.....	Transcranial Magnetic Stimulation

CHAPTER 1
INTRODUCTION

Millions of people suffer the loss of motor function due to spinal cord injury, loss of limb, or degenerative disease. Typically, motor output signals are sent from neurons in the brain (motor cortex neurons) to cells in the spinal cord (motoneurons) and on to muscles of the body. Motor cortex neurons direct spinal motoneurons to perform movements such as walking, reaching, chewing and breathing. Neurological disorders and injury that disrupt that signaling result in weakening, wasting away, uncontrollable twitching, or stiffness of limb muscles. Eventually, the ability to control voluntary movement can be lost completely. Everyday, scientific research on the brain's control of movement gets closer to finding cures and treatments for these disorders. In the last decade alone, brain machine interface technology has allowed people to move a computer cursor by just thinking about it. "Locked in" patients can now send email communications to their loved ones. Thousands have been relieved of Parkinson's tremor using deep brain stimulation of the basal ganglia. Not only is there an effort to treat motor disorders, but also to understand the properly functioning system. If we can understand how the system should work, it will be easier to diagnose and treat the problems.

Voluntary movements are initiated in the higher order motor centers of the brain. Sensory stimuli are first perceived, followed by a series of transformations that include a spatiotemporal motor plan and eventually the muscle activity necessary to achieve the movement. Descending inputs

make their way to the motor cortex which projects to the spinal motoneurons (Figure 1.1). Primary motor cortex (M1) was long thought of as the “final common pathway” to the motoneurons of the spinal cord and has therefore been the most widely studied region of motor cortex. Recently six premotor regions have been characterized as having a set of corticospinal neurons (Dum and Strick 1991; He et al., 1993, 1995). However, the descending input from M1 is much stronger than any of the individual premotor areas (Boudrias et al., 2006).

Organization and function of the corticomotor system

Fritsch and Hitzig (1870) reported the first evidence that the frontal cortex was electrically excitable, specifically the region just rostral to the central sulcus. That region was later called the primary motor cortex due to its low threshold for eliciting movements when stimulated. Since then, electrical stimulus has been an important tool useful for studying the organization of motor regions of the brain. Penfield and Boldrey (1937) used a stimulating current to show a somatotopic representation of the human body. Stimulating the medial portion of M1 produced leg movements, as the current was placed more laterally the trunk responded, followed by the arm, face and mouth. The same somatotopic organization was later discovered in the monkey (Woolsey 1952).

Since the pioneering works of Penfield and Woolsey, mapping methods have improved and are now much higher resolution. Intracortical

microstimulation (ICMS) is one such method (Stoney et al., 1968). A form of ICMS known as stimulus-triggered averaging (StTA) of electromyographic (EMG) activity allows mapping M1 output to individual muscles (Figure 1.2 A). A systematic mapping of M1 using StTA of EMG activity from 24 muscles of the forelimb revealed an overlapping output pattern (Park et al., 2001). The intra-areal organization of the forelimb representation contained a core of neurons, located mostly in the bank of the precentral gyrus, which projected to only distal muscles. That core was surrounded by a horse-shoe shaped region with output to both proximal and distal muscles and further surrounded by neurons which projected to only proximal muscles. It had previously been shown that a single neuron projected to motoneuron pools of multiple muscles, including combinations of proximal and distal muscles (McKiernan et al., 1998). The diverging output from M1 onto combinations of muscles may form an anatomical substrate for the functional muscle synergies underlying reaching and grasping movements.

M1 corticospinal neurons send direct monosynaptic connections to the alpha motoneurons in lamina IX of the spinal cord (Armand et al., 1997; Dum and Strick 1996; Kuypers 1981). The emergence of a direct monosynaptic connection, present in old world primates and humans, is presumed to underlie the ability for skilled movements of the hand and digits and particularly independent movements of the digits (Maier et al., 1997; Porter and Lemon, 1993). Neurons that project directly to motoneurons are called

corticomotoneuronal (CM) cells. Such a direct connection to motoneurons is assumed to drive motoneuron activity and ultimately muscle activity.

The synaptic inputs to motoneurons create either an excitatory post synaptic potential (EPSP) or an inhibitory postsynaptic potential (IPSP). A single EPSP is not strong enough to bring a motoneuron to its firing threshold. However, multiple EPSPs will sum together and result in a greater membrane depolarization. This will increase the likelihood that the motoneuron reaches its firing threshold.

The motoneuron is only one part of the functional unit known as the motor unit. The motor unit is comprised of a motoneuron and all the muscle fibers it innervates. The motor unit is the basic unit of a muscle contraction. Each time the motoneuron is brought to threshold and fires an action potential every muscle fiber of the motor unit will contract. Since the firing ratio between a motoneuron and its innervated muscle fibers is one to one; it's viewed as a single functional entity.

Organization and function of the motor periphery

Peripheral feedback about the changing state of the musculoskeletal system also supplies input to the motoneurons (Figure 1.3). Muscle spindles are located in parallel with muscle fibers. They have both a motor component, under the control of the gamma motor system, and a sensory component. The sensory component is sensitive to muscle stretch and responds through group 1a afferent sensory neurons. Group 1a afferents

increase their firing onto homonymous motoneurons resulting in a contraction which opposes the stretch. They also inhibit the activity of the antagonist muscle's motoneurons. Golgi tendon organs lie in series with muscle fibers and provide feedback about force development in the muscle through 1b afferent fibers. Inputs to motoneurons can be further modified within the spinal cord through interneurons which serve to integrate synaptic inputs to the motoneurons. Other parallel descending drive to motoneurons can include the cortical premotor areas and brainstem descending systems (reticulospinal, rubrospinal, and vestibulospinal systems).

Continuing controversies concerning the functional role of M1

It has been known for more than a century that M1 is important for making voluntary movements. A complete understanding of the function of M1 however remains controversial. It has long been assumed that CM cells are responsible for driving motoneuron activity during voluntary movements. But what is encoded in the actual signal? Do CM cells communicate information in the language of the motoneuron (muscle activity) or some higher order parameter (direction of movement)? Are the coordination, selection and timing of muscle activity done in M1 or the spinal cord? Studies have shown that M1 cell discharge is related to a variety of kinematic and dynamic parameters including movement velocity (Ashe and Georgopoulos, 1994), direction of hand movement (Georgopoulos et al., 1982), force (Evarts,

1968; Cheney and Fetz, 1980) limb geometry (Caminiti et al., 1990; Kalaska et al., 1989; Scott and Kalaska, 1997) and muscle EMG (Morrow and Miller, 2003). However, these studies are complicated by the fact that movement direction, force and EMG activity all covary and most studies have not made any attempt to dissociate the relationships between these parameters. The studies that have attempted to dissociate these variables have demonstrated that the activity of many cortical cells encode muscle related variables such as force or EMG activity (Takei et al., 1999). Even so, few of these studies have identified neurons with synaptic connections to motoneurons.

Spike-triggered averaging reveals the synaptic connections of individual neurons

In order to study the function of a brain region, neurons must be studied in their natural relation to external stimuli. Spike-triggered averaging (SpTA) of EMG activity is one such method. SpTA is used to detect facilitation and suppression of EMG activity associated with underlying excitatory and inhibitory synaptic linkages. Each time the cell fires an action potential travels down the corticospinal tract to the motoneurons in Rexed lamina IX of the spinal cord. Since SpTA is performed in awake behaving animals, the muscles of the limbs are active and the motoneurons are either at or near their firing threshold. Therefore, each action potential that reaches the primed motoneurons has a high probability of causing the motor unit to fire. If the motoneuron does fire, all the muscle fibers it innervates will also

fire in a one to one ratio. If there is a synaptic connection between the CM cell and motor units being recorded, their activity will be time locked. SpTA allows the identification of transient increases (post-spike facilitation) and decreases (post-spike suppression) in EMG activity. Muscles with post-spike facilitation (PSPF) or post-spike suppression (PSPS) are referred to as the cell's target muscles. An important advantage of the SpTA method is that it can be applied in awake behaving animals where relationships between the cortical cell activity and target muscles can also be investigated.

ICMS methods enable the study of corticomotor system functional organization

ICMS approaches have historically been used to reveal basic features of somatotopic organization of motor cortex. Since the original findings with ICMS (Stoney et. al., 1968), different variations of this method have been used to map and investigate motor cortex output properties. The classic approach (repetitive short duration ICMS; Figure 1.2 B) consists of a train of 10 symmetrical biphasic stimulus pulses (negative--positive with total duration of 0.4 ms) at a frequency of 330 Hz (Asanuma and Rosén 1972). It is supra-threshold for movements and is easily detected as a muscle twitch.

StTA of EMG activity (Figure 1.2 A) involves applying microstimuli (2-60 μ A at 10-20 Hz) through an electrode that can also be used to record the activity of individual neurons (Cheney and Fetz, 1985). This method has a major advantage over other stimulation methods that produce simple evoked

movements in that the sign (excitation or inhibition), strength and latency of synaptic effects on specific muscles can be quantified. StTA of EMG activity is one method of ICMS that has an advantage in that the low rate of stimulation (15 Hz) does not allow temporal summation of excitatory postsynaptic potentials at the motoneuron and therefore is below threshold for a muscle contraction. The low stimulus intensity helps maintain a concentrated current which is focused on a small cluster of neurons surrounding the electrode tip (Asanuma et al., 1976; Jankowska et al., 1975; Ranck 1975; Stoney et al., 1968; Tehovnik 1996). It has been estimated that StTA at 10 μ A activates 1 – 12 large pyramidal tract neurons (Cheney and Fetz 1985).

Long duration repetitive ICMS (RL-ICMS) is a relatively new approach (Graziano et al., 2002). It involves the application of high frequency ICMS for relatively long durations (Figure 1.2 C), typically 500ms; close to the duration of a normal movement. This method has yielded novel and interesting results concerning the functional organization of motor cortex output. For example, RL-ICMS produces natural appearing arm movements that end with the hand positioned in different parts of extrapersonal space depending on the cortical area stimulated, but independent of the initial arm posture. The movements are described as being similar to the natural movements that are involved in visually guided manipulation of objects. It has been reported that during RL-ICMS, the EMG pattern in a particular muscle switches from excitation to

inhibition depending on the initial posture of the arm. For example, the authors state that “each cortical site did not appear to have a fixed mapping to biceps or triceps”. These results raise fundamental questions about the reproducibility of ICMS based mapping studies. Further, Graziano and colleagues (2004) have interpreted their results as supporting a map of “desired” arm postures in motor cortex. Since their original findings with RL-ICMS, several studies have been published to provide support for their hypothesis that M1 neurons provide “higher order signals instructing the limb to move to a certain posture regardless of the initial posture” (Aflalo and Graziano 2006a,b; Graziano et al., 2004, 2005). However, little is known about the mechanism responsible for RL-ICMS evoked movements.

Specific aims of this study

M1 neurons with a demonstrable synaptic linkage to motoneurons, as revealed through spike triggered averaging (SpTA) of electromyographic (EMG) activity, are termed corticomotoneuronal (CM). The goal of this body of work is to study the output properties of both individual and ensembles of CM cells to 24 muscles of the primate forelimb. What does CM cell activity encode? How well does the firing activity of individual CM cells covary with that of their target muscles? Are populations of CM cells better predictors of target muscle activity? If populations of CM cells can predict EMG activity with a high level of reliability, it is a strong argument supporting the

hypothesis that M1 output signals to motoneurons specify muscle based parameters.

Another way to study the output properties of M1 is through the use of ICMS. Stimulus-triggered averaging (StTA) of EMG activity allows one to document the output properties of a small cluster of neurons to muscles of the limbs. Another aim of this research is to investigate various methods of ICMS and the nature of the relationship between stimulation parameters, task conditions, and the resulting output effects. To what extent do task conditions affect, through afferent joint position feedback, the output properties of M1? How stable are those output properties when obtained with different stimulus intensities, frequencies and train durations?

Specific Aim 1 - Covariation of individual CM cells and their target muscles

The goal of this aim was set to test the hypothesis that CM cells and their target muscles have common peaks of activity. If M1 neurons with a demonstrable synaptic linkage to motoneurons (CM cells) are encoding muscle activity, a reasonable expectation would be that the cell's activity covaries closely with that of its target muscles. We set out to ascertain the degree to which M1 neurons and their target muscles show peaks of activity in the same segment of a natural, multi-joint reaching task.

Specific Aim 2 - Covariation of CM cell populations and their target muscles

The goal of this aim was set to test the hypothesis that populations of CM cells are strong predictors of target muscle EMG activity. Our objective was to show that a population of neurons influencing the same muscle is a strong predictor of EMG activity. A single CM cell can not depolarize a motoneuron to a sustained level of firing and must therefore be viewed as one of many inputs necessary for producing the motoneuron activity associated with movement. Under steady state conditions, a motoneuron encodes synaptic input by firing at a frequency that is linearly related to the magnitude of the inputs (Powers and Binder, 1996). If the same relationship exists under the dynamic condition of a population of CM cells converging onto and driving motoneuron output during movement, target muscle activity should reflect that linear relationship.

Specific Aim 3 – Task dependence of motor output with StTA of EMG activity

The goal of this aim was set to test the hypothesis that corticospinal output effects obtained with StTA of EMG activity will not vary significantly under different task conditions. One possible interpretation of the output effects obtained with the RL-ICMS method is that the changes in output to antagonist muscle pairs reflects the changing levels of muscle spindle afferent input to the motoneuron pool with changing joint angle. For example, in the ketamine sedated monkey, Graziano (2002) reported a small excitatory effect from RL-ICMS in an elbow flexor muscle with the elbow joint flexed but a larger effect

with the elbow joint extended. Further, StTA of EMG activity showed similar dependence on elbow joint angle. Excitatory 1a afferent input to elbow flexor muscles will increase with extension of the elbow joint because flexor muscle length will increase and, in turn, this will increase the excitability of flexor motoneurons. The results will have important implications for the interpretation of StTA based mapping studies of cortical motor areas and for understanding the organization of corticospinal output.

Specific Aim 4: Task dependence of motor output with RL-ICMS and the interpretation of RL-ICMS evoked movements

The goal of this aim was set to distinguish between two possible mechanisms of RL-ICMS evoked movements. We will focus on determining whether RL-ICMS evoked EMG activity in target muscles begins immediately upon stimulation and is sustained over the time course of stimulation; as would occur with the equilibrium point mechanism. Or does the EMG activity during RL-ICMS shows time and position dependent EMG modulation, for example facilitation for movement in one direction and suppression for movement in the opposite direction, similar to that associated with the monkey's own active movements; as would occur if a natural brain circuit were activated. The results of RL-ICMS are subject to two different interpretations. One is that the movements produced appear to have normal qualities and appear purposeful because stimulation is activating the natural neural circuit that is normally

used by the internal motor program to produce that same movement (natural circuit hypothesis). An alternative interpretation (equilibrium point hypothesis) is that RL-ICMS evokes tonic contraction of agonist and antagonist muscles at multiple joints, bringing the limb to a final posture that is sustained for the duration of stimulation. This position represents an equilibrium between the forces generated by antagonist muscle pairs at each joint.

Specific aim 5: Mechanism of neural circuit activation with repetitive ICMS

We will test the hypothesis that RL-ICMS evoked EMG activity does not sum with the existing level of activity, but instead forces a new level of activity independent of voluntary background. Although ICMS methods have been in use for over a century, the mechanism of action is not fully understood. The equilibrium point hypothesis can describe the peripheral mechanism of RL-ICMS evoked movements, but is a consequence of the forelimb's musculoskeletal architecture. How does the stimulus affect the cortical output from the area with which it has been applied?

Specific aim 6: Comparison of M1 output obtained with different microstimulation methods

The goal of this aim was to document the relationships between motor output effects (muscle distribution, sign and strength) and the characteristics (frequency, duration and magnitude) of the stimulation applied. ICMS

methods are widely used to study the organization of motor areas of the brain. Are the output effects obtained with different forms of ICMS comparable? StTA of EMG activity is sub-threshold for movements and can only be seen in averages of EMG activity. Short and long train repetitive ICMS on the other hand are supra-threshold and evoke muscle twitches and whole limb movements. Long train duration ICMS also has a potential for physiological spread of current. Is the output from M1 the same using different ICMS parameters?

Figure 1.1. Cortical projections to motoneurons. Primary motor cortex (M1) neurons send synaptic projections down the corticospinal tract (which decussates in the medulla) to synapse directly onto motoneurons (monosynaptic) or onto interneurons (polysynaptic) which then synapse onto motoneurons. Motoneurons in turn synapse on muscle fibers.

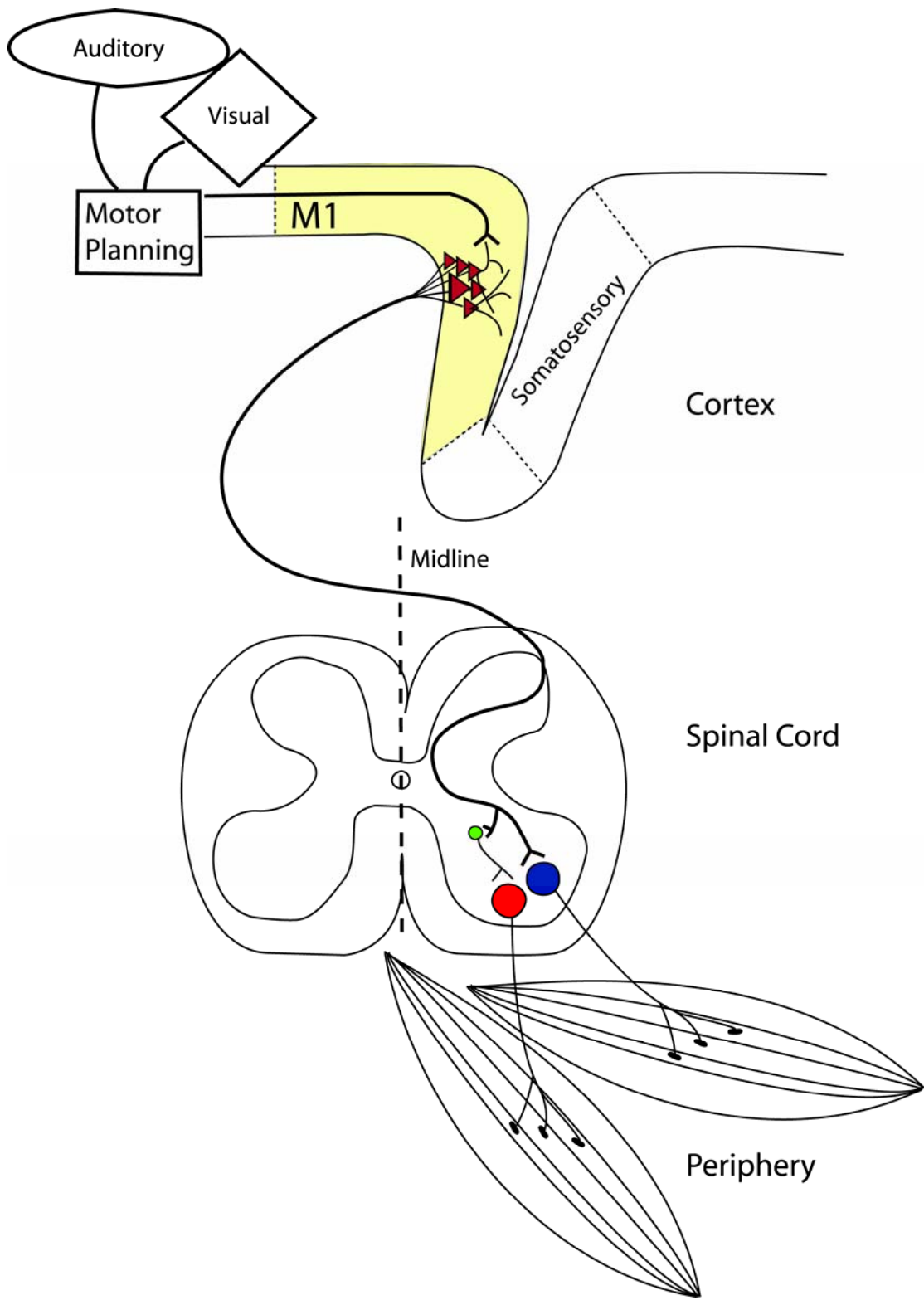


Figure 1.2. Different forms of intracortical microstimulation (ICMS).

Schematic of a rhesus monkey brain highlights primary motor cortex (M1) forelimb region. A microelectrode is placed in layer V of M1 forelimb representation. A. Stimulus-triggered averaging (StTA) of electromyographic (EMG) activity. 1. Stimulating current excites corticospinal neurons with monosynaptic projections to a motoneuron. An excitatory post synaptic potential (EPSP) increases the firing probability of the motoneuron. Averaging EMG activity with respect to the stimulus pulse reveals a transient increase in EMG activity time locked to the stimulus pulse; referred to as post-stimulus facilitation (PStF). 2. Averaging EMG activity with respect to the stimulus pulse reveals a transient decrease in EMG activity due to an inhibitory post synaptic potential (IPSP), likely mediated through an inhibitory interneuron; referred to as a post-stimulus suppression (PStS). 3. Averaging EMG activity with respect to the stimulus pulse reveals no stimulus mediated effect. B. Repetitive short duration ICMS (RS-ICMS). The stimulus train evokes a muscle twitch and an increase in EMG activity. C. Repetitive long duration ICMS (RL-ICMS). The stimulus train evokes a limb movement at higher stimulus intensities and an increase in EMG activity. For repetitive ICMS methods, the first pulse of each stimulus train is used as a trigger to compute averages of EMG activity. Stimulus parameters and number of trigger events also given.

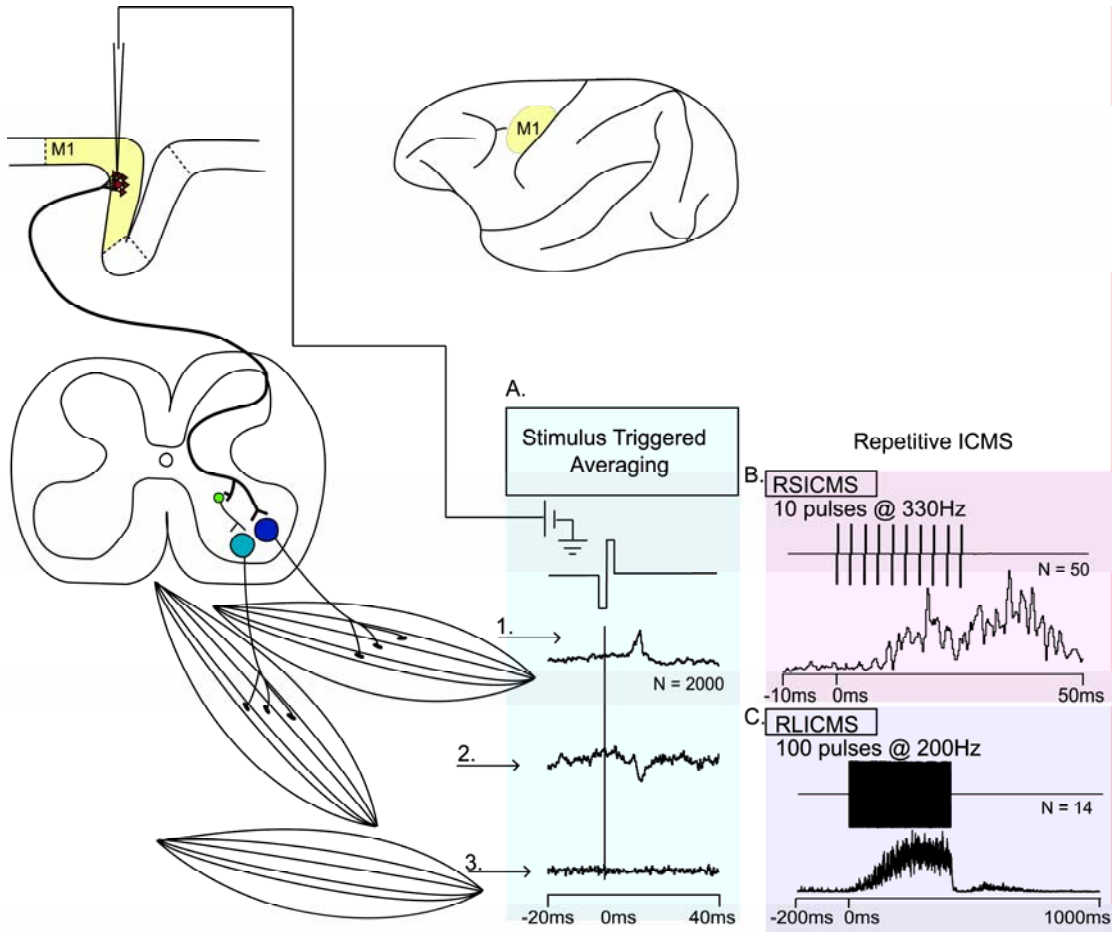
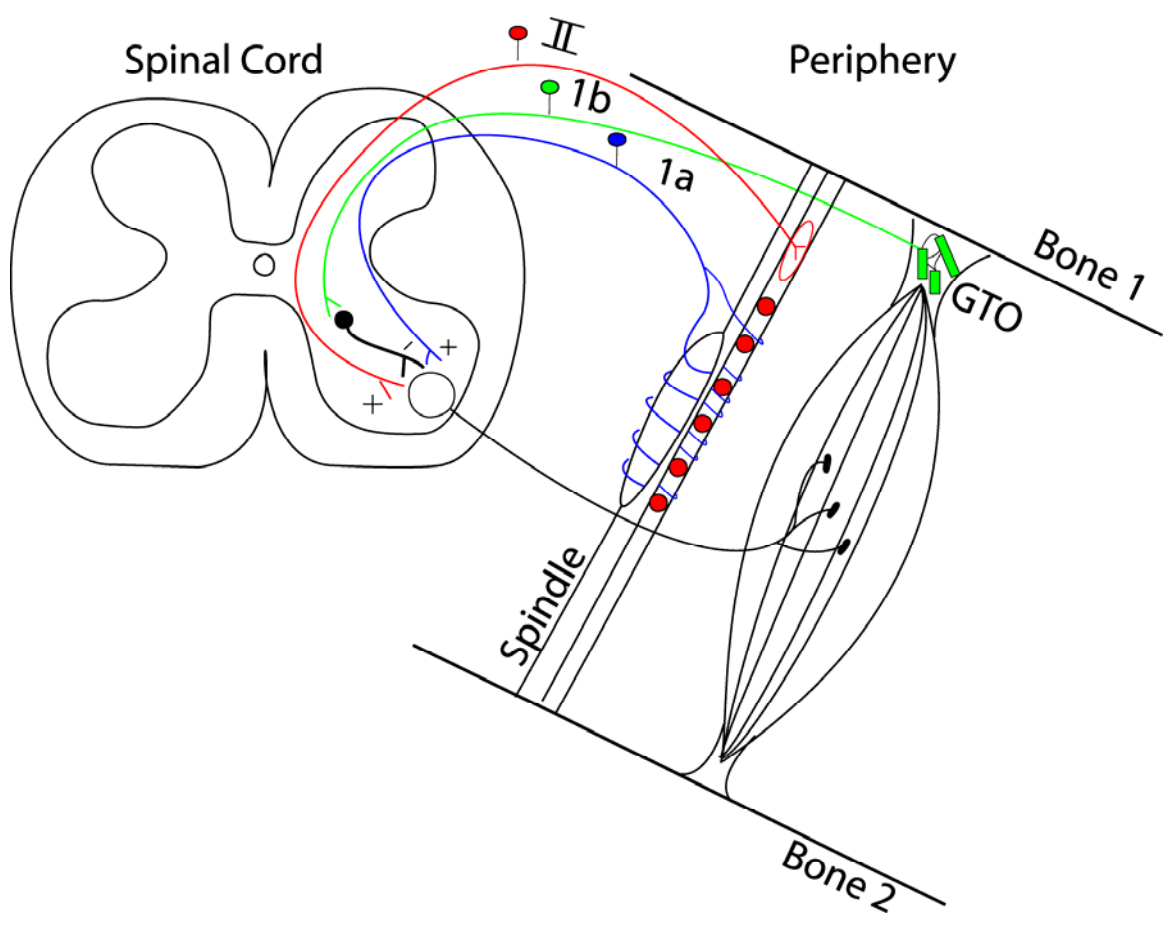


Figure 1.3. Afferent feedback to the motoneuron is supplied by muscle spindles and Golgi tendon organs (GTO).



REFERENCES

- Aflalo TN, Graziano MS (2006a) Possible origins of the complex topographic organization of motor cortex: reduction of a multidimensional space onto a two-dimensional array. *J Neurosci* 26(23): 6288-97.
- Aflalo TN, Graziano MS (2006b) Partial tuning of motor cortex neurons to final posture in a free-moving paradigm. *Proc Natl Acad Sci U S A* 103(8): 2909-14.
- Aflalo TN, Graziano MS (2007) Relationship between unconstrained arm movements and single-neuron firing in the macaque motor cortex. *J Neurosci* 27(11): 2760-80.
- Armand J, Olivier E, Edgley SA, Lemon RN (1997) The postnatal development of corticospinal projections from motor cortex to the cervical enlargement in the macaque monkey. *J Neurosci* 17: 251-266.
- Asanuma H, Rosén I (1972) Topographical organization of cortical efferent zones projecting to distal forelimb muscles in the monkey. *Exp Brain Res* 14(3): 243-56.
- Asanuma H, Arnold A, Zarzecki P (1976) Further study on the excitation of pyramidal tract cells by intracortical microstimulation. *Exp Brain Res* 26(5): 443-61.
- Boudrias MH, Belhaj-Saïf A, Park MC, Cheney PD (2006) Contrasting properties of motor output from the supplementary motor area and primary motor cortex in rhesus macaques. *Cereb Cortex* 16(5): 632-8.
- Caminiti R, Johnson PB, Urbano A (1990) Making arm movements within different parts of space: dynamic aspects in the primate motor cortex. *J Neurosci* 10(7): 2039-2058.
- Cheney PD, Fetz EE (1985) Comparable patterns of muscle facilitation evoked by individual corticomotoneuronal (CM) cells and by single intracortical microstimuli in primates: evidence for functional groups of CM cells. *J Neurophysiol* 53(3): 786-804.

- Cheney PD, Fetz EE (1980) Functional classes of primate corticomotoneuronal cells and their relation to active force. *J Neurophysiol* 44(4): 773-91.
- Dum RP, Strick PL (1991) The origin of corticospinal projections from the premotor areas in the frontal lobe. *J Neurosci* 11(3): 667-89.
- Dum RP, Strick PL (1996) Spinal cord terminations of the medial wall motor areas in macaque monkeys. *J Neurosci* 16(20): 6513-6525.
- Evarts EV (1968) Relation of pyramidal tract activity to force exerted during voluntary movement. *J Neurophysiol* 31: 14-27.
- Fritsch G and Hitzig E (1870). *Über die elektrische Erregbarkeit des Grosshirns. Archs Anat. Physiol. Wiss. Med.* 37, 300-332. (Translation by Bonin, G. Von. *In The cerebral cortex*, pp. 73-96. Thomas, Springfield, Illinois).
- Georgopoulos AP, Kalaska JF, Caminiti R, Massey JT (1982) On the relations between the direction of two-dimensional arm movements and cell discharge in primate motor cortex. *J Neurosci* 2: 1527-1537.
- Graziano MS, Aflalo TN, Cooke DF (2005) Arm movements evoked by electrical stimulation in the motor cortex of monkeys. *J Neurophysiol* 94(6): 4209-23.
- Graziano MSA, Kaushal PT, Taylor CSR (2004) Mapping from motor cortex to biceps and triceps altered by elbow angle. *J Neurophysiol* 92: 395-407.
- Graziano MSA, Taylor CSR, Moore T (2002) Complex movements evoked by microstimulation of precentral cortex. *Neuron* 34: 841-851.
- He SQ, Dum RP, Strick PL (1993) Topographic organization of corticospinal projections from the lateral lobe: motor areas on the lateral surface of the hemisphere. *J Neurosci* 13(3): 952-80.
- He SQ, Dum RP, Strick PL (1995) Topographic organization of corticospinal projections from the lateral lobe: motor areas on the medial surface of the hemisphere. *J Neurosci* 15(5): 3284-306.

- Jankowska E, Padel Y, Tanaka R (1975) The mode of activation of pyramidal tract cells by intracortical stimuli. *J Physiol* 249(3): 617-36.
- Takei S, Hoffman DS, Strick PL (1999) Muscle and movement representations in the primary motor cortex. *Science* 285(5436): 2136-2139.
- Kalaska JF, Cohen DAD, Hude ML, Prud'Homme MA (1989) Comparison of movement direction- related versus load direction- related activity in primate motor cortex, using a two-dimensional reaching task. *J Neurosci* 9: 2080-2102.
- Kuypers HGJM (1981) Anatomy of the descending pathways. Handbook of Physiology. The Nervous System. Motor Control. Bethesda, MD, Am Physiol Soc II: 597-666.
- Maier MA, Olivier E, Baker SN, Kirkwood PA, Morris T, Lemon RN (1997) Direct and indirect corticospinal control of arm and hand motoneurons in the squirrel monkey (*Saimiri sciureus*). *J Neurophysiol* 78: 721-733.
- McKiernan BJ, Marcario JK, Karrer JH, Cheney PD (1998) Corticomotoneuronal postspike effects in shoulder, elbow, wrist, digit and intrinsic hand muscles during a reach and prehension task. *J Neurophysiol* 80: 1961-1980.
- Morrow MM, Miller LE (2003) Prediction of muscle activity by populations of sequentially recorded primary motor cortex neurons. *J Neurophysiol* 89: 2279-2288.
- Park MC, Belhaj-Saïf A, Gordon M, Cheney PD (2001) Consistent features in the forelimb representation of primary motor cortex in rhesus macaques. *J. Neurosci* 21(8): 2784-2792.
- Penfield W, Boldrey E (1937) Somatic motor and sensory representation in the cerebral cortex of man as studied by electrical stimulation. *Brain* 60, 389-443.

- Porter R, Lemon RN (1993) Corticospinal Function and Voluntary Movement. Oxford, UK, Oxford Univ. Press.
- Powers RK., Binder MD (1996) Experimental evaluation of input-output models of motoneuron discharge. *J Neurophysiol* 75(1): 367-79.
- Ranck JB Jr. (1975) Which elements are excited in electrical stimulation of mammalian central nervous system: a review. *Brain Res* 98(3): 417-40. Review.
- Scott SH, Kalaska JF (1997) Reaching Movements with similar hand paths but different arm orientations. I. Activity of individual cells in motor cortex. *J Neurophysiol* 77: 826-852.
- Stoney SD Jr., Thompson WD, Asanuma H (1968) Excitation of pyramidal tract cells by intracortical microstimulation: effective extent of stimulating current. *J Neurophysiol* 31(5): 659-69.
- Tehovnik EJ (1996) Electrical stimulation of neural tissue to evoke behavioral responses. *J Neurosci Methods* 65(1): 1-17. Review.
- Woolsey CN (1958) Organization of somatic sensory and motor areas of the cerebral cortex. Biological and Biochemical Basis of Behavior: 63-79.

CHAPTER TWO

DO CORTICOMOTONEURONAL CELLS PREDICT TARGET

MUSCLE EMG ACTIVITY?

The studies described in this chapter have been published in the *Journal of Neurophysiology*, 2008, volume 99, pages 1169-1986.

ABSTRACT

Data from two rhesus macaques was used to investigate the pattern of cortical cell activation during reach-to-grasp movements in relation to the corresponding activation pattern of the cell's facilitated target muscles. The presence of post-spike facilitation (PSPF) in spike-triggered averages (SpTA) of electromyographic (EMG) activity was used to identify cortical neurons with excitatory synaptic linkages with motoneurons. EMG activity from 22-24 muscles of the forelimb was recorded together with the activity of M1 cortical neurons. The extent of covariation was characterized by: 1) identifying the task segment containing the cell and target muscle activity peaks, 2) quantifying the timing and overlap between CM cell and EMG peaks, and 3) applying Pearson correlation analysis to plots of CM cell firing rate versus EMG activity of the cell's facilitated muscles. At least one firing rate peak, for nearly all (95%) CM cells tested matched a corresponding peak in the EMG activity of the cell's target muscles. Although some individual CM cells had very strong correlations with target muscles, overall, substantial disparities were common. We also investigated correlations for ensembles of CM cells sharing the same target muscle. The ensemble population activity of even a small number of CM cells influencing the same target muscle produced a relatively good match ($r \geq 0.8$) to target muscle EMG activity. Our results provide evidence in support of the notion that corticomotoneuronal output from primary motor cortex encodes movement in a framework of muscle

based parameters, specifically, muscle activation patterns as reflected in EMG activity.

INTRODUCTION

The presence of post-spike facilitation (PSpF) in spike-triggered averages of EMG activity provides a means of identifying cortical neurons with demonstrable excitatory synaptic linkages to motoneurons (Buys et al., 1986; Fetz and Cheney 1980; Schieber and Rivlis 2005). Similarly, post-spike suppression (PSpS) identifies the presence of underlying inhibitory synaptic linkages (Kasser and Cheney 1985). Muscles with PSpF or PSpS are defined as the cell's target muscles. PSpF effects with durations at half magnitude of 9 ms or less can be attributed to underlying monosynaptic connections (Baker and Lemon 1998; Schieber and Rivlis 2005). Accordingly, cells producing these PSpF effects can be more confidently categorized as corticomotoneuronal (CM) cells.

Given that the presence of PSpF is evidence of an underlying synaptic linkage and that neurons producing PSpF represent the output signal from motor cortex to spinal motoneurons, a fundamental issue concerns the extent to which the activity of these cortical cells predicts or even encodes target muscle EMG activity (Schieber and Rivlis 2007; Townsend et al., 2006; Hamed et al., 2007). There is an underlying assumption that if post-spike effects on muscle activity are functionally meaningful, then the cells producing the effects and their target muscles should show some level of covarying activity during task performance. Our previous work (McKiernan et al., 2000), using long duration cross-correlations of continuous data (Houk et al., 1987),

suggests this is true for identified CM cells. Taking this analysis a step further, one might also expect that the temporal pattern of activity of an individual CM cell might closely resemble the temporal pattern of target muscle EMG activity. However, these expectations must be tempered by the fact that muscle activation reflects the summation of converging EPSPs from many cells terminating within the motoneuron pool. A single cell will only make a small contribution to overall motor unit activation so its relationship to the pattern of target muscle activity may be weak and variable. In view of this, one minimal expectation might be that the activity of the majority of CM cells and their facilitated muscles should at least show coactivation during the same segment of a movement task and that their peaks of activity should exhibit overlap. Although individual CM cells might have temporal patterns of activation that closely match the pattern of target muscle EMG activity, this is not essential. However, it is true that the ensemble activity of an identified population of CM cells sharing a common target muscle should have a temporal pattern of activity during movement that closely resembles the pattern of EMG activity, assuming that CM input to the motoneuron pool is a major factor driving motoneuron depolarization underlying an EMG peak and assuming a relatively linear transformation of cortical spike trains into EMG activity.

To further investigate the extent of covariation between CM cells and their target muscles, we have identified where peaks in their activity occur

during a forelimb reach-to-grasp task and have quantified the extent of overlap between them. The results show that 71% of CM cell peaks match a target muscle peak in the same task segment. CM cell peaks show an average of 74% overlap with peaks in their target muscles. We also report significantly improved correlations between the ensemble activity of a population of CM cells influencing the same target muscle and that muscle's EMG activity compared to the individual CM cell correlations.

MATERIALS AND METHODS

Behavioral task

Two male rhesus macaques were trained to perform a reach-to-grasp task as described previously (McKiernan et al., 1998). Inside a sound attenuating chamber, the monkey was seated in a custom built primate chair facing a computer monitor providing audiovisual cues. The monkey's left arm was comfortably restrained and the task was performed with the right arm. The task was initiated when the monkey placed his right hand, palm down, on a pressure detecting plate (home plate) at waist level in front of him on the right side. Holding the plate down for a preprogrammed length of time (1-2 seconds) triggered the release of a food reward into a cylindrical well at arms length from the monkey. The monkey then grasped and brought the food reward to its mouth. This task provided a robust paradigm in which to test relationships between CM cell and target muscle activity. The task broadly coactivated both proximal and distal forelimb muscles while at the same time yielding a relatively high level of fractionation in terms of the detailed structure of the EMG pattern in different muscles.

Surgical procedures

After training, a 22 mm diameter stainless steel chamber was centered over the hand area of M1 of the left hemisphere of each monkey and anchored to the skull with 12 vitallium screws and dental acrylic. Threaded

stainless steel nuts were also attached over the occipital aspect of the skull using 12 additional vitallium screws and dental acrylic. These nuts provided a point of attachment for a flexible head restraint system during recording (McKiernan et al., 1998, 2000).

EMG activity was recorded with pairs of insulated, multi-stranded stainless steel wires inserted transcutaneously into each of the target muscles (McKiernan et al., 1998, 2000). Electrode locations were confirmed by stimulation through the electrode pair and observation of appropriate muscle twitches. Electrode wires and connector terminals were affixed using medical adhesive tape. Following surgery, the monkeys wore a Kevlar vest and sleeve to protect the implant. EMG activity was recorded simultaneously from 22-24 forelimb muscles (Table 1).

For all surgeries, the monkeys were tranquilized with Ketamine (10 mg/kg) and anesthetized with isoflurane gas. Surgeries were performed in a facility accredited by the Association for Assessment and Accreditation of Laboratory Animal Care (AAALAC) using full sterile procedures. All work involving these monkeys conformed to the procedures outlined in the *Guide for the Care and Use of Laboratory Animals* published by the U.S. Department of Health and Human Services and the National Institutes of Health.

Cortical recording

Single cells in primary motor cortex (M1) were recorded using glass and mylar insulated platinum-iridium electrodes with typical impedances between 0.7 and 1.5 M Ω . A recording electrode was positioned within the chamber using an X-Y coordinate manipulator and was advanced into the cortex with a manual hydraulic microdrive (FHC Corp.). Electrode orientation was at a right angle to the cortical surface.

Spike-triggered averages

Cortical cell activity, EMG activity and position signals were recorded on analog tape using a 28-channel TEAC instrumentation recorder. Spike-triggered averages and response averages were compiled off-line using a custom software package (Windows Neural Averager, Larry Shupe, University of Washington, Seattle). The action potentials of single cells in M1 served as the triggers for computing SpTAs. Single unit spikes were isolated using an Alpha Omega MSD spike discriminator. EMG activity was routinely filtered from 30 Hz to 1 KHz, digitized at 4 KHz and full-wave rectified. Averages were compiled using an epoch of 60 ms, extending from 20 ms before to 40 ms after the unit spike.

Segments of EMG activity associated with each spike were evaluated by the software and accepted for averaging only if the average of all data points over the entire epoch was $\geq 5\%$ of full scale input. This prevented

averaging EMG segments where activity was minimal or absent (McKiernan et al., 1998).

Categorization and quantification of post-spike effects and cell firing frequency

The CM cells analyzed here were used in previous studies of post-spike effects in forelimb muscles (McKiernan et al., 1998, 2000). For the present analysis, the post-spike effects of many of the cells were recomputed from tape playback and enhanced by increasing the number of trigger events.

Categorization of effects in spike triggered averages was based on the latency and width of effects. We estimated the minimum reasonable latency for PSpF of muscles at different joints to be: 3.4 ms for shoulder muscles, 4.2 ms for elbow muscles, and 6.0 ms for intrinsic hand muscles (McKiernan et al., 1998, 2000). Effects with shorter latencies were presumed to have synchrony components. Schieber and Rivlis (2005) evaluated PSpF effects using a criterion developed by Baker and Lemon (1998) derived from a spike-triggered averaging simulation model. This model suggests that pure PSpF effects arising from underlying monosynaptic connections with motoneurons can be identified based on the peak width of PSpF at half magnitude (PWHM). A PWHM of 9 ms or less was suggested as an effective criterion for identifying PSpF effects that are most likely due to underlying monosynaptic PSpF (Baker and Lemon 1998). A PWHM of 9 ms was the

criterion applied by Schieber and Rivlis (2005) and we have also adopted this criterion. Taking into account these latency and width factors, in this study we categorized PSpF effects as: 1) pure PSpF if this was the only effect present and its PWHM was 9 ms or less; 2) PSpF on synchrony (PSpF+Sync) if a primary PSpF could be identified based on a discontinuity in the slope of the rising phase of an underlying synchrony facilitation and the primary PSpF effect possessed a latency consistent with a minimum cortex to muscle pathway (Flament et al., 1992); 3) late widening PSpF (Schieber and Rivlis 2005) if only a primary effect was present but the PWHM was greater than 9 ms and its latency could be explained without requiring the presence of synchrony; and 4) pure synchrony facilitation (SyncF) if the effect was broad with an onset latency inconsistent with a realistic minimum cortex to muscle pathway and no primary PSpF could be identified as a sharp peak riding on a broad synchrony peak. A similar categorization was used for suppression effects. Although synchrony effects are of interest and may contain a component mediated by a synaptic output linkage between the cortical cell and motoneurons, for the purposes of this study, we have excluded synchrony effects from the analysis. All effects included in this study were either pure PSpF or late widening PSpF effects. For convenience, we will refer to cortical cells producing these effects as CM cells.

All identified post-spike effects were assigned a ranking of weak, moderate, or strong based on the magnitude of the effect (Figure 2.1).

Nonstationary, ramping baseline activity was routinely subtracted from SpTAs using our analysis software. The EMG values from a range of bins in the pre-trigger period were averaged to arrive at a baseline mean and standard deviation (SD). The baseline typically was determined by averaging a 10 ms segment of each record during the pre-trigger period. The onset and offset of each peak were determined as the points where the record crossed a level equivalent to + 2 SD above the mean of the baseline EMG (see McKiernan et al., 1998; Figure 4 A). Peaks less than 2 SD of baseline and peaks that remained above 2 SD for less than a 0.75 ms period were considered insignificant, and the average was categorized as having no effect (Figure 2.1). The color coding of effects based on magnitude used in Figure 2.1 is maintained throughout all figures of the paper.

The peak of each effect was defined as the highest point of the PSpF. The magnitude of each PSpF was quantified in terms of its peak percent increase (PPI) above baseline, peak-to-noise ratio (P/N), and P/N normalized to 10,000 trigger events. P/N magnitudes were normalized based on the principle that signal-to-noise ratios should increase as the square root of the number of trigger events (Belhaj-Saïf et al., 1998). Ten thousand was approximately equal to the median of the number of trigger events for all PSpE analyzed (Park et al., 2004). Expressions for these measures are as follows:

$PPI = 100 (\text{Maximum bin value} - \text{baseline mean}) / \text{baseline mean}$

$P/N = (\text{PSpF peak} - \text{baseline mean}) / \text{baseline standard deviation}$

$\text{Normalized P/N} = \sqrt{10,000 / \# \text{trigger events}} \times P / N$

After normalizing the P/N ratio, the magnitude of PSpF effects were categorized as follows (Figure 2.1). Weak PSpF effects had peaks greater than 2 SD of mean baseline activity but less than 4 SD; moderate effects had peaks equal to or greater than 4 SD of mean baseline activity but less than 7 SD; and strong PSpF effects had peaks of 7 SD or greater.

The depth of modulation (DOM) in CM cell firing rate (Hz) was measured for all peaks using response average records referenced to different parts of the movement sequence. CM cell activity peaks were identified in segments of the record that exceeded 2 SD of the baseline points. Baseline was determined from activity while the monkey's hand was on home plate (segment #1 in Figure 2.2) and EMG activity was largely absent. DOM was then calculated by subtracting the cell's lowest firing rate during baseline activity from its highest firing rate during the peak of activity. Peaks in CM cell activity were then ranked by magnitude as primary (highest peak value), secondary (2nd highest peak value) tertiary (3rd highest), and quaternary (4th highest).

Response averages consisting of unit firing rate, full wave rectified EMG activity for each of 22 to 24 implanted forelimb muscles, the home plate

signal and the food well signal were aligned to each of the four segments of the task: leaving home plate, entering target food well, exiting target food well and returning to home plate. Response averages were typically based on 40-60 trials and were four seconds in duration. The bin width for unit spikes was 10 ms and the sampling rate for all analog channels (EMG and movement parameters) was 100 Hz or 10 ms/point. EMG was full-wave rectified and low pass filtered.

Quantification of cell-muscle covariation

For each response average, peaks in CM cell and EMG activity were assigned to one of 10 segments of the reach-to-grasp task as illustrated in Figure 2.2. The details of timing for defining the boundaries of each task segment are given in the legend for Figure 2.2. These segments were then used as the criterion for determining if peaks in CM cell activity were associated with peaks in target muscle EMG activity. Peaks in CM cell and target muscle EMG activity were considered “matching” if they both fell within the same segment of the task. The durations of segments 1 (on home plate) and 5 (in the food cylinder) were considerably longer than other segments and potentially could allow non-overlapping peaks in CM cell and muscle activity to be called “matching”. However, the mean peak time difference between CM cell and target muscle EMG activity was not significantly greater for these movement segments compared to other movement segments.

Our goal in segmenting the reach-to-grasp task was not only to identify the location of CM cell firing rate peaks relative to functionally distinct task segments, but also to establish a sufficient number of segments to provide reasonable temporal resolution. The onset and duration of segment 8 (at the mouth) were estimated based on the fact that the monkey's hand reached his mouth about half way between exiting the food well and depressing home plate.

As noted above, one objective of this approach was to document what phase of the reach-to-grasp task engaged the activity of each CM cell and its target muscles. This approach also provided a measure of the extent to which peaks in CM cell and target muscle activity occurred during the same functionally distinct task segment. Given the fact that a single CM cell is just one of hundreds of cells contributing to the activity of motoneurons belonging to the target muscle, it is unreasonable to expect that the cell and muscle peaks should necessarily be completely overlapping and coincident. However, if the cell is part of a larger neural network causally involved in generating muscle activity, it is reasonable to expect that the peaks of activity should at least be partially overlapping and would occur during the same functional task segment. To quantify the temporal coupling between CM cell and target muscle EMG activity we measured the time difference between their matching peaks, that is, peaks falling within the same segment of the task, and the extent of overlap between peaks.

Covariation was visualized and quantified by plotting CM cell firing rate in response averages against target muscle EMG point-for-point as a scatter plot (Griffin et al., 2004; Schieber and Rivlis 2007). Pearson correlation coefficients (r) were then calculated for these scatter plots. Four response averages were generated for each CM cell as described above. The analysis period was sufficiently long to contain the entire movement cycle within each average. However, the average producing the highest peak in cell activity revealed the aspect of movement the cell was best related to and this average was used to calculate the correlation coefficient. For example, in Figure 2.4, all four averages show a peak in CM cell activity corresponding to exiting the food well. However, the peak was most sharply defined in the average triggered from exiting the food well so that average was selected for performing the correlation analysis. However, the correlation coefficients were very similar for all four sets of averages belonging to a particular cell.

Measurement of EMG cross-talk

Cross-talk between EMG electrodes was evaluated by constructing EMG triggered averages. This procedure involved using the motor unit potentials from one muscle as triggers for compiling averages of rectified EMG activity of all other muscles. The criterion established by Buys et al., (1986) was used to eliminate effects with cross-talk. To be accepted as a valid post-spike effect; the ratio of PSpF between test and trigger muscle

needed to exceed the ratio of their cross-talk peaks by a factor of two or more. One muscle of any muscle pair that did not meet this criterion was eliminated from the data base. Based on this criterion, we eliminated a total of 11 effects from both monkeys over the course of four EMG implants.

Cortical Maps

The procedure used for producing a two-dimensional rendering of the location of cortical sites was described previously (Park et al., 2001). Briefly, the cortex was unfolded and the location of cells were mapped onto a two dimensional cortical sheet based on the cell's X-Y coordinate, known architectural landmarks and observations noted during the cortical implant surgeries (Figure 2.3).

RESULTS

Data were collected from the left M1 cortex in two rhesus monkeys. A total of 44 task related CM cells were recorded, 22 in monkey N and 22 in monkey K. CM cells used in this study were derived from the same database used in two previous reports (McKiernan et al., 1998, 2000). Spike-triggered averaging of EMG activity from 22-24 forelimb muscles yielded 187 post-spike and synchrony effects as follows: 135 pure PSpF or late widening PSpF effects, 14 syncF, 7 PSpF+S, and 31 pure PSpS. The total number of pure or late widening PSpF effects obtained by joint was: 18 shoulder, 28 elbow, 27 wrist, 23 intrinsic hand, and 39 digit. Of the total, 13% were strong effects (>7 times the SD of the baseline points), 41% were moderate effects (4-7 times the SD of the baseline points) and 46% were weak effects (2-4 times the SD of the baseline points). Eighty percent of the CM cells facilitated more than one muscle; 61% facilitated three or more muscles.

CM cell-target muscle modulation during reach-to-grasp

Response averages referenced to leaving home plate, entering the food well, leaving the food well and returning to home plate were generated for each CM cell (Figures 2.2 and 2.4). The maximum DOM observed among the 44 CM cells during the reach-to-grasp task ranged from 186 Hz for the 1° peak to 12 Hz for the 4° peak. The overall mean DOM for primary peaks was 80 Hz and 56 Hz across all peaks. Figure 2.4 shows an example of a

complete set of four response averages compiled for one CM cell. As noted in the Methods, the analysis period was sufficiently long that all segments of the task are present in each response average. The peak in activity for the cell in Figure 2.4 was strongest in the response average triggered from exiting the target food well, although the peak of activity actually occurred about midway through segment 5 of the task (digits in the food well). The discharge peaked about 300 ms before leaving the food well with a DOM of 97Hz. All four of the cell's facilitated target muscles (green and blue records corresponding to moderate and weak PSpF effects respectively) show a peak in EMG activity within the same segment of the task (gray shading), defined as a "matching" peak. Several non-target muscles also showed matching peaks of activity including ECU, ED2,3, ED4,5, EDC, ECR, FCU, and TLON. The peaks in activity of the cell's facilitated muscles lagged the CM cell's peak by 30–140 ms but they all (except FDI) began to rise in advance of the CM cell's peak. All of the target muscle peaks were present in the same segment of the task and overlapped substantially with the cell's peak.

For 1 of 3 CM cells with single peaks of activity, the primary EMG peaks in all facilitated target muscles occurred in the same segment of the task (100% matching); the match was 25% (i.e., one of four target muscles) for another cell and for the 3rd cell, the primary target muscle EMG peaks were in different segments of the task. However, most CM cells had multiple peaks of modulation during the task. The total number of activity peaks was

as follows: three had one peak, six had two peaks, 14 had three peaks, and 21 had four peaks.

The peaks in CM cell activity were distributed over the entire movement cycle. Figure 2.5 shows a histogram of all the CM cell peaks associated with each segment of the task coded for whether it was the cell's primary (strongest) peak or a weaker peak. The majority of firing rate peaks (44%) occurred in segments 4 (entering target food well), 5 (in target food well) and 6 (exiting target food well) of the movement cycle. A substantial number (28%) were also associated with segments 8 (at the mouth) and 9 (in transit back to home plate). It is noteworthy that these are all phases of task that most heavily rely on skilled use of the distal muscles and correlates with the fact that a majority of cells (52%) facilitated distal muscles exclusively or most strongly. For example, the cell in Figure 2.4 facilitated digit and wrist flexor muscles and showed a single strong peak in segment five of the task, undoubtedly associated with flexion of the wrist and digits related to grasp of the food pellet. The concentration of peaks in activity associated with activity in the food well and at the mouth reflects the importance of CM cells in controlling distal muscles associated with shaping the hand, grasping the reward and release of the food pellet into the mouth. Relatively few CM cell peaks (3.5%) were associated with segments 10 (depression of home plate) and 1 (hold on home plate). The EMG levels during these segments of the task were also relatively low.

Do peaks in CM cell activity match EMG peaks in their facilitated target muscles?

Peaks in CM cell firing rate and target muscle EMG activity were compared to determine the extent to which they occurred in the same segment of the reach-to-grasp movement task (defined as matching peaks). This approach is based on the rationale that while the timing and duration of peaks in individual CM cells and target muscles would not be expected to correlate perfectly, they should at least be associated with the same functional segment of the task and show some overlap. Figure 2.6 shows the results obtained using criteria that varied in the level of rigor needed to conclude that the cell's peaks matched the target muscle's peaks, with Figure 2.6 A being the most rigorous and 6C the least rigorous. In Figure 2.6 A, we determined the number of cells whose 1° peak was in the same segment of the task as the 1° EMG peaks of the target muscles. Since most CM cells had multiple target muscles, the percentage given for each cell reflects the fraction of target muscles that met the criterion. Secondary firing rate peaks were ignored. For 64% of CM cells (numbers 1-28) none of the target muscle primary peaks matched the cell's primary peak. For this strictest criterion, the mean CM cell-target muscle peak match was 20% including the cells with zero matches. Some CM cells (7.0%) showed a 100% match, that is, all the cell's target muscles had their primary peak in the same segment of the task

as the CM cell. The outcome did not correlate with either the number of facilitated muscles or the number of muscle peaks. We then relaxed the criterion and determined for each CM cell whether its 1^o peak was in the same segment of the task as any peak in the target muscle EMG (Figure 2.6 B). Once again the percentage given for each cell reflects the number of target muscles that met this criterion. This yielded a mean CM cell-target muscle peak match of 45%, that is, 45% of target muscles had a peak of some magnitude in the same segment of the task as the primary peak of the CM cell. In Figure 2.6 C, we determined for each CM cell the percent of target muscles that had a peak of any magnitude that matched a CM cell peak of any magnitude. This yielded an average match of 85%. Overall, 71% of CM cell firing rate peaks had a matching target muscle EMG peak. Nearly all CM cells (95%) had at least one peak that matched a peak in a target muscle.

Finally, for each CM cell, we determined the percent of CM cell firing rate peaks with matching EMG peaks relative to the number of total possible matches (Figure 2.6 D). For example, if a CM cell had two peaks of activity, each of its target muscles would need to show two corresponding peaks in the same segments of the task for a 100% match. If the same CM cell facilitated four target muscles, the total possible chances for matching peaks would be eight. Therefore a 50% match for this cell would reflect any combination of cell and target muscle peak matches where there were four

EMG peaks that matched a CM cell peak. This yielded an average CM cell-target muscle peak match of 45% (Figure 2.6 D). In three cases, all the peaks in CM cell activity were matched by corresponding peaks in target muscle EMG activity.

Figure 2.7 shows two examples of identifying matching peaks in CM cell firing rate and EMG activity (peaks occurring in the same segment of the task) and how this data was used to construct the plots in Figure 2.6. A subset of task segments are color coded and labeled 4-9 at the bottom of the figure. CM cell 105N6, represented by the black bars in Figure 2.6, and CM cell 65N6, represented by the grey bars in Figure 2.6, both show four peaks of activity. Both cells have a primary peak (highest firing rate) associated with segment 6 (exiting the target food well) of the reach-to-grasp task. Only 105N6 has a primary peak that matches a primary peak of EMG activity in one of its facilitated muscles (APB). Since 105N6 had seven target muscles, 14% of all target muscles had primary peaks that matched the cell's primary peak. Similarly, 65N6 showed a 0% match (0/3) to primary peaks in its target muscles. However, 105N6's primary peak matches three of the non-primary peaks in its muscles (the tertiary peak of TLAT and the secondary peak of both BRA and BR). This yields a 57% match between the cell's primary peak and any target muscle EMG peak (Figure 2.6 B). 65N6 shows only one target muscle peak match with its primary peak (secondary peak of ED45) yielding a 33% match based on the criterion of Figure 2.6 B. Taking this analysis

further, all seven of 105N6's target muscles show at least one peak that matched one of the cell's peaks yielding a value of 100% in Figure 2.6 C. By this same criterion, 65N6 had two target muscles with peaks that matched one of the cell's peaks yielding a 67% match in Figure 2.6 C. Since 105N6 has 4 peaks of activity and facilitates 7 muscles, the total possible matches would be 28. However, only 14 peaks in EMG activity actually match peaks in CM cell activity - a 50% match in Figure 2.6 D. 65N6 has 4 peaks of activity and facilitates 3 muscles yielding 12 total possible matches. However, only 2 actual matches were observed for this cell and its target muscles - a 17% match in Figure 2.6 D.

Timing between peaks in CM cell and target muscle activity

To provide detailed information on timing, we measured the time lag between matching peaks in CM cell and target muscle EMG activity. Figures 2.8 A and B show the distribution of time lags plotted according to the strength of synaptic connection (magnitude of PSpF; Figure 2.1) and cell firing rate modulation (DOM). Cell-muscle peak time difference was determined using the time corresponding to the highest point in the peak for both unit and EMG activity. Fifty-six percent of peaks were within ± 100 ms of each other. Based on analysis of 190 matching activity peaks, the CM cell peak led the target muscle EMG peak by an average of 23 ms ± 150 (Table 2). The median CM cell to EMG peak time differences were not statistically

significant for the different distributions based on magnitude of PSpF ($P = 0.68$, Kruskal-Wallis) or DOM ($P = 0.18$, Mann-Whitney). The peaks in the timing distributions for different strengths of PSpF were similar. However, the tightest coupling (smallest range) between peak time in CM cell activity and target muscle EMG activity occurred for cell-muscle pairs exhibiting strong and moderate PSpF ($P < .01$, Levene median test). A similar result was obtained for DOM. The distribution of timing between CM cell and target muscle EMG peaks was narrower (less variability) for CM cells with high DOM, greater than 75 Hz, compared to those with DOM less than 75 Hz ($P < .05$, Levene median test). The same result was obtained with a DOM cutoff of 50 Hz. Note that DOM and strength of PSpF were not significantly correlated ($r = 0.01$, $P = 0.95$).

Figures 2.8 C and D quantify the extent of overlap in matching peaks of cell and target muscle activity. Peak width was evaluated in terms of the percent of overlap with respect to both muscle activity and CM cell activity. Figure 2.8 C shows the percent of each CM cell peak that was overlapped by matching, facilitated target muscle EMG peaks while Figure 2.8 D shows the percent of the target muscle EMG peak that was overlapped by the CM cell peak. Note that the distribution is narrower with more pairs toward the greater overlap end of the distribution for strong PSpF effects. This was true for both the extent of overlap of the CM cell peak by the muscle peak and the overlap of the target muscle EMG peak by the CM cell peak. On average,

74% of the CM cell peak was overlapped by the facilitated target muscle peak and this rose to 90% for muscles with strong PSpF (Table 2, $P < .05$, Kruskal-Wallis). Conversely, 57% of the target muscle peak was overlapped by the CM cell peak and this was also higher for muscles with strong PSpF. We quantified the number of CM cell – target muscle EMG peaks with 50% or greater overlap: 81% of CM cell peaks showed 50% or more overlap by one or more individual target muscles.

Correlations between CM cell activity and target muscle EMG activity

Cell-target muscle covariation during the reach-to-grasp task was quantified by plotting the average CM cell firing rate during reach-to-grasp against target muscle EMG (Figure 2.9). Scatter plots were generated from this procedure and subjected to correlation analysis. Pearson's correlation coefficient (r) was used to quantify the covariation of CM cell and target muscle activity during the reach-to-grasp movement cycle. Firing rate was plotted against EMG activity with no time shift based on the rationale that the time delay between the firing of a CM cell and its effect on muscle activity should be roughly equal to the conduction time through the CM pathway to muscles and should be approximated by the peak latency of PSpF (see Discussion). This latency is in the range of 8-14 ms (Park et al., 2004) depending on the muscle and can be ignored for this analysis because it is close to our sampling rate, that is, one sample point. Firing rates and

corresponding target muscle EMGs that have the same temporal profile with no phase shift should have correlations close to one. In Figure 2.9, the bulk of points in the > 60Hz firing rate range are from a part of the response average record containing the cell's primary activity peak. During much of this time, ECR's EMG activity was relatively flat. This generates a group of points that are relatively constant on the EMG axis but vary over the range from 60–100Hz on the CM cell firing rate axis. These points tend to diminish the overall correlation since throughout most of the remainder of the record, CM cell and muscle activity covary more closely. The broader, slower trends in firing rate and EMG activity contribute significantly to the overall strength of the correlation.

The distribution of correlation coefficients for all CM cell-target muscle pairs with matching peaks of activity is given in Figure 2.10. The median correlation coefficient was 0.46 with a peak between 0.5 and 0.6. Eighty-four percent of the correlations were positive and 16% were negative despite the presence of PSpF. However, PSpF was weak for 50% of the muscles with negative correlations; none of these muscles had strong PSpF.

PSpF magnitude relationships

The magnitude of pure PSpF (PPI and normalized P/N ratio) was plotted against the Pearson correlation coefficient (r) for all 135 cell-target muscle pairs which showed PSpF and had 2,000 or more sweeps in the

SpTA. Although the correlations were weak, PSpF magnitude measured as P/N showed a significant positive relationship with CM cell-target muscle covariation ($r = 0.25$, $P < 0.01$), but this weakened to only a trend toward significance when P/N was normalized ($r = 0.13$, $P = 0.14$). Using PPI as a measure of PSpF yielded no significance or trend ($r = 0.03$, $P = 0.72$). It is worth noting that differences in baseline magnitude can potentially distort the true strength of PSpF based on PPI measurements.

DOM relationships

DOM of individual CM cell firing rate peaks were plotted against Pearson's correlation of the covariation between the cell firing rate and target muscle EMG activity. One-hundred fifteen cell-muscle pairs had at least one "matching" peak of activity. In the case of multiple "matching" peaks, the values used were based on the response average with the highest DOM peak. There was no statistically significant tendency for r to be higher for greater DOMs. There was no relationship between DOM and any measure of PSpF magnitude.

Covariation and PSpS

For 31 cell-target muscle pairs which exhibited PSpS, 29% (9/31) had a negative r (compared to 16% of cell-target muscle pairs producing PSpF effects). The magnitudes of pure PSpS effects (PPI and normalized P/N)

were plotted against r for all 31 cell-target muscle pairs which showed PSpS and had 2,000 or more sweeps in the SpTA. PSpS magnitude did not show a statistically significant relationship with r nor did the relationship change when the analysis was limited to moderate and strong effects.

Covariation and synchrony effects

The analysis thus far was limited to PSpF or PSpS without evidence of early onset synchrony. However, we did identify synchrony effects and test their relationship to the strength of covariation. The magnitude of synchrony effects expressed as PPI or normalized P/N was plotted against r for all 21 cell-target muscle pairs which showed either SyncF ($n = 14$) or PSpF+Sync ($n = 7$) and had 2,000 or more sweeps in the SpTA. The strength of covariation between CM cell and target muscle activity based on r was not significantly correlated with SyncF magnitude. This was also true for effects rated as moderate or strong.

Correlations with a CM cell's full muscle field

One factor that might contribute to weak covariation between CM cells and their target muscles is the fact that the output from most CM cells is not limited to one muscle but rather diverges to influence multiple muscles. This raises the possibility that the activity of a CM cell might covary more closely with the summed activity of all of its target muscles rather than with any one

muscle. To test this hypothesis, the response averages of all target muscles for 12 representative CM cells were summed together after weighting by the magnitude of PSpF for each muscle. CM cells were selected using the criteria that the PSpF in at least one muscle had to be strong or moderate. Scatter plots were generated by plotting each CM cell's firing rate record against the summed EMG activity of all of its facilitated target muscles. The resulting correlation coefficient was then evaluated for improvement compared to that of the individual cell-target muscle pairs. Only 3 of 12 CM cells showed stronger correlations with the summed target muscle EMG record compared to the best correlation with an individual muscle. All three of these were CM cells with a distal only or proximal only muscle field. Also, the mean of correlations between the CM cell's firing rate record and the summed EMG of all its target muscles was not significantly different from the corresponding mean of all the individual CM cell – target muscle EMG correlations ($P=0.41$).

Populations of CM cells converging on a common target muscle

A major contributor to disparities evident above between CM cell and target muscle covariation is undoubtedly the fact that the activation of muscles is the result of synaptic input from many CM cells (and other cells), not just the recorded cell. Clearly, the input from one cell alone will have only a weak effect on the firing of motoneurons and based on that it is perhaps

unrealistic to expect that the activity of one CM cell should correlate closely with the activity of a particular muscle, even though the cell directly facilitates that muscle. However, it is reasonable to expect that a population of CM cells influencing the same muscle should be a much better predictor of the pattern of EMG activity (Fetz et al., 1989; Griffin et al., 2004; Schieber and Rivlis 2007). To test this hypothesis, we identified populations of CM cells influencing the same target muscle and correlated the summed population activity to the muscle's EMG activity. Of course, the optimal way to perform this experiment would be to simultaneously record from many CM cells that all have at least one target muscle in common. However, lacking this type of data, which would undoubtedly be very difficult to obtain, we have tried to take advantage of our existing data from sequentially recorded individual CM cells. To simulate the conditions that would exist with simultaneously recorded CM cells, we have only selected cells for which the temporal pattern of EMG activity in the muscle of interest was very similar. For example, Figure 2.11 B shows the EMG records for ED2,3 recorded with three different CM cells (Figure 2.11 A) aligned on entering the food well (Figure 2.11 E). The EMG records for ED2,3 in Figure 2.11 B have the same number of peaks with similar timing and width thereby meeting the criterion for creating a population from the corresponding CM cells. The average firing rate records of these CM cells were then summed together as were their associated EMG records (Table 3). Our data base contained many more individual CM cells

that facilitated each of these muscles, but we excluded them based on the dissimilarity in their EMG pattern during the reach-to-grasp task.

Figure 2.11 is an example of this procedure for ED2,3 population 1 (Table 3). The individual ED2,3 EMG records for each of the three CM cells used to generate the population average are shown in Figure 2.11 B. Note the similarity they have to each other and to the summed EMG record. Figure 2.11 A shows the average firing rate records during the reach-to-grasp task for all three CM cells as well as the population firing rate record. These CM cells produced moderate to strong PSpF of ED2,3 (Figure 2.11 C). Note that the population CM cell firing rate record created by summing together the individual records has a temporal pattern very similar to the EMG record and even shows evidence of the multiple peaks that are clear in the EMG record. The population CM cell firing rate record was plotted point for point against the summed EMG record for ED2,3 (Figure 2.11 D). The resulting linear correlation coefficient was very strong ($r = .90$; $P < 0.001$) demonstrating relatively tight covariation of population CM cell activity with ED2,3 EMG activity. The individual CM cell-ED2,3 EMG correlation coefficients ranged from 0.34 to 0.91 and included one cell-muscle pair with a correlation coefficient that was essentially equal to the population correlation coefficient. However, most noteworthy is the fact that the population CM cell-target muscle correlation of 0.90 is much stronger than the mean of the individual cell-target muscle correlations (0.60).

We were able to apply this analysis to seven muscles in total (Table 3). For four of these muscles, the criterion that the temporal pattern of EMG activity for the muscle of interest had to be similar for each individual CM cell required splitting the CM cells for these muscles into multiple populations. Our final data set consisted of 10 CM cell populations ranging in size from 3 cells to 5 cells. For all but two (Table 3, ED2,3-2, ECR) of these CM cell populations, the population correlation coefficient was either equal to or greater than the correlation coefficient of any individual cell-target muscle pair in the population. However, all but one of the 10 population correlation coefficients were greater than the corresponding means of the individual cell-target muscle correlations. Additionally, the overall mean of the 10 population correlation coefficients was significantly greater than the overall mean of the individual correlation coefficients for each population ($r = 0.75$ versus 0.58 , $P = 0.02$).

We went to great lengths to select CM cells that had a very similar pattern of EMG activity for the muscle in question. The lowest value of the correlation coefficients between each muscle in a set and the summed EMG for that set ranged from $0.79 - 0.96$ (Table 3, column F). Nevertheless, to further test the possibility that improvement in the correlation between the population CM cell firing rate and summed EMG records could have been due to some nonspecific smoothing effect of summing records together, we compared the set of r values obtained from correlating the population CM cell

activity and summed EMG, (Table 3, column E) to the mean r values obtained from correlations of the population CM cell activity to the individual EMG records (Table 3, column G). This comparison was not significant ($P = 0.43$, Mann-Whitney test) supporting the contention of statistical equivalence between the summed and individual EMG records. Finally, we also compared the mean r from the individual CM cell-muscle pair correlations (Table 3, column D) against the mean r derived from correlating the population CM cell activity with each individual muscle EMG (Table 3, column G). The population CM cell activity yielded a stronger correlation although falling slightly below the 0.05 level of statistical significance ($r = 0.55$ versus 0.44, $P = 0.08$). Nevertheless, it seems reasonable to conclude that using the population CM cell activity was a major factor contributing to the improvement in CM cell-muscle EMG correlations, not the summing together the EMG records.

DISCUSSION

Predicting EMG activity from individual CM cells

The interpretation of data presented in this paper is subject to two points of view. On the one hand it could be argued that for neurons comprising a descending system which is supposedly driving muscle activity, the level of mismatch between the firing rate peaks of individual CM cells and their target muscles seems rather astounding. For example, on average, only 20% of CM cells had their primary peaks in the same segment of the task as the primary peaks in their target muscles. Relaxing the criterion to include any magnitude EMG peak occurring in the same segment of the task as the cell's primary peak resulted in a match of 45% - better but still surprisingly low.

Alternatively, the similarities in activity between the temporal pattern of activity in CM cells and their target muscles could be emphasized. For example, nearly all CM cells (95%) had a least one firing rate peak that matched (occurred in the same task segment) an EMG peak in at least one of its target muscles. CM cell firing rate peaks also showed substantial overlap (mean = 74%) with peaks in individual target muscle EMG records and the amount of overlap increased to 90% for cell-muscle pairs producing strong PSpF. In this case, it should be noted that even though CM cell and target muscle peaks overlap, the activity of the two may have actually been

negatively correlated during part of overlap period with one signal increasing and another decreasing. Nevertheless, these results are evidence in support of the general conclusion that CM cells exhibit relatively strong and consistent coactivation with their target muscles and this is particularly true of CM cell - target muscle pairs exhibiting strong PSpF.

This conclusion supports the findings of McKiernan and colleagues (2000) which study used long duration cross correlation analysis. Although the long duration cross correlation method has its strengths, for example, it yields a coefficient that describes the correlation and a measure of time lag; it lacks information about where the activity for both the cell and muscle are occurring relative to the task. In the present study, we have been able to describe where CM cell activity peaks occur in relation to their target muscles in a linear non-shifted correlation. This study also demonstrates that the highest peak of cell activity is often not associated with the activity peak of the cell's target muscle and therefore shifting the EMG signal to match the highest cell activity peak may be imposing an arbitrary association. Also, since the long duration cross correlation method uses single continuous trial records, it is subject to trial by trial variability. The analysis method of this study uses averages of multiple trials which removes the trial by trial variability. We have made the argument that if CM cells are linearly encoding EMG activity, using the present analysis methods, one would expect to see

correlation coefficients approaching one without shifting the signals relative to one another.

Correlation studies are an approach to quantifying the extent of linear covariation between CM cells and EMG activity. We plotted the average firing rate records of CM cells against the corresponding target muscle EMG records and subjected the resulting scatter plots to correlation analysis (Figure 2.9). The correlation coefficients ranged from -0.69 to 0.91 for individual cell-muscle pairs with PSpF. The median r value was 0.46 with a peak between 0.5 and 0.6 (Figure 2.10). Overall, the correlations for individual cell-muscle pairs would have to be judged as relatively weak and this result is consistent with the findings of other studies on cortical cells and their facilitated muscles (Schieber and Rivlis 2007). One might expect our results to show even weaker correlation coefficients than those of the Schieber and Rivlis study (2007) since we have used a highly complex multi-joint reaching task which broadly activates forelimb muscles while at the same time fractionating peaks of activity into unique synergies and ultimately providing a robust paradigm with which to test relationships between CM cell and target muscle activity.

What factors might contribute to the existence of major disparities in the location of movement related activity peaks in CM cells compared to their target muscles and to associated weak correlation coefficients? Certainly a major issue is the fact that the depolarization of motoneurons underlying

muscle EMG activity results not from the action of just one CM cell but from many CM cells converging on a particular motoneuron pool. In addition, there are numerous additional sources of input to the motoneuron pool that can influence motoneuron activity independent of corticospinal input. At any given time during movement, a single motoneuron is receiving modulated input from hundreds if not thousands of afferent neurons. Another factor that might degrade the fidelity of covariation between a CM cell and its target muscles is the fact that most CM cells do not influence just one muscle; rather they influence multiple muscles as a synergy. We tested the possibility that correlations might be stronger if a CM cell's complete muscle field were taken into account. Each muscle of a CM cell's muscle field was weighted according to the magnitude of PSpF and the resulting EMG records were then summed together. The summed record was correlated with the cell's firing rate record. However, in most cases, the summed record did not result in significantly stronger correlations than the individual muscle EMG records. Using a similar approach, Schieber and Rivlis (2007) also reported that summing the EMG records of all the target muscles failed to substantially improve the correlations. However, in an interesting modification of this type of analysis, Townsend et al., (2006) recently showed that the EMG activity of all a cell's target muscles could be used to accurately predict CM cell activity and that the prediction accuracy increased with the size of the muscle field.

In view of the potential sources of disparity, it is only reasonable to predict major dissimilarities in the pattern of activity of any single CM cell and its target muscles. In fact, it might be considered remarkable that the timing of firing rate peaks between single CM cells and target muscle EMG activity are as close as they are and that the correlation coefficients are as strong as they are.

Predicting EMG from population CM cell activity

Assume that corticospinal input to motoneurons is the principal driving force under at least some conditions, essentially eliminating multiple sources of synaptic input as a factor contributing to degradation in the strength and quality of covariation between CM cell and EMG activity. In this case, motoneurons would be depolarized by the actions of multiple CM cells and other corticospinal neurons. The ensemble firing rate record of a sufficiently large population of CM cells synaptically coupled to motoneurons of the same muscle might then approach a perfect correlation with the muscle's EMG activity. To the extent that this was possible within our data set, we attempted to test this possibility. We found that in many cases (6 of 10), the temporal pattern of the ensemble firing rate record for the CM population closely resembled ($r \geq 0.8$) the EMG activity of the common target muscle (Figure 2.11). Perhaps most noteworthy is the fact that in all cases except one, the population correlation coefficient was greater than the corresponding mean of

the individual cell-target muscle correlations (Table 3). The one exception was ECR where the population and individual r values were essentially the same. Moreover, the mean of the population correlation coefficients for all 10 muscles tested was significantly greater ($P = 0.02$) than the mean of all the individual cell-target muscle correlations. Finally, in all cases except two (Table 3), the population r was essentially equal to or greater than the highest individual cell-muscle correlation.

Some individual cell-target muscle pairs had very strong correlations as Schieber and Rivlis (2007) have also reported. However, the key issues are whether the population correlation is better than the individual cell-target muscle correlations and whether the final population correlation achieves a level consistent with concluding that the cells as a population could potentially account for large part of time varying pattern of EMG activity during movement. We believe our data is consistent with this interpretation and adds further support to the notion that CM cell output encodes muscle activation (EMG) and should be viewed within the context of a muscle based coordinate system (Hamed et al., 2007; Holdefer and Miller 2002; Morrow et al., 2007; Morrow and Miller 2003; Mussa-Ivaldi 1988; Todorov 2000; Townsend et al., 2006).

Due to the small size of our populations, we could not analyze, in any meaningful way, changes in the population r with addition of new cells and increase in the size of the population. However, Schieber and Rivlis (2007)

were able to do this, using larger populations of CM cells recorded in relation to finger movements. They showed that the pattern of improvement or decline with cell number depended on the order in which cells were added into the population. Using an order that was essentially random, the population r value fluctuated over a large range with small numbers of cells but then converged toward the final population r . However, despite larger populations of CM cells, the correlations reported by Schieber and Rivlis (2007) were weaker overall than those we have reported in this study. Their strongest population r value was 0.657 (R^2 value of 0.431). In contrast, 60% (6 of 10) of our CM cell populations had greater correlations than this and the overall mean r value was 0.75. The reason for this difference is unclear. The muscles that form our CM cell populations are entirely distal muscles, mostly digit muscles. Although our behavioral task was an unconstrained “free-form” task that might have provided a greater opportunity for yielding a higher level of sculpting of individual muscle EMG activity than the digit flexion/extension task used by Schieber and Rivlis (2007), the fact that their correlations included 12 separate movement conditions potentially added a much greater opportunity for disparities to occur between cell and muscle activity and this may have contributed to the differences in the strength of correlations between our two studies.

Our results also suggest that cortical input to the motoneuron pool dominates the activity of the motoneurons during the reach-to-grasp

movement. If not, other excitatory inputs to the motoneuron pool must show temporal modulation closely matching that of the CM cell input. A significant contributor to the strength of correlations observed in our data is the broader periods of coactivation. We agree with the interpretation of Townsend et al., (2006) that this broad coactivation “accounts for the general correlation between the envelopes of cell and muscle activity”. Superimposed on this broad coactivation are peaks and valleys of activity. Our analysis of these peaks in activity showed a relatively poor correlation between the existence of CM cell primary activity peaks and primary peaks or lesser peaks in the target muscle EMG activity. However, it was true that for 73% of the CM cells, at least one peak in each of the cell’s target muscles had a matching peak of some size in CM cell activity. Moreover, the timing of the peaks was relatively tight (25 ms mean with EMG peak lagging, Table 2).

CM cell effects on motor unit firing: timing issues

What timing should be expected between peaks in CM cell activity and the effect of that activity on motor unit firing rate? Many studies going back to the original work of Evarts (1968) have demonstrated that cells in motor cortex show a wide range of timing relationships relative to movement onset with some neurons beginning to fire before the onset of movement and others following the onset of movement. However, nearly all these studies have shown that the mean onset time of the cortical cell population ranges from 60-

150 ms before the onset of movement (Porter and Lemon 1993). Extending this analysis to CM cells, Fetz and Cheney (1980) showed that the mean onset of activity relative to the onset of target muscle EMG activity for a simple alternating wrist flexion-extension task was 71 ms (phasic-tonic CM cells). Despite these findings, we agree with Schieber and Rivlis (2007) that logical analysis would suggest that the timing should equal the conduction time through the pathway from cortical cell discharge to motor unit discharge (Morrow and Miller 2003; Townsend et al., 2006). This time can be estimated from the onset latency of PSpF. However, the cell's peak effect on motor unit firing would more likely correspond to the peak latency of PSpF. It is reasonable to conclude that the timing difference between a CM cell's firing rate peak and its maximum effect on motor units should also be the peak latency of PSpF. Peak PSpF latencies range from 9-13 ms depending on the muscle (McKiernan et al., 1998). Our sampling rate for response averages was 100 Hz or 10 ms for both unit activity and EMG channels. This means that the time shift expected between a CM cell's firing rate and its affect on motoneurons is about equal to one sample point, in other words, negligible for our purposes. Accordingly, in plotting CM cell firing rate against EMG activity and performing the Pearson correlation analysis, we did not time shift the records in an effort to achieve stronger correlations. Time shifting records might have provided stronger correlations in some cases, but we believe that such time shifting does not match the reality of timing that should exist

between peaks in CM cell activity and when that activity should exert its maximum excitatory influence over motoneurons (Morrow and Miller 2003; Schieber and Rivlis 2007, Townsend et al., 2006).

Our data provide some support for this view of the timing between CM cell activity and target muscle EMG. Of the 190 cell-target muscle activity peaks occurring during the same segment of the reach-to-grasp task, the peak of CM cell activity led the peak in target muscle EMG by an average of $25 \text{ ms} \pm 150$ (Table 2). This number is very close to the estimated time of 9-13 ms based on the peak latency of PSpF. Restricting this analysis to peaks occurring during the same segment of the task is justified because other peaks would be unlikely to be causally related. It is also noteworthy that the tightest coupling (smallest range) between peak time in CM cell activity and target muscle EMG activity occurred for cell-muscle pairs exhibiting strong PSpF effects.

The mean EMG peak time lag is notably shorter than the 71 ms reported in a previous study of the timing between CM cell (phasic-tonic cells) and muscle activity (Cheney and Fetz 1980). This difference may be due to differences in the behavioral tasks. The step-tracking task used by Cheney and Fetz (1980) in which wrist movement alternated between flexion and extension position zones engaged the activity of wrist and digit muscles in a heavily reciprocal pattern. While in one zone, the antagonist muscles were generally inactive and their motoneurons were hyperpolarized. Movement

toward the opposite target zone then involved activation of the CM cells for that direction. However, before the appearance of agonist muscle EMG for that direction, the CM cells need to depolarize motoneurons from their hyperpolarized level to firing threshold. The amount of time needed for motoneurons to reach threshold and start firing would contribute to the time delay between the onset of CM cell firing and the onset of target muscle EMG activity. The reach-to-grasp task we have used in the present study differs fundamentally from the reciprocal wrist movement task in that it requires a “free-form”, coordinated, multi-joint reaching movement to a visual target where a food morsel is grasped and carried to the mouth and then the hand is returned to the starting point. EMG activity during this task shows broad coactivation throughout most of the task with specific sculpting of EMG peaks and valleys evident for individual muscles. What is significant about this task is that EMG activity is always present (except on home plate) so peaks in CM cell firing rate should be translated immediately into firing rate changes of the motoneuron without the need to first depolarize the motoneuron to threshold. This fact could have significantly reduced the time difference observed in this study between CM cell firing rate peaks and corresponding target muscle EMG peaks.

Schieber and Rivlis (2007) tested the effect of time shifting the population activity of cortical cells with respect to the cell’s target muscle and found that, in one monkey, the maximum correlation was obtained with the

EMG delayed 40-60 ms from the cell activity. The effect of time shifting was not near as dramatic in another monkey. How might this time shift be reconciled with expectations based on conduction time in the corticospinal pathway? It is tempting to suggest that in the finger flexion/extension task of Schieber and Rivlis (2007), the possible lack of background EMG and need to raise motoneurons to firing threshold might also apply. However, as pointed out by Morrow and Miller (2003), it is difficult to explain the results of correlation studies involving activity over the whole movement cycle, if the delay of 40-60 ms is only present at the onset of movement. They further raise the possibility that persistent inward currents in motoneurons (Lee and Heckman 1998) essentially act as a low-pass filtered amplifier to produce currents that are substantially delayed from and greater than the synaptic currents. While the correct explanation of these timing disparities remains unknown, the findings we have reported in this paper suggest that the disparity may not be as large as previously thought.

Overall summary and conclusions

In this paper we report the results of a study of the functional activity patterns of 44 identified CM cells and their target muscles in relation to a free-form reach-to-grasp task. The peaks in activity of individual CM cells were about evenly distributed throughout the movement task, except for the starting position where EMG activity was minimal or absent. CM cell peaks

occurred during segments of the task that in general correlated with the occurrence of peaks in target muscle EMG activity. Although many examples of strong correlations between the activity of individual CM cells and their facilitated target muscles were found, overall, the correlations were relatively weak. However, this should not be surprising given the large number of synaptic inputs driving motoneurons and the relatively small contribution made by any single input neuron. While individual cell-target muscle correlations were relatively weak, the ensemble firing rate records of populations of CM cells sharing a common target muscle produced significantly stronger correlations than the mean of the individual cell-target muscle correlations. The results provide further evidence in support of the notion that cortical output encodes muscle based parameters, specifically, muscle activation as reflected in EMG activity. Morrow and Miller (2003) demonstrated that the ensemble activity of a relatively small number of unidentified cortical cells, time shifted according to the phase differences observed in analog cross-correlations, very closely matched the EMG activity of agonist muscles. Our data extends this to identified CM cells and shows that without any time shifting, the ensemble activity of small populations of CM cells produces a relatively good match ($r \geq 0.8$) to target muscle EMG activity.

Table 2.1. Muscles Recorded

<u>Abbreviation</u>	<u>Muscle</u>
<u>Proximal muscles</u>	
Shoulder	
Pectoralis Major	SHL
Anterior Deltoid	PEC
Posterior Deltoid	ADE
Teres Major	PDE
Latissimus Dorsi	TMAJ
	LAT
Elbow	
Short Head of the Biceps	ELB
Long Head of the Biceps	BIS
Brachialis	BIL
Brachioradialis	BRA
Lateral Head of the Triceps	BR
Long Head of the Triceps	TLAT
Dorsal Epitrochlearis	TLON
	DE*
<u>Distal muscles</u>	
Wrist	
Flexor Carpi Radialis	WRS
Palmaris Longus	FCR
Flexor Carpi Ulnaris	PL*
Extensor Carpi Radialis	FCU
Extensor Carpi Ulnaris	ECR
	ECU
Intrinsic	
Abductor Pollicis Brevis	INT
First Dorsal Interosseus	APB
	FDI
Digit	
Flexor Digitorum Suprficialis	DIG
Flexor Digitorum Profundus	FDS
Extensor Digitorum Communis	FDP
Extensor Digitorum 2, 3	FDC
Extensor Digitorum 4, 5	ED23
	ED45

*These muscles were recorded in monkey K but not monkey N.

Table 2.2. Timing and percentage overlap of peaks in CM cell activity relative to matching peaks in facilitated target muscle EMGs. In all cases, the mean EMG peak lagged the CM cell peak.

	Mean	Median
<u>Peak Time Difference (ms)</u>		
All Effects	25 ± 156	30
Strong Effects	40 ± 127	70
Moderate Effects	25 ± 111	30
Weak Effects	22 ± 183	30
DOM ≥ 75	43 ± 113	30
DOM < 75	19 ± 167	30
DOM ≥ 50	37 ± 145	30
DOM < 50	13 ± 166	30
<u>% of CM cell peak overlapped by muscle peak</u>		
All Effects	75 ± 28	85
Strong Effects	89 ± 15	*98
Moderate Effects	74 ± 28	83
Weak Effects	73 ± 29	81
<u>% of target muscle peak overlapped by CM cell peak</u>		
All Effects	58 ± 31	56
Strong Effects	64 ± 27	68
Moderate Effects	59 ± 29	57
Weak Effects	55 ± 32	53

* There is a statistically significant difference in the median values between strong PSpF and both moderate and weak PSpF (Mann-Whitney, P < 0.05).

Table 2.3. Analysis of CM cell populations for individual muscles.

A CM Cell Population	B # CM Cells	C Range of individual muscle to individual CM cell r values	D Mean of individual muscle to individual CM cell r values	E Population CM cell to summed muscle r value	F Lowest individual muscle to summed muscle r value	G Mean of individual muscle to population CM cell r values
ED2,3-1	3	0.342 - 0.912	0.604	0.900	0.891	0.884
ED2,3-2	4	0.069 - 0.813	0.552	0.608	0.918	0.583
APB-1	4	0.288 - 0.627	0.457	0.590	0.904	0.567
APB-3	4	0.473 - 0.753	0.574	0.847	0.787	0.725
ECU	3	0.675 - 0.870	0.742	0.867	0.903	0.828
FDP	4	0.395 - 0.778	0.653	0.876	0.959	0.852
ECR	4	0.159 - 0.900	0.482	0.471	0.810	0.411
FDI	5	-0.233 - 0.617	0.299	0.574	0.840	0.516
ED4,5-1	4	0.604 - 0.909	0.786	0.917	0.944	0.911
ED4,5-2	3	0.367 - 0.910	0.620	0.838	0.922	0.797

Figure 2.1. Examples of Spike-triggered averages of EMG activity illustrating the criteria used for categorizing the strength of PSpF effects. The zero line corresponds to the action potential of the CM cell used as a trigger for averaging. For this figure and throughout the paper the colors used for each average represent the magnitude of effects as follows: red = strong PSpF, green = moderate PSpF, blue = weak PSpF, black = no effect, yellow = weak PSpS and purple = moderate PSpS. The number of trigger events is given in parentheses.

Standard Deviations
From Baseline

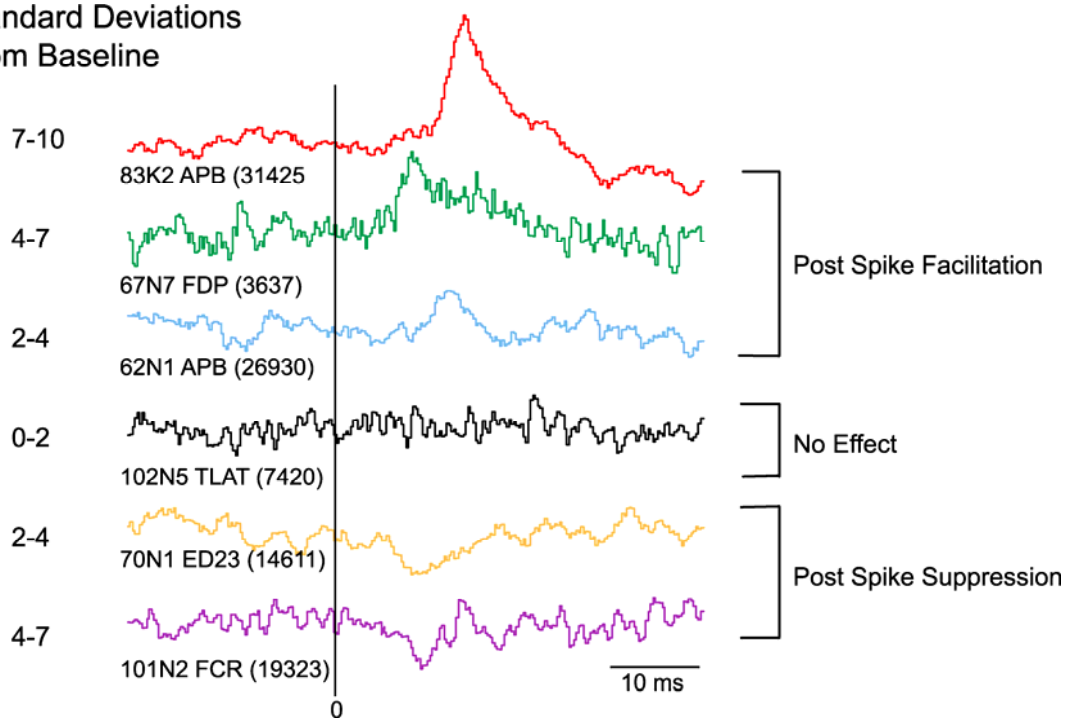


Figure 2.2. Segmentation of the reach-to-grasp task and approximate timing of the individual segments: (1) on home plate; ~250 ms duration, (2) leaving home plate; 100 ms flanking the release of home plate, (3) hand in transit to the food well; beginning 100 ms after release of home plate and extending to 50 ms before digit entry into the target food well, (4) entering food well; beginning 50 ms before and extending to 150 ms after digit entry into the food well, (5) in food well; beginning 150 ms after digit entry into the food well and extending up to 100 ms before digit exit from the food well, (6) exiting food well; beginning 100 ms before and extending to 100 ms after digit exit from the food well, (7) hand in transit to the mouth; 100-300 ms after digit exit from the food well, (8) hand at the mouth; beginning 300 ms after digit exit from the food well and extending to 450 ms before depression of home plate, (9) hand in transit back to home plate; beginning 450 ms before and extending to 50 ms before depression of home plate, (10) contact with home plate; 50 ms before to 150 ms after depression of home plate. The length of the movement cycle and durations of individual components given above represent a typical response. Although total movement durations varied somewhat, the two monkeys used in this study were highly over trained and the responses tended to be consistent and stereotyped. The goal was to assign peaks to the movement segment they were most closely related to functionally. It was not uncommon for the shoulder of a peak to be broad enough to exist in multiple movement segments but assignment was based on the location of the highest point in the peak.

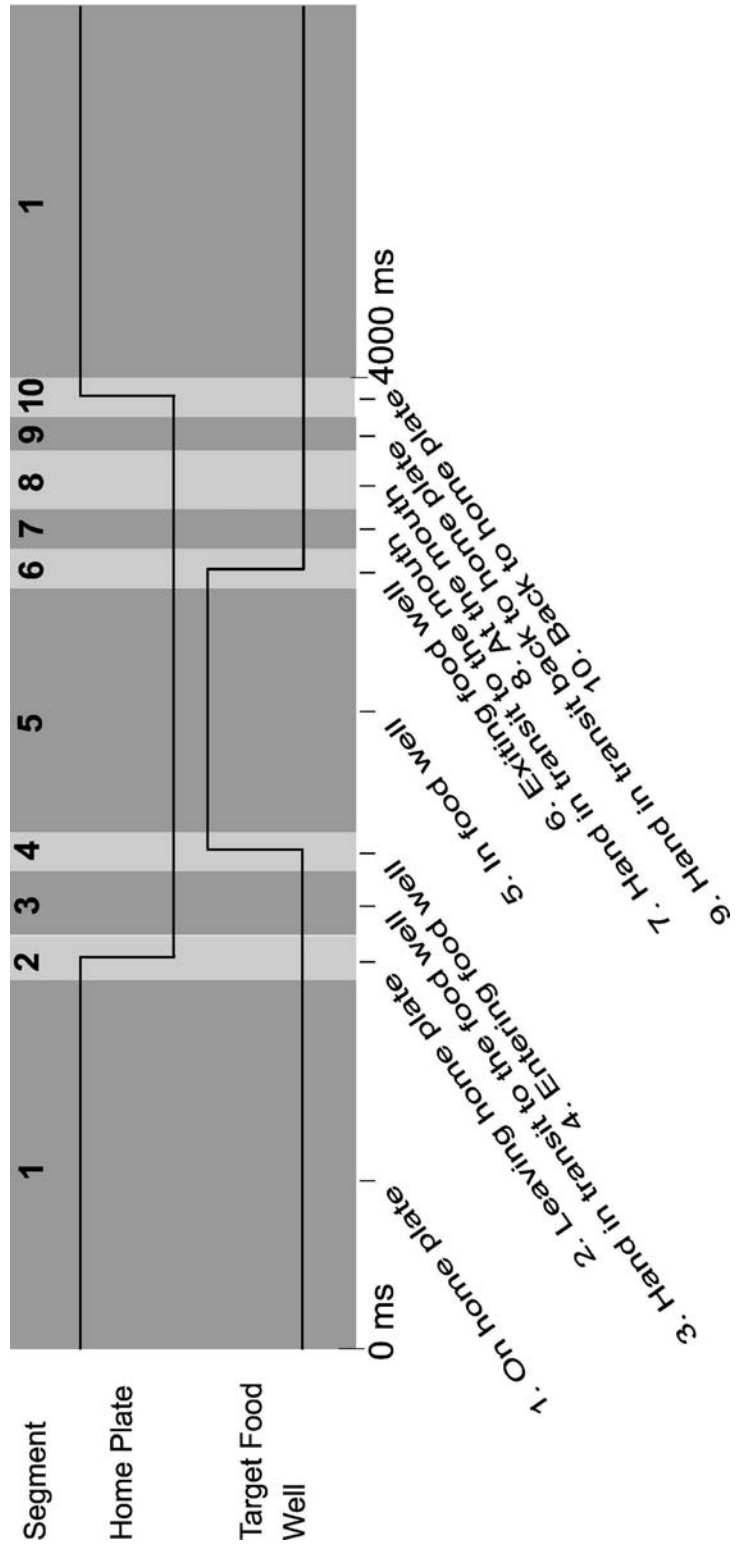
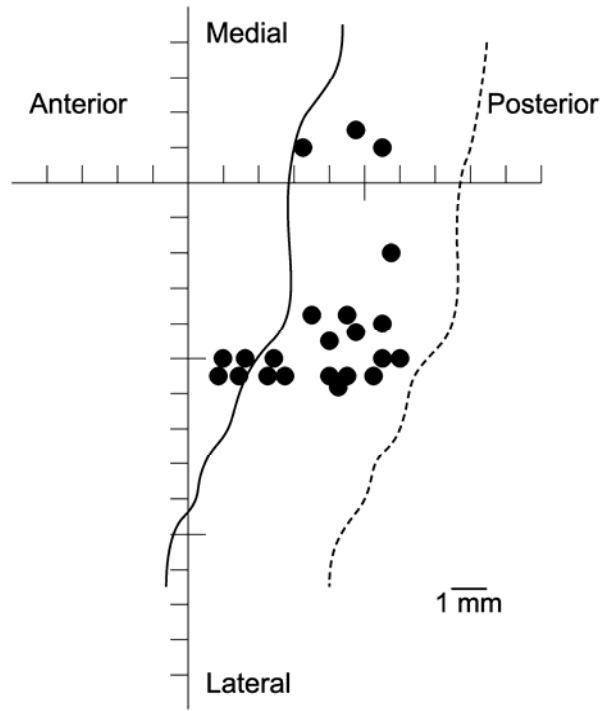


Figure 2.3. Cortical locations of the 44 CM cells investigated in this study plotted on an unfolded map of the cortex. The solid line is the convexity of the central sulcus and the dotted line is the fundus. Intersection of axes represents the center of the recording chamber.

A. Monkey K



B. Monkey N

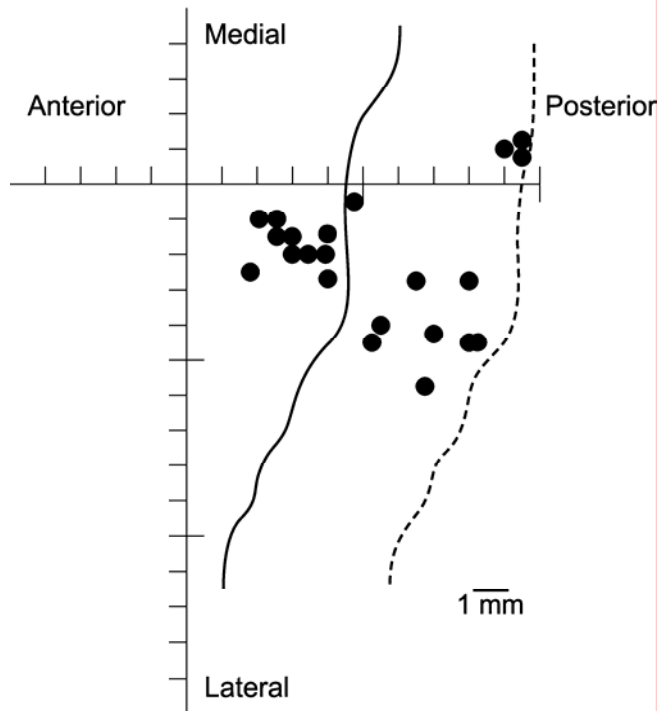


Figure 2.4. Example of response averages for cell 110N3 and 22 simultaneously recorded muscles. Four response averages are shown referenced to: A) leaving home plate, B) entering the food well, C) exiting the food well, and D) returning to home plate. Note a single peak in CM cell activity occurs in segment 5 (in the food well) of the reach-to-grasp task. Color coding of EMG records reflects the magnitude of post-spike effects (Figure 2.1).

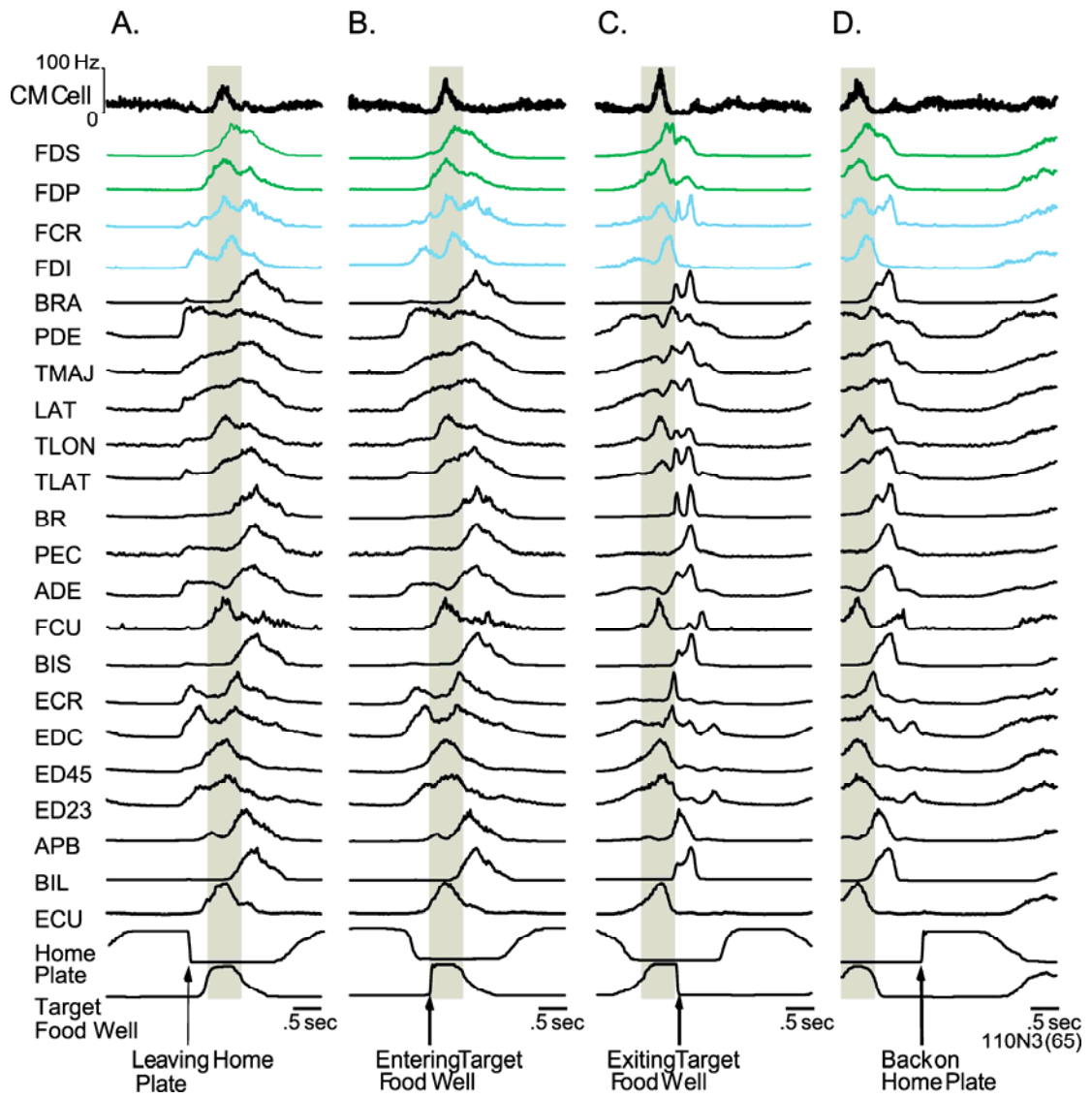


Figure 2.5. Histogram showing the segment location in the reach-to-grasp task of the firing rate peaks for the 44 CM cells analyzed in this study.

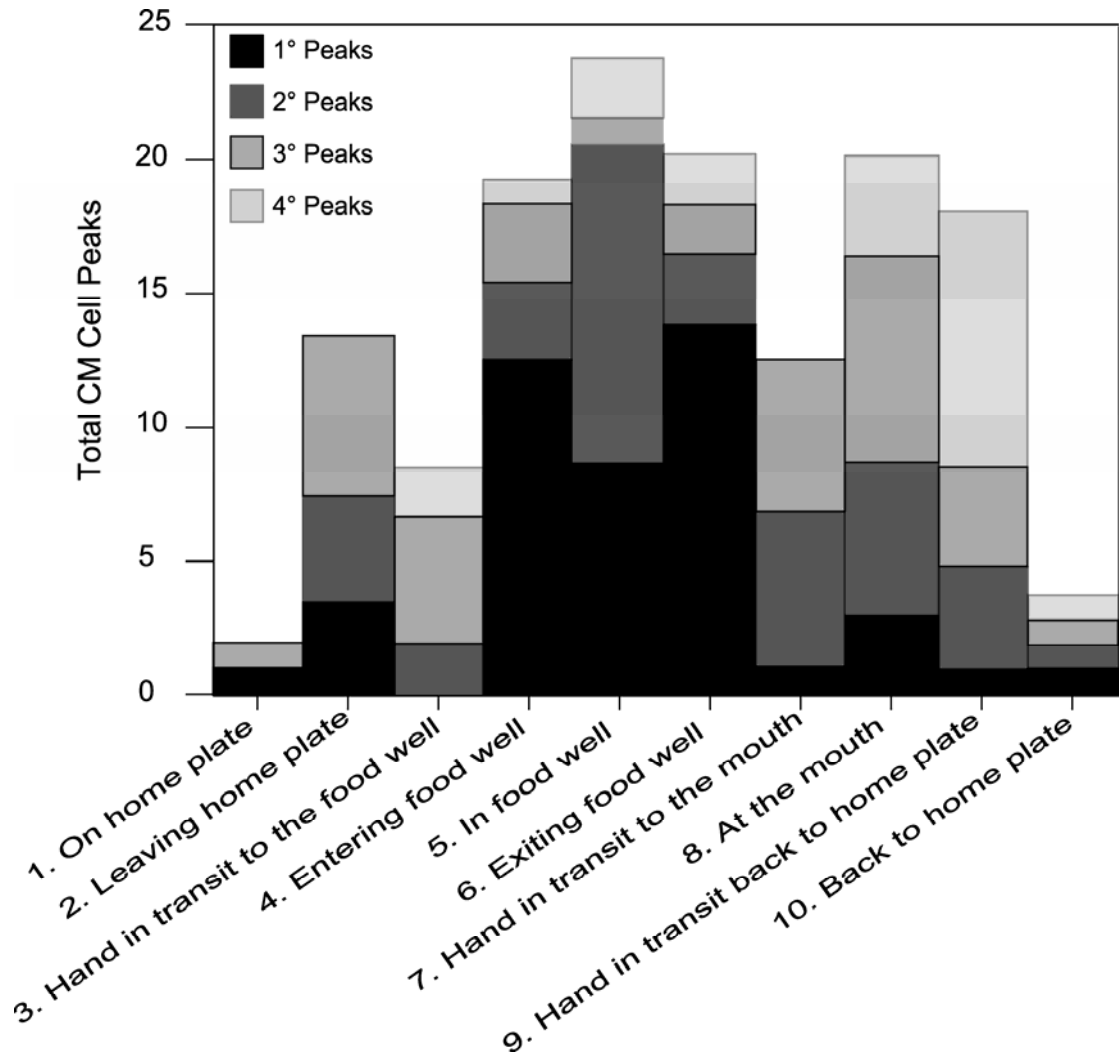
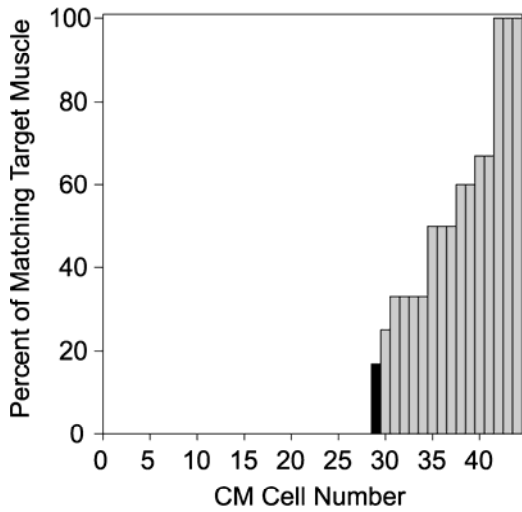
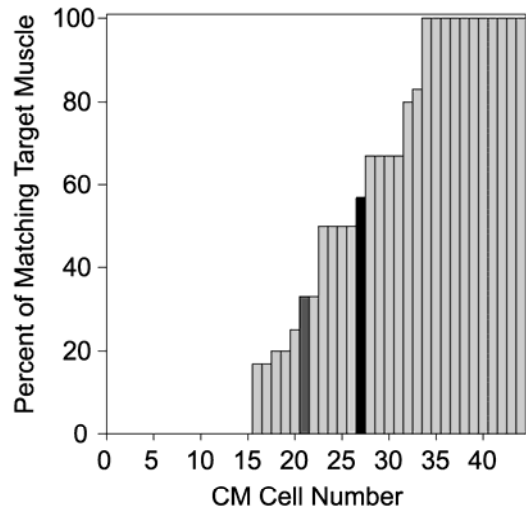


Figure 2.6. Analysis of the extent to which peaks in CM cell activity have matching peaks of EMG activity in the cell's facilitated target muscles. Matching peaks were ones that occurred in the same segment of the task. Each bar represents one of the 44 CM cells studied. A. Most rigorous criterion: the 1° peaks of both the CM cell and facilitated target muscle were in the same segment of the reach-to-grasp task. B. Less rigorous: the 1° peak of the CM cell was in the same segment as any peak of the facilitated target muscle. C. Least rigorous: any CM cell peak matched any EMG peak in a facilitated target muscle. D. Percent of all possible CM cell peaks that matched facilitated target muscle EMG peaks (see text). Black bars represent data from CM cell 105N6 and grey bars represent data from 65N6 (illustrated in Figure 2.7).

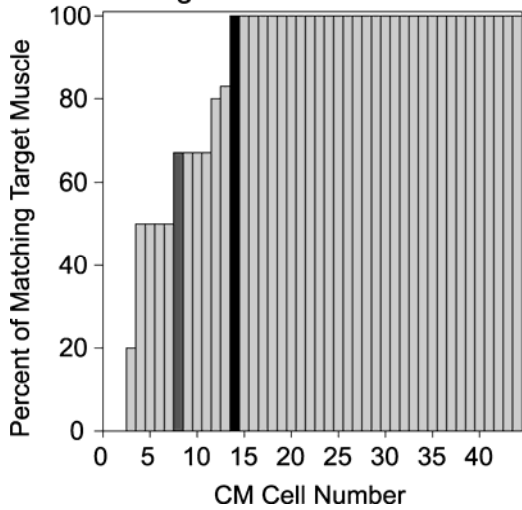
A. CM Cell Primary Peak Matches Target Muscle Primary Peak



B. CM Cell Primary Peak Matches any Target Muscle Peak



C. Any CM Cell Peak Matches Any Target Muscle Peak



D.

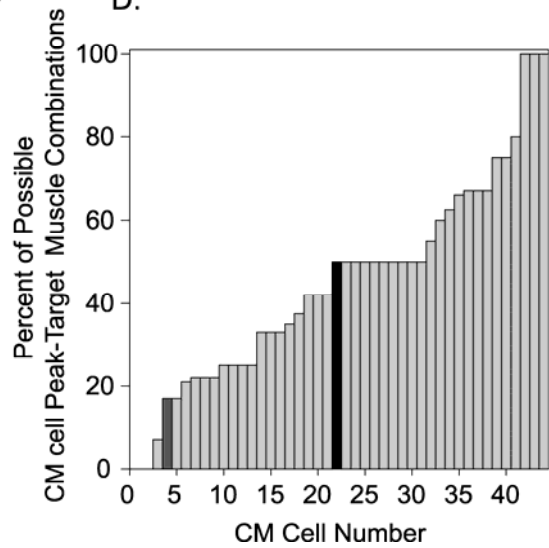


Figure 2.7. Identification of matching peaks in CM cell and target muscle activity. An example of two CM cells with multiple peaks of activity during the reach-to-grasp task and associated peaks of activity in the cell's facilitated target muscles. Task segments 4-9 are color coded. CM cell and muscle peaks were defined as matching if they occurred in the same task segment. In Figure 6, CM cell 105N6 is represented as a black bar and 65N6 as a grey bar.

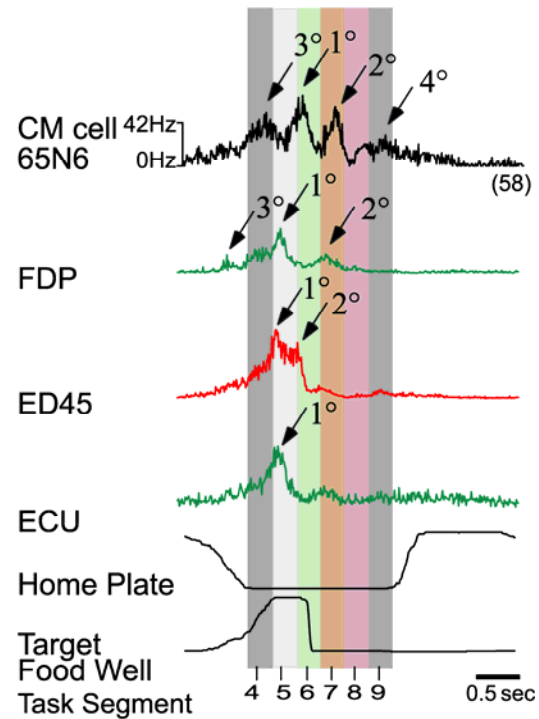
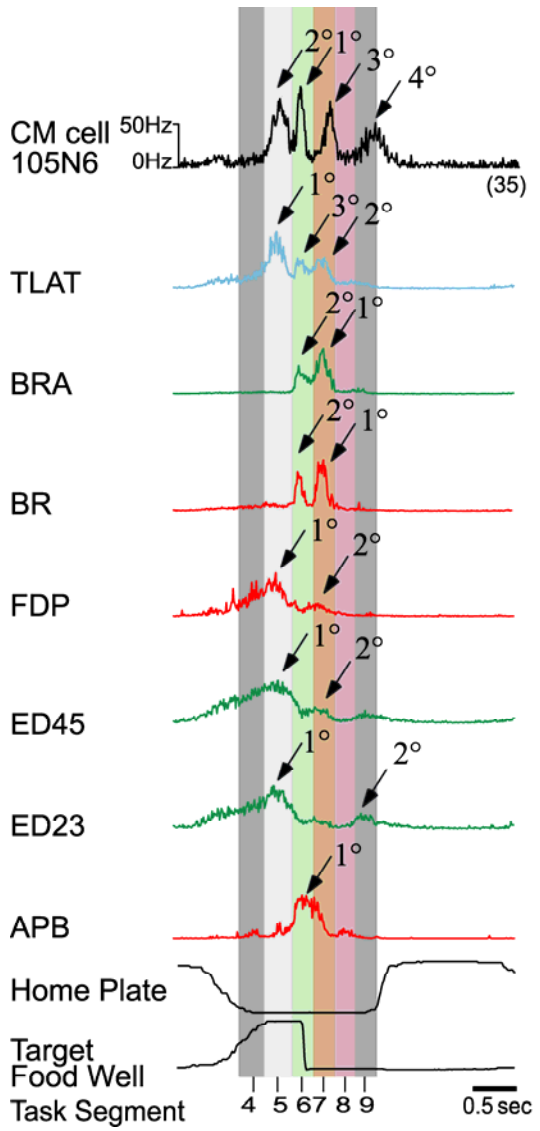


Figure 2.8. Timing between all matching CM cell peaks and facilitated target muscle EMG peaks. A: Distribution of peak time differences shaded according to magnitude of effects. B: Distribution of peak time differences shaded according to DOM. C: Percent of CM cell peaks overlapped by matching muscle peaks. D: Percent of muscle peaks overlapped by matching CM cell peaks.

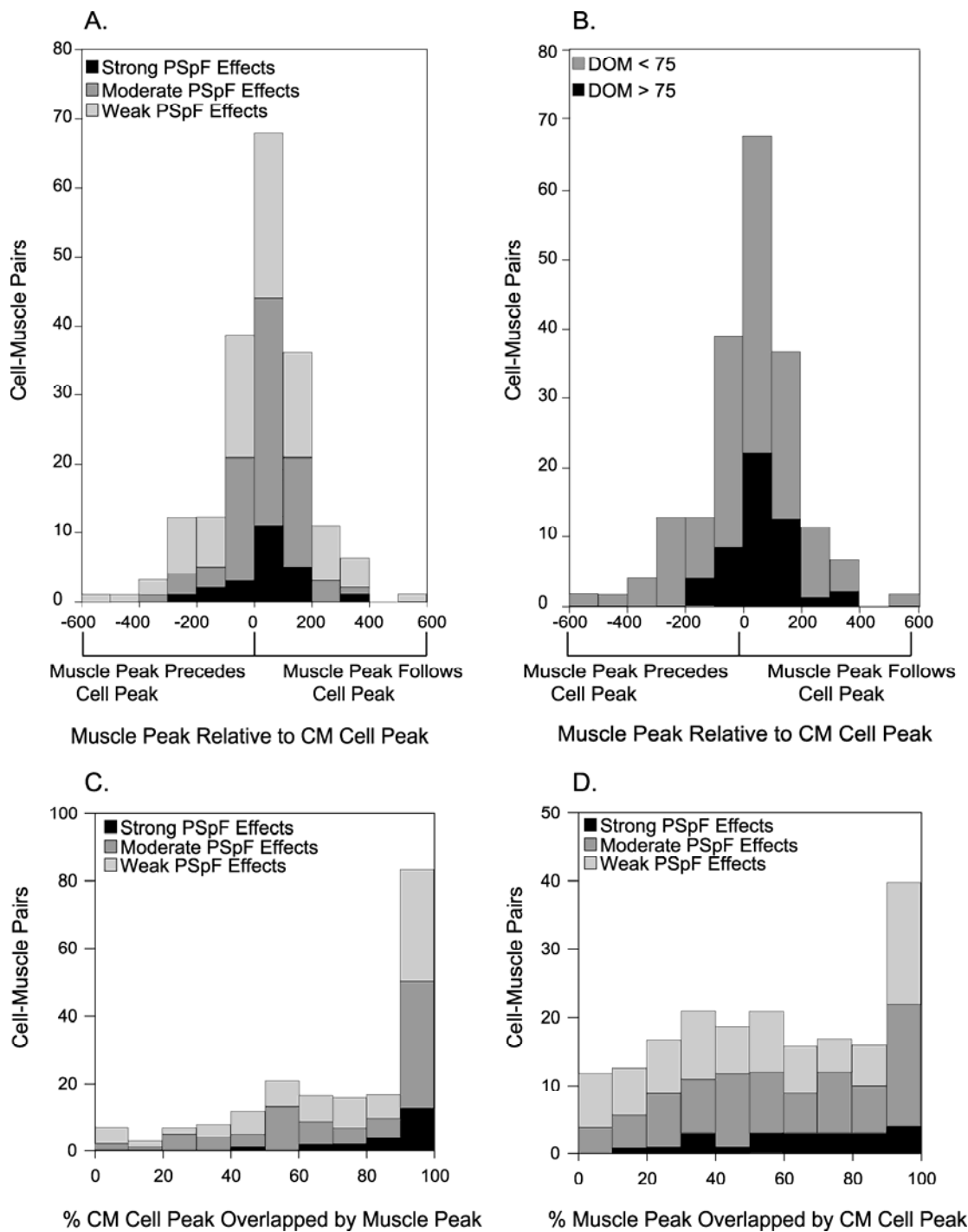
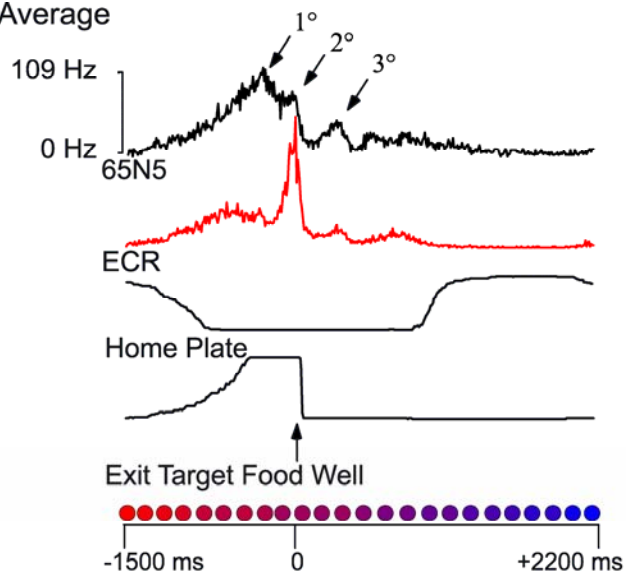
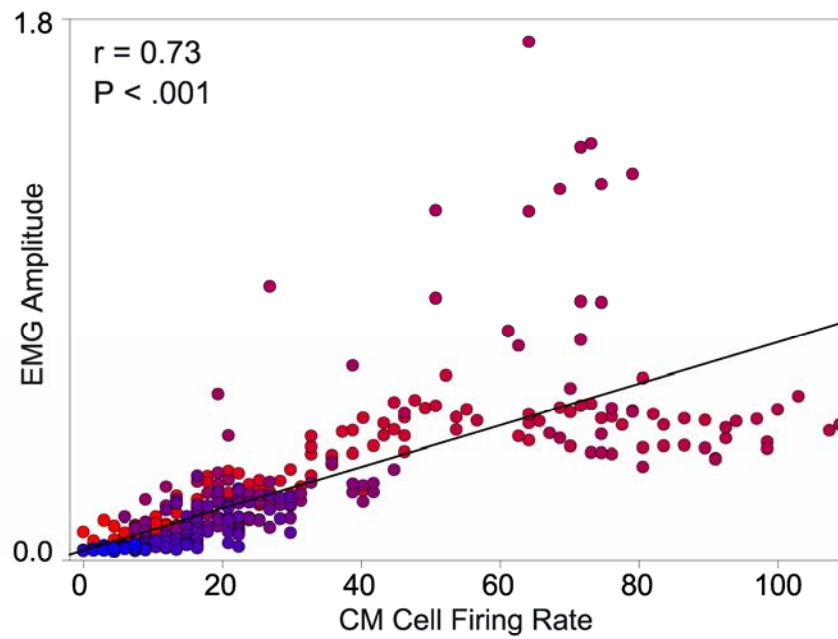


Figure 2.9. Response average and scatter plot for a cell-target muscle pair with strong PSpF. In the scatter plot, points are color coded according to time. Points at the beginning of the record are red. See color code at the bottom of the response average. Red transitions to purple and then blue represents points at the end of the record.

A. Response Average



B. Scatter Plot



C. Spike Triggered Average

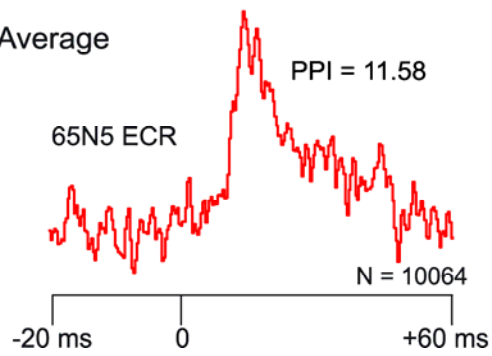


Figure 2.10. Distribution of Pearson correlation coefficients (r) for CM cell-target muscle pairs. Correlation coefficients were derived from plotting CM cell firing rate against target muscle EMG activity. Only pairs exhibiting PSpF were included.

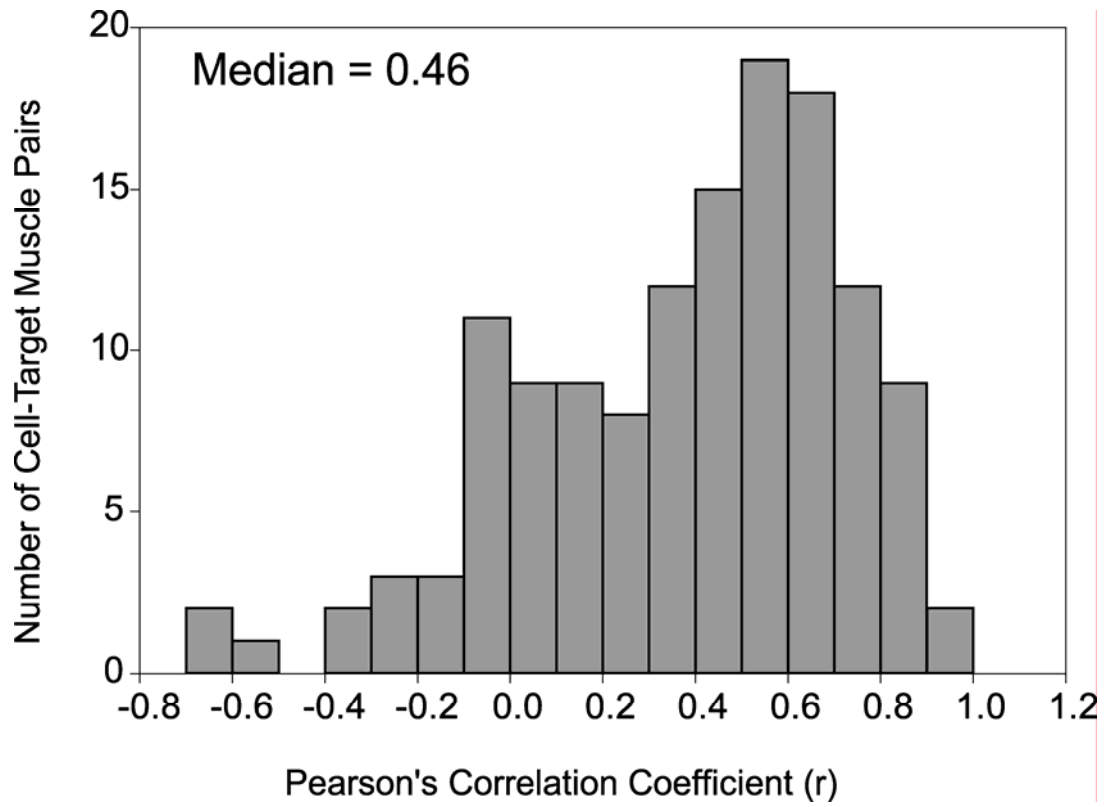
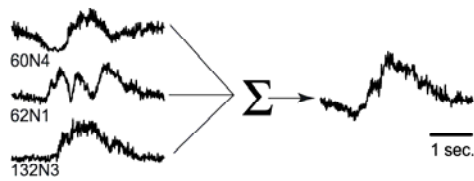
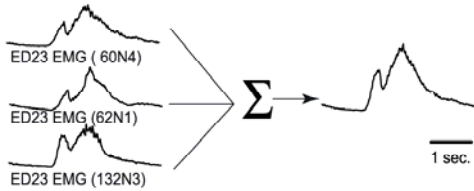


Figure 2.11. Analysis of CM cell populations sharing a common target muscle. A. Individual CM cell firing rate histograms for three CM cells that all facilitated ED2,3. On the right is the population CM cell record obtained by summing the individual records. B. Individual EMG records of ED2,3 recorded with the individual CM cells in A. Note the similarity in the temporal pattern of activity. On the right is the ensemble EMG record obtained by summing the individual records. C. PSpF for each of the CM cell – target muscle pairs in panels A and B. D. Scatter plot obtained by plotting the population CM cell firing rate record against the summed EMG record of ED2,3. E. Population CM cell activity (sum of all three CM cells) and summed EMG activity in relation to task performance.

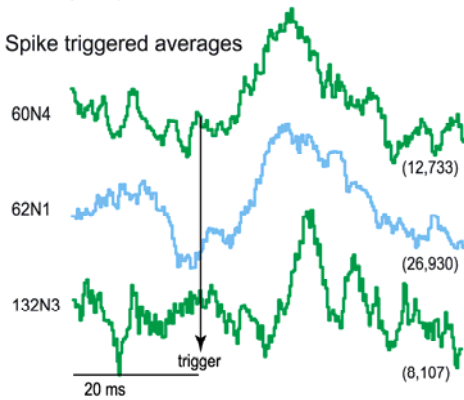
A. Individual CM cell firing rate



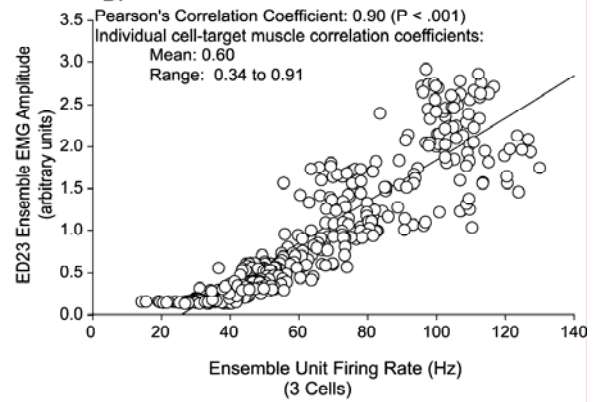
B. Corresponding EMG records



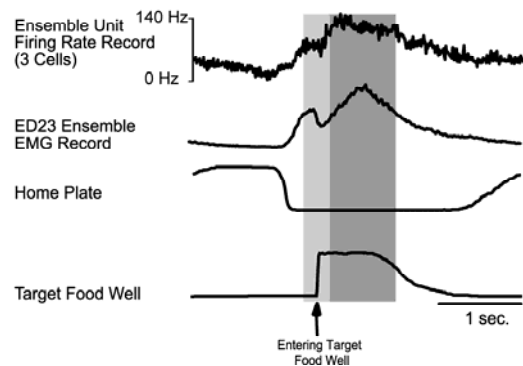
C. Spike triggered averages



D.



E. Ensemble firing rate and EMG records



REFERENCES

- Baker SN and Lemon RN (1998) Computer simulation of post-spike facilitation in spike-triggered averages of rectified EMG. *J Neurophysiol* 80(3): 1391-406.
- Belhaj-Saïf A, Hill Karrer J, and Cheney PD (1980) Distribution and characteristics of poststimulus effects in proximal and distal forelimb muscles from red nucleus in the monkey. *J Neurophysiol* 79: 1777-1789.
- Buys EJ, Lemon RN, Mantel GW, and Muir RB (1986) Selective facilitation of different hand muscles by single corticospinal neurones in the conscious monkey. *J Physiol* 381: 529-549.
- Evarts EV (1968) Relation of pyramidal tract activity to force exerted during voluntary movement. *J Neurophysiol* 31(1): 14-27.
- Fetz EE and Cheney PD (1980) Postspike facilitation of forelimb muscle activity by primate corticomotoneuronal cells. *J Neurophysiol* 44(4): 751-72.
- Fetz EE, Cheney PD, Mewes K, and Palmer S (1989) Control of forelimb muscle activity by populations of corticomotoneuronal and rubromotoneuronal cells. *Prog Brain Res* 80: 437-449.
- Flament D, Fortier PA, and Fetz EE (1992) Response patterns and postspike effects of peripheral afferents in dorsal root ganglia of behaving monkeys. *J Neurophysiol* 67: 875-888.
- Griffin DM, Hudson HM, Boudrias MH, Belhaj-Saïf A, McKiernan BJ and Cheney PD (2004) Patterns of activation of primary motor cortex neurons (M1) and their target muscles during a reach-to-grasp task. Program No. 655.9. *Abstract Viewer/Itinerary Planner*. Washington, DC: Society for Neuroscience, Online.
- Hamed SB, Schieber MH, and Pouget A (2007) Decoding M1 neurons during multiple finger movements. *J Neurophysiol* 98:327-333.

- Holdefer RN and Miller LE (2002) Primary motor cortical neurons encode functional muscle synergies. *Exp. Brain Res* 146: 233-243.
- Houk JC, Dessem DA, Miller LE, and Sybirska FH (1987) Correlation and spectral analysis of relations between single unit discharge and muscle activities. *J Neurosci Methods* 21(2-4): 201-24.
- Kasser RJ and Cheney PD (1985) Characteristics of corticomotoneuronal postspike facilitation and reciprocal suppression of EMG activity in the monkey. *J Neurophysiol* 53(4): 959-78.
- Lee RH and Heckman CJ (1998) Bistability in spinal motoneurons in vivo: systematic variation in persistent inward currents. *J Neurophysiol* 80: 583-593.
- McKiernan BJ, Marcario JK, Hill Karrer J, and Cheney PD (2000) Correlations between corticomotoneuronal (CM) cell postspike effects and cell-target muscle covariation. *J Neurophysiol* 83: 99-115.
- McKiernan BJ, Marcario JK, Hill Karrer J, and Cheney PD (1998) Corticomotoneuronal postspike effects in shoulder, elbow, wrist, digit, and intrinsic hand muscles during a reach and prehension task. *J Neurophysiol* 80(4): 1961-1980.
- Morrow MM Jordan LR and Miller LE (2007) Direct comparison of the task-dependent discharge of M1 in hand space and muscle space. *J Neurophysiol* 97: 1786-1798.
- Morrow MM and Miller LE (2003) Prediction of muscle activity by populations of sequentially recorded primary motor cortex neurons. *J Neurophysiol* 89: 2279-2288.
- Mussa-Ivaldi FA. (1988) Do neurons in motor cortex encode movement direction? An alternative hypothesis. *Neurosci Lett* 91: 106-111.

- Park MC, Belhaj-Saïf A, and Cheney PD (2004) Properties of primary motor cortex output to forelimb muscles in rhesus macaques. *J Neurophysiol* 92(5): 2968-2984.
- Park MC, Belhaj-Saïf A, Gordon M, and Cheney PD (2001) Consistent features in the forelimb representation of primary motor cortex in rhesus macaques. *The J Neurosci* 21: 2784-2792.
- Porter R and Lemon RN (1993) Corticospinal Function and Voluntary Movement. Clarendon Press, Oxford.
- Schieber MH and Rivlis G (2005) A spectrum from pure post-spike effects to synchrony effects in spike-triggered averages of electromyographic activity during skilled finger movements. *J Neurophysiol* 94(5): 3325-41.
- Schieber MH and Rivlis G (2007) Partial reconstruction of muscle activity from a pruned network of diverse motor cortex cells. *J. Neurophysiol* 97: 70-82.
- Todorov E. Direct cortical control of muscle activation in voluntary arm movements: a model. *Nat Neurosci* 3: 391-398, 2000.
- Townsend BR, Paninski, L and Lemon RN (2006) Linear encoding of muscle activity in primate motor cortex and cerebellum. *J Neurophysiol* 96: 2578-2592.

CHAPTER THREE

STABILITY OF OUTPUT EFFECTS FROM MOTOR CORTEX TO FORELIMB MUSCLES IN PRIMATES

ABSTRACT

Stimulus-triggered averaging (StTA) of electromyographic (EMG) activity is a form of intracortical microstimulation that enables documentation in awake animals of the sign, magnitude, latency and distribution of output effects from cortical and brainstem areas to motoneurons of different muscles. In this study, we show that the properties of effects in StTAs are stable and largely independent of task conditions. StTAs of EMG activity from 24 forelimb muscles were collected from two male rhesus monkeys while they performed three tasks: 1) an isometric step tracking wrist task, 2) an isometric whole arm push-pull task, and 3) a reach-to-grasp task. Layer V sites in primary motor cortex were identified and microstimuli were applied at intensities ranging from 15 μ A to 120 μ A at a low rate (15 Hz). In 98% (1471/1498) of StTAs, the same effect (facilitation, suppression, or no effect) was present independent of joint angle changes within a task. The magnitude of effects in both proximal and distal forelimb muscles were highly correlated at the most extreme shoulder, elbow and wrist angles. Our results demonstrate that M1 output effects obtained with StTA of EMG activity are highly stable across widely varying joints angles and motor tasks. This study further validates the use of StTA for mapping and other studies of cortical motor output.

INTRODUCTION

Stimulus-triggered averaging (StTA) of electromyographic (EMG) activity involves applying microstimuli at a low rate while an animal actively performs a movement task (Cheney and Fetz, 1985; Kasser and Cheney, 1985; Cheney, 2002; Park et al., 2004). This method provides relatively high spatial resolution (depending on stimulus strength), which is enhanced by the use of stimulus rates (15 Hz) that avoid spread of activation by temporal summation. This method yields effects that can be rigorously quantified and is also capable of detecting both excitatory and inhibitory events (Kasser and Cheney, 1985). The fact that the rank order of output effects across muscles obtained with StTA consistently matches the output effects obtained with spike triggered averaging from single cells at the same site reinforces the potential power and resolution provided by this approach (Cheney and Fetz, 1985).

StTA has been widely used to characterize output from primary motor cortex (M1), pre-motor areas, somatosensory cortex and various brainstem descending nuclei to muscles of the limbs (Cheney and Fetz, 1985; Cheney et al., 1985; Palmer and Fetz, 1985; Hummelsheim et al., 1986; Cheney et al., 1991; Widener and Cheney, 1997; Baker et al., 1998; Belhaj-Saïf et al., 1998; Perlmutter et al., 1998; Schieber, 2001; Davidson and Buford, 2004, 2006; Graziano et al., 2004; Park et al., 2004; Bretzner and Drew 2005a, b; Boudrias et al., 2006; Davidson et al., 2007; Moritz et al., 2007) and to map

the distribution of M1 output to forelimb muscles (Park et al., 2001; Boudrias et al., 2007). These studies have revealed important new features of motor cortex functional organization.

Because StTA is being widely applied to characterize the sign, strength, latency and distribution of output from various brain motor areas to motoneurons of different muscles, the question of stability of post-stimulus effects becomes important. Do the measures of motor output obtained from StTA remain constant under varying task conditions? Studies using supra-threshold stimulation methods such as high frequency intracortical microstimulation (ICMS) in animals and transcranial magnetic stimulation (TMS) in monkeys and humans have reported changes in output effects as a function of joint position (Gellhorn and Hyde, 1953; Sanes et al., 1992; Ginannesch et al., 2005, 2006) and phase of a movement (Armstrong and Drew, 1985; Drew, 1991; Baker et al., 1995; Lemon et al., 1995). In ketamine tranquilized monkeys, Graziano et al., (2004) reported that the magnitude of facilitation in StTAs of EMG activity varied as a function of elbow joint angle. Moreover, some effects switched from facilitation to suppression depending on joint angle.

In this study, we tested the stability of motor output effects in StTA of EMG activity in awake monkeys actively performing a variety of movements tasks. We have characterized M1 output effects in terms of the sign (facilitation or suppression), strength and distribution of effects across

muscles in StTAs. Our results show that output effects in StTAs of EMG activity from M1 cortex are remarkably stable under different task conditions and largely independent of changes in joint angle or limb posture.

MATERIALS AND METHODS

Behavioral tasks

Data were collected from two male rhesus monkeys (*Macaca mulatta*; ~10kg, 9 years old) trained to perform three tasks: 1) an isometric step tracking wrist task with up to three different fixed wrist positions (Figure 3.1 A), 2) an isometric whole arm push-pull task with up to nine different shoulder and elbow positions (Figure 3.1 B), and 3) a reach-to-grasp task (Figure 3.1 C). During each data collection session, the monkey was seated in a custom built primate chair inside a sound-attenuating chamber. The left forearm was restrained during task performance. All tasks were performed with the right arm.

For the isometric wrist task (Figure 3.1 A), the monkey's lower and upper arm was restrained. The hand, with digits extended, was placed in a padded manipulandum that rotated about the wrist. The wrist was aligned with the axis of rotation of the torque wheel to which the manipulandum was attached. The manipulandum was locked in place at three different wrist positions including 30 degrees in flexion, 30 degrees in extension and 0 degrees (wrist and digits aligned with the forearm). The monkey was required to generate ramp and hold trajectories of wrist torque alternately between flexion and extension target zones. The inner and outer boundaries of the torque window were 0.025 Nm and 0.05 Nm respectively. Delivery of an

applesauce reward was contingent upon the monkey holding within each zone for one second.

For the isometric whole arm push-pull task (Figure 3.1 B), the monkeys were required to grip a handle fixed to a force transducer (Grass Medical Instruments, West Warwick, RI) on a linear XYZ positioning system. Each axis had a calibrated scale which ensured accurate replication of handle positions between recording sessions. Monkeys were required to generate ramp and hold trajectories of torque alternately between push (arm extension) and pull (arm flexion) target zones. The inner and outer boundaries of the torque window were 1 N and 2 N respectively. Delivery of an applesauce reward was contingent upon the monkey holding within each zone for one second. The handle was locked into place at up to nine different positions within the monkeys work space (Figure 3.1 B a). Shoulder and elbow angles for each handle position are listed in Table 1. Joint angles were measured using photographs of the monkey's arm at each of the handle positions. Digital images were processed in Image J using the shoulder, ribcage, elbow and wrist joints as base points on the body. Final angle measurements are an average from several sessions. Figure 3.1 B illustrates how the shoulder and elbow measurements were made in both the vertical (b) and horizontal (c) plane.

Each monkey was also trained to perform a reach-to-grasp task (Figure 3.1 C) as described previously (Belhaj-Saïf et al., 1998; McKiernan et

al., 1998). The task was initiated when the monkey placed its right hand, palm down, on a pressure detecting plate (home plate). The home plate was located at waist level in front and to the right of the monkey. Holding the plate down for a preprogrammed length of time (2-3 seconds) triggered the release of a food reward into a cylindrical well at arms length from the monkey. The monkey then grasped and brought the food reward to its mouth. The task was completed by returning the hand to the pressure plate.

Surgical procedures

After training, a 30-mm inside diameter titanium chamber was stereotaxically centered over the forelimb area of M1 on the left hemisphere of each monkey and anchored to the skull with 12 titanium screws (Stryker Leibinger, Germany) and dental acrylic (Lux-it Inc., Blue Springs, MO). Threaded titanium nuts (Titanium Unlimited, Houston, TX) were also attached over the occipital aspect of the skull using 12 additional titanium screws and dental acrylic. These nuts provided a point of attachment for a flexible head restraint system during data collection sessions. The chambers were centered at anterior 16 mm, lateral 18 mm (Monkey V), and anterior 16 mm, lateral 22 mm (Monkey A), at a 30° angle to the sagittal plane.

EMG activity was recorded from 24 muscles of the forelimb with pairs of insulated, multi-stranded stainless steel wires (Cooner Wire, Chatsworth, CA) implanted during an aseptic surgical procedure (Park et al., 2000). Pairs

of wires for each muscle were tunneled subcutaneously from an opening above the elbow to their target muscles. The wires of each pair were bared of insulation for ~ 2 - 3 mm at the tip and inserted into the muscle belly with a separation of ~ 5 mm. Implant locations were confirmed by stimulation through the wire pair and observation of appropriate muscle twitches. EMG connector terminals (ITT Cannon, White Plains, NY) were affixed to the upper arm using medical adhesive tape. Following surgery, the monkeys wore a Kevlar jacket (Lomir Biomedical Inc., Malone, NY) reinforced with fine stainless steel mesh (Sperian Protection Americas Inc., Attleboro Falls, MA) to protect the implant. EMG activity was recorded from five shoulder muscles: pectoralis major (PEC), anterior deltoid (ADE), posterior deltoid (PDE), teres major (TMAJ), and latissimus dorsi (LAT); seven elbow muscles: biceps short head (BIS), biceps long head (BIL), brachialis (BRA), brachioradialis (BR), triceps long head (TLON), triceps lateral head (TLAT) and dorso-epitrochlearis (DE); five wrist muscles: extensor carpi radialis (ECR), extensor carpi ulnaris (ECU), flexor carpi radialis (FCR), flexor carpi ulnaris (FCU), and Palmaris longus (PL); five digit muscles: extensor digitorum communis (EDC), extensor digitorum 2 and 3 (ED2,3) extensor digitorum 4 and 5 (ED4,5), flexor digitorum superficialis (FDS), and flexor digitorum profundus (FDP); and two intrinsic hand muscles: abductor pollicis brevis (APB) and first dorsal interosseus (FDI).

All surgeries were performed under deep general anesthesia and aseptic conditions. Postoperatively, monkeys were given an analgesic (Buprenorphine 0.5 mg/kg every 12h for 3-4 days) and antibiotics (Penicillin G, Benzathine / Procaine combination, 40,000 IU/kg every 3 days). All procedures were in accordance with the Association for Assessment and Accreditation of Laboratory Animal Care (AAALAC) and the Guide for the Care and Use of Laboratory Animals, published by the US Department of Health and Human Services and the National Institutes of Health.

Data collection

Sites in M1 were stimulated using glass and mylar insulated platinum-iridium electrodes with impedances ranging from 0.5 to 1.5 M Ω (Frederick Haer & Co., Bowdoinham, ME). The electrode was positioned within the chamber using an X-Y coordinate manipulator and was advanced at approximately a right angle into the cortex with a manual hydraulic microdrive (Frederick Haer & Co., Bowdoinham, ME). Rigid support for the electrode was provided by a 22 gage cannula (Small Parts Inc., Miami Lakes, FL) inside of a 25 mm long, 3 mm diameter stainless steel post which served to guide the electrode to the surface of the dura.

StTA of EMG activity was used to map the cortical representation of 24 simultaneously recorded forelimb muscles. While the monkeys performed the isometric wrist task and the reach-to-grasp task, stimuli (15 μ A at 15 Hz) were

applied through the electrode and served as triggers for computing StTAs (Park et al., 2001). Electrode track penetrations were made systematically in precentral cortex at 1 mm grid intervals. In tracks down the bank of the precentral gyrus, StTAs were collected at 0.5 mm intervals. First cortical unit activity was noted and the electrode was lowered 1.5 mm below this point to layer V. In order to distinguish layer V from more superficial layers, particularly in the bank of the precentral gyrus, neuronal activity was evaluated for the presence of large action potentials that were often modulated with the task and StTAs for clear, robust effects at 15 μ A. Because our MRI data was collected in register with the cortical chamber coordinates, images of sections taken at particular electrode positions were also helpful in localizing electrode tracks relative to cortical anatomy.

If no post-stimulus effects (PStEs) were detected at 15 μ A, averages were computed at 30 μ A. These sites were not included in the unfolded muscle maps because they generally were from electrode positions located outside (dorsal and ventral premotor cortex) the M1 forelimb region. When no PStEs were detected at 30 μ A, repetitive ICMS was applied to determine if a motor output representation could be identified for that site. Repetitive ICMS allowed the identification of M1 regions not implanted with electrodes (face and trunk). Repetitive ICMS consisted of a train of 10 symmetrical biphasic stimulus pulses of 30 μ A at 330 Hz (Asanuma and Rosen, 1972). White matter was identified by a sharp decrease or loss of unit activity and in some

cases by the presence of small, short duration, positive-negative spikes typical of fibers. Sensory cortex was identified by the presence of distinctive spike activity and characteristic receptive fields (Widener and Cheney, 1997).

Since it is known that an electrode penetration through the dura matter will cause dimpling of the cortical surface and potential hysteresis upon reversal of electrode direction, steps were taken to ensure the electrode was not “drifting” from the original site of StTA collection. To ensure that electrode position remained stable in the cortex between changes in task position and for the collection of multiple averages, the first task position was typically repeated at the end of each set of StTAs. If the first and last set of StTAs matched, the series of StTAs was considered valid. When possible, electrode drift was also monitored by tracking a task related neuron near the electrode. If a task related neuron was present at the site of stimulation, it was monitored between task position changes and used to ensure a constant electrode position.

Individual stimuli were symmetrical bi-phasic pulses: a 0.2 ms negative pulse followed by a 0.2 ms positive pulse. EMG activity was generally filtered from 30 Hz to 1 KHz, digitized at a rate of 4 kHz and full-wave rectified. Averages were compiled over a 60 ms epoch, including 20 ms before the trigger to 40 ms after the trigger. Stimuli were applied throughout all phases of the tasks, and the assessment of effects was based on StTAs of at least 500 trigger events. Segments of EMG activity associated with each stimulus

were evaluated and accepted for averaging only when the mean of all EMG data points over the entire 60 msec epoch was $\geq 5\%$ of full-scale input. This prevented averaging segments in which EMG activity was minimal or absent (McKiernan et al., 1998). EMG recordings were tested for cross-talk by computing EMG-triggered averages (Cheney and Fetz, 1980). This procedure involved using the EMG peaks from one muscle as triggers for compiling averages of rectified EMG activity of all other muscles. To be accepted as a valid post-stimulus effect; the ratio of post-stimulus facilitation (PStF) between test and trigger muscle needed to exceed the ratio of their cross-talk peaks by a factor of two or more (Buys et al., 1986). Based on this criterion, none of the effects obtained in this study needed to be eliminated.

Data analysis

At each stimulation site, averages were obtained for all 24 muscles. All StTAs with a minimum of 500 triggers were evaluated for PStEs. Post-stimulus facilitation (PStF) and post-stimulus suppression (PStS) effects were computer-measured as described in detail by Mewes and Cheney (1991, 1994). Nonstationary, ramping baseline activity was subtracted from StTAs using custom analysis software. Mean baseline activity and the standard deviation (SD) of baseline EMG activity was measured from the pre-trigger period typically consisting of the first 12.5 ms of each average. StTAs were considered to have a significant post-stimulus effect (PStF or PStS) if the

points of the record crossed a level equivalent to 2 SD of the mean of the baseline EMG for a period ≥ 0.75 ms or more (Park et al., 2001). The magnitude of PStF and PStS was expressed as the percent increase (+ ppi) or decrease (- ppi) in EMG activity above (PStF) or below (PStS) baseline EMG activity (Cheney and Fetz, 1985; Kasser and Cheney, 1985; Cheney et al., 1991).

Imaging

Structural MRIs were obtained from a 3 Tesla Siemens Allegra system. Images were obtained with the monkey's head mounted in an MRI compatible stereotaxic apparatus so the orientation and location of the cortical recording chamber and electrode track penetrations could be determined. A three-dimensional rendering of each monkey's brain (Figure 3.2 A&B) was obtained using CARET software (Computerized Anatomical Reconstruction and Editing Tool Kit) and surface visualization (Van Essen et al., 2001). A two-dimensional rendering of cortical layer V was constructed for each monkey. The method for flattening and unfolding cortical layer V in the anterior bank of the central sulcus has been previously described in detail (Park et al., 2001). Briefly, the cortex was unfolded and the location of StTAs were mapped onto a two dimensional cortical sheet based on the electrode's depth and X-Y coordinate, known architectural landmarks, MRI images, and observations noted during the cortical implant surgeries.

Statistical data analysis

Effects of joint position changes within tasks and changes between tasks were compared using the Student's *t*-test, the Mann-Whitney Rank Sum Test and linear regression. In all tests, statistical significance was based on a P value ≤ 0.05 .

RESULTS

Data were obtained from the left M1 cortex in two rhesus monkeys. StTAs (15 μ A @ 15 Hz) were collected at a total of 253 M1 layer V sites while the monkeys performed one or more of the three tasks (Figure 3.1). This included 132 sites in monkey V and 121 sites in monkey A. Figure 3.2 illustrates the three dimensional reconstruction of each monkey's left hemisphere with placement of the cortical recording chamber marked as well as an enlarged view of the M1 forelimb region (Figure 3.2 A&B). Figure 3.2 C&D are unfolded maps of the precentral cortex. The grid of black dots indicates cortical stimulation sites in layer V which were collected while the monkeys performed the reach-to-grasp task. These sites were used in combination with effects elicited while the monkeys performed the isometric wrist task to map the intra-areal muscle representation of forelimb M1. Layer V sites showing PStEs in only the distal muscles are color coded in blue (distal only muscle representation), sites showing PStEs in both proximal and distal muscles are color coded in purple (proximal-distal representation) and sites showing PStEs in only the proximal muscles are color coded in red (proximal only muscle representation).

The maps confirm the intra-areal organization of the proximal and distal muscle representation described by Park et al., (2001). These maps also allowed the selection of specific sites for further testing in this study. Sites located in the distal only muscle representation and sites in the

proximal-distal representation that produced clear effects in distal muscles were tested for stability of PStEs using the isometric wrist task (white dots in Figure 3.3 A&B). Sites located in the proximal only representation and sites in the proximal-distal muscle representation that produced clear effects in proximal muscles were used to test the stability of PStEs using the isometric push-pull task (pink dots in Figure 3.3 B) and the reach-to-grasp task (pink dots with black centers in Figure 3.3 B).

Stability of post-stimulus effects across wrist positions

Wrist angle changes are most likely to have an influence on the synaptic efficacy of M1 projections to the motoneuron pools of the distal muscles. We therefore chose to focus on the distal only muscle representation to test the stability of StTAs across wrist angles, although some sites in the proximal-distal representation were also tested using the isometric wrist task. Low intensity StTAs (15 μ A) were collected at 43 sites, in the distal only and proximal-distal representations of M1 and were evaluated for stability at different wrist positions while the monkeys performed the isometric wrist task. StTAs were collected at two different wrist positions (30 degrees in flexion, 30 degrees in extension) for all 43 layer V sites. First we quantified the stability of StTAs by comparing the sign of effect (facilitation, suppression, no effect) across the two wrist positions. If the sign of the effect was the same for both wrist positions, it was considered a stable effect.

Table 2 (row 2) summarizes these results. The number of muscles evaluated at each site was not always the same due to the inactivity of some muscles during performance of this task (intrinsic hand and proximal muscles) and low baseline EMG level. This meant that the number of triggers for some muscles did not meet our criterion ($N \geq 500$) and were excluded. Stable effects were present (PStF, PStS, or no effect) in 98% (879/897) of all StTAs (Table 2 column 2).

Figure 3.4 illustrates an example of a typical layer V site showing highly stable effects in StTAs for all recorded muscles at the two wrist positions (30 degrees in flexion and 30 degrees in extension). The StTAs collected with the wrist at 30 degrees of flexion are illustrated as a mirror image of those collected with the wrist at 30 degrees of extension. PStF effects are color coded red, PStS are blue and no effects are black. All recorded muscles (24/24; 100%) showed matching PStEs at the two wrist positions. At 74% of sites, all effects evaluated were stable across the two wrist positions. Even at the site with the greatest instability (47V2), 86% of the effects matched. At this site, 22 muscles were evaluated (APB and TLAT were not evaluated due to trigger numbers < 500) and three muscles showed different qualitative effects in the StTAs collected at the two wrist positions. FDI and BIL showed PStF and FDP showed PStS when the monkey performed the task with the wrist flexed 30° but no effect was present in FDI or BIL and FDP was facilitated with the wrist at 30° in extension.

All 43 sites tested with the isometric wrist task exhibited clear PStF in the distal muscles. Sites in the proximal-distal representation also showed clear PStF in proximal muscles. We initially analyzed all muscles because it has been reported that changes in position at one joint can affect responses in muscles at other joints (Ginanneschi et al., 2005). However, since the proximal muscles would have shown no or minimal length change (shoulder and elbow joints were restrained) during the isometric wrist task, we also re-analyzed the data limiting it to forearm muscles only (FDS, FDP, FCR, FCU, PL, EDC, ED23, ED45, ECR and ECU). In this case, the example discussed above (47V2), yielded 80% (8/10 effects) stability. Overall, after limiting the data to just the forearm muscles, 97% (416/430) of effects were stable (Table 2 column 3). Limiting the analysis further by excluding muscles with no effect also did not change the overall results; 96% (356/370) of PStF and PStS effects remained stable in this case (Table 2 column 4).

At 13 of the 43 sites tested for stability of PStEs between wrist positions, StTAs were also collected at 0 degrees. For sites where StTAs were collected with the wrist in all three positions, the 0° position was evaluated to ensure that StTAs at a neutral position of the wrist were not different than the two more extreme positions. There were no cases where a PStE at the 0° wrist position did not match one of the other two PStEs or both.

The analysis thus far has focused on stability in terms of the sign of effects (facilitation, suppression or no effect). Another aspect of stability

concerns the magnitudes of effects. For 356 forearm muscle post-stimulus effects that remained qualitatively stable across wrist angles, we measured and compared the magnitude (ppi) of the effects at both wrist positions. If the magnitudes were identical at both wrist positions, plotting magnitude at wrist flexion against the magnitude at wrist extension should yield a correlation coefficient of one and a regression line with a slope of one. Figure 3.5 A shows the scatter plot generated from the magnitudes of forearm StTAs at the two wrist positions. The magnitude of effects in forearm muscles were highly correlated ($R = 0.87$, $P < 0.001$). The black line represents the linear regression of the points and the grey line is the unity line (regression line with a slope of one). The regression slope for the forearm muscle PStE magnitudes was close to one (slope = 1.04). The wrist flexor effects are color coded dark grey and the extensors are light grey. Plotting the flexor and extensor muscles separately yields a stronger correlation for flexor muscles ($R = 0.92$, $P < 0.001$) than extensor muscles ($R = 0.83$, $P < 0.001$) although the regression line slopes in both cases were very close to one (Flexors: slope = 0.93; Extensors: slope = 1.04)

Another question is whether changes in the magnitude of PStEs could be attributed to changes in the level of EMG activation at the two joint positions. In fact, forearm muscle EMG activation levels were significantly different at the two wrist positions ($P < 0.05$, Mann Whitney) and changed in a way that was consistent with the length-tension properties of the muscles.

For example, the flexors showed significantly higher levels of EMG activity when they were shorter (30° flexion wrist position) compared to when they were longer (30° extension wrist position). Similarly, the extensors showed significantly higher levels of EMG activity at 30° extension compared to 30° flexion wrist position. However, Figure 3.5 B shows that these EMG activation level changes did not have a consistent role in producing the observed changes in magnitude of PStEs. The percent change in EMG level was calculated in going from the position with the low EMG to the position with the higher EMG and plotted against the corresponding change in the magnitude of PStF (gray dots) and PStS (black triangles). First, it is clear that increases in EMG level do not translate into greater PStE magnitudes because many of the points for change in ppi magnitude are negative. Figure 3.5 B also shows that changes in the level of EMG activation at the two wrist positions cannot account for the variations in ppi magnitude observed in Figure 3.5 A.

Eighteen PStEs were classified as unstable based on the fact that the sign of the effect (PStF, PStS, no effect) changed between the two wrist positions. Fifty percent of unstable effects were observed in the forearm flexors and the other 50% were divided between the intrinsic hand muscles (5%) forearm extensors (22.5 %) and proximal muscles (22.5%). Figure 3.6 shows the PStEs for each of these 18 cases, categorized by type, and the changes in EMG activation level for each pair. Eight were cases in which a

PStF effect was present in one wrist position (either 30° flexion or 30° extension) and a PStS was present at the other wrist position. Interestingly, most of these (5/8) involved the same muscle (FDP). Seven were cases in which a PStF effect was present in one position and no effect was present at the other wrist position. Three were cases in which a PStS effect was present in one wrist position and no effect was present at the other position. What might underlie these qualitative changes in output effects? First, it is important to note that all unstable effects had weak magnitudes (based on criteria described in Park et al., 2004). Weak effects might be more unstable because cortical neurons producing these effects are on the fringe of the activation sphere associated with the stimulus making them more vulnerable to biasing synaptic inputs. Do the changes observed in unstable effects correlate with either change in EMG activation level or the direction of wrist position changes? Figure 3.6 shows that the EMG activation level differences between the two wrist positions did not show a consistent relationship with the direction of changes in PStEs. For example, effects that changed from PStF to PStS were not consistently associated with either an increase or decrease in the level of EMG activation, although in most cases EMG level was increased. Nor was there a consistent decrease in EMG activation level when going from PStF to no effect. The EMG activation level differences, between the two wrist positions, were not statistically different for any of the unstable effects that switched sign, either for PStF going to no effect or PStS

going to no effect. Finally, changes in the sign of the effect did not correlate with expected changes in spindle afferent input associated with different wrist positions. The same was true of changes in magnitude.

Effects also remained stable at higher stimulus intensities. At 19 sites, StTAs were collected at a range of stimulus intensities including 30 μ A, 60 μ A and 120 μ A. Stable effects were present (PStF, PStS, or no effect) for 96% (284/297) of StTAs collected at 30 μ A, 96% (258/270) of StTAs collected at 60 μ A and 95% (237/250) of StTAs collected at 120 μ A. Effects that were unstable at lower intensities tended to strengthen and become stable at higher intensities. For example, all PStEs that were unstable at 30 μ A became stable at 60 μ A.

Influence of elbow and shoulder position on post-stimulus effects

Elbow and shoulder angle changes may have an influence on the synaptic efficacy of M1 projections to the motoneuron pools of both the proximal and distal muscles. We focused on electrode track penetrations in the proximal only and the proximal-distal representation of M1 to test the stability of StTAs at different proximal joint angles (pink dots in Figure 3.3 B). StTAs were collected at 26 layer V sites in M1 while the monkey performed the isometric push-pull task at different elbow and shoulder positions. Several of the nine possible push-pull handle positions were tested (Figure 3.1 B) each of which produced substantial changes in elbow and shoulder

angles (Table 1). Due to the many degrees of freedom available for positioning the isometric push-pull handle around the monkey's work space, positions were typically chosen to maximize the change in angle of the joint most represented in the PStEs obtained at that site. For example, at a site that facilitated one or more shoulder muscles, push-pull positions A, B, D and E were chosen. In the case of a site that facilitated only elbow muscles, push-pull positions G, B and D were chosen. Since one of the goals of this study was to assess the stability of StTAs at different shoulder and elbow angles, the aforementioned push-pull handle sites (A,B,D,E and G) were the most commonly used. Push-pull handle positions H and I proved difficult for the monkey to perform and were therefore only tested rarely. Push-pull handle positions C and F were considered to be closer to a neutral shoulder and elbow angle and therefore were also rarely used.

StTAs were collected at two push-pull positions for eight sites, three push-pull positions for seven sites, four push-pull positions for eight sites, five push-pull positions for two sites and six push-pull positions for one site. Table 2 (row 3) summarizes the number of muscles showing stable PStEs at all handle positions tested for each cortical site. If the sign (facilitation, suppression, no effect) of the PStE was the same for all push-pull handle positions tested, it was considered a stable effect. As was the case with the wrist task, StTAs collected at different push-pull handle positions were highly stable. Overall, 592 of 601 total effects (98.5%) remained stable at all handle

positions tested (Table 2, column 2). An example of a typical layer V site illustrating the stability of effects in StTAs for all recorded muscles at four different push-pull handle positions is illustrated in Figure 3.7. PStEs were the same at all handle positions and thus showed 100% stability. Since 100% stability required each muscle to show the same qualitative effect at all handle positions tested, the one site that was tested at six different push-pull handle positions had the greatest opportunity for inconsistencies. However, even at that site, only one muscle (DE) showed inconsistent effects (PStF at handle positions B, D, E, and F; PStS at positions A and C). This site, therefore, yielded 23/24 matching PStEs at the six handle positions tested (96% stability).

We also compared the magnitudes of the effects focusing on the most extreme elbow positions (G and D) and the most extreme shoulder positions (horizontal plane: B and D; vertical plane: E and D). The magnitude of the effects at the extreme elbow angles were highly correlated ($R = 0.85$, $P < 0.001$) as were the magnitudes measured at the extreme shoulder angles in the horizontal and vertical plane respectively ($R = 0.95$, $R = 0.94$; $P < 0.001$). The slopes of the regression lines relating the magnitude of PStEs in one position to magnitude in the most extreme other position were all close to one (elbow positions, slope = 0.98; horizontal shoulder positions, slope = 1.03; and vertical shoulder positions; slope = 0.94). The difference in magnitudes measured across joint angles were not influenced by EMG activity levels,

since the EMG activity levels showed no significant changes at any of the extreme proximal joint positions for any muscle group (elbow flexors, elbow extensors, shoulder abductors, shoulder adductors, wrist and digit flexors, wrist and digit extensors or intrinsic hand muscles). Further, the median PStF and PStS magnitudes were not significantly different across any of the elbow or shoulder angles for any muscle group.

Figure 3.8 shows polar plots illustrating the stability of both the sign of output effects (PStF, PStS) and their magnitude at a cortical site where five different push-pull handle positions were tested (site 7dA4). The polar plot on the left contains the legend which shows the color coding for each muscle. The concentric circles give the magnitude scale for the polar plots. The heavy black circle represents no effect ($ppi=0$). Wedges extending beyond this line were facilitation effects plotted as positive ppi magnitude, shorter wedges falling inside the line were suppression effects plotted as negative ppi . At this site, all 24 muscles were evaluated and 23/24 showed matching PStEs at all handle positions (A, E, B, D and G). DE was the only muscle with an inconsistent PStE; it shows PStF (ppi range = 10 – 32) at four handle positions and a PStS ($ppi = -30$) at one.

We also limited the analysis to shoulder and elbow muscles only (ADE, PEC, TMAJ, PDE, LAT, BIS, BIL, BRA, BR, TLAT, TLON, and DE), where joint angle changes with different handle positions were the greatest. This still yielded a high level of stability (305/312, 98%), as did limiting the analysis

further by omitting muscles without PStF or PStS (143/150, 95%). For proximal muscle StTAs that remained qualitatively stable across elbow and shoulder angles, we compared the magnitude of the effects. Elbow muscle PStE magnitudes measured at the two most extreme elbow positions (G and D) were highly correlated ($R = 0.88$, $P < 0.001$) and the slope of the regression line was very close to one (1.04). Shoulder muscle PStE magnitudes measured at the two most extreme horizontal (B and D) and vertical (E and D) shoulder positions were also highly correlated ($R = 0.90$, $R = 0.91$; $P < .001$) and the slope of the regression lines were also close to one (1.05 and 0.95 respectively).

Nine PStEs were classified as unstable based on the fact that the sign of the effect (PStF, PStS, no effect) was not the same at all of the push-pull handle positions tested. Four were cases in which a PStF effect was present in one or more push-pull handle positions and a PStS effect was present in one or more of the other push-pull positions. Four were cases in which a PStF effect was present in one or more push-pull handle positions and no effect was present in one or more of the other push-pull handle positions. There was only one case in which a PStS effect was present in one or more push-pull handle positions and no effect was present at one of the other push-pull handle positions. Fifty-five percent of inconsistent effects were observed in the shoulder abductors (DE, LAT, and PDE) and the other 45% were

divided between the elbow flexors (22.5%) and distal muscles (22.5%). All unstable effects had weak magnitudes.

PStEs compared across movement tasks

In order to maximize the opportunity for PStEs to show instability under different task conditions, we decided to compare two tasks that differ fundamentally in terms of basic task characteristics. The push-pull task is isometric and robustly activates forelimb muscles in a tonic pattern with minimal changes in muscle length at a given handle position. The reach-to-grasp task on the other hand is free-form in nature and requires dynamic movement of the forelimb while fractionating peaks of activity into unique muscle synergies. Fourteen layer V sites, in the proximal only or proximal-distal representation of M1 (pink dots with black dot insert in Figure 3.3 D) were evaluated for stability of PStEs across the two tasks. Table 2 (row 4) summarizes the results from testing the stability in StTAs across different tasks. Stability was calculated for each site by comparing the qualitative effects present in the StTAs for both the push-pull handle position tested and the reach-to-grasp task. If the PStE was qualitatively the same for both tasks, it was considered a stable effect.

Stable effects were present (PStF, PStS, or no effect) in 93% (287/307) of all StTAs (Table 2 column 2). Limiting the analysis further by omitting muscles without PStF or PStS yielded 81% (96/118) stability. Overall

the magnitude of effects, in the same muscle across tasks, were highly correlated ($R = 0.76$, $P < 0.001$) and the slope of the regression line was very close to one (1.03). Statistical comparison of median PStF and PStS magnitudes for the two tasks were not significant for any muscle group (elbow flexors, elbow extensors, shoulder abductors, shoulder adductors, wrist and digit flexors, wrist and digit extensors or intrinsic hand muscles). Statistical comparison of the EMG activity levels showed no significant differences between the two tasks for any muscle group.

Twenty two PStEs (7%) were classified as unstable based on the fact that the sign of the effect (PStF, PStS, no effect) changed between the two tasks. Five were cases in which a PStF was present while the monkey performed one of the tasks and a PStS was present while the monkey performed the other task. Fourteen were cases in which a PStF was present while the monkey performed one of the tasks and no effect was present during performance of the other task. There were also three cases in which a PStS was present while the monkey performed one of the tasks and no effect was present during performance of the other task. Seventy-five percent of inconsistent effects were observed in the distal muscles (40% extensors and 35% flexors) and the other 25% were divided between the shoulder muscles (10%) and elbow muscles (15%). Inconsistent effects were largely weak in magnitude (18/22) although 4/22 had moderately strong magnitudes based on the classification scheme of Park et al., (2004).

DISCUSSION

Data presented in this paper demonstrate that effects in StTAs of forelimb muscle EMG are remarkably stable under a variety of different task conditions. Our results show that the sign (facilitation or suppression), strength and distribution of effects in StTAs are highly stable independent of joint angle position changes of the forelimb for both isometric tasks (98%) and comparing isometric tasks with the dynamic movement conditions present in the reach-to-grasp task (93%). PStEs were stable for both distal and proximal muscles whose length changed with joint angle changes for each of the isometric tasks. When wrist position was changed in the isometric wrist task, 96% (411/430) of forearm muscle PStEs (PStF, PStS, no effect) remained stable (same qualitative effect). When the shoulder and elbow positions were changed in the push-pull task, 97% (304/312) of proximal PStEs remained stable. This shows that M1 output to forelimb muscles, as evident in PStEs, is not heavily influenced by joint angle position or limb posture.

Occasionally, effects in StTAs changed across joint angle positions for each of the tasks. However, it is important to note that almost all (90%) cases of inconsistent effects were weak and no case involved a strong effect (based on criteria of Park et al., 2004). Cortical neurons producing unstable, weak effects might be on the fringe of the activation sphere associated with the

stimulus making them more vulnerable to cortical or motoneuron excitability changes.

Not only did the sign of effects remain stable (PStF, PStS and no effect) under different task conditions but so did the magnitude (ppi) of effects. To investigate magnitude relationships more closely we plotted the PStE magnitudes obtained at different joint angles and for different tasks against each other. If the magnitudes of PStEs were identical under all task conditions the regression slope for these plots would be one. In fact, the actual slopes we obtained were all very close to one (0.93 – 1.05). Moreover, the correlation coefficients relating PStE magnitudes obtained under different task conditions were all statistically significant and approached one (0.76 – 0.95). Nevertheless, it should also be noted that individual effects could show rather substantial changes in magnitude at different joint angles (~300%, see Figure 3.5). These larger deviations more frequently involved extensor muscles which also had PStF effects that were higher in magnitude. Changes in magnitude of effects at different joint angles were not correlated with changes in baseline EMG activity and could not be explained by possible changes in spindle afferent input related to muscle length changes.

Peripheral feedback to both the spinal cord and the cortex will differ with different joint angle positions and arm postures. These changes in afferent feedback were hypothesized to underlie shifts in the boundaries between forelimb and vibrissa representations identified by repetitive ICMS in

the rat (Sanes et al., 1992). For example, when the limb was moved from a retracted position (wrist extension and elbow flexion) to a protracted position (wrist flexion and elbow extension) forelimb EMG activity was evoked from eight sites which had previously only evoked vibrissa movement. The expansion of the forelimb representation was attributed primarily to changing somatic sensory input to M1 although they note that the “immediate” plasticity could also be related to changes in the synaptic efficacy at sub-cortical levels. How can this result be reconciled with our finding that PStF does not change with joint position or arm posture? One important difference between our study and that of Sanes and colleagues is that they were looking at boundary changes between representations whereas we examined output effects from single sites well within the forelimb representation of M1. Another difference is that stimulus-triggered averaging of EMG activity at low intensity is a sub-threshold approach to activation of cortical motor output. Individual stimuli do not produce overt responses observable in the raw EMG record. Still other differences between our studies are that we used unanesthetized primates performing a trained behavioral task whereas Sanes et al., (1992) use rats that were anesthetized with ketamine.

Transcranial magnetic stimulation (TMS) studies in humans have shown differing results regarding the stability of motor evoked potentials (MEP) in the presence of passive and active joint angle changes. Lewis and Byblow (2002) demonstrated stability in MEP amplitude and latency in

humans during fixed wrist postures (45 degrees in flexion and extension) with the subject at rest. However, MEP amplitudes did show changes (exceeding 5-fold) during passive wrist movement, suggesting that afferent input associated with dynamic movement, at least passive movement, can alter cortical and/or motoneuronal excitability sufficiently to produce changes in MEP magnitude. Ginannesch and colleagues have shown MEP changes in forearm muscles (2006) and hand muscles (2005) related to changes in shoulder joint angle. Also, forearm rotation was shown to change MEPs of both elbow and intrinsic hand muscles (Mitsuhashi et al., 2007). Lemon et al., (1995) reported amplitude and latency changes in EMG responses related to phase of a reach-to-grasp and lift task. One possible reason for the discrepancy between these studies and ours is the difference in stimulus parameters between TMS and StTA. StTA is a sub-threshold method of determining output effects to muscle in which low intensity stimuli are delivered at a low rate (15 Hz) minimizing temporal summation of EPSPs at the motoneuron and reducing physical spread of current (Stoney et al., 1968; Jankowska et al., 1975; Ranck, 1975; Asanuma et al., 1976; Tehovnik et al., 2006,). Signal averaging in the presence of background EMG activity is required to detect effects. On the other hand, TMS activates a larger cortical area producing supra-threshold effects clearly visible with single stimuli in the presence or absence of background EMG activity. The magnitude of TMS effects are known to be dependent on motoneuron excitability and the level of

baseline EMG activity (Hasegawa et al., 2001; Mitchell et al., 2007). In comparison, our data show no consistent relation between the level of background EMG activity and the magnitude of PStF or PStS.

The TMS approach to investigating cortical output to motoneurons differs quite substantially from stimulus-triggered averaging of EMG so it is perhaps not surprising that our results differ from those using TMS. However, a recent report by Graziano et al., (2004) using stimulus-triggered averaging of EMG activity also reported clear changes in output effects as a function of elbow joint angle. They reported that the magnitude of triceps PStF increased as elbow angle was moved toward flexion (stretching triceps) and biceps decreased while the opposite pattern was obtained as elbow angle was moved toward extension. In both cases, effects became stronger as the muscles were lengthened. All sites tested in their paper seem to follow this pattern. They studied a total of 35 cortical sites looking at effects on triceps and biceps and reported consistent patterns of change with joint angle at all sites for the biceps and 34 of 35 sites for the triceps. It is interesting to note that all of these changes are consistent with expected changes in muscle spindle input associated with the joint angle changes under passive conditions. If muscle spindle input does change motoneuron excitability such that the same descending signal produces activation of more motoneurons, why is this not reflected in our results? Not only did we see a high level of stability in output effects between joint angle changes, the changes that did

occur were not always consistent with an explanation based on motoneuron excitability brought about by expected changes in spindle afferent input. One possible important difference between the approaches in our two studies is that Graziano and colleagues collected their stimulus-triggered averaging data with the monkey under ketamine anesthesia. It is feasible that in the absence of voluntary movement and the related changes in descending input to the spinal cord, motoneuron excitability might have become heavily dominated by changes in spindle afferent input associated with joint angle changes.

Our results show that the excitability of the corticospinal system remains stable under a wide variety of task conditions involving large changes in the position of different individual joints as well as changes in global arm posture. Joint angle changes about the wrist, elbow and shoulder produced little or no effect on the sign and distribution of M1 output effects in StTAs of forelimb muscles. Although some individual cases showed relatively large changes in PStF magnitude with changes in joint position, overall, magnitudes at different joints positions and arm postures were highly correlated with regression slopes close to one. Stimulus-triggered averaging of EMG activity has been used extensively to quantify output effects from cortical and sub-cortical descending systems to motoneurons and for mapping cortical output (Hummelsheim et al., 1986; Baker et al., 1998; Perlmutter et al., 1998; Park et al., 2001, 2004; Schieber 2001; Boudrias et

al., 2006; Davidson and Buford 2006; Moritz et al., 2007). Our results further validate the use of stimulus-triggered averaging of EMG activity as a powerful and effective method for studying the organization and function of cortical and sub-cortical motor areas.

Table 3.1. Joint angles achieved in the isometric push-pull task

1. Push-Pull handle position	2. Joint	3. Angle
A.	Shoulder	50° Horizontal Plane
		115° Vertical Plane
	Elbow	105° Horizontal Plane
B.	Shoulder	50° Horizontal Plane
		125° Vertical Plane
	Elbow	115° Horizontal Plane
C.	Shoulder	90° Horizontal Plane
		125° Vertical Plane
	Elbow	120° Horizontal Plane
D.	Shoulder	110° Horizontal Plane
		125° Vertical Plane
	Elbow	135° Vertical Plane
E.	Shoulder	110° Horizontal Plane
		115° Vertical Plane
	Elbow	120° Vertical Plane
F.	Shoulder	90° Horizontal Plane
		115° Vertical Plane
	Elbow	120° Vertical Plane
G.	Shoulder	110° Horizontal Plane
		160° Vertical Plane
	Elbow	70° Vertical Plane
H.	Shoulder	50° Horizontal Plane
		140° Vertical Plane
	Elbow	65° Vertical Plane
I.	Shoulder	50° Horizontal Plane
		120° Vertical Plane
	Elbow	70° Vertical Plane

Angles estimated to the nearest 5 degrees.
See Figure 1 for identification of handle positions.

Table 3.2. Stability results from different tasks (15 μ A)

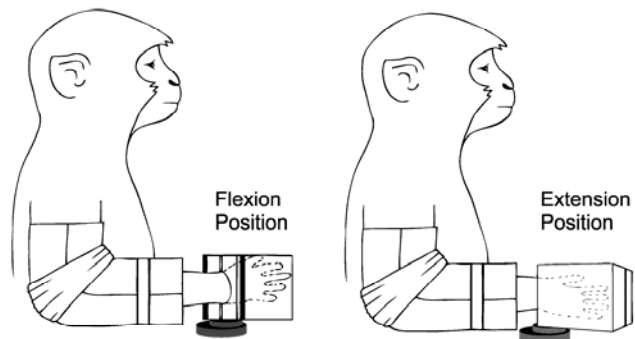
1. Task	2. Stable*/Total (All StTAs**)	3. Stable*/Total (Specific Muscle Groups)	4. Stable*/Total (Specific Muscle Groups; excluding muscles with no effect)
Isometric Wrist	879/897 (98%)	Forearm muscles: 416/430 (97%)	Forearm muscles: 356/370 (96%)
Isometric Push- Pull	592/601 (98.5%)	Proximal muscles: 305/312 (98%)	Proximal muscles: 143/150 (95%)
Isometric Push- Pull Vs. Reach-to-Grasp	287/309 (93%)	N.A.	96/118 (81%)

* Same qualitative effects (PStF, PStS, no effect)

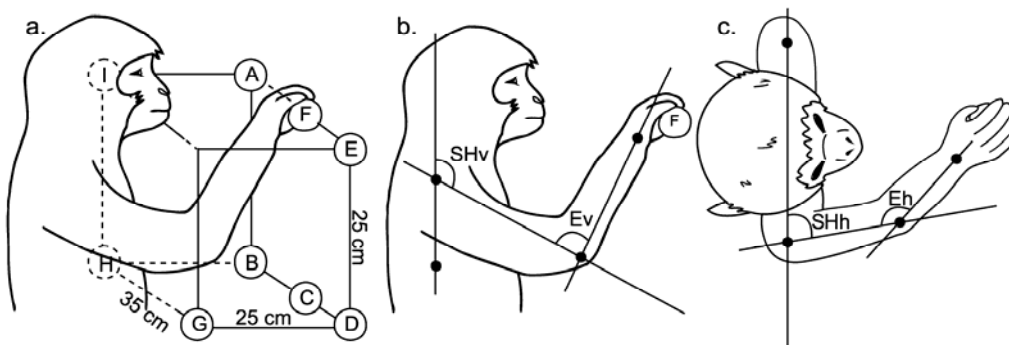
** Includes all records (PStF, PStS and no effect) and muscles at all joints

Figure 3.1. Illustrations depicting the tasks used to test the stability of output effects from motor cortex to forelimb muscles. A) isometric wrist task. B) isometric push-pull task a. lettered circles in the first illustration depict the push-pull handle positions further described in Table 1. The second two illustrations depict how the joint angles were measured. for the a. vertical shoulder angle (SHv), vertical elbow angle (Ev), b. horizontal shoulder angle (SHh), and horizontal elbow angle (Eh). C) Reach-to-grasp task.

A. Isometric Wrist Task



B. Isometric Push-Pull Task



C. Reach-to Grasp Task

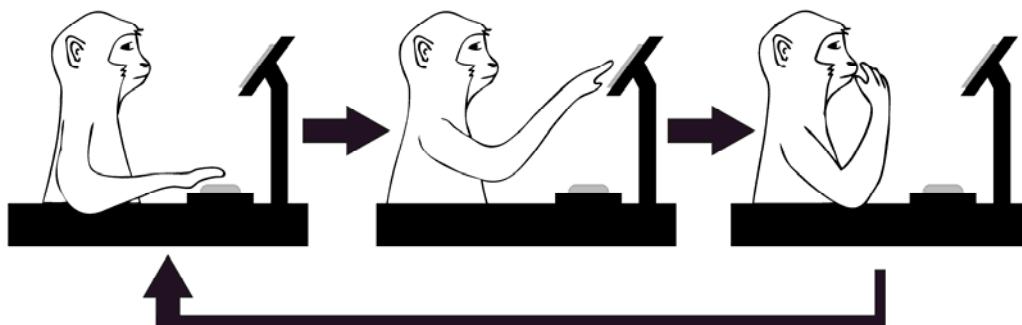


Figure 3.2. A,B). Three-dimensional reconstructions of the left hemisphere of monkeys V and A, respectively. The circles represent the area under the cortical recording chambers. An enlarged view shows the central sulcus (CS), arcuate sulcus (AS) and the precentral dimple (PcD). C,D). Muscle maps of M1 for monkeys V and A, respectively, represented in two-dimensional coordinates after unfolding the precentral gyrus. Black dots represent electrode track penetrations.

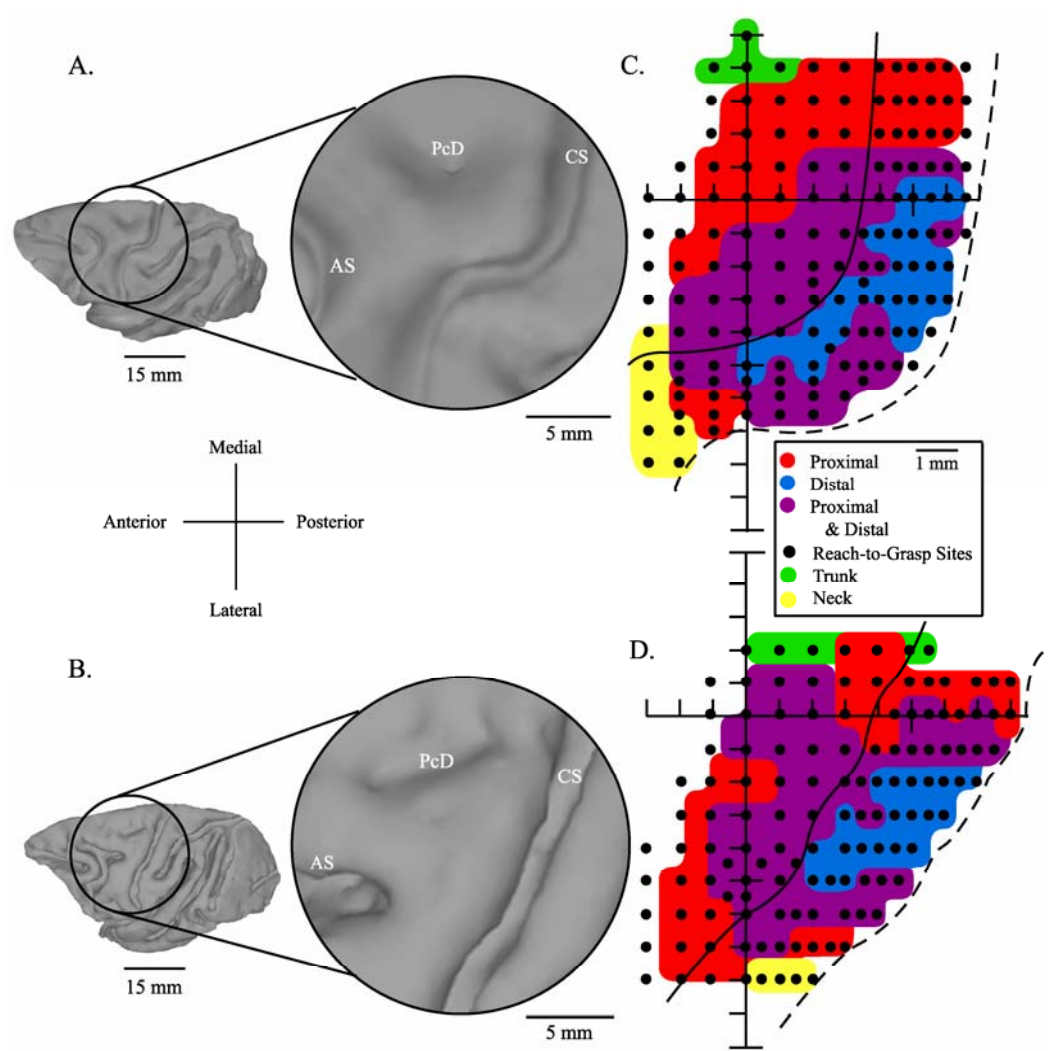


Figure 3.3. Sites used to test the stability of effects in StTAs of EMG activity with the isometric wrist task (white dots), isometric push-pull task (pink dots), and between the isometric push-pull task and the reach-to-grasp task (pink dots with black dot inserts) represented in two-dimensional coordinates after unfolding the precentral gyrus and overlaid on the monkey's respective muscle map.

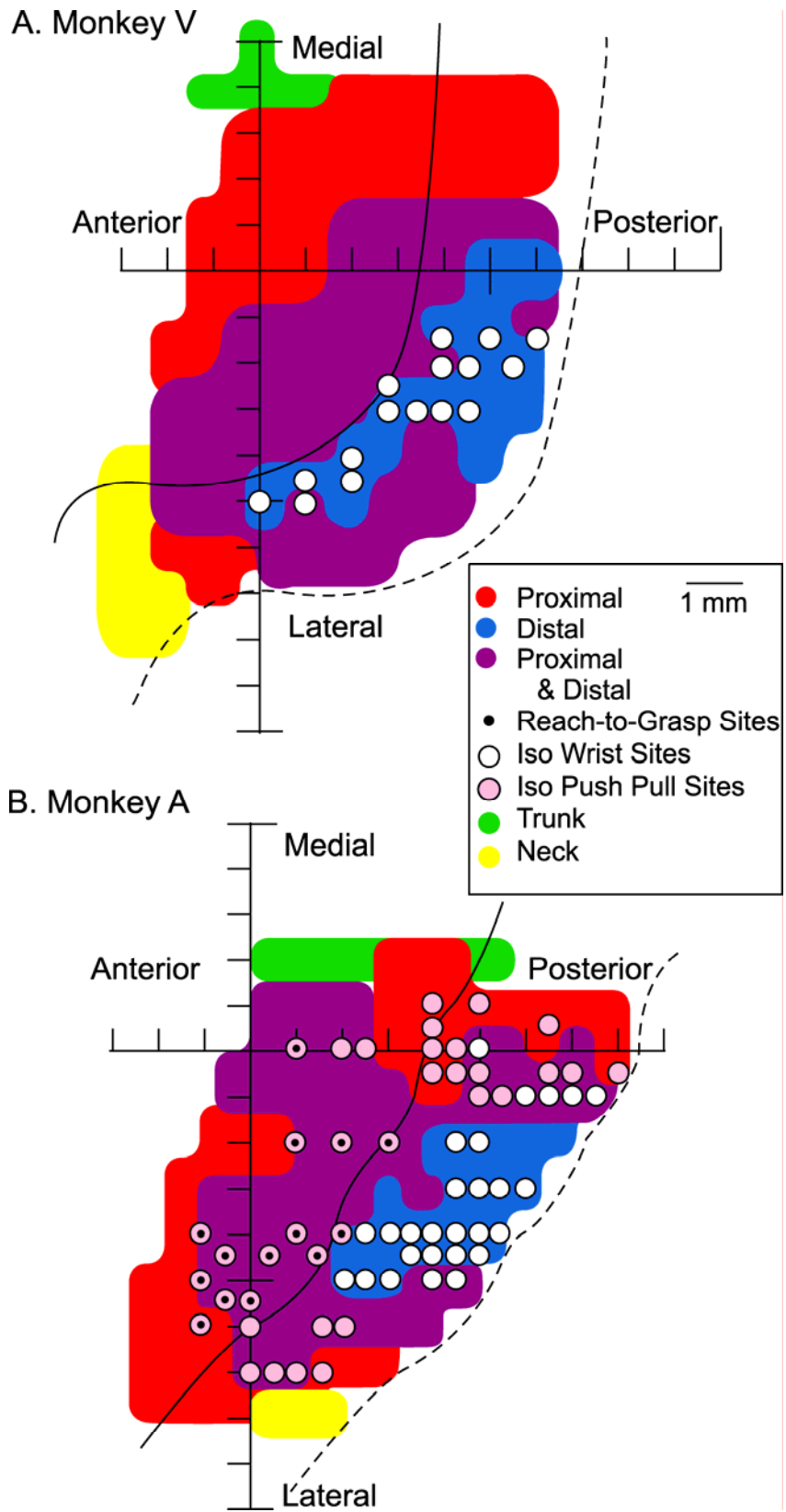
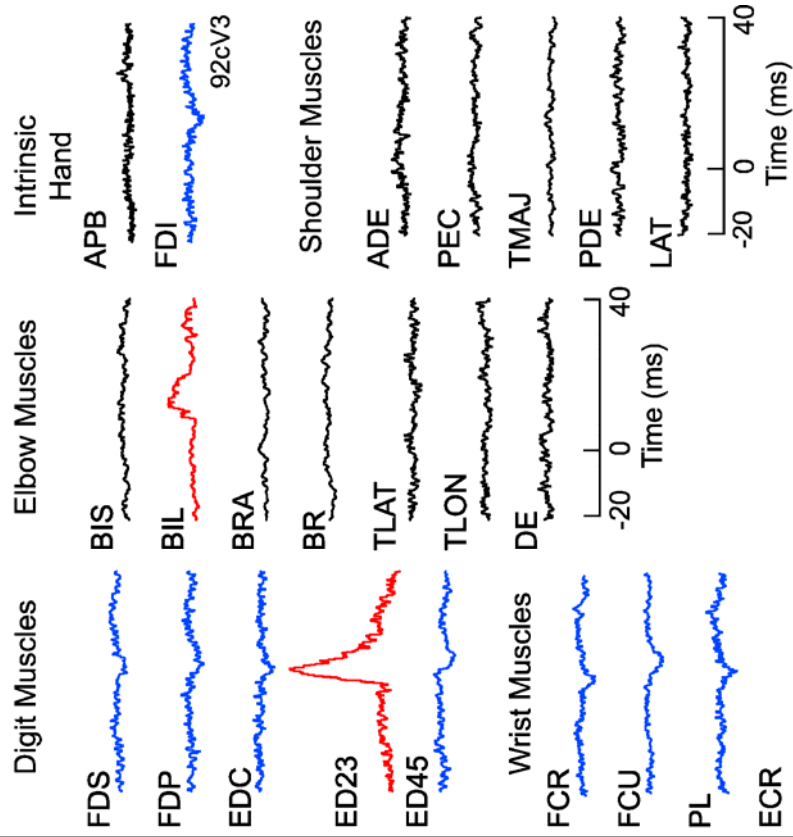


Figure 3.4. A typical layer V site with stable effects in all muscles at both the flexion 30 degrees and extension 30 degrees wrist positions of the isometric wrist task. PStF effects were present in both proximal (BIL) and distal (ED23) forelimb muscles (proximal-distal site). PStS effects were present in distal (FDI, FDS, FDP, EDC, ED45, FCR, FCU, PL, ECU) forelimb muscles. Stimulus intensity was 15 μ A.

B. Wrist Position = 30 degrees Extension



A. Wrist Position = 30 degrees Flexion

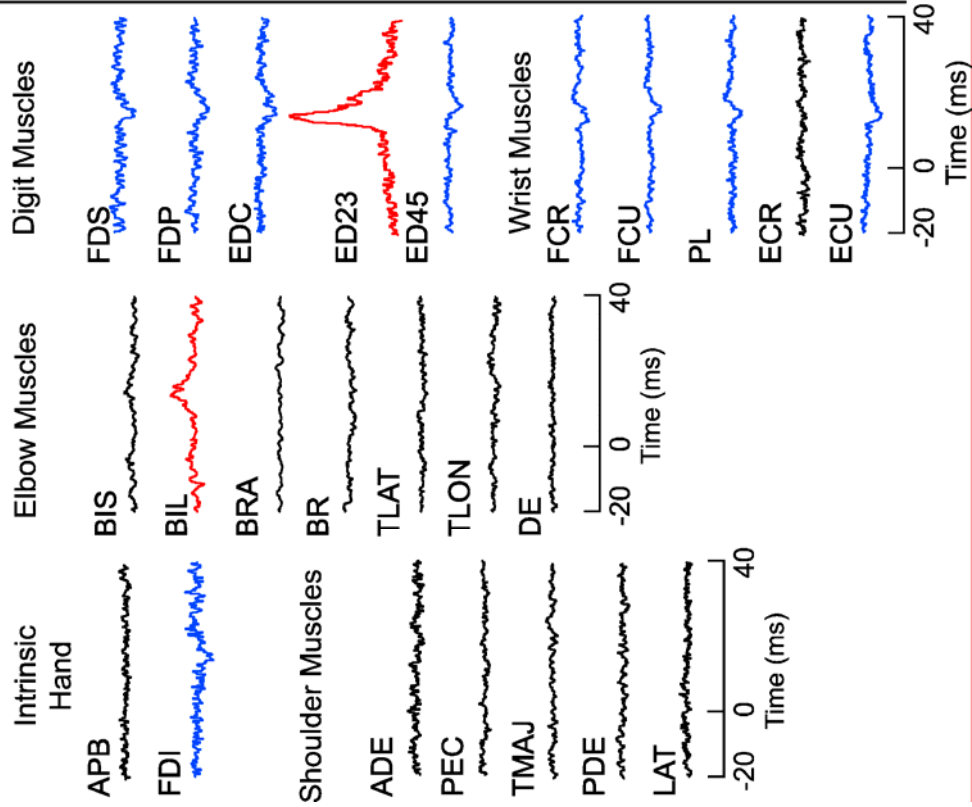
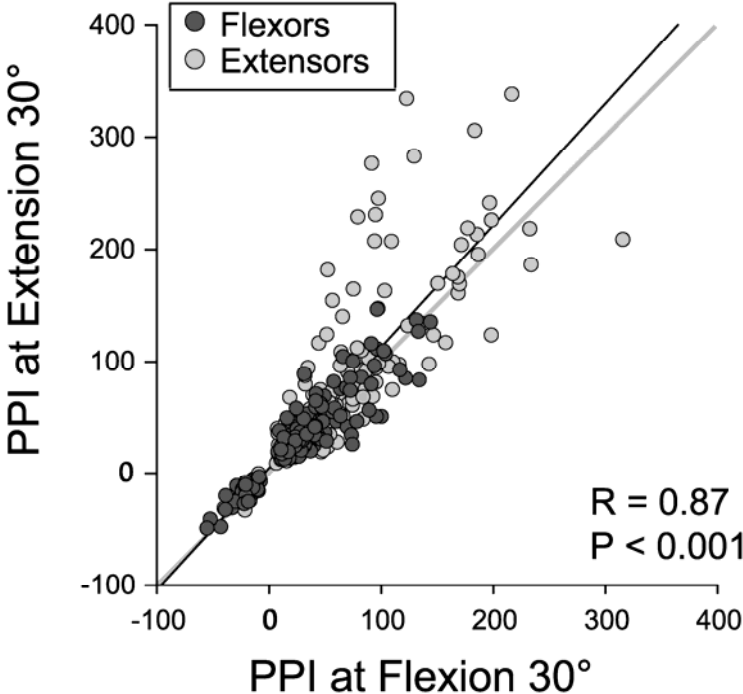


Figure 3.5. Consistent PStEs relationships. A) Consistent Effects in Forearm Muscles. Relationship between the magnitudes of PStEs (ppi) at the two most extreme wrist positions. Both PStF (positive ppi) and PStS (negative ppi) effects are included. Dark grey dots represent forearm flexors and light grey dots represent forearm extensors. Grey line represents a line with slope = 1. B) Role of Baseline EMG Changes. Relationship between the EMG level change (from low level EMG to high level EMG expressed as a percent) and the corresponding change in magnitude of PStE (expressed as a percent) measured in the two most extreme wrist positions. The light grey dots represent PStF and the dark grey triangles represent PStS. For both plots, linear regression lines are plotted and correlation coefficients (R) and P values are given.

A. Consistent Effects (Distal Muscles)



B. Role of Baseline EMG Changes

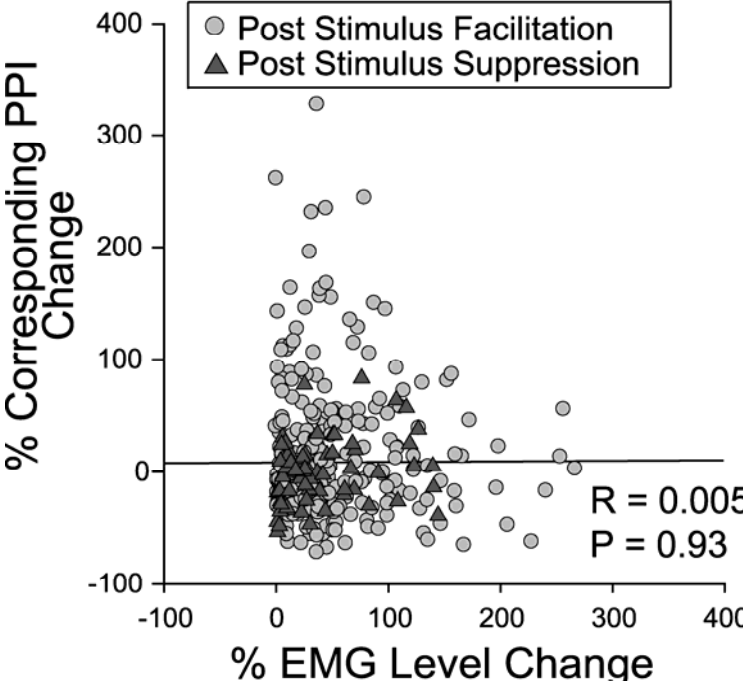
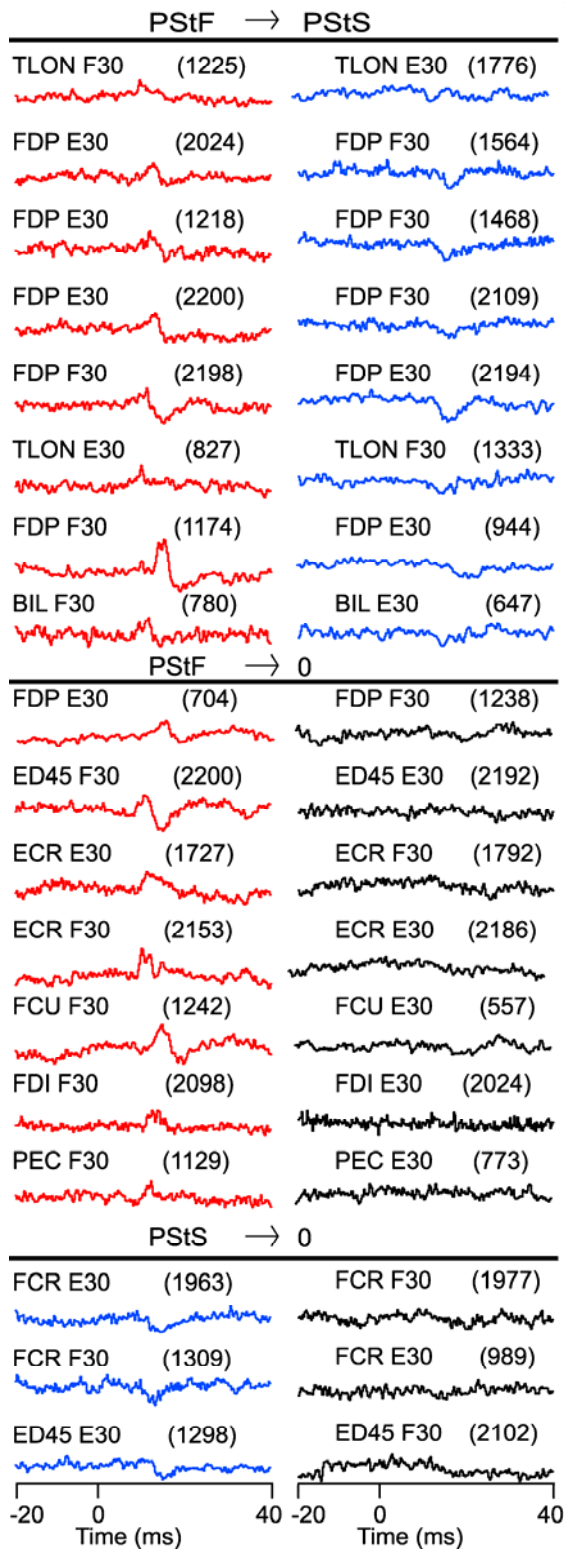


Figure 3.6. All 18 inconsistent effects observed during performance of the isometric wrist task and the corresponding percentage of EMG activity level change (from left column EMG to right column EMG expressed as a percent) measured across the two wrist positions.

A. Inconsistent Effects



B. % EMG Level Change

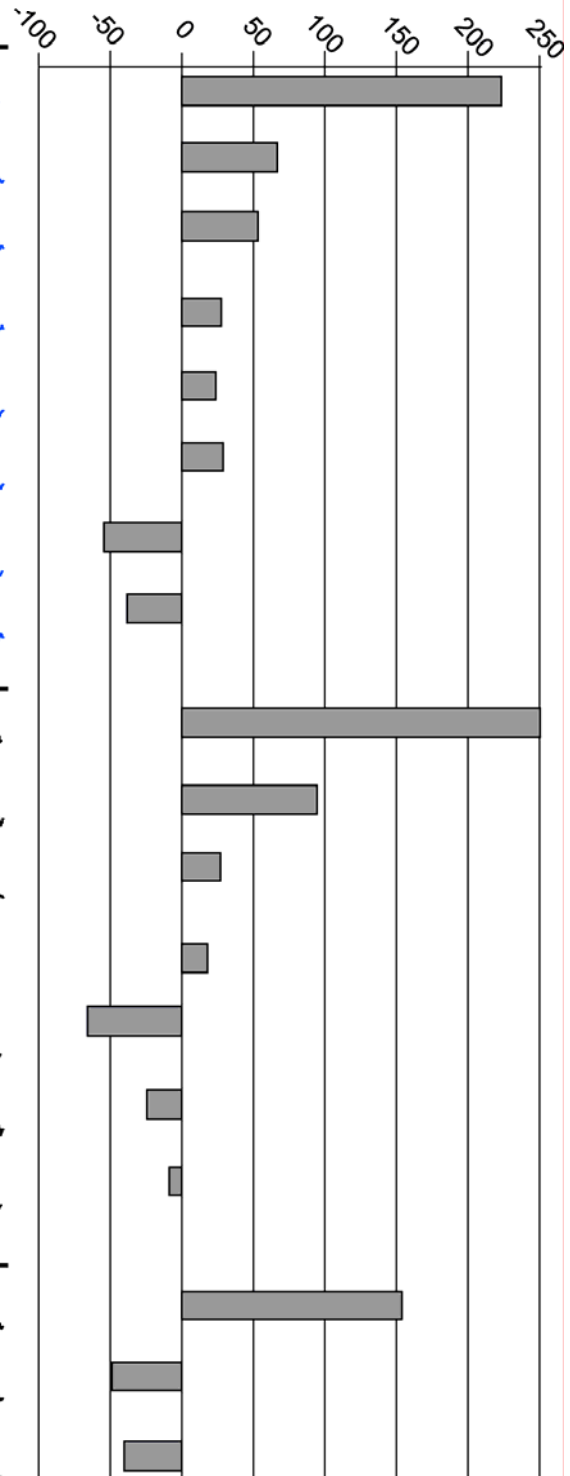


Figure 3.7. A typical layer V site with stable effects in all muscles observed during performance of the push-pull task at four different positions. The distribution of PStE in forelimb muscles is from a proximal-distal site. PStF effects were present in both proximal (BIS, BIL, BRA, PDE) and distal (FDP, ED45, FDI, PL) forelimb muscles. PStS effects were also present in proximal (BR) and distal (ECU) forelimb muscles.

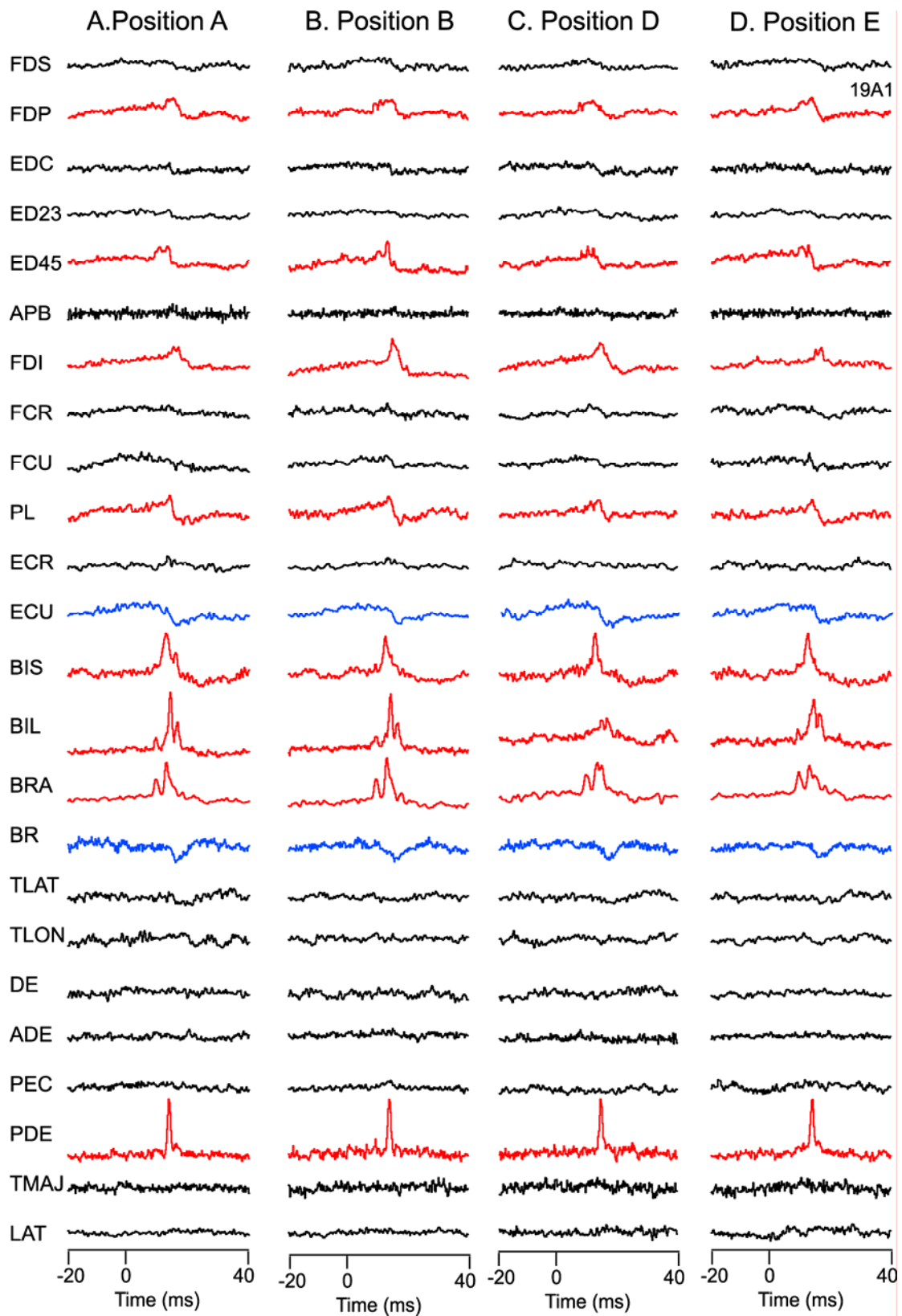
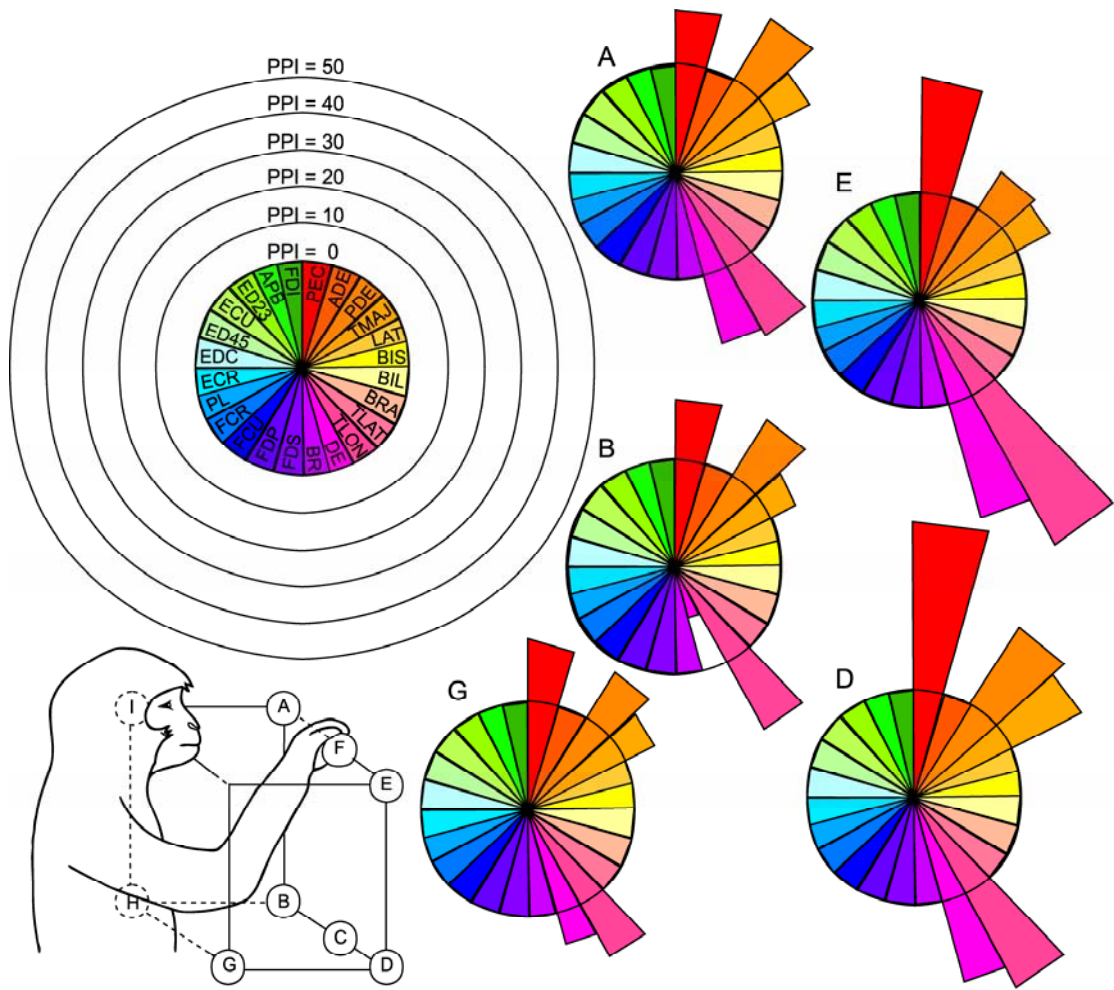


Figure 3.8. Polar plots of the distributions of magnitudes (ppi) for each of 24 muscles at five different workspace locations assuming a uniform distribution for ppi = 0. The top left polar plot represents the legend with a uniform distribution of ppi = 0 for all muscles. The concentric circles represent a magnitude scale for ppi increments of 10. Letters represent each handle position tested.



REFERENCES

- Armstrong DM, Drew T (1985) Forelimb electromyographic responses to motor cortex stimulation during locomotion in the cat. *J Physiol* 367: 327-51.
- Asanuma H, Rosén I (1972) Topographical organization of cortical efferent zones projecting to distal forelimb muscles in the monkey. *Exp Brain Res* 14(3): 243-56.
- Asanuma H, Arnold A, Zarzecki P (1976) Further study on the excitation of pyramidal tract cells by intracortical microstimulation. *Exp Brain Res* 26(5): 443-61.
- Baker SN, Lemon RN (1998) Computer simulation of post-spike facilitation in spike-triggered averages of rectified EMG. *J Neurophysiol* 80(3): 1391-406.
- Baker SN, Oliver E, Lemon RN (1995) Task-related variation in corticospinal output evoked by transcranial magnetic stimulation in the macaque monkey. *J Physiol* 488.3: 795-801.
- Belhaj-Saïf A, Hill Karrer J, Cheney PD (1998) Distribution and characteristics of post-stimulus effects in proximal and distal forelimb muscles from red nucleus in the monkey. *J Neurophysiol* 79: 1777-1789.
- Boudrias MH, Belhaj-Saïf A, Park MC, Cheney PD (2006) Contrasting properties of motor output from the supplementary motor area and primary motor cortex in rhesus macaques. *Cereb Cortex* 16(5): 632-8.
- Boudrias MH, McPherson RL, Cheney PD (2007) Contrasting output properties of rostral and caudal parts of the primary motor cortex (M1) in rhesus macaques. Program No. 292.17 *Abstract Viewer/Itinerary Planner*. Washington DC: Society for Neuroscience. Online.
- Bretzner F, Drew T (2005a) Changes in corticospinal efficacy contribute to the locomotor plasticity observed after unilateral cutaneous denervation of the hindpaw in the cat. *J Neurophysiol* 94(4): 2911-27.

- Bretzner F, Drew T. (2005b) Contribution of the motor cortex to the structure and the timing of hindlimb locomotion in the cat: a microstimulation study. *J Neurophysiol* 94(1): 657-72.
- Buys EJ, Lemon RN, Mantel GW, Muir RB (1986) Selective facilitation of different hand muscles by single corticospinal neurons in the conscious monkey. *J Physiol* 381: 529-49.
- Cheney PD (2002) Electrophysiological Methods for Mapping Brain Motor and Sensory Circuits. In: *Brain Mapping: The Methods, Second Edition* (A. W. Toga, J. C. Mazziotta, eds), pp189-226. New York, NY: Academic Press.
- Cheney PD, Fetz EE (1980) Functional classes of primate corticomotoneuronal cells and their relation to active force. *J Neurophysiol* 44(4): 773-91.
- Cheney PD, Fetz EE (1985) Comparable patterns of muscle facilitation evoked by individual corticomotoneuronal (CM) cells and by single intracortical microstimuli in primates: evidence for functional groups of CM cells. *J Neurophysiol* 53(3): 786-804.
- Cheney PD, Fetz EE, Palmer SS (1995) Patterns of facilitation and suppression of antagonist forelimb muscles from motor cortex sites in the awake monkey. *J Neurophysiol* 53(3): 805-20.
- Cheney PD, Mewes K, Widener G (1991) Effects on wrist and digit muscle activity from microstimuli applied at the sites of rubromotoneuronal cells in primates. *J Neurophysiol* 66(6): 1978-92.
- Davidson AG, Buford JA (2004) Motor outputs from the primate reticular formation to shoulder muscles as revealed by stimulus-triggered averaging. *J Neurophysiol* 92(1): 83-95.

- Davidson AG, Buford JA (2006) Bilateral actions of the reticulospinal tract on arm and shoulder muscles in the monkey: stimulus triggered averaging. *Exp Brain Res* 173(1): 25-39.
- Davidson AG, Schieber MH, Buford JA (2007) Bilateral spike-triggered average effects in arm and shoulder muscles from the monkey pontomedullary reticular formation. *J Neurosci* 27(30): 8053-8.
- Drew T (1991) Functional organization within the medullary reticular formation of the intact unanesthetized cat III. Microstimulation during locomotion. *J Neurophysiol* 66: 919-938.
- Gellhorn E, Hyde J (1953) Influence of proprioception on map of cortical responses. *J Physiol* 122(2): 371-85.
- Ginanneschi F, Del Santo F, Dominici F, Gelli F, Mazzocchio R, Rossi A (2005) Changes in corticomotor excitability of hand muscles in relation to static shoulder positions. *Exp Brain Res* 161(3): 374-82.
- Ginanneschi F, Dominici F, Biasella A, Gelli F, Rossi A (2006) Changes in corticomotor excitability of forearm muscles in relation to static shoulder positions. *Brain Res* 1073-1074: 332-8.
- Graziano MS, Patel KT, Taylor CS (2004) Mapping from motor cortex to biceps and triceps altered by elbow angle. *J Neurophysiol* 92(1): 395-407.
- Hasegawa Y, Kasai T, Kinoshita H, Yahagic S (2001) Modulation of a motor evoked response to transcranial magnetic stimulation by the activity level of the first dorsal interosseous muscle in humans when grasping a stationary object with different grip widths. *Neurosci Lett* 299: 1-4.
- Hummelsheim H, Wiesendanger M, Bianchetti M, Wiesendanger R, Macpherson J (1986) Further investigations of the efferent linkage of the supplementary motor area (SMA) with the spinal cord in the monkey. *Exp Brain Res* 65(1): 75-82.

- Jankowska E, Padel Y, Tanaka R (1975) The mode of activation of pyramidal tract cells by intracortical stimuli. *J Physiol* 249(3): 617-36.
- Kasser RJ, Cheney PD (1985) Characteristics of corticomotoneuronal postspike facilitation and reciprocal suppression of EMG activity in the monkey. *J Neurophysiol* 53(4): 959-78.
- Lemon RN, Johansson RS, Westling G (1995) Corticospinal control during reach, grasp, and precision lift in man. *J Neurosci* 15(9): 6145-56.
- Lewis GN, Byblow WD (2002) Modulations in corticomotor excitability during passive upper-limb movement: is there a cortical influence? *Brain Res* 943(2): 263-75.
- McKiernan BJ, Marcario JK, Hill Karrer J, Cheney PD (1998) Corticomotoneuronal postspike effects in shoulder, elbow, wrist, digit, and intrinsic hand muscles during a reach and prehension task. *J Neurophysiol* 80(4): 1961-1980.
- Mewes K, Cheney PD (1991) Facilitation and suppression of wrist and digit muscles from single rubromotoneuronal cells in the awake monkey. *J Neurophysiol*. 66(6): 1965-77.
- Mewes K, Cheney PD (1994) Primate rubromotoneuronal cells: parametric relations and contribution to wrist movement. *J Neurophysiol* 72: 14-30.
- Mitchell KW, Baker MR, Baker SN (2007) Muscle responses to transcranial stimulation in man depend on background oscillatory activity. *J Physiol* 583.2: 567-79.
- Mitsuhashi K, Seki K, Akamatsu C, Handa Y (2007) Modulation of excitability in the cerebral cortex projecting to upper extremity muscles by rotational positioning of the forearm. *Tohoku J Exp Med* 212(3): 221-8.
- Moritz CT, Lucas TH, Perlmutter SI, Fetz EE (2007) Forelimb movements and muscle responses evoked by microstimulation of cervical spinal cord in sedated monkeys. *J Neurophysiol* 97(1): 110-20.

- Palmer SS, Fetz EE (1985) Effects of single intracortical microstimuli in motor cortex on activity of identified forearm motor units in behaving monkeys. *J Neurophysiol* 54(5): 1194-1212.
- Park MC, Belhaj-Saïf A, Cheney PD (2000) Chronic recording of EMG activity from large numbers of forelimb muscles in awake macaque monkeys. *J Neurosci Methods* 15;96(2): 153-60.
- Park MC, Belhaj-Saïf A, Cheney PD (2004) Properties of primary motor cortex output to forelimb muscles in rhesus macaques. *J Neurophysiol* 92(5): 2968-2984.
- Park MC, Belhaj-Saïf A, Gordon M, Cheney PD (2001) Consistent features in the forelimb representation of primary motor cortex in rhesus macaques. *The J Neurosci* 21: 2784-2792.
- Perlmutter SI, Iwamoto Y, Baker JF, Peterson BW (1998) Interdependence of spatial properties and projection patterns of medial vestibulospinal tract neurons in the cat. *J Neurophysiol* 79(1): 270-84.
- Ranck JB Jr. (1975) Which elements are excited in electrical stimulation of mammalian central nervous system: a review. *Brain Res* 98(3): 417-40. Review.
- Sanes JN, Wang J, Donoghue JP (1992) Immediate and delayed changes of rat motor cortical output representation with new forelimb configurations. *Cereb Cortex* 2(2):141-52.
- Schieber MH (2001) Constraints on somatotopic organization in the primary motor cortex. *J Neurophysiol* 86(5): 2125-43. Review.
- Stoney SD Jr, Thompson WD, Asanuma H (1968) Excitation of pyramidal tract cells by intracortical microstimulation: effective extent of stimulating current. *J Neurophysiol* 31(5): 659-69.
- Tehovnik EJ, Tolia AS, Sultan F, Slocum WM, Logothetis NK (2006) Direct and indirect activation of cortical neurons by electrical microstimulation. *J Neurophysiol* 96(2): 512-21. Review.

Van Essen DC, Drury HA, Dickson J, Harwell J, Hanlon D, Anderson CH
(2001) An integrated software suite for surface-based analyses of
cerebral cortex. *J Am Med Inform Assoc* 8(5): 443-59.

Widener GL Cheney PD (1997) Effects on muscle activity from microstimuli
applied to somatosensory and motor cortex during voluntary
movement in the monkey. *J Neurophysiol* 77(5): 2446-65.

CHAPTER FOUR

EMG ACTIVATION PATTERNS ASSOCIATED WITH LONG

DURATION ICMS OF PRIMARY MOTOR CORTEX

ABSTRACT

Repetitive, long duration intracortical microstimulation (RL-ICMS) of primary motor cortex (M1) in primates has been shown to produce hand movements to a common final end-point regardless of the starting position (Graziano et al., 2002). We have confirmed this general conclusion and have investigated the electromyography (EMG) activation patterns responsible for producing these movements. Our primary objectives were to determine the extent to which the sign (facilitation or suppression) strength and distribution of effects in RL-ICMS evoked EMG activity are dependent on task conditions including limb posture, and to compare the temporal profiles of EMG activation associated with RL-ICMS evoked movements. Layer V sites in forelimb M1 were identified and microstimuli ranging in intensity from 60 μ A to 120 μ A were applied at 200 Hz for 500 ms. The first pulse of each train was used as a trigger to compute averages of EMG activity from 24 muscles of the forelimb including shoulder, elbow, wrist, digit and intrinsic hand muscles. RL-ICMS was applied in two male rhesus macaques while the monkeys performed a number of tasks which resulted in a hand starting position in various positions within the work space. RL-ICMS evoked EMG activity was largely stable in sign, strength, and distribution independent of starting position of the hand. The most common temporal profile of RL-ICMS evoked EMG activity (58% of responses) was a sharp rise to a plateau which was then maintained essentially constant for the entire duration of the stimulus

train. This pattern was qualitatively different from the largely bell-shaped profile of EMG activity associated with natural active movements made over a similar trajectory. Our data support a model in which RL-ICMS produces sustained co-activation of multiple agonist and antagonist muscles which then generates joint movements according to the length-tension properties of the muscles until an equilibrium position is achieved.

INTRODUCTION

Intracortical microstimulation (ICMS) is a high resolution method for studying the organization and function of the motor areas of the brain (Stoney et al., 1968). It is thought to stimulate neurons somewhat indirectly (Gustaffson and Jankowska 1976; Jankowska et al., 1975; Nowak and Bullier 1998a,b; Porter 1963; Rattay 1999; Swadlow 1992; Tehovnik et al., 2006) and, when using low intensities, has a small current spread (Asanuma et al., 1976; Ranck 1975; Shinoda et al., 1976; Stoney et al., 1968). ICMS is a powerful tool that has been used to characterize output from primary motor cortex (M1), pre-motor areas and various brainstem areas to muscles of the limbs (Baker et al., 1998; Boudrias et al., 2006; Cerri et al., 2003; Davidson and Buford 2006; Hummelsheim et al., 1986; Lemon et al., 2002; Moritz et al., 2007; Park et al., 2004; Perlmutter et al., 1998; Schieber 2001), to map the distribution of M1 and pre-motor areas output to muscles of the limbs (Godschalk et al., 1995; Hatanaka et al., 2001; Luppino et al., 1991; Mitz and Wise 1987; Park et al., 2001; Raos et al., 2003) and to characterize the plasticity of motor cortex following injury (Frost et al., 2003; Nudo and Milliken 1996; Schmidlin et al., 2004) or motor skill learning (Kleim et al., 2004; Martin et al., 2005; Nudo et al., 1996).

Although ICMS can be used to study motor control in a detailed way, there is a lack of information which relates ICMS input-output properties to the internal motor program's selection of motor cortex neurons during voluntary

movement. The production of movements related to repetitive long train (500 ms) ICMS (RL-ICMS) has provided interesting new insight to cortical motor output with ICMS (Aflalo and Graziano 2006a,b; Graziano et al., 2002). One result derived from this method was the demonstration that at a single site of stimulation in frontal cortex, RL-ICMS would drive the hand to a consistent final endpoint position regardless of hand starting position. These results could suggest that high level parameters, such as a global representation of movements, are encoded in motor cortex. These studies have served to fuel the muscle versus movement debate that has surrounded M1 as well as spark a new debate concerning the use of long stimulus trains and high stimulus intensities to study motor cortex function (Strick 2002). We understand the urge for caution when interpreting these results as the stimulus may have spread, via synaptic activation, beyond the original site of stimulation.

This complication arises from the fact that M1 is not a homogeneous population of neurons. The subset of CM cells, neurons with direct monosynaptic connections to spinal motoneurons, likely encode muscle activation parameters. However physiological spread of current due to repetitive stimulus trains likely activate muscles indirectly through other pathways; by way of M1 neurons which project to the basal ganglia, cerebellum, red nucleus, reticular formation and other brainstem descending pathways. This makes it difficult to separate muscle activation reflective of

any single pathway. Also, there is no guarantee that RL-ICMS activation of several pathways would reflect the dynamic activation mediated by the internal motor program to generate the same movements.

The mechanism responsible for RL-ICMS evoked movements has not been clarified. Although the technique has been extensively used and has resulted in new conceptual views of motor cortex and its control of movements, there lacks investigation of the evoked muscle activity resultant of RL-ICMS movements. One mechanism that might explain the results of RL-ICMS is that evoked electromyograph (EMG) activation patterns vary depending on the direction of the required joint movement. For example, to achieve the same end-point position of the hand, RL-ICMS might produce activation of flexors and suppression of extensors at a joint for one starting arm posture but the reverse muscle activation pattern for another starting posture where the joint must move in the opposite direction. Another possible mechanism that might explain the results of RL-ICMS is that it produces the same pattern of muscle activation regardless of initial arm posture. In this case, the joint movement would occur as a function of the length-tension properties of the activated muscles and would continue until an equilibrium position was achieved. The objective of this study was to investigate the muscle activation patterns responsible for RL-ICMS evoked movements. We have quantified the extent to which the pattern and magnitude of RL-ICMS evoked EMG activity varies as a function of arm posture.

MATERIALS AND METHODS

Behavioral tasks

RL-ICMS was applied in the left M1 of two male rhesus monkeys (*Macaca mulatta*; ~10kg, 9 years old) while they reached with their right hand for a food reward or a handle placed in various positions within the workspace (Figure 4.1 Aa) or performed a wrist task that 1) alternated between flexion and extension, or 2) was locked into place at two different wrist positions (Figure 4.1 B). During each data collection session, the monkey was seated in a custom built primate chair inside a sound-attenuating chamber. The left forearm was restrained during task performance. All tasks were performed with the right arm/hand.

Hand starting positions of the reaching tasks are illustrated in Figure 4.1 Aa. Monkeys were offered peanuts in various positions around the work space (Numbers in Figure 4.1 Aa). RL-ICMS was delivered as the monkey's hand entered the target starting position, but before the monkey grasped his reward. Alternatively, the monkeys were required to grip a handle fixed to a force transducer (Grass Medical Instruments) on a linear XYZ positioning system. The handle was locked into place at up to 4 different positions within the monkeys work space (letters in Figure 4.1 Aa). RL-ICMS was delivered using handle position as an indicator of starting hand position. Shoulder and elbow angles for each starting hand position from both the whole limb reaching tasks are listed in Table 4.1. Joint angles were measured using

photographs of the monkey's arm at each of the starting hand positions. Digital images were processed in Image J using the shoulder, ribcage, elbow and wrist joints as base points on the body. Final angle measurements are an average from several sessions. Figure 4.1 A illustrates how the shoulder and elbow measurements were made in both the vertical (b) and horizontal (c) plane.

For the wrist tasks (Figure 4.1 B), the monkey's lower and upper arm was restrained. The hand, with digits extended, was placed in a padded manipulandum that rotated about the wrist. The wrist was aligned with the axis of rotation of the torque wheel to which the manipulandum was attached. The monkey was required to alternate between flexions and extensions of the wrist into electronically detected hold zones (15° - 20° in both directions). RL-ICMS was delivered as the position sensor reached the outer boundary of the target hold zone. Alternatively, the manipulandum was locked in place at two different wrist positions including 30 degrees in flexion and 30 degrees in extension. The monkey was required to generate ramp and hold trajectories of wrist torque alternately between flexion and extension target zones. The inner and outer boundaries of the torque window were 0.025 Nm and 0.05 Nm respectively. RL-ICMS was delivered as the force sensor reached the outer boundary of the target hold zone. Since delivery of an applesauce reward was contingent upon the monkey holding within each zone for one second, RL-ICMS was delivered once every 2-3 trials.

Surgical procedures

After training, a 30-mm inside diameter titanium chamber was stereotaxically centered over the forelimb area of M1 on the left hemisphere of each monkey and anchored to the skull with 12 titanium screws (Stryker Leibinger, Germany) and dental acrylic (Lux-it Inc., Blue Springs, MO). Threaded titanium nuts (Titanium Unlimited, Houston, TX) were also attached over the occipital aspect of the skull using 12 additional titanium screws and dental acrylic. These nuts provided a point of attachment for a flexible head restraint system during data collection sessions. The chambers were centered at anterior 16 mm, lateral 18 mm (Monkey V), and anterior 16 mm, lateral 22 mm (Monkey A), at a 30° angle to the sagittal plane.

EMG activity was recorded from 24 muscles of the forelimb with pairs of insulated, multi-stranded stainless steel wires (Cooner Wire, Chatsworth, CA) implanted during an aseptic surgical procedure (Park et al., 2000). Pairs of wires for each muscle were tunneled subcutaneously from an opening above the elbow to their target muscles. The wires of each pair were bared of insulation for ~ 2 - 3 mm at the tip and inserted into the muscle belly with a separation of ~ 5 mm. Implant locations were confirmed by stimulation through the wire pair and observation of appropriate muscle twitches. EMG connector terminals (ITT Cannon, White Plains, NY) were affixed to the upper arm using medical adhesive tape. Following surgery, the monkeys wore a

Kevlar jacket (Lomir Biomedical Inc., Malone, NY) reinforced with fine stainless steel mesh (Sperian Protection Americas Inc., Attleboro Falls, MA) to protect the implant. EMG activity was recorded from five shoulder muscles: pectoralis major (PEC), anterior deltoid (ADE), posterior deltoid (PDE), teres major (TMAJ), and latissimus dorsi (LAT); seven elbow muscles: biceps short head (BIS), biceps long head (BIL), brachialis (BRA), brachioradialis (BR), triceps long head (TLON), triceps lateral head (TLAT) and dorso-epitrochlearis (DE); five wrist muscles: extensor carpi radialis (ECR), extensor carpi ulnaris (ECU), flexor carpi radialis (FCR), flexor carpi ulnaris (FCU), and Palmaris longus (PL); five digit muscles: extensor digitorum communis (EDC), extensor digitorum 2 and 3 (ED2,3) extensor digitorum 4 and 5 (ED4,5), flexor digitorum superficialis (FDS), and flexor digitorum profundus (FDP); and two intrinsic hand muscles: abductor pollicis brevis (APB) and first dorsal interosseus (FDI).

All surgeries were performed under deep general anesthesia and aseptic conditions. Postoperatively, monkeys were given an analgesic (Buprenorphine 0.5 mg/kg every 12h for 3-4 days) and antibiotics (Penicillin G, Benzathaine / Procaine combination, 40,000 IU/kg every 3 days). All procedures were in accordance with the Association for Assessment and Accreditation of Laboratory Animal Care (AAALAC) and the Guide for the Care and Use of Laboratory Animals, published by the US Department of Health and Human Services and the National Institutes of Health.

Data collection

Sites in M1 were stimulated using glass and mylar insulated platinum-iridium electrodes with impedances ranging from 0.5 to 1.5 M Ω (Frederick Haer & Co., Bowdoinham, ME). The electrode was positioned within the chamber using an X-Y coordinate manipulator and was advanced at approximately a right angle into the cortex with a manual hydraulic microdrive (Frederick Haer & Co., Bowdoinham, ME). Rigid support for the electrode was provided by a 22 gage cannula (Small Parts Inc., Miami Lakes, FL) inside of a 25 mm long, 3 mm diameter stainless steel post which served to guide the electrode to the surface of the dura.

First cortical unit activity was noted and the electrode was lowered 1.5 mm below this point to layer V. In order to distinguish layer V from more superficial layers, particularly in the bank of the precentral gyrus, neuronal activity was evaluated for the presence of large action potentials that were often modulated with the task and stimulus-triggered averages (StTAs) for the presence of both clear and robust effects at 15 μ A. Individual stimuli were symmetrical bi-phasic pulses: a 0.2 ms negative pulse followed by a 0.2 ms positive pulse. EMG activity was generally filtered from 30 Hz to 1 KHz, digitized at a rate of 4 kHz and full-wave rectified. Stimuli (15, 30, 60 and 120 μ A) were applied throughout all phases of the task.

- Stimulus-triggered averages

Layer V sites in forelimb M1 were identified and microstimuli were applied at 15 Hz. The assessment of StTA effects was based on averages of at least 500 trigger events. Segments of EMG activity associated with each stimulus were evaluated and accepted for averaging only when the mean of all EMG data points over the entire 60 msec epoch was $\geq 5\%$ of full-scale input. This prevented averaging segments in which EMG activity was minimal or absent (McKiernan et al., 1998). EMG recordings were tested for cross-talk by computing EMG-triggered averages (Cheney and Fetz, 1980). This procedure involved using the EMG peaks from one muscle as triggers for compiling averages of rectified EMG activity of all other muscles. To be accepted as a valid post-stimulus effect; the ratio of PStF between test and trigger muscle needed to exceed the ratio of their cross-talk peaks by a factor of two or more (Buys et al., 1986). Based on this criterion, none of the effects obtained in this study needed to be eliminated.

- RL- ICMS triggered averages

Layer V sites with clear StTA effects in forelimb muscles were identified and selected for data collection with RL-ICMS. RL-ICMS consisted of a train of 100 symmetrical biphasic stimulus pulses at 200 Hz (500 ms). The assessment of effects was based on averages of 4 - 8 trigger events.

Data analysis

At each stimulation site, averages were obtained for all 24 muscles. The onset latency of the post-stimulus effect was based on visual inspection of the record and was marked where the activity inflected relative to the pre-trigger baseline of EMG. Baseline EMG level was measured from the pre-trigger period in all averages.

- Stimulus-triggered averages

Averages were compiled over a 60 ms epoch, including 20 ms before the trigger to 40 ms after the trigger. Post-stimulus facilitation (PStF) and post-stimulus suppression (PStS) effects were computer-measured as described in detail by Mewes and Cheney (1991, 1994). Nonstationary, ramping baseline activity was subtracted from single pulse ICMS triggered averages using custom analysis software. Mean baseline activity and the standard deviation (SD) of baseline EMG activity was measured from the pre-trigger period typically consisting of the first 12.5 ms of each average. Single pulse ICMS triggered averages were considered to have a significant post-stimulus effect (PStF or PStS) if the points of the record crossed a level equivalent to 2 SD of the mean of the baseline EMG for a period ≥ 0.75 ms or more (Park et al., 2001). The magnitude of PStF and PStS was expressed as the percent increase (+ ppi) or decrease (- ppi) in EMG activity above (PStF)

or below (PStS) baseline EMG activity (Cheney and Fetz, 1985; Kasser and Cheney, 1985; Cheney et al., 1991).

- RL-ICMS triggered averages

RL-ICMS triggered averages were compiled over a 1.2 s epoch, including 200 ms before the trigger to 1,000 ms after the trigger. Mean baseline activity was measured from the pre-trigger period typically consisting of the first 100 ms of each average. The first pulse of each train was used as a trigger to compute averages of EMG activity. The magnitude of the EMG response was expressed as the mean EMG level present after the first RL-ICMS pulse and throughout the stimulus train. In addition, the magnitude of the EMG response was measured for the first and last 100 ms of the stimulus train.

Imaging

Structural MRIs were obtained from a 3 Tesla Siemens Allegra system. Images were obtained with the monkey's head mounted in an MRI compatible stereotaxic apparatus so the orientation and location of the cortical recording chamber and electrode track penetrations could be determined. A two-dimensional rendering of experimental sites was constructed for each monkey. The method for flattening and unfolding cortical layer V in the anterior bank of the central sulcus has been previously described in detail

(Park et al., 2001). Briefly, the cortex was unfolded and the location of experimental sites were mapped onto a two dimensional cortical sheet based on the electrode's depth and X-Y coordinate, known architectural landmarks, MRI images, and observations noted during the cortical implant surgeries.

Statistical data analysis

Effects of starting hand position changes tasks were compared using the Student's *t*-test, the Mann-Whitney Rank Sum Test and linear regression. In all tests, statistical significance was assumed if the P value was ≤ 0.05 .

RESULTS

Data were obtained from the left M1 cortex in two rhesus monkeys. RL-ICMS (200 Hz, 500 ms) triggered averages of EMG activity were collected at a total of 42 sites while the monkeys performed one of the tasks (Figure 4.1). This included 14 sites in monkey V (Figure 4.2 A) and 28 sites in monkey A (Figure 4.2 B). Figure 4.2 A&B show the RL-ICMS stimulation sites overlaid on the monkey's respective muscle maps (see Chapter 3 for details). Sites where RL-ICMS triggered averages were obtained while the monkeys performed one of the whole limb tasks (reach for peanuts or handle) are marked with white dots and wrist tasks (isometric and concentric) are marked with grey dots. StTAs of EMG activity (15 μ A – 120 μ A @ 15 Hz) were performed before each series of RL-ICMS experiments to verify the intra-areal muscle representation and for comparison with RL-ICMS averages of EMG activity.

Movements elicited with RL-ICMS

RL-ICMS was delivered as the monkey's hand reached the target starting position. For the reaching tasks, this was just before the monkey grasped his food reward or as the monkey put his food reward into his mouth. Alternatively RL-ICMS was delivered while the monkey's hand was on the push-pull handle. The offered food reward or handle were used to accurately replicate starting hand position around the monkey's work space while

maximizing the change in elbow and shoulder angles. Joint angles associated with each starting hand position can be found in Table 4.1.

RL-ICMS was applied to 32 sites with 60 μ A or 120 μ A while the monkeys performed the whole limb tasks. Most sites (29/32) were in the proximal and proximal-distal forelimb representation, as that is where whole limb movements were most likely produced. In 94% of sites tested (30/32), the arm movements drove the hand to converge toward a final common endpoint regardless of starting hand position. RL-ICMS elicited arm movements resulted in the hand being brought toward the midline of the monkey at 10 sites, toward the contralateral side at 14 sites and down from the starting position at 6 sites. RL-ICMS elicited movements at these sites often involved more than one joint. A full range of shoulder and elbow movements were observed including elbow flexion, elbow extension, shoulder abduction, shoulder adduction and shoulder rotation. RL-ICMS was applied to 10 sites in the distal only muscle representation. Wrist extension and full digit flexion (resulting in the hand taking on a fist appearance) were the only distal movements observed with RL-ICMS with the exception of one site which produced movement toward flexion for the first part of the stimulus and eventually ended with the wrist in extension. Since this study did not fully explore the distal muscle representation of both monkeys, it is possible that sites exist that would produce full flexion of the wrist and extension of the digits.

RL-ICMS evoked EMG activation patterns

A total of 2,736 RL-ICMS triggered averages of EMG activity were analyzed yielding 1,498 RL-ICMS evoked EMG activity patterns. Figure 4.3 illustrates the different temporal patterns of EMG activity elicited from RL-ICMS in M1 and shows the most common (Tonic: 58% of all responses) was a sharp rise to a plateau which was essentially constant for the entire duration of the stimulus train. The second most common pattern (Phasic-Tonic: 14% of all responses) was an initial burst of activation followed by a decline to a plateau which was then constant for the duration of the stimulus. These two activity patterns combined (72% of all responses) may be typical of movements performed which require holding a position against a load, however they are not the typical bell shaped patterns associated with reaching to a target. Similarly, most suppression effects (9.5% of all responses) were sharp and immediate (relative to stimulus onset) and occasionally a gradual decline to full suppression was observed (16% of all suppression effects). The activity patterns we characterized as phasic, ramp and delayed ramp are similar to activation patterns associated with reaching movements, however they accounted for only 13% of the total responses observed. Therefore, if the phasic, ramp and delayed ramp patterns are showing a natural activation of muscles by RL-ICMS, it is not the typical mechanism. It is possible that muscles activated in a tonic or phasic-tonic

pattern are being activated by the stimulus in the most direct route to the motoneurons and the other patterns are reaching the motoneuron pools through an indirect route (physiological spread of current).

Since the presence of clear post-stimulus effects demonstrate a strong functional connection between a cluster of neurons surrounding the microelectrode and their target muscles, we wondered if the presence of post-stimulus effects in StTAs were more likely to predict the presence of a tonic or phasic-tonic activity pattern when using the RL-ICMS stimulus parameters. At 27 sites where RL-ICMS and StTAs were performed back to back at the same stimulus intensity, 80% of muscles with a clear post-stimulus effect showed the tonic or phasic-tonic activation pattern. Only 56% of muscles showed the tonic or phasic-tonic activation patterns when there was no PStF present. Similarly, does the absence of a post-stimulus effect predict the occurrence of the phasic, ramp, phasic ramp or delayed ramp activation pattern? Only 12% of muscles with clear post-stimulus effects present in the StTA displayed these four activation patterns during RL-ICMS compared to 20% of muscles without a post-stimulus effect present.

Stability of RL-ICMS evoked EMG activation patterns

All eight EMG activity patterns were present in both proximal and distal muscles during performance of both the reaching tasks and the wrist tasks. The presence of eight qualitatively different activity patterns shows that RL-

ICMS is capable of eliciting various muscle activation patterns; not just tonic activation or suppression. Therefore, there is a possibility that RL-ICMS evokes different activation patterns at different starting positions of the hand. One important question concerning RL-ICMS is whether or not the EMG activation patterns evoked at different starting hand positions display time and position dependent modulation as occur for the monkey's own active movements. One way to assess the variation in RL-ICMS evoked EMG activity was to determine how stable the sign of effects were for each muscle at all starting hand positions tested. In 98% (2,211/2,256) of RL-ICMS triggered averages, the same sign of effect was present (facilitation, suppression, no effect) and independent of starting hand positions associated with the reaching tasks. Similarly, in 98% (468/480) of RL-ICMS triggered averages, the same sign of effect was present independent of starting hand positions associated with the wrist tasks. This reflects the stability of the sign and distribution of cortical motor output in terms of activated muscles from RL-ICMS.

Another way to assess the variation in RL-ICMS evoked EMG activity was to determine how stable the patterns of activation were for each muscle at all starting hand positions tested. Limiting the analysis to the muscles which displayed a qualitatively characterized activation pattern, 66% (367/551) showed the same RL-ICMS evoked EMG activity pattern for all starting hand positions tested during the reach task and 62.5% (75/120) were

the same for the two starting hand positions of the wrist tasks. Typically, two to four different hand starting positions were tested to maximize the change of each joint angle. For example, to maximize the change in shoulder angle, starting hand positions 1 and 2 were tested. Alternatively, A and D or B and C were used. To maximize the change in elbow angle, starting hand positions 3 and 4 were tested. To maximize the change in wrist angle, the wrist tasks were used. At one site, a large number of hand starting positions were tested using the whole arm reach task. Figure 4.4 shows this example. This site was one in which RL-ICMS consistently drove the hand to the mouth. The variability of EMG activation patterns can be seen in the EMG records. Only 35% (8/23) of muscles at this site show the same EMG activation patterns at all seven hand starting positions. Muscles TMAJ, TLAT, DE, FCU, PL, ECU, ED23 and ED45 consistently show tonic activation patterns for all starting hand positions. Interestingly, if the analysis is limited to comparing EMG activation patterns associated with hand starting positions 1 and 2 (extreme shoulder positions that also straddle the end point position) the percentage of muscle match improves with the addition of muscles PEC, LAT, BR, EDC, FDP, FDS, FCR, ECR and FDI to 74%. Also, if the analysis is limited to comparing the EMG activation patterns associated with hand starting positions 3 and 4 (extreme elbow positions) the percentage of muscle match improves with the addition of PEC, LAT, ADE, BIL, FDP, ECR and EDC to 65%.

Thus far, the analysis of RL-ICMS evoked EMG activity has focused on qualitative measures of the effects. Another way to analyze the RL-ICMS evoked effects in EMG is to measure the EMG activation level associated with the stimulus and determine if it is stable with different hand starting positions. Figure 4.5 illustrates the measures of RL-ICMS evoked mean EMG levels across the hand starting positions that produced the two most extreme shoulder angles (Figure 4.5 A), the two most extreme elbow angles (Figure 4.5 B) and the two most extreme wrist angles (Figure 4.5 C). Not only were the mean EMG levels highly correlated across shoulder ($R = 0.95$), elbow ($R = 0.96$) and wrist ($R = 0.96$) angles, but also the regression slopes associated with the shoulder, elbow and wrist angle measurements were close to one (range = 0.96 - 1.06). Since these measures are of the entire RL-ICMS effect, they do not take into account the fact that the activity patterns may be different for each of the starting hand positions. For example, in a scenario where ADE showed ramp activation when the hand started at position 1 and decrementing ramp activation when the hand started at position 2, the measured mean EMG activation could still be the same assuming the amplitude and slope of the effects were similar. In order to take the possible difference in activity patterns and onset-offset latencies into account we also measured the first and last 100 ms of the EMG triggered averages (relative to onset and offset of the stimulus) for comparison across starting hand positions which produced the largest change in joint angles. Similar to the

overall mean comparisons, the mean EMG levels for the first and last 100ms of each record were highly correlated across shoulder ($R = 0.90; 0.94$), elbow ($R = 0.91; 0.98$) and wrist ($R = 0.92; 0.96$) angles respectively. Clearly the last 100ms of the records are more similar than are the first 100 ms. This likely reflects the fact that the first 100 ms of the records are the most sensitive to differences in activity patterns and onset latencies. On the other hand, the last 100ms of the records are more stable. This could be due in part to the increased probability that the stimulus evoked component of cortical output has become the dominant process. The regression slopes associated with the shoulder, elbow and wrist measures were close to one (range = 0.91 – 1.20).

Thus far, the data analysis has included all the activated muscles at each site stimulated. Since there is evidence that changes in arm posture or proximal joint positions may affect muscles at other joints (Ginanneschi et al., 2005; 2006) we feel this type of broad analysis is an important part of studying RL-ICMS effects on muscles. However, there is a possibility that RL-ICMS effects are more prominent on the muscles where individual joint angle changes for individual hand starting positions were greatest. For example, starting hand positions 1 and 2 achieve the largest difference in shoulder angle and may affect shoulder muscles more prominently than elbow, forearm or hand muscles. In order to test this possibility, we have divided the data into subsets of muscle groups. Table 4.2 summarizes the

stability of EMG activity patterns at different hand starting positions for muscles at different joints. The percentage of matching EMG activity patterns showed similar levels of stability for individual muscle groups as did all muscles when evaluated at different starting hand positions. However the mean EMG level measurements for only the first 100 ms of the records showed similar correlations for digit and wrist muscles across the two wrist positions ($R = 0.92$ and $R = 0.93$). The regression slope for this measurement was very close to one (1.14). Shoulder and elbow muscles showed lower correlations across the two most extreme shoulder and elbow angles ($R = 0.90$ versus $R = 0.75$; $R = 0.91$ versus $R = 0.88$) respectively. Similarly, the regression slopes associated with these measures decreased (shoulder = 0.75; elbow = 0.94). The correlation coefficients associated with mean EMG level measurements for the last 100 ms either stayed the same (digit and wrist muscle group) or decreased (shoulder and elbow muscles groups). The regression slopes associated with all three joint angle measures were close to one (range = 0.93 – 1.04).

Although a large percentage of RL-ICMS effects show stability in the evoked EMG activation pattern and mean EMG levels, some disparities exist. Is there a difference between proximal and distal muscles? Since M1 neurons send more monosynaptic projections to the distal muscle motoneuron pools than to those of the proximal muscles, RL-ICMS could be directly activating distal muscles more often than proximal muscles.

However, when comparing the RL-ICMS evoked EMG activation pattern's onset latencies for each of the three muscle groups from table 4.2, the activity pattern's onset latencies were comparable for all three groups with the wrist and digit muscles having a slightly higher percentage of onset latencies below 40ms (74%) compared to the elbow muscles (66%) and shoulder muscles (64%). Elbow muscles showed the highest percentages of tonic and phasic-tonic activation patterns (70%) compared to the wrist and digit muscles (58%) and the shoulder muscles (39%).

We have shown that RL-ICMS does elicit different EMG activation patterns across 34% of effects observed at different hand starting positions. Do these cases show consistent patterns that would indicate RL-ICMS can produce muscle activity in a reproducible and functionally meaningful way? One way to test this would be to look at a subset of data where the hand was consistently driven to a center point around which different starting hand positions straddling the endpoint could be tested. In this study, no sites were observed which drove the hand to a neutral wrist or elbow position, however 10 sites drove the hand to the midline of the monkey's body (in front of the face or abdomen). Since starting hand positions 1 and 2 were used to test all 10 of these sites and straddle the midline of the monkey's body, we have an opportunity to test this possibility. Analysis was limited to the 38 effects observed in the shoulder muscles, at starting hand positions 1 and 2. In 58% of effects, the same RL-ICMS evoked EMG activation pattern was observed.

Sixteen muscles showed different activation patterns across the two hand starting positions. In order for the muscle activation patterns to be functionally relevant, TMAJ, LAT and PDE should show activation when the hand is at starting position 1 and either a decrease in activation or suppression when the hand is at starting position 2. This was found to occur in four cases (44%). In two instances involving PDE and two instances involving TMAJ, a tonic effect or no effect was observed for starting hand position 1 and a suppression effect was present at starting hand position 2. However, the mean EMG activation levels present in TMAJ, LAT and PDE during RL-ICMS at these sites were highly correlated ($R = 0.88$) and the regression slope was close to one. Also, ADE and PEC should show the opposite pattern (decreased activation when the hand is at starting position 1 and increased activation at starting hand position 2). In two instances involving ADE that scenario was observed (29%). Similarly, the overall mean EMG activation levels present in ADE and PEC during RL-ICMS at these sites were highly correlated ($R = 0.88$) and the regression slope was close one.

What is producing different patterns of activation in muscles at different hand starting positions (34% of effects observed at different hand starting positions of the reach task and 37.5% of effects observed at different hand starting positions of the wrist task)? These results have shown that the patterns of activation of shoulder muscles are only functionally related to

achieving a final endpoint position in 37.5% (6/16) of observed instances. Could there be another explanation behind the presence of unstable activation patterns? One possibility could be that as the limb is moving toward the final hand endpoint position, afferent feedback to the motoneuron pool changes and is reflected in the recorded EMG activation pattern. A subset of our data is particularly relevant to this issue because RL-ICMS was performed during conditions of the isometric wrist task (forelimb, wrist and digits are locked in place) and the concentric wrist task (rotation about the wrist was the only movable joint). When the analysis was limited to only the wrist muscles, the patterns of activation were more likely to be stable when the wrist was locked into place (78%) than when the wrist was able to move in response to the RL-ICMS stimulus (40%). This could suggest that feedback about dynamic joint movement affects the EMG activation patterns.

Figure 4.6 shows a site where RL-ICMS was delivered during both the isometric and concentric task conditions. This site is exemplary of the stability of RL-ICMS effects but was also interesting because RL-ICMS produced wrist extension when the hand started at flexion 30 degrees and flexion for the first half of the stimulus, when the hand started at extension 30 degrees. The hand was not driven to an endpoint position in the middle of the two positions however because after 250 ms of the RL-ICMS stimulus, the movement switched and drove the hand to a final endpoint near 30 degrees of extension. The first two columns show the RL-ICMS activation patterns

associated with the concentric wrist task and the last two are the isometric wrist task. The second column shows the RL-ICMS activation patterns while the monkey performed the concentric wrist task and therefore the stimulus produced movement toward flexion (first 250 ms) and extension (last 250 ms). One interesting note about this column is that RL-ICMS caused movement in two opposite directions for the first half and last half of the stimulus duration. However, that fact does not reveal itself in the RL-ICMS produced EMG activation patterns. This was a site which showed 92% (11/12) stability across the EMG activation patterns associated with the isometric tasks (FCU was inconsistent). Only 75% (9/12) of activity patterns were stable with the concentric task. The inconsistent effects were observed in FDS, FCR and PL. Although the inconsistent effects follow the necessary functional pattern associated with RL-ICMS driving the wrist to extension (suppression of flexors in the flexion 30 degree target), the same pattern is not observed with the isometric task conditions.

DISCUSSION

We present data that support the finding that RL-ICMS produces movements of the forelimb and that these movements are capable of driving the hand to a final endpoint position independent of starting position (Graziano et al., 2002, 2005). These results are subject to two possible interpretations. One, the arm movements are the result of the stimulus activating a natural brain circuit. In this case, RL-ICMS produces muscle activation patterns that resemble the natural muscle activation scheme of the motor program. If this hypothesis is correct, RL-ICMS output to muscles will show position dependent variability. The second is that the stimulus indiscriminately activates the descending inputs available to it, resulting in a broad co-activation of forelimb muscles. In this case, stimulus output to muscles will be stable and independent of changes in limb posture. We further investigated the EMG activation patterns associated with RL-ICMS initiated movements to determine whether they were position dependent or stable.

RL-ICMS output to muscles is stable

Data presented here demonstrate that the EMG activation patterns associated with generating hand movements to a final common endpoint are largely stable (98%) in sign of effect (facilitation, suppression or no effect). This demonstrates that at any single site in M1, RL-ICMS consistently

activated the same set of muscles regardless of the starting or ending hand position. Further, RL-ICMS did not activate a set of agonist muscles for movements in one direction and antagonists for movements in the opposite direction. Arm posture or joint angle changes rarely caused opposing muscle activation patterns in the same muscle (facilitation at one starting hand position and suppression at another).

Further, varying starting hand position did not change the magnitude of RL-ICMS evoked muscle activity. The magnitudes of the RL-ICMS elicited effects were correlated at different hand starting positions that produced the largest joint angle changes in shoulder ($R = 0.95$), elbow ($R = 0.96$) and wrist ($R = 0.96$). Further, the regression lines fit to the points which compared the magnitudes had slopes which were close to one across extreme shoulder (0.98), elbow (0.96) and wrist (1.06) joint positions. When the analysis was limited to muscles showing the most displacement from joint angle changes across starting hand positions, the magnitude of effects were correlated (Shoulder $R = 0.88$, Elbow $R = 0.92$, Wrist $R = 0.95$) and regression line slopes were close to one (Shoulder $R = 0.91$, Elbow $R = 1.13$, Wrist = 1.06). This demonstrates that at any single site in M1, RL-ICMS activated muscles to the same level of activity independent of the starting or ending hand position. In other words, RL-ICMS did not produce stronger activation of agonist muscles for movements in one direction and weaker activation of the same muscles for movements in the opposite direction. Arm posture or joint

angle changes rarely caused disparate muscle activation levels in the same muscle (high level at one starting hand position and low level at another).

These results conflict with those of Graziano and colleagues (2002, 2004) who reported changes in output effects as a function of elbow joint angle. Their studies involved recording RL-ICMS elicited activity from biceps and triceps at different elbow angles. They reported that stimulus elicited effects became stronger as the muscles were lengthened. One potentially important difference between our approaches is that Graziano and colleagues collected their EMG data with the monkey under ketamine anesthesia. It is feasible that in the absence of voluntary movement and related modulation of spinal cord inputs, motoneuron excitability might become more heavily dominated by spindle afferent input associated with joint angle changes.

Mechanism of RL-ICMS evoked movements

RL-ICMS produced 8 patterns of muscle activation, none of which could be considered the triphasic EMG activity pattern typical of fast reaching movements (Brown and Cooke 1990; Lestienne 1979; Sanes and Jennings, 1984). Few were characterized as biphasic (phasic ramp; 2%) or bell shaped (phasic or delayed ramp; 8%). The most common EMG activation pattern observed (58% of all responses) was tonic activation; characterized as a sharp rise to a plateau which was maintained throughout the duration of the stimulus train. The tonic activation pattern produced by RL-ICMS was

observed in both proximal and distal muscles independent of starting hand position. This type of tonic co-activation is not typical of the natural activation patterns characteristic of reaching movements. When RL-ICMS triggered averages did display different qualitative effects at different starting hand positions, there was no consistent muscle activation relationship between prime mover agonist and antagonists to suggest the final hand endpoint was produced in a functionally meaningful way.

The occurrence of other temporal EMG patterns in addition to tonic activation and suppression could be due to pathway excitability changes due to lengthening and shortening of muscles during dynamic movement. It is likely that afferent feedback to the motoneuron pool is present during RL-ICMS produced movements, but is visible in the EMG activation patterns when there were weaker or fewer routes present for the stimulus to activate motoneurons. In addition, if the stimulus is reaching the motoneuron pool through mostly indirect routes (through physiological activation of brainstem descending systems or spinal inter-neurons) the changing levels of motoneuron excitability likely add to the instability of the EMG activation profiles.

Our data suggest that RL-ICMS activates muscles with synaptic connections to the cortical site stimulated. RL-ICMS output effects obtained at individual sites in M1 were consistent across different starting hand positions, with reference to both the set of muscles activated and the

activation levels of those muscles. The stimulus elicited co-activation of multiple forearm muscles produces active forces against the joints resulting in movements of the arm. The amount of force each muscle generates is dependent on its length (Gordon et al., 1966) and level of activation (Rothwell, 1994). Length-tension curves describe the change in muscle length, plotted as change in joint angle, given the level of activation associated with two prime mover muscles. The intersection of two length-tension curves represents the equilibrium position of the joint where the joint torque produced by flexors equals the opposing torque produced by extensors (Rothwell, 1994). Muscle tension is known to be linearly related to the mean level of EMG activity (Milner-Brown and Stein 1975). The slopes of the length-tension curves can be shifted upwards or downwards depending on the level of muscle activation.

Figure 4.7 illustrates how the length-tension relationships of biceps and triceps interact to specify elbow joint angle. The solid line represents the length-tension curve of biceps and the dotted line triceps at given muscle activity levels. The grey squares represent the levels of muscle tension produced by biceps and triceps at the starting hand positions which produce a certain elbow angle (y-axis). Given this level of RL-ICMS evoked biceps and triceps activity, these muscles will produce movement from any starting hand position to a final hand position reflecting the equilibrium position; represented by the black square. For example, with starting hand position 1, triceps

tension is greater than biceps. Triceps will shorten along its length-tension curve as biceps lengthens (indicated by heavy arrows) until the forces produced by both muscles reaches equilibrium. With starting hand position 2, biceps tension is greater than triceps. Biceps will shorten along its length-tension curve as triceps lengthens (indicated by light arrows) until the forces reach equilibrium. A different level of RL-ICMS evoked EMG activity would produce a different set of length-tension curves, resulting in movement to a new final hand position reflecting the equilibrium position between those forces. Our data shows RL-ICMS produces essentially the same level of muscle activity independent of starting hand position. Therefore, RL-ICMS produces the same final posture because the forces acting upon the joints are largely the same. This result need not be dependent on a cortical circuit encoding hand positions; instead our results reflect the biomechanical forces acting upon the limb. In conclusion, our data support a model in which RL-ICMS produces sustained co-activation of multiple agonist muscles which then generate joint movements according to their length-tension properties until an equilibrium position is achieved. The final hand endpoint position represents the equilibrium position of forces acting at the forearm joints due to all activated muscles at a given cortical site.

Table 4.1. Joint angles achieved with different hand starting positions

1. Hand starting positions	2. Joint	3. Angle
A.	Shoulder	50° Horizontal Plane
		115° Vertical Plane
	Elbow	105° Horizontal Plane
B.	Shoulder	50° Horizontal Plane
		125° Vertical Plane
	Elbow	115° Horizontal Plane
C.	Shoulder	110° Horizontal Plane
		125° Vertical Plane
	Elbow	135° Vertical Plane
D.	Shoulder	110° Horizontal Plane
		115° Vertical Plane
	Elbow	120° Vertical Plane
1.	Shoulder	50° Horizontal Plane
		120° Vertical Plane
	Elbow	70° Vertical Plane
2.	Shoulder	110° Horizontal Plane
		120° Vertical Plane
	Elbow	70° Vertical Plane
3.	Shoulder	90° Horizontal Plane
		120° Vertical Plane
	Elbow	170° Vertical Plane
4.	Shoulder	90° Horizontal Plane
		120° Vertical Plane
	Elbow	90° Vertical Plane
5.	Shoulder	90° Horizontal Plane
		90° Vertical Plane
	Elbow	90° Vertical Plane

Angles estimated to the nearest 5 degrees.

Letters represent starting hand positions of the push pull task.

Numbers represent starting hand positions of the reach task.

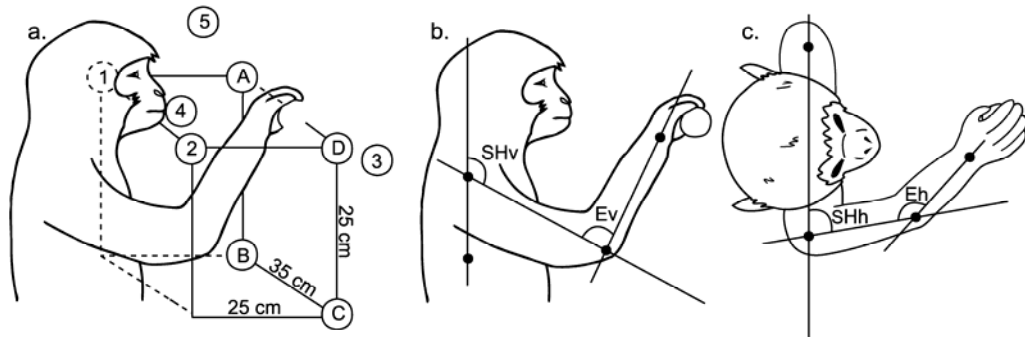
See Figure 4.1 for identification of starting hand positions

Table 4.2. Stability of RL-ICMS evoked EMG activity

Joint	Starting Hand Positions	# Cortical Sites	N	Stable EMG Activity Pattern	Correlation 1 st 100ms	Correlation Last 100ms
Shoulder	1 and 2	28	94	76%	R = 0.75	R = 0.91
Elbow	3 and 4	9	46	69%	R = 0.80	R = 0.91
Wrist	Flexion and Extension	10	70	64%	R = 0.93	R = 0.96

Figure 4.1. Illustrations depicting the tasks used to study the EMG activation patterns associated with RL-ICMS of M1. A) Whole limb tasks a. Numbered circles depict hand starting positions when the monkeys reached for peanuts. Lettered circles depict hand starting positions when the monkeys reached for a handle. The second two illustrations depict how the joint angles were measured for the b. vertical shoulder angle (SHv), vertical elbow angle (Ev), c. horizontal shoulder angle (SHh) and horizontal elbow angle (Eh). B) Wrist flexion and extension positions of the wrist tasks.

A. Whole Limb Tasks



B. Wrist Tasks

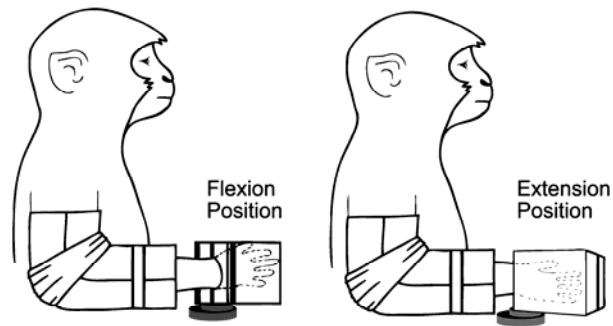


Figure 4.2. Experimental sites used to study EMG activity patterns associated with RL-ICMS of primary motor cortex. A,B) Sites where RL-ICMS triggered EMG activity was collected with the whole limb tasks (white circles) and the wrist tasks (grey circles) represented in two-dimensional coordinates after unfolding the precentral gyrus and overlaid on the monkey's respective muscle map.

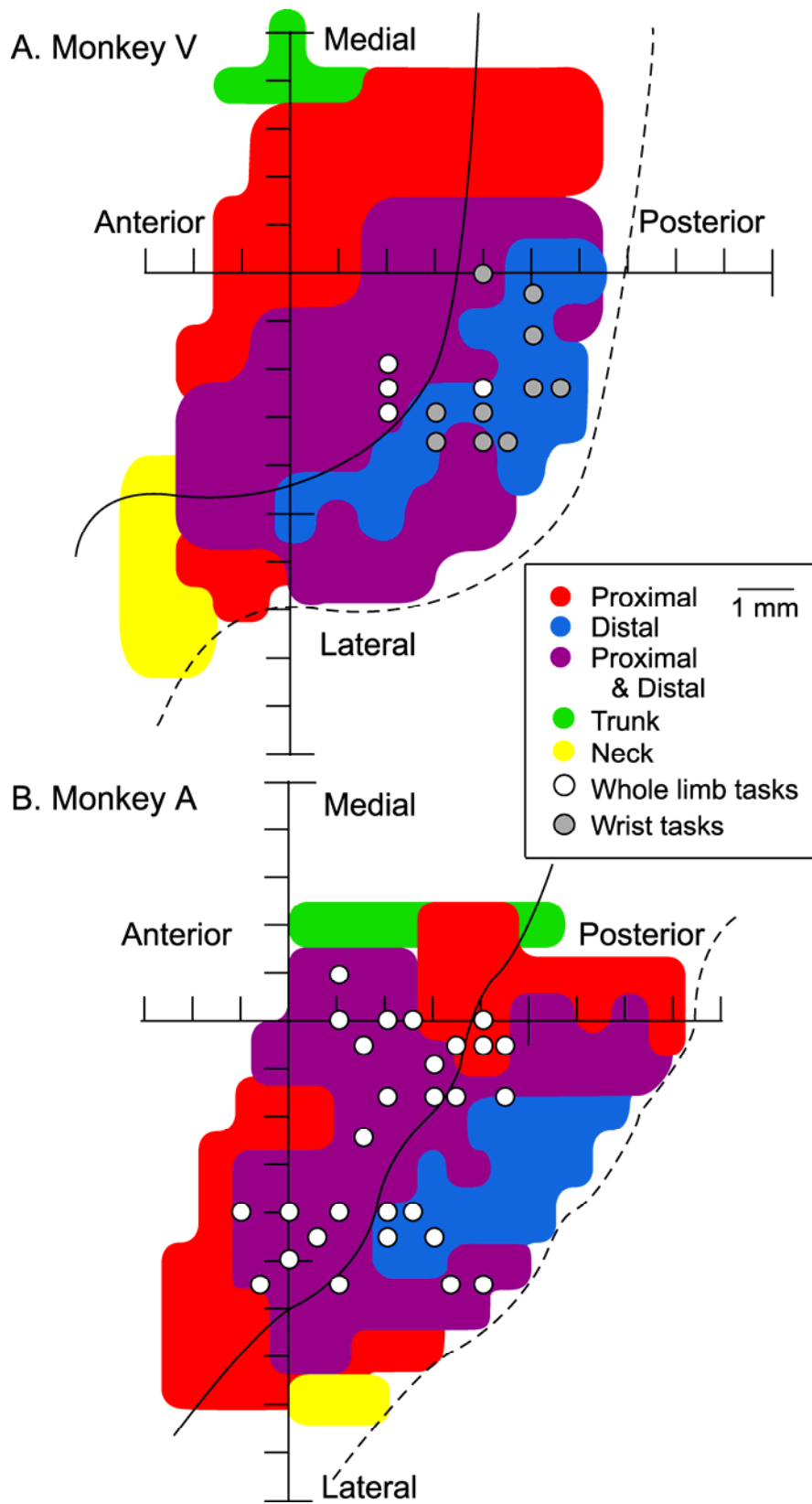


Figure 4.3. Qualitative characterization of EMG activity patterns evoked with RL-ICMS and the percentage of their occurrence during performance of the whole limb and wrist tasks. Grey bar represents 500 ms stimulus train.

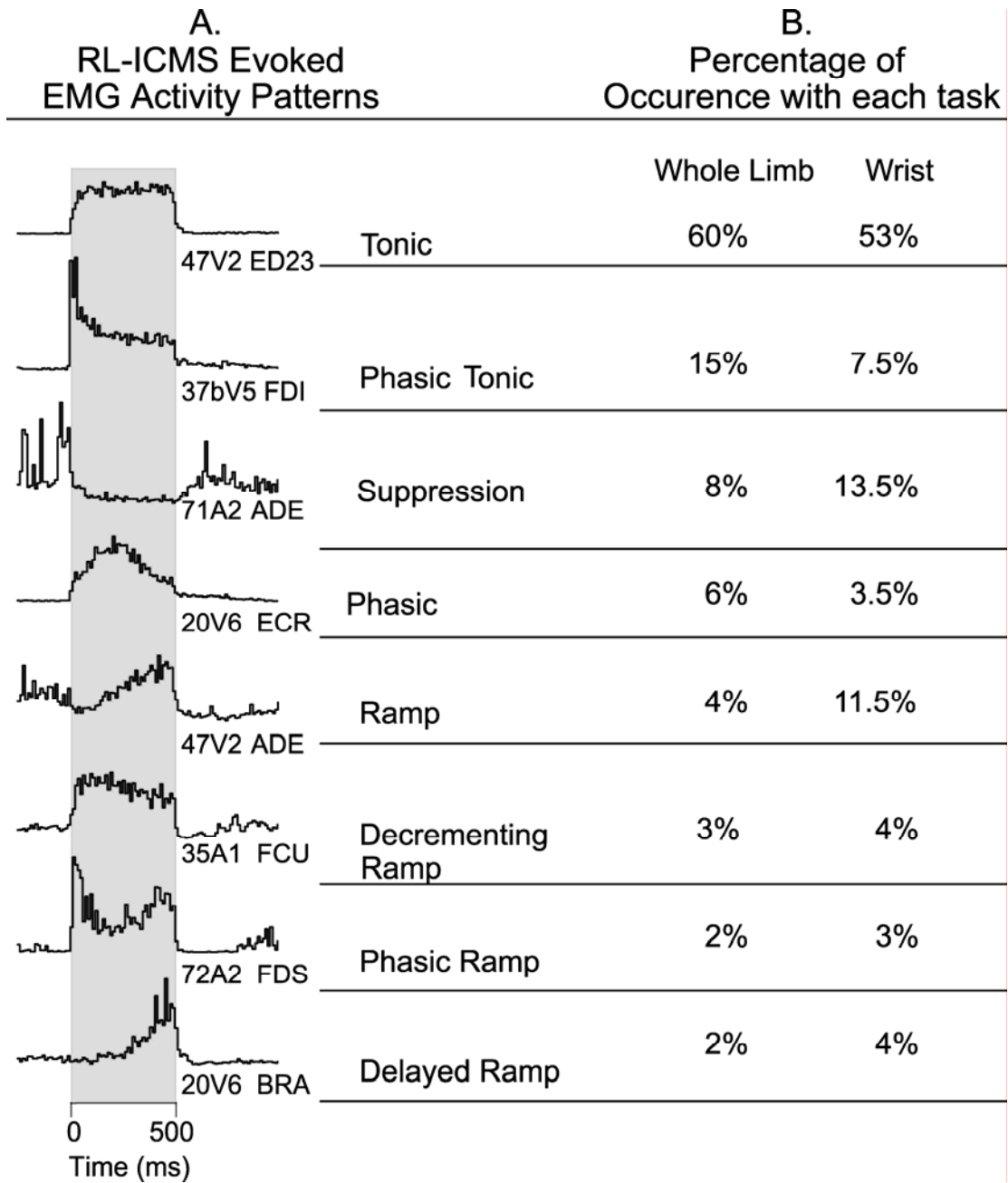


Figure 4.4. RL-ICMS elicited EMG activation patterns associated with 7 starting hand positions at a layer V site. Numbered and lettered circles represent the starting hand positions within the monkey's work space as depicted in figure 4.1. Grey bar represents 500 ms stimulus train. Each muscle is calibrated across all starting hand positions.

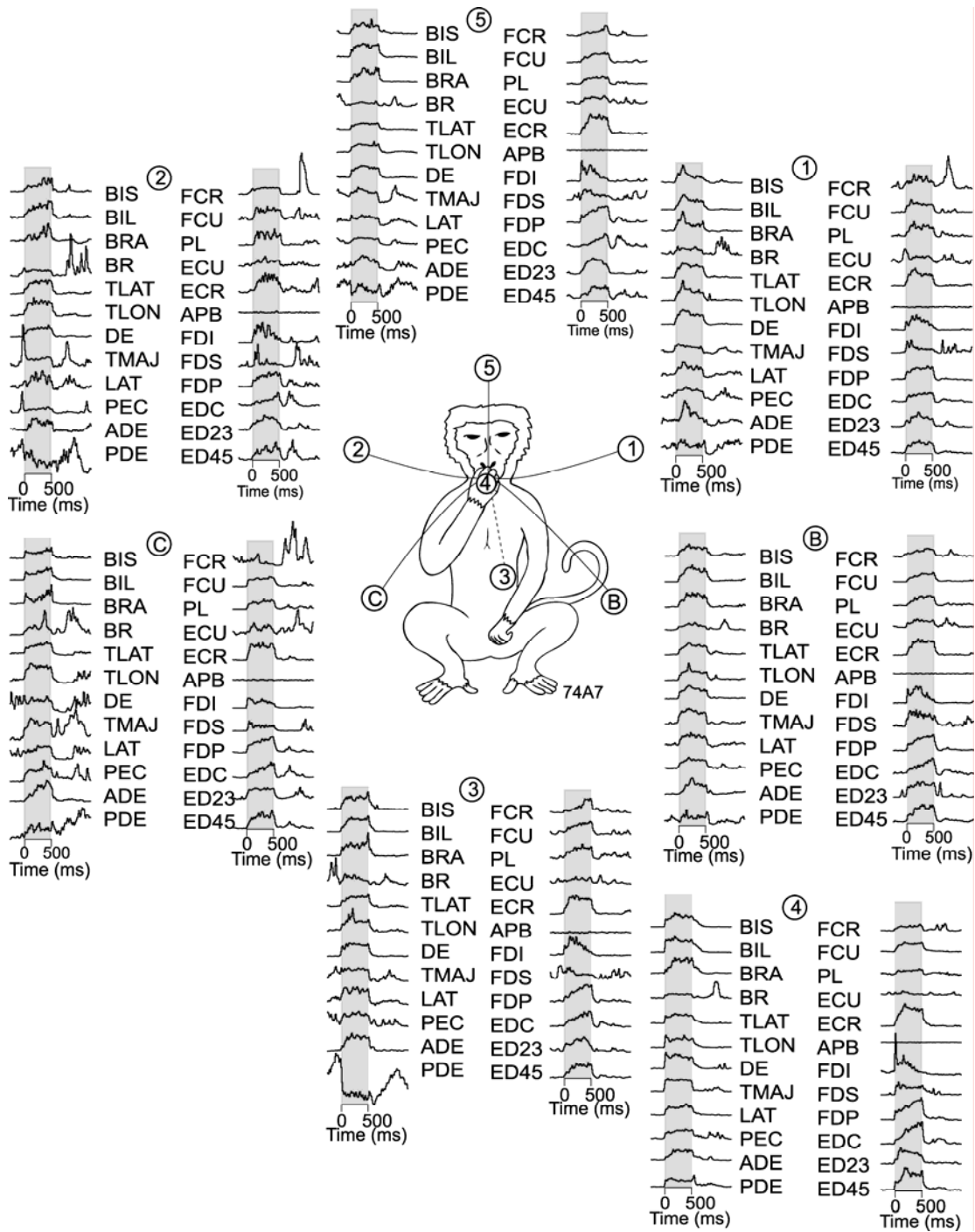


Figure 4.5. Relationship between the magnitudes of RL-ICMS evoked EMG activity at starting hand positions that produced the most extreme A) shoulder, B) elbow and C) wrist positions. Linear regression lines are plotted and correlation coefficients (R) and P values given. The grey line has a slope = 1.

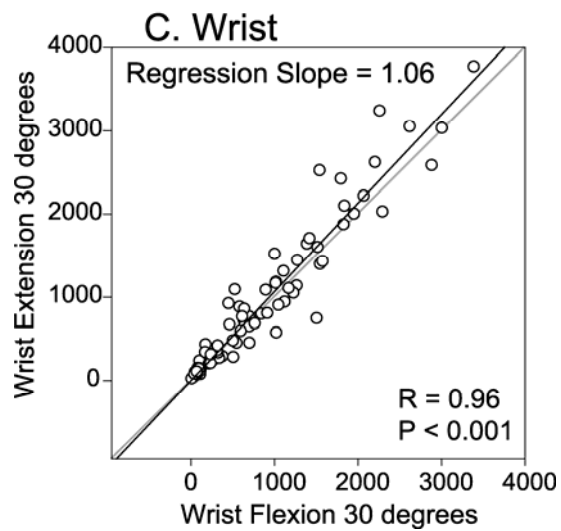
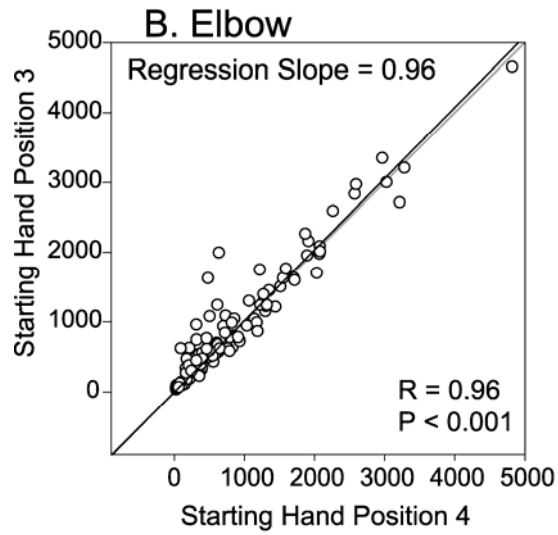
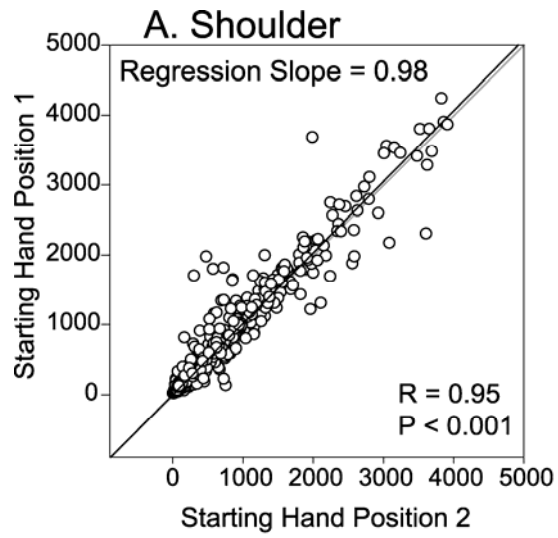
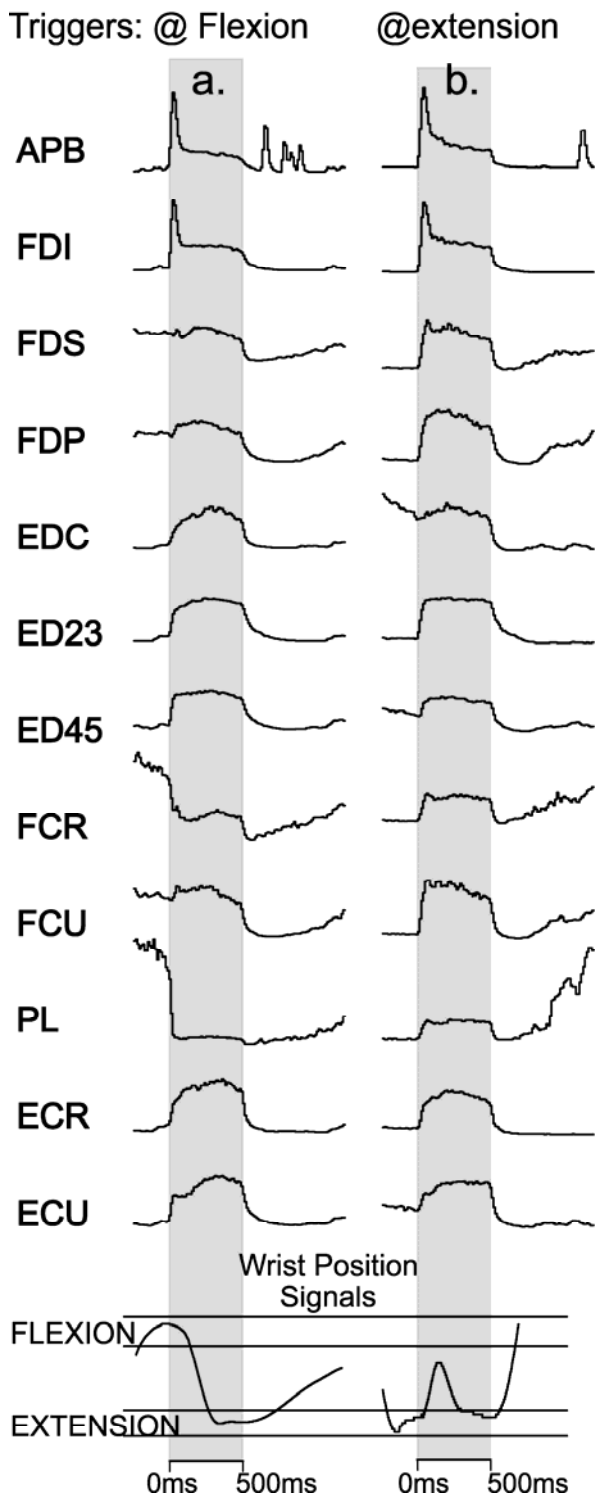


Figure 4.6. RL-ICMS elicited EMG activation patterns associated with hand starting positions during the a,b) concentric wrist task and c,d) isometric wrist task. Grey bars represent 500 ms stimulus train. Each muscle is calibrated across all starting hand positions.

A. Concentric Wrist Task



B. Isometric Wrist Task

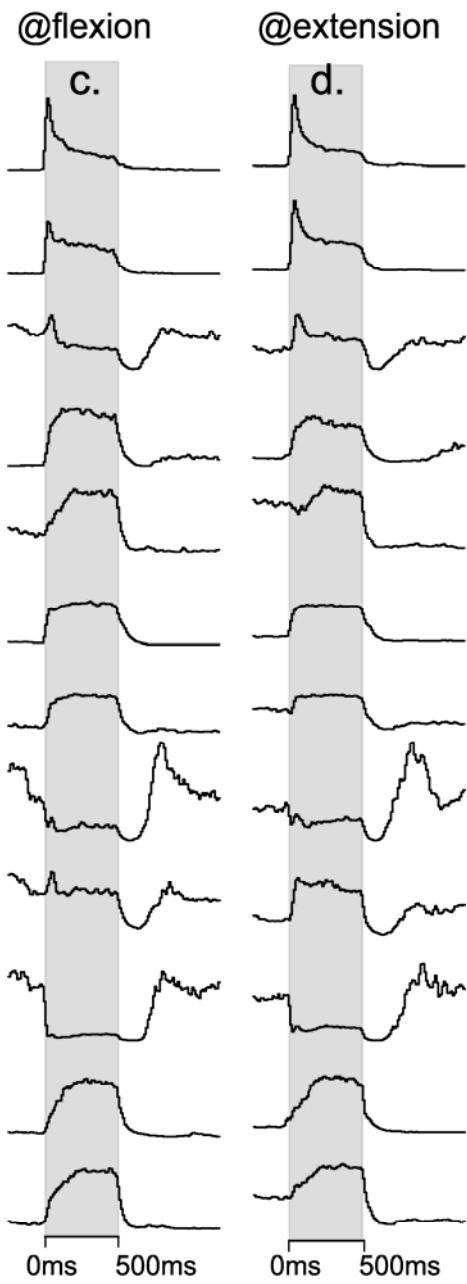
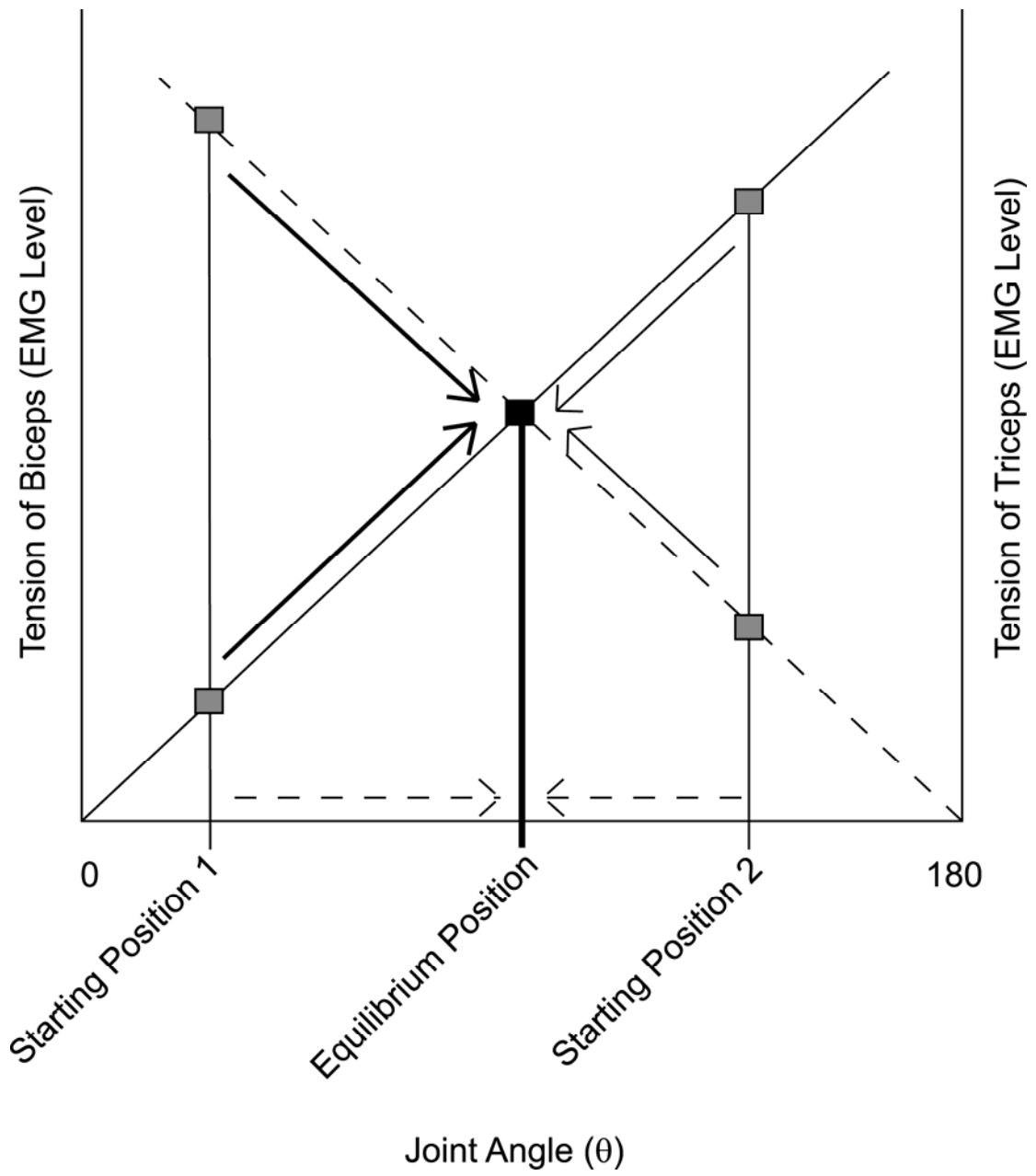


Figure 4.7. Illustration depicting how the length-tension relationships of biceps and triceps specify elbow joint angle. Muscle tension is plotted along the x-axis and against angle of the elbow joint (θ), rather than muscle length. The solid line represents the length-tension curve of biceps and the dotted line triceps at given muscle activity levels. Grey squares represent levels of muscle tension produced by biceps and triceps at the two example starting hand positions. Given this level of RL-ICMS evoked biceps and triceps activity, these muscles will produce movement from either starting hand position to a final hand position reflecting the equilibrium point (heavy and light diagonal arrows). The black square represents the point of intersection between length-tension curves; the equilibrium position of the joint (heavy vertical line). Dotted Horizontal lines represent corresponding changes in elbow angle associated with movement toward the equilibrium position.



REFERENCES

- Aflalo TN, Graziano MS (2006a) Partial tuning of motor cortex neurons to final posture in a free-moving paradigm. *Proc Natl Acad Sci U S A*. 103(8):2909-14.
- Aflalo TN, Graziano MS (2006b) Possible origins of the complex topographic organization of motor cortex: reduction of a multidimensional space onto a two-dimensional array. *J Neurosci* 26(23):6288-97.
- Asanuma H, Arnold A, Zarzecki P (1976) Further study on the excitation of pyramidal tract cells by intracortical microstimulation. *Exp Brain Res* 26(5): 443-61.
- Baker SN, Olivier E, Lemon RN (1998) An investigation of the intrinsic circuitry of the motor cortex of the monkey using intra-cortical microstimulation. *Exp Brain Res* 123(4):397-411.
- Boudrias MH, Belhaj-Saïf A, Park MC, Cheney PD (2006) Contrasting properties of motor output from the supplementary motor area and primary motor cortex in rhesus macaques. *Cereb Cortex* 16(5): 632-8.
- Brown SH, Cooke JD (1990) Movement-related phasic muscle activation. I. Relations with temporal profile of movement. *J Neurophysiol* 63(3):455-64.
- Buys EJ, Lemon RN, Mantel GW, Muir RB (1986) Selective facilitation of different hand muscles by single corticospinal neurons in the conscious monkey. *J Physiol* 381: 529-49.
- Cerri G, Shimazu H, Maier MA, Lemon RN (2003) Facilitation from ventral premotor cortex of primary motor cortex outputs to macaque hand muscles. *J Neurophysiol* 90(2):832-42.
- Cheney PD, Fetz EE (1985) Comparable patterns of muscle facilitation evoked by individual corticomotoneuronal (CM) cells and by single intracortical microstimuli in primates: evidence for functional groups of CM cells. *J Neurophysiol* 53(3): 786-804.

- Cheney PD, Fetz EE (1980) Functional classes of primate corticomotoneuronal cells and their relation to active force. *J Neurophysiol* 44(4): 773-91.
- Cheney PD, Mewes K, Widener G (1991) Effects on wrist and digit muscle activity from microstimuli applied at the sites of rubromotoneuronal cells in primates. *J Neurophysiol* 66(6): 1978-92.
- Davidson AG, Buford JA (2006) Bilateral actions of the reticulospinal tract on arm and shoulder muscles in the monkey: stimulus triggered averaging. *Exp Brain Res* 173(1): 25-39.
- Frost SB, Barbay S, Friel KM, Plautz EJ, Nudo RJ (2003) Reorganization of remote cortical regions after ischemic brain injury: a potential substrate for stroke recovery. *J Neurophysiol* 89(6):3205-14.
- Ginanneschi F, Del Santo F, Dominici F, Gelli F, Mazzocchio R, Rossi A (2005) Changes in corticomotor excitability of hand muscles in relation to static shoulder positions. *Exp Brain Res* 161(3): 374-82.
- Ginanneschi F, Dominici F, Biasella A, Gelli F, Rossi A (2006) Changes in corticomotor excitability of forearm muscles in relation to static shoulder positions. *Brain Res* 1073-1074: 332-8.
- Godschalk M, Mitz AR, van Duin B, Van Der Burg H (1995) Somatotopy of monkey premotor cortex examined with microstimulation. *Neurosci Res* 23(3):269-79.
- Gordon AM, Huxley AF, Julian FJ (1966) The variation in isometric tension with sarcomere length in vertebrate muscle fibres. *J Physiol* 184: 170-192.
- Graziano MS, Aflalo TN, Cooke DF (2005) Arm movements evoked by electrical stimulation in the motor cortex of monkeys. *J Neurophysiol* 94(6):4209-23.
- Graziano, M.S.A., Taylor, C.S.R., Moore, T (2002) Complex movements evoked by microstimulation of precentral cortex. *Neuron* 34: 841-851.

- Gustafsson B, Jankowska E (1976) Direct and indirect activation of nerve cells by electrical pulses applied extracellularly. *J Physiol* 258(1):33-61.
- Hatanaka N, Nambu A, Yamashita A, Takada M, Tokuno H (2001) Somatotopic arrangement and corticocortical inputs of the hindlimb region of the primary motor cortex in the macaque monkey. *Neurosci Res* 40(1):9-22.
- Hummelsheim H, Wiesendanger M, Bianchetti M, Wiesendanger R, Macpherson J (1986) Further investigations of the efferent linkage of the supplementary motor area (SMA) with the spinal cord in the monkey. *Exp Brain Res* 65(1): 75-82.
- Jankowska E, Padel Y, Tanaka R (1975) The mode of activation of pyramidal tract cells by intracortical stimuli. *J Physiol* 249(3): 617-36.
- Kasser RJ, Cheney PD (1985) Characteristics of corticomotoneuronal postspike facilitation and reciprocal suppression of EMG activity in the monkey. *J Neurophysiol* 53(4): 959-78.
- Kleim JA, Hogg TM, VandenBerg PM, Cooper NR, Bruneau R, Rempel M (2004) Cortical synaptogenesis and motor map reorganization occur during late, but not early, phase of motor skill learning. *J Neurosci* 24(3):628-33.
- Lemon RN, Maier MA, Armand J, Kirkwood PA, Yang HW (2002) Functional differences in corticospinal projections from macaque primary motor cortex and supplementary motor area. *Adv Exp Med Biol* 508:425-34. Review.
- Lestienne F (1979) Effects of inertial load and velocity on the braking process of voluntary limb movements. *Exp Brain Res* 35(3):407-18.
- Luppino G, Matelli M, Camarda RM, Gallese V, Rizzolatti G (1991) Multiple representations of body movements in mesial area 6 and the adjacent cingulate cortex: an intracortical microstimulation study in the macaque monkey. *J Comp Neurol* 311(4):463-82.

- Martin JH, Engber D, Meng Z (2005) Effect of forelimb use on postnatal development of the forelimb motor representation in primary motor cortex of the cat. *J Neurophysiol* 93(5):2822-31.
- McKiernan BJ, Marcario JK, Hill Karrer J, Cheney PD (1998) Corticomotoneuronal postspike effects in shoulder, elbow, wrist, digit, and intrinsic hand muscles during a reach and prehension task. *J Neurophysiol* 80(4): 1961-1980.
- Mewes K, Cheney PD (1991) Facilitation and suppression of wrist and digit muscles from single rubromotoneuronal cells in the awake monkey. *J Neurophysiol.* 66(6): 1965-77.
- Mewes K, Cheney PD (1994) Primate rubromotoneuronal cells: parametric relations and contribution to wrist movement. *J Neurophysiol* 72: 14-30.
- Milner-Brown HS, Stein RB (1975) The relation between the surface electromyogram and muscular force. *J Physiol* 246(3): 549-569.
- Mitz AR, Wise SP (1987) The somatotopic organization of the supplementary motor area: intracortical microstimulation mapping. *J Neurosci* 7(4):1010-21.
- Moritz CT, Lucas TH, Perlmutter SI, Fetz EE (2007) Forelimb movements and muscle responses evoked by microstimulation of cervical spinal cord in sedated monkeys. *J Neurophysiol* 97(1): 110-20.
- Nowak LG, Bullier J (1998a) Axons, but not cell bodies, are activated by electrical stimulation in cortical gray matter. I. Evidence from chronaxie measurements. *Exp Brain Res* 118(4):477-88.
- Nowak LG, Bullier J (1998b) Axons, but not cell bodies, are activated by electrical stimulation in cortical gray matter. II. Evidence from selective inactivation of cell bodies and axon initial segments. *Exp Brain Res* 118(4):489-500.

- Nudo RJ, Milliken GW, Jenkins WM, Merzenich MM (1996) Use-dependent alterations of movement representations in primary motor cortex of adult squirrel monkeys. *J Neurosci* 16(2):785-807.
- Nudo RJ, Milliken GW (1996) Reorganization of movement representations in primary motor cortex following focal ischemic infarcts in adult squirrel monkeys. *J Neurophysiol* 75(5):2144-9.
- Park MC, Belhaj-Saïf A, Cheney PD (2000) Chronic recording of EMG activity from large numbers of forelimb muscles in awake macaque monkeys. *J Neurosci Methods* 15;96(2): 153-60.
- Park MC, Belhaj-Saïf A, Cheney PD (2004) Properties of primary motor cortex output to forelimb muscles in rhesus macaques. *J Neurophysiol* 92(5): 2968-2984.
- Park MC, Belhaj-Saïf A, Gordon M, Cheney PD (2001) Consistent features in the forelimb representation of primary motor cortex in rhesus macaques. *J Neurosci* 21(8):2784-92.
- Perlmutter SI, Iwamoto Y, Baker JF, Peterson BW (1998) Interdependence of spatial properties and projection patterns of medial vestibulospinal tract neurons in the cat. *J Neurophysiol* 79(1): 270-84.
- Porter R (1963) Focal Stimulation of Hypoglossal Neurones in the cat. *J Physiol* 169:630-40.
- Ranck JB Jr. (1975) Which elements are excited in electrical stimulation of mammalian central nervous system: a review. *Brain Res* 98(3): 417-40. Review.
- Raos V, Franchi G, Gallese V, Fogassi L (2003) Somatotopic organization of the lateral part of area F2 (dorsal premotor cortex) of the macaque monkey. *J Neurophysiol* 89(3):1503-18.
- Rattay F (1999) The basic mechanism for the electrical stimulation of the nervous system. *Neurosci* 89(2):335-46.

- Rothwell JC (1994) *Control of Human Voluntary Movement*. London, UK: Chapman & Hall.
- Sanes JN, Jennings VA (1984) Centrally programmed patterns of muscle activity in voluntary motor behavior of humans. *Exp Brain Res* 54(1):23-32.
- Schieber MH (2001) Constraints on somatotopic organization in the primary motor cortex. *J Neurophysiol* 86(5): 2125-43. Review.
- Schmidlin E, Wannier T, Bloch J, Rouiller EM (2004) Progressive plastic changes in the hand representation of the primary motor cortex parallel incomplete recovery from a unilateral section of the corticospinal tract at cervical level in monkeys. *Brain Res* 1017(1-2):172-83
- Shinoda Y, Arnold AP, Asanuma H (1976) Spinal branching of corticospinal axons in the cat. *Exp Brain Res* 26(3):215-34.
- Stoney SD Jr, Thompson WD, Asanuma H (1968) Excitation of pyramidal tract cells by intracortical microstimulation: effective extent of stimulating current. *J Neurophysiol* 31(5): 659-69.
- Strick PL (2002) Stimulating research on motor cortex. *Nat Neurosci* 5(8):714-5.
- Swadlow HA (1992) Monitoring the excitability of neocortical efferent neurons to direct activation by extracellular current pulses. *J Neurophysiol* 68(2):605-19.
- Tehovnik EJ, Tolias AS, Sultan F, Slocum WM, Logothetis NK (2006) Direct and indirect activation of cortical neurons by electrical microstimulation. *J Neurophysiol* 96(2): 512-21. Review.
- Van Essen DC, Drury HA, Dickson J, Harwell J, Hanlon D, Anderson CH (2001) An integrated software suite for surface-based analyses of cerebral cortex. *J Am Med Inform Assoc* 8(5): 443-59.

Widener GL Cheney PD (1997) Effects on muscle activity from microstimuli applied to somatosensory and motor cortex during voluntary movement in the monkey. *J Neurophysiol* 77(5): 2446-65.

CHAPTER FIVE

INSIGHTS INTO THE MECHANISM OF NEURAL CIRCUIT

ACTIVATION WITH REPETITIVE INTRACORTICAL

MICROSTIMULATION

ABSTRACT

High frequency repetitive microstimulation has been widely used as a method of investigating the properties of cortical motor output. Despite its widespread use, few studies have investigated how activity evoked by high frequency stimulation may interact with the existing natural background firing of cortical cells. A reasonable assumption might be that the stimulus evoked activity sums with the existing background activity. However, another possibility is that the stimulus-evoked firing of cortical neurons might block and replace the natural activity. We refer to this possibility as “neural hijacking”. Evidence presented in this paper provides support for the neural hijacking hypothesis. In a previous study, we documented the muscle activation patterns associated with repetitive, high frequency, long duration intracortical microstimulation (RL-ICMS) of primary motor cortex (M1) in rhesus monkeys. As part of that study, we found 40 instances (6% of all cortical site-muscle pairs tested) in which RL-ICMS produced apparent suppression at some starting hand positions and activation at other positions. However, upon further investigation, we determined that stimulation was actually driving muscle activity to a new stimulus-evoked level of activity, independent of the starting EMG level or the starting hand position. At some starting hand positions where existing EMG level for a particular muscle was high, achieving the stimulus driven level of activity required a decrease in EMG level, which appeared to be suppression; whereas at other positions

where background EMG as low, achieving the same stimulus driven level of activity required an increase in level and this appeared as activation.

However, in both cases the same stimulus driven level of EMG activity was achieved suggesting that the decrease in activity was not actually true suppression but rather substitution of a stimulus evoked level of activity in place of the natural level of activity. Computing stimulus-triggered averages of EMG activity (StTA) for muscles with apparent suppression confirmed that the true effect was actually facilitation. Our data support a model in which RL-ICMS blocks (“hijacks”) the natural activity of cortical neurons and replaces it with pure stimulus evoked activity.

INTRODUCTION

Repetitive ICMS is supra-threshold for movements and is easily detected as a muscle twitch or whole limb movement. Short duration repetitive ICMS (RS-ICMS), consists of a train of 10 symmetrical biphasic stimulus pulses at a frequency of 330 Hz (Asanuma and Rosén 1972), has been used extensively to define output representations in motor cortex (Andersen et al., 1975; Asanuma et al., 1982; Baker et al., 1998; Burish et al., 2008; Dancause et al., 2006; Donoghue et al., 1992; Friel et al., 2007; Kosar et al., 1985; Kwan et al., 1978; Lemon et al., 1987; Macpherson et al., 1982; Mori et al., 1983; Sato and Tanji 1989; Schieber and Deuel 1997; Schmidlin et al., 2004; Schmidt and McIntosh 1990; Tandon et al., 2008; Thompson and Fernandex 1975; Waters and Asanuma 1983; Weinrich and Wise 1982). Long duration repetitive ICMS (RL-ICMS) consists of a train of 100 symmetrical biphasic stimulus pulses at a frequency of 200 Hz for 500 ms and can produce limb and eye movements (Ethier et al., 2006; Ferrier 1875; Fritsch and Hitzig 1875; Graziano et al., 2002, 2005; Ramanathan et al., 2006). Both ICMS methods can be used to study output effects in either sedated or awake behaving animals. Due to the ease of its use, it is a popular tool for studying the organization and function of motor areas of the brain.

Although these ICMS methods are being used extensively, the mechanism responsible for stimulus related muscle activity is not fully understood. One possibility is that the stimulus sums with the natural

descending input commands to the motoneuron pools. If this is the case, the stimulus evoked muscle activity should add to the existing background EMG levels present at the time the stimulus is applied. However, our data suggests that this is not the case. Here, we present evidence that RL-ICMS evoked EMG activity does not sum with the existing level of EMG activity; rather it forces a new EMG level that is independent of existing voluntary activity. Our data support a model in which repetitive ICMS blocks natural afferent input to corticospinal neurons and replaces it with a stimulus evoked input.

MATERIALS AND METHODS

Behavioral tasks

RL-ICMS was applied in the left M1 of two male rhesus monkeys (*Macaca mulatta*; ~10kg, 9 years old) while they reached with their right hand for a food reward or a handle placed in various positions within the workspace (Figure 4.1 Aa) or performed 1) a concentric wrist task which alternated between flexion and extension targets, or 2) an isometric wrist task which was locked into place at two different wrist positions (Figure 4.1 B). During each data collection session, the monkey was seated in a custom built primate chair inside a sound-attenuating chamber. The left forearm was restrained during task performance. All tasks were performed with the right arm/hand.

Hand starting positions of the reaching tasks are illustrated in Figure 4.1 Aa. Monkeys were offered peanuts in various positions around the work space (Numbers in Figure 4.1 Aa). RL-ICMS was delivered as the monkey's hand entered the target starting position, but before the monkey grasped the reward. Alternatively, the monkeys were required to grip a handle fixed to a force transducer (Grass Medical Instruments) on a linear XYZ positioning system. The handle was locked in place at up to 4 different positions within the monkey's work space (letters in Figure 4.1 Aa). RL-ICMS was elicited using the handle position as an indicator of starting hand position. Shoulder and elbow angles for each starting hand position for both the whole limb reaching tasks are listed in Table 4.1. Joint angles were measured using

photographs of the monkey's arm at each of the starting hand positions. Digital images were processed in Image J using the shoulder, ribcage, elbow and wrist joints as base points on the body. Final angle measurements are an average from several sessions. Figure 4.1 A illustrates how the shoulder and elbow measurements were made in both the vertical (b) and horizontal (c) plane.

For the wrist tasks (Figure 1 B), the monkey's lower and upper arm was restrained. The hand, with digits extended, was placed in a padded manipulandum that rotated about the wrist. The wrist was aligned with the axis of rotation of the torque wheel to which the manipulandum was attached. The monkey was required to alternate between flexions and extensions of the wrist into electronically detected hold zones (15° - 20° in both directions). RL-ICMS was delivered as the position sensor reached the outer boundary of the target hold zone. Alternatively, the manipulandum was locked in place at two different wrist positions including 30 degrees in flexion and 30 degrees in extension. The monkey was required to generate ramp and hold trajectories of wrist torque alternately between flexion and extension target zones. The inner and outer boundaries of the torque window were 0.025 Nm and 0.05 Nm respectively. RL-ICMS was delivered as the force sensor reached the outer boundary of the target hold zone. Since delivery of an applesauce reward was contingent upon the monkey holding within each zone for one second, RL-ICMS was delivered once every 3-4 trials.

Surgical procedures

After training, a 30-mm inside diameter titanium chamber was stereotaxically centered over the forelimb area of M1 on the left hemisphere of each monkey and anchored to the skull with 12 titanium screws (Stryker Leibinger, Germany) and dental acrylic (Lux-it Inc., Blue Springs, MO). Threaded titanium nuts (Titanium Unlimited, Houston, TX) were also attached over the occipital aspect of the skull using 12 additional titanium screws and dental acrylic. These nuts provided a point of attachment for a flexible head restraint system during data collection sessions. The chambers were centered at anterior 16 mm, lateral 18 mm (Monkey V), and anterior 16 mm, lateral 22 mm (Monkey A), at a 30° angle to the sagittal plane.

EMG activity was recorded from 24 muscles of the forelimb with pairs of insulated, multi-stranded stainless steel wires (Cooner Wire, Chatsworth, CA) implanted during an aseptic surgical procedure (Park et al., 2000). Pairs of wires for each muscle were tunneled subcutaneously from an opening above the elbow to their target muscles. The wires of each pair were bared of insulation for ~ 2 - 3 mm at the tip and inserted into the muscle belly with a separation of ~ 5 mm. Implant locations were confirmed by stimulation through the wire pair and observation of appropriate muscle twitches. EMG connector terminals (ITT Cannon, White Plains, NY) were affixed to the upper arm using medical adhesive tape. Following surgery, the monkeys wore a

Kevlar jacket (Lomir Biomedical Inc., Malone, NY) reinforced with fine stainless steel mesh (Sperian Protection Americas Inc., Attleboro Falls, MA) to protect the implant. EMG activity was recorded from five shoulder muscles: pectoralis major (PEC), anterior deltoid (ADE), posterior deltoid (PDE), teres major (TMAJ), and latissimus dorsi (LAT); seven elbow muscles: biceps short head (BIS), biceps long head (BIL), brachialis (BRA), brachioradialis (BR), triceps long head (TLON), triceps lateral head (TLAT) and dorso-epitrochlearis (DE); five wrist muscles: extensor carpi radialis (ECR), extensor carpi ulnaris (ECU), flexor carpi radialis (FCR), flexor carpi ulnaris (FCU), and Palmaris longus (PL); five digit muscles: extensor digitorum communis (EDC), extensor digitorum 2 and 3 (ED2,3) extensor digitorum 4 and 5 (ED4,5), flexor digitorum superficialis (FDS), and flexor digitorum profundus (FDP); and two intrinsic hand muscles: abductor pollicis brevis (APB) and first dorsal interosseus (FDI).

All surgeries were performed under deep general anesthesia and aseptic conditions. Postoperatively, monkeys were given an analgesic (Buprenorphine 0.5 mg/kg every 12h for 3-4 days) and antibiotics (Penicillin G, Benzathaine / Procaine combination, 40,000 IU/kg every 3 days). All procedures were in accordance with the Association for Assessment and Accreditation of Laboratory Animal Care (AAALAC) and the Guide for the Care and Use of Laboratory Animals, published by the US Department of Health and Human Services and the National Institutes of Health.

Data collection

Sites in M1 were stimulated using glass and mylar insulated platinum-iridium electrodes with impedances ranging from 0.5 to 1.5 M Ω (Frederick Haer & Co., Bowdoinham, ME). The electrode was positioned within the chamber using an X-Y coordinate manipulator and was advanced at approximately a right angle into the cortex with a manual hydraulic microdrive (Frederick Haer & Co., Bowdoinham, ME). Rigid support for the electrode was provided by a 22 gage cannula (Small Parts Inc., Miami Lakes, FL) inside of a 25 mm long, 3 mm diameter stainless steel post which served to guide the electrode to the surface of the dura.

First cortical unit activity was noted and the electrode was lowered 1.5 mm below this point to layer V. In order to distinguish layer V from more superficial layers, particularly in the bank of the precentral gyrus, neuronal activity was evaluated for the presence of large action potentials that were often modulated with the task and stimulus triggered averages (StTAs) for the presence of both clear and robust effects at 15 μ A. Individual stimuli were symmetrical bi-phasic pulses: a 0.2 ms negative pulse followed by a 0.2 ms positive pulse. EMG activity was generally filtered from 30 Hz to 1 KHz, digitized at a rate of 4 kHz and full-wave rectified. Stimuli (15, 30, 60 and 120 μ A) were applied throughout all phases of the task.

- Stimulus triggered averages

Layer V sites in forelimb M1 were identified and microstimuli were applied at 15 Hz. The assessment of StTA effects was based on averages of at least 500 trigger events. Segments of EMG activity associated with each stimulus were evaluated and accepted for averaging only when the mean of all EMG data points over the entire 60msec epoch was $\geq 5\%$ of full-scale input. This prevented averaging segments in which EMG activity was minimal or absent (McKiernan et al., 1998). EMG recordings were tested for cross-talk by computing EMG-triggered averages (Cheney and Fetz, 1980). This procedure involved using the EMG peaks from one muscle as triggers for compiling averages of rectified EMG activity of all other muscles. To be accepted as a valid post-stimulus effect; the ratio of PStF between test and trigger muscle needed to exceed the ratio of their cross-talk peaks by a factor of two or more (Buys et al., 1986). Based on this criterion, none of the effects obtained in this study needed to be eliminated.

- RL- ICMS triggered averages

Layer V sites with clear StTA effects in forelimb muscles were identified and selected for data collection with RL-ICMS. RL-ICMS consisted of a train of 100 symmetrical biphasic stimulus pulses at 200 Hz (500 ms). The assessment of effects was based on averages of 4 - 8 trigger events.

Data analysis

At each stimulation site, averages were obtained for all 24 muscles. The onset latency of the post-stimulus effect was based on visual inspection of the record and was marked where the activity inflected relative to the pre-trigger baseline of EMG. Baseline EMG level was measured from the pre-trigger period in all averages.

- Stimulus triggered averages

Averages were compiled over a 60 ms epoch, including 20 ms before the trigger to 40 ms after the trigger. Post-stimulus facilitation (PStF) and post-stimulus suppression (PStS) effects were computer-measured as described in detail by Mewes and Cheney (1991, 1994). Nonstationary, ramping baseline activity was subtracted from single pulse ICMS triggered averages using custom analysis software. Mean baseline activity and the standard deviation (SD) of baseline EMG activity was measured from the pre-trigger period typically consisting of the first 12.5 ms of each average. Single pulse ICMS triggered averages were considered to have a significant post-stimulus effect (PStF or PStS) if the points of the record crossed a level equivalent to 2 SD of the mean of the baseline EMG for a period ≥ 0.75 ms or more (Park et al., 2001). The magnitude of PStF and PStS was expressed as the percent increase (+ ppi) or decrease (- ppi) in EMG activity above (PStF)

or below (PStS) baseline EMG activity (Cheney and Fetz, 1985; Kasser and Cheney, 1985; Cheney et al., 1991).

- RL-ICMS triggered averages

RL-ICMS triggered averages were compiled over a 1.2 s epoch, including 200 ms before the trigger to 1,000 ms after the trigger. Mean baseline activity was measured from the pre-trigger period typically consisting of the first 100 ms of each average. The first pulse of each train was used as a trigger to compute averages of EMG activity. The magnitude of the EMG response was expressed as the mean EMG level present after the first RL-ICMS pulse and throughout the stimulus train.

Imaging

Structural MRIs were obtained from a 3 Tesla Siemens Allegra system. Images were obtained with the monkey's head mounted in an MRI compatible stereotaxic apparatus so the orientation and location of the cortical recording chamber and electrode track penetrations could be determined. A two-dimensional rendering of experimental sites was constructed for each monkey. The method for flattening and unfolding cortical layer V in the anterior bank of the central sulcus has been previously described in detail (Park et al., 2001). Briefly, the cortex was unfolded and the location of experimental sites were mapped onto a two dimensional cortical sheet based

on the electrode's depth and X-Y coordinate, known architectural landmarks, MRI images, and observations noted during the cortical implant surgeries.

Statistical data analysis

Effects of starting hand position changes tasks were compared using the Student's *t*-test, the Mann-Whitney Rank Sum Test and linear regression. In all tests, statistical significance was assumed if the P value was ≤ 0.05 .

RESULTS

Previously, we reported that 34% (229/671) of evaluated forelimb muscles showed qualitatively different RL-ICMS evoked EMG activation patterns (tonic activation, inclining, declining, suppression, etc.) at different starting hand positions of both a whole limb reaching task and a wrist task (Chapter 4). Interestingly, 40 of these were instances where RL-ICMS produced what appeared to be suppression at one starting hand position and facilitation at another. Figure 5.1 provides four examples of “opposite” muscle activation patterns elicited by RL-ICMS at two sites in the cortex. Column A shows the activity patterns elicited when RL-ICMS was delivered at a starting hand position near the monkey’s mouth (hand position 4 in figure 4.1). Column B shows the activity patterns of those same muscles elicited when RL-ICMS was delivered at starting hand position slightly to the right and in front of the monkey (hand position C in figure 4.1). At this site, RL-ICMS consistently drove the hand to a final end point position near the monkey’s abdomen. RL-ICMS resulted in an increase in EMG activity when the hand started at position 4 and a decrease in EMG activity when the hand started at position C. Column C shows the activity patterns of two muscles when RL-ICMS was delivered at the same starting hand position in column B (hand position C in figure 4.1). Column D shows the activity patterns of those same muscles elicited when RL-ICMS was delivered at a starting hand position to the left and in front of the monkey (hand position D in figure 4.1). At this site,

RL-ICMS drove the hand to a final end point position near the monkey's chest. RL-ICMS resulted in what appeared to be an increase in EMG activity when the hand started at position C and a decrease in EMG activity when the hand started at position D. However, for all four examples, the overall mean EMG activation levels during stimulation are nearly the same regardless of starting position. In fact, even the pattern of activity during the stimulation shows features that match, despite the fact that in one case it follows a higher existing EMG level while in the other case it rises from a lower existing EMG level. RL-ICMS is not actually producing a facilitation or suppression, but it is producing an increase or decrease in EMG activity relative to the baseline. The stimulus evoked EMG activation levels in all these muscles for both starting hand positions however, are very similar (table 5.1). Since RL-ICMS results in the same level of EMG activity, independent of starting hand position, it is the pre-stimulus level of baseline EMG activity which accounts for the different qualitative results.

Figure 5.2 further illustrates these points. Column A displays the RL-ICMS evoked EMG activity present when there was a low level of pre-stimulus baseline EMG. Column B displays the RL-ICMS evoked EMG activity present when there was a high level of pre-stimulus baseline EMG activity. In Column C, the RL-ICMS evoked EMG activity traces from columns A and B are superimposed illustrating the stability of EMG activation during the RL-ICMS stimulus train. For example, LAT shows a ramp increase

pattern during the stimulus train in both EMG records. TLON shows a ramp decrease pattern during the stimulus train in both EMG records. In the records of DE, the RL-ICMS evoked activity pattern remains tonic throughout the stimulus train. In all three examples, the RL-ICMS evoked activity levels are very similar.

Another way to demonstrate that RL-ICMS is producing a consistent level of EMG activity that is independent of voluntary background EMG, is to show that RL-ICMS evoked EMG activity is quantitatively the same across the two different starting hand positions which produced the opposite muscle activation pattern. If the EMG activity levels were identical at both hand starting positions, plotting mean EMG activity level at one position against mean EMG activity level present at the other position should yield a correlation coefficient of one, a regression line with a slope of one and a y intercept of zero. Figure 5.3 illustrates the stability of RL-ICMS evoked mean EMG activation levels associated with all 40 effects at the two different starting hand positions which produced the opposite qualitative effect. The mean EMG activation levels were highly correlated ($R = 0.91$, $P < 0.001$). Furthermore, the regression line fitted to these points had a slope that was very close to one (slope = 0.98) and an intercept close to zero (y intercept = -0.002). The black line represents the linear regression of the points and the grey line is the unity line (regression line with a slope of one). Even though the pre-stimulus baseline EMG activity was very different across the two

starting hand positions, it did not affect the RL-ICMS evoked EMG activity level. Instead, RL-ICMS forced a new EMG activity level that was independent of background EMG activity.

At a few sites it was observed that RL-ICMS caused the monkey to drop his arm straight down from the hand starting position. Figure 5.4 shows the shoulder muscle's EMG activation patterns associated with stimulation of one site which produced this effect. All of the shoulder muscles show a decrease in EMG activity relative to pre-stimulus voluntary activity. In this case, ADE and PDE were the only two shoulder muscles determined to be true suppression whereas PEC, TMAJ and LAT showed an increase in EMG activity relative to baseline at one starting hand position and a decrease relative to baseline at another. Further, no effects were observed in stimulus triggered averages of these muscles's EMG activity at 15 μ A. This suggests that RL-ICMS elicited these effects through neurons outside of the immediate vicinity of the electrode. It further provides evidence to suggest the RL-ICMS pulse is capable of blocking the natural supply of input to the area. This likely occurs by antidromic spread of current back to the somas supplying descending input as well as orthodromic spread along horizontal collaterals.

An alternative explanation for the decrease in EMG activity at the onset of the stimulus train is that the monkey feels the stimulus and actively "lets go" removing all natural input to muscles in the process. Figure 5.5 illustrates that this explanation is unlikely because latencies between the onset of the

stimulus train and the onset of the decline in EMG activity were much less than voluntary reaction times to somatosensory stimuli which are typically 180 – 280 ms (Naito et al., 2000; Nelson et al., 1990).

DISCUSSION

In each of the 40 qualitatively different RL-ICMS evoked EMG activity patterns (increase from baseline versus decrease) investigated in this study, a high level of voluntary activity was present in the muscle at one starting hand position and a lower level of voluntary activity was present at another starting hand position. This natural voluntary activity is that which is present before the onset of stimulation. In the case where the voluntary EMG activity was high, RL-ICMS drove the EMG activity to a new level that was lower than the pre-stimulus baseline level. Although this appears to be an active inhibitory process, it is actually substitution of a stimulus evoked level of activity for the existing natural level of activity. In the case where the voluntary EMG activity was low, RL-ICMS drove the EMG activity to the same level as before, however, the resultant level was high relative to the pre-stimulus baseline. In other words, RL-ICMS did not sum with the existing voluntary activity, but instead produced a new EMG level independent of existing voluntary EMG activity. Since it appears that high frequency stimulation blocks the existing activity of cortical neurons related to natural synaptic inputs and replaces with pure stimulus driven activity, it seems appropriate to refer to this phenomenon as “neural hijacking”.

Figure 5.6 summarizes the proposed RL-ICMS mechanism suggested by our findings. First, the RL-ICMS pulse blocks the natural supply of input to the area by antidromic spread along the axons of descending inputs as well

as horizontal collaterals. RL-ICMS activates neurons in the vicinity of the electrode as well as those excited outside the immediate area due to the antidromic spread of current. This creates a descending input that forces a new level of stimulus evoked muscle activity.

Although the mechanism above seems most likely, another possibility is that high frequency stimulation of the cortex powerfully activates the cortical GABA network which, in turn, inactivates corticospinal output neurons and renders them totally unresponsive to natural excitatory synaptic inputs. A similar phenomenon occurs with transcranial magnetic stimulation of the cortex (Di Lazzaro et al., 1998; Nakamura et al., 1997; Sanger et al., 2001). However, because it is clear that RL-ICMS continues to produce EMG activation, if the GABA system were the mechanism by which stimulation blocks natural activation of cortical output neurons, this would suggest that ICMS must be capable of by-passing the inhibition. Assuming that corticospinal neurons are among the cells shut down under the influence of ICMS-evoked GABA inhibition, then ICMS might be activating output neurons directly rather than synaptically. Although there is considerable evidence supporting predominant activation of corticospinal neurons (Gustaffson and Jankowska 1976; Nowak and Bullier 1998a,b; Porter 1963; Rattay 1999; Swadlow 1992), modeling studies typically suggest that direct activation should also occur (McIntyre and Grill 2000, 2002). It is also possible that antidromic activation of afferent inputs by ICMS quickly “drives back”

conduction of natural action potentials to points along the axon more proximal than branch points allowing stimulus-evoked action potentials to then propagate orthodromically to cortical sites outside of the area shut down by GABA inhibition. Additional work is needed to determine the exact mechanism by which high frequency ICMS eliminates cortical signals responsible for natural activation of motoneurons.

To conclude, our results suggest that high frequency ICMS blocks natural signals generated by the internal motor program for the activation of corticospinal output neurons. These natural signals are then replaced with output signals that reflect solely the efficacy of ICMS in activating cortical output neurons. In this sense, high frequency ICMS can be viewed as “hijacking” cortical output to motoneurons.

Table 5.1. RL-ICMS evoked EMG activation levels in Figure 5.1

1. Muscle	2. EMG activation level (μ V) Start: Position 4	3. EMG activation level (μ V) Start: Position C
LAT	0.262	0.273
DE	1.180	1.620
1. Muscle	2. EMG activation level (μ V) Start: Position C	3. EMG activation level (μ V) Start: Position B
TLON	0.580	0.710
DE	1.040	0.950

Figure 5.1. Examples of “opposite” muscle activation patterns elicited by RL-ICMS at a single cortical site. A. Activity patterns elicited when RL-ICMS was delivered at a starting hand position near the monkey’s mouth. B. Activity patterns elicited when RL-ICMS was delivered at starting hand position slightly to the right and in front of the monkey. RL-ICMS consistently drove the hand to a final end point position near the monkey’s abdomen at this site. See figure 4.1 for an illustration of starting hand positions. Grey bar represents stimulus train duration. Each muscle is calibrated across all starting hand positions.

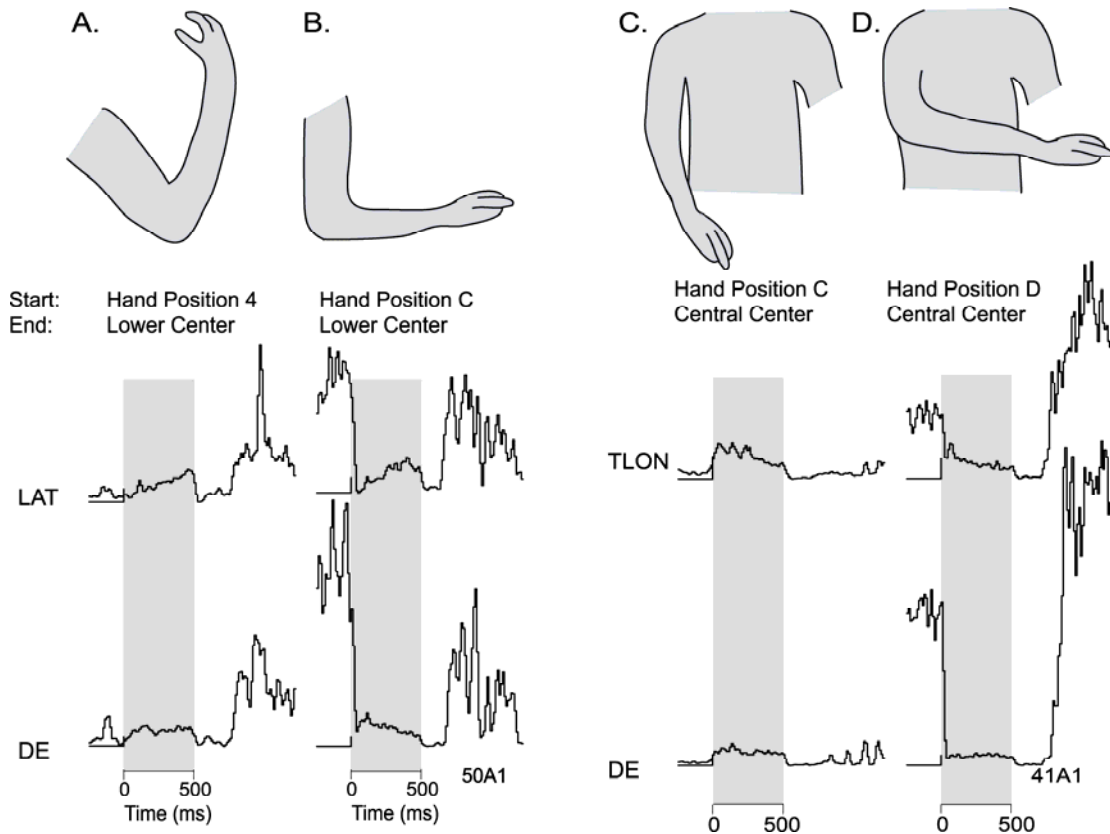


Figure 5.2. Superimposed examples of “opposite” muscle activation patterns elicited by RL-ICMS at a single cortical site. A. RL-ICMS evoked EMG activity present at a low level of pre-stimulus baseline EMG activity. B. RL-ICMS evoked EMG activity present at a high level of pre-stimulus baseline EMG activity. C. RL-ICMS evoked EMG activity traces from the previous two columns overlapping one another. Grey bar represents stimulus train duration. Each muscle is calibrated across all starting hand positions.

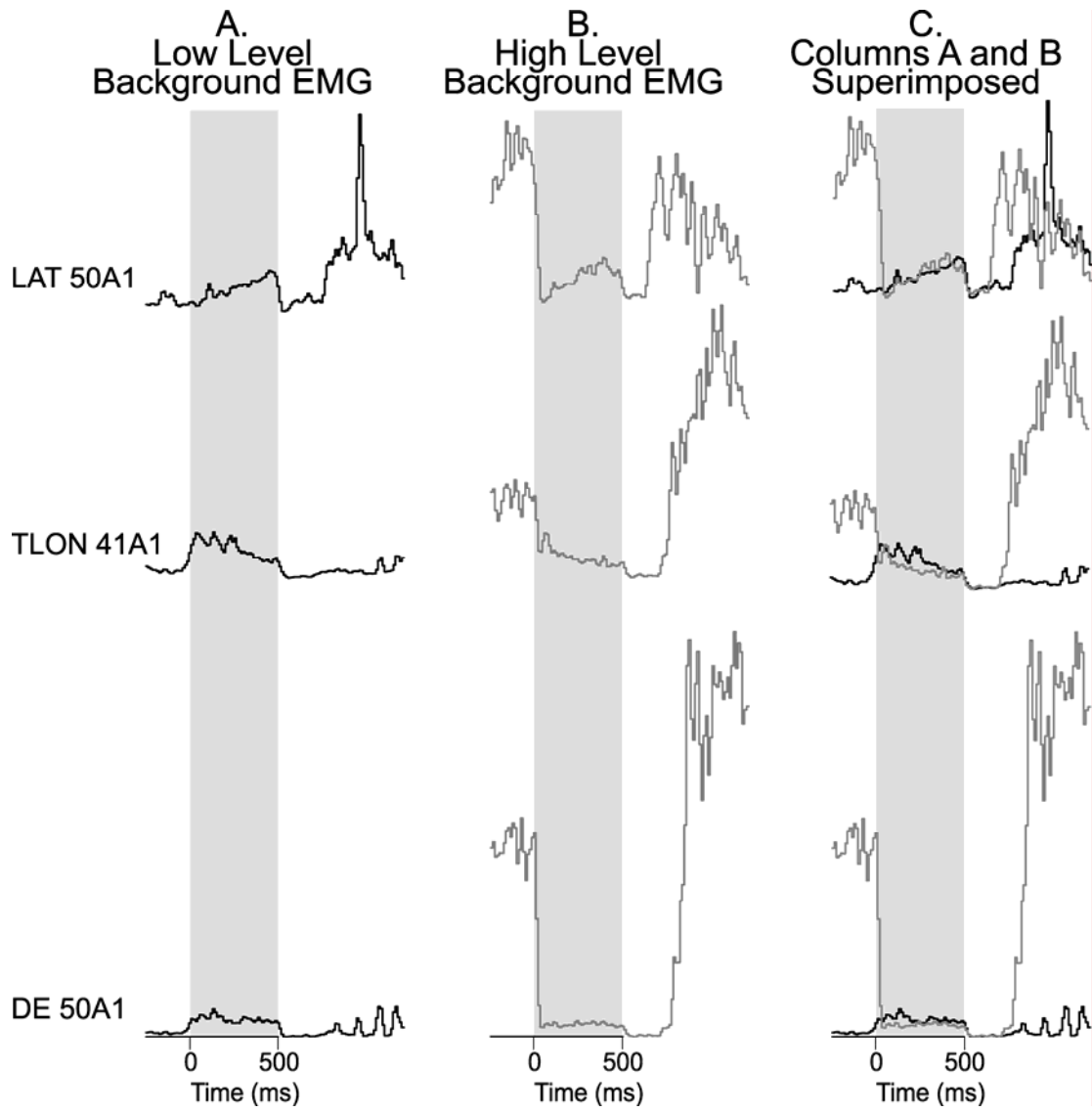


Figure 5.3. Relationship between RL-ICMS evoked mean EMG levels at different starting hand positions. The black line is the linear regression line. The slope of the regression line, correlation coefficient (R) and P value are given. The grey line has a slope = 1.

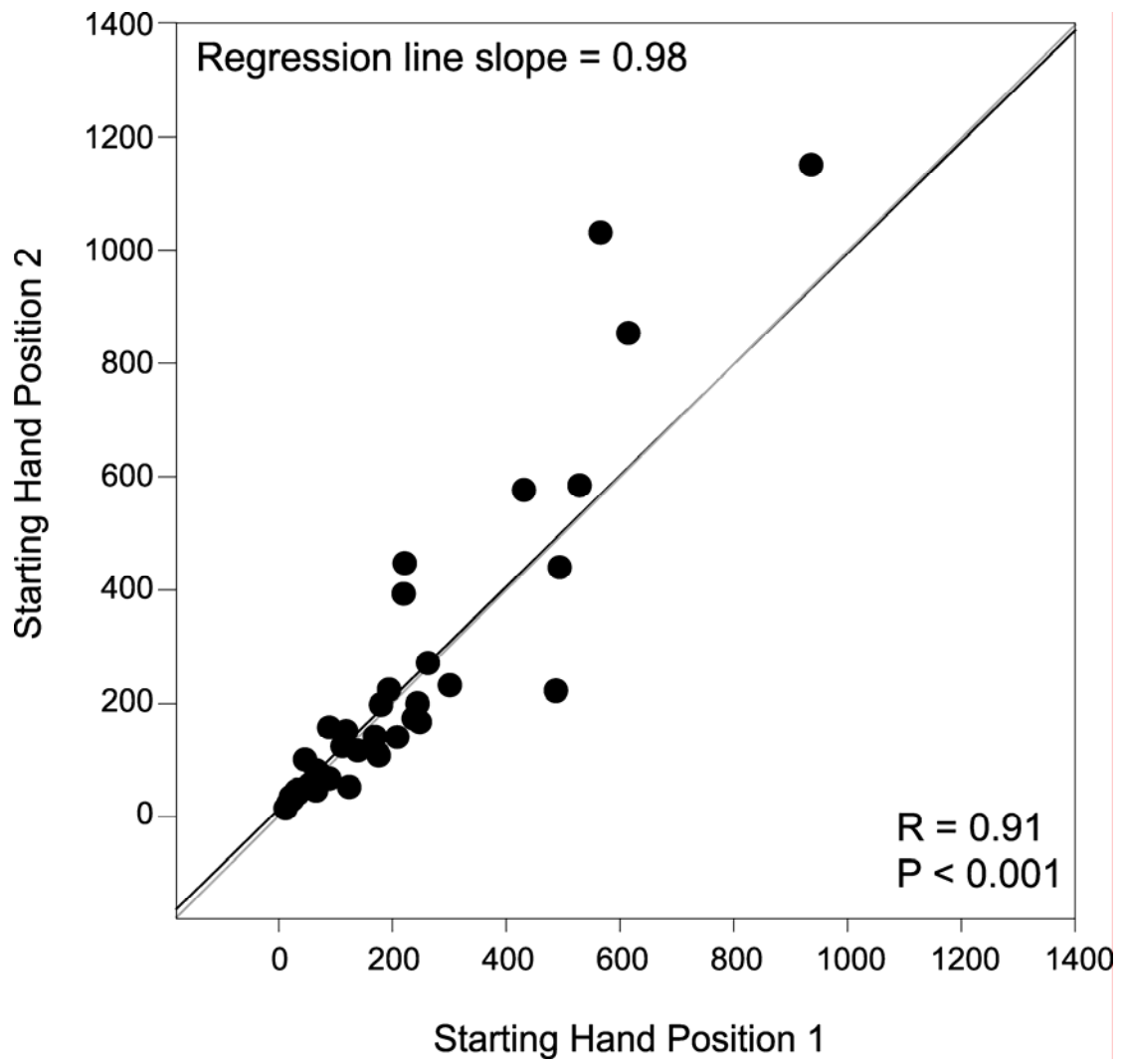


Figure 5.4. A layer V site and the RL-ICMS elicited shoulder muscle EMG activation patterns associated with stimulus interrupted movement. Grey bar represents 500 ms stimulus train. Individual averages are scaled to fit the window.

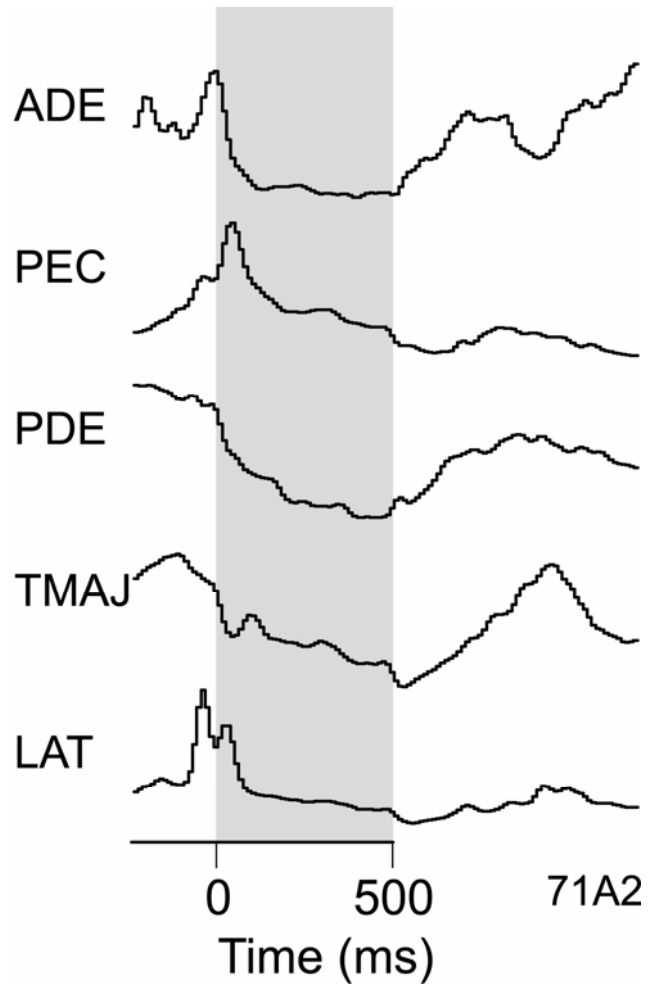


Figure 5.5. Distribution of declining EMG onset latencies measured relative to the stimulus train onset.

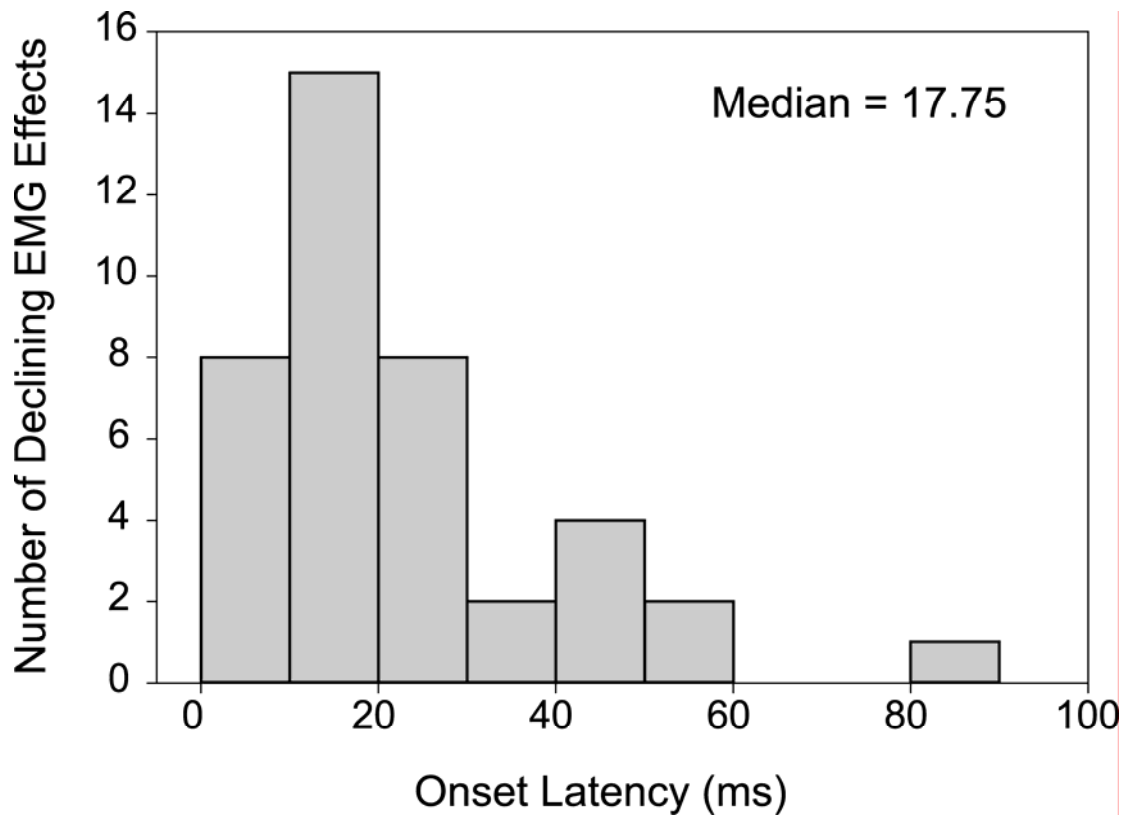
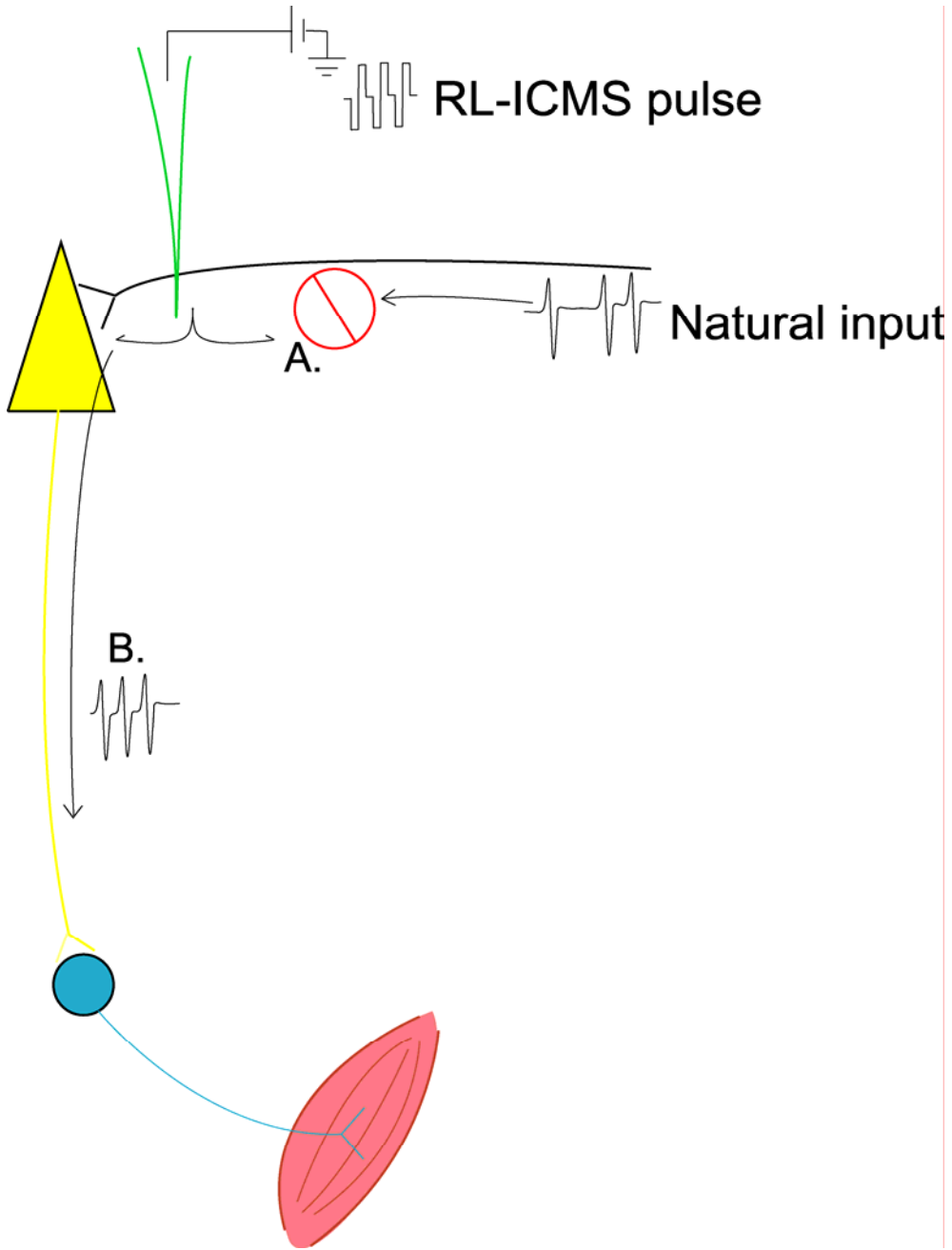


Figure 5.6. Diagram of proposed RL-ICMS mechanism. A. The RL-ICMS stimulus pulse travels orthodromically and antidromically along descending inputs and horizontal collaterals. The antidromic signal collides with and blocks the natural descending input. B. The stimulus evoked input to the replaces the natural supply of descending input.



REFERENCES

- Andersen P, Hagan PJ, Phillips CG, Powell TP (1975) Mapping by microstimulation of overlapping projections from area 4 to motor units of the baboon's hand. *Proc R Soc Lond B Biol Sci* 188(1090): 31-6.
- Asanuma H, Rosén I (1972) Topographical organization of cortical efferent zones projecting to distal forelimb muscles in the monkey. *Exp Brain Res* 14(3): 243-56.
- Asanuma H, Waters RS, Yumiya H (1982) Physiological properties of neurons projecting from area 3a to area 4 gamma of feline cerebral cortex. *J Neurophysiol* 48(4):1048-57.
- Baker SN, Olivier E, Lemon RN (1998) An investigation of the intrinsic circuitry of the motor cortex of the monkey using intra-cortical microstimulation. *Exp Brain Res* 123(4):397-411.
- Burish MJ, Stepniowska I, Kaas JH (2008) Microstimulation and architectonics of frontoparietal cortex in common marmosets (*Callithrix jacchus*). *J Comp Neurol* 507(2):1151-68.
- Buys EJ, Lemon RN, Mantel GW, Muir RB (1986) Selective facilitation of different hand muscles by single corticospinal neurons in the conscious monkey. *J Physiol* 381: 529-49.
- Cheney PD, Fetz EE (1985) Comparable patterns of muscle facilitation evoked by individual corticomotoneuronal (CM) cells and by single intracortical microstimuli in primates: evidence for functional groups of CM cells. *J Neurophysiol* 53(3): 786-804.
- Cheney PD, Fetz EE (1980) Functional classes of primate corticomotoneuronal cells and their relation to active force. *J Neurophysiol* 44(4): 773-91.
- Cheney PD, Mewes K, Widener G (1991) Effects on wrist and digit muscle activity from microstimuli applied at the sites of rubromotoneuronal cells in primates. *J Neurophysiol* 66(6): 1978-92.

- Dancause N, Barbay S, Frost SB, Zoubina EV, Plautz EJ, Mahnken JD, Nudo RJ (2006) Effects of small ischemic lesions in the primary motor cortex on neurophysiological organization in ventral premotor cortex. *J Neurophysiol* 96(6):3506-11.
- Di Lazzaro V, Restuccia D, Oliviero A, Profice P, Ferrara L., Insola A, Mazzone P, Tonali P, Rothwell JC (1998) Magnetic transcranial stimulation at intensities below active motor threshold activates inhibitory circuits. *Exp Brain Res* 119, 265-268.
- Donoghue JP, Leibovic S, Sanes JN (1992) Organization of the forelimb area in squirrel monkey motor cortex: representation of digit, wrist, and elbow muscles. *Exp Brain Res* 89(1):1-19.
- Ethier C, Brizzi L, Darling WG, Capaday C (2006) Linear summation of cat motor cortex outputs. *J Neurosci* 26(20):5574-81.
- Ferrier D (1875) Experiments on the brain of monkeys-No. 1. *Proc R Soc Lond B* 23, 409-30.
- Friel KM, Barbay S, Frost SB, Plautz EJ, Stowe AM, Dancause N, Zoubina EV, Nudo R (2007) Effects of a rostral motor cortex lesion on primary motor cortex hand representation topography in primates. *Neurorehabil Neural Repair* 21(1):51-61.
- Fritsch, G. and Hitzig, E (1870) Über die elektrische Erregbarkeit des Grosshirns. *Archs Anat Physiol Wiss. Med.* 37, 300-332. (Translation by Bonin, G. Von. *In The cerebral cortex*, pp. 73-96. Thomas, Springfield, Illinois).
- Graziano MS, Aflalo TN, Cooke DF (2005) Arm movements evoked by electrical stimulation in the motor cortex of monkeys. *J Neurophysiol* 94(6):4209-23.
- Graziano MSA, Taylor CSR, Moore T (2002) Complex movements evoked by microstimulation of precentral cortex. *Neuron* 34: 841-851.

- Gustafsson B, Jankowska E (1976) Direct and indirect activation of nerve cells by electrical pulses applied extracellularly. *J Physiol* 258(1):33-61.
- Kasser RJ, Cheney PD (1985) Characteristics of corticomotoneuronal postspike facilitation and reciprocal suppression of EMG activity in the monkey. *J Neurophysiol* 53(4): 959-78.
- Kosar E, Waters RS, Tsukahara N, Asanuma H (1985) Anatomical and physiological properties of the projection from the sensory cortex to the motor cortex in normal cats: the difference between corticocortical and thalamocortical projections. *Brain Res* 345(1):68-78.
- Kwan HC, Mackay WA, Murphy JT, Wong YC (1978) An intracortical microstimulation study of output organization in precentral cortex of awake primates. *J Physiol (Paris)*. 74(3):231-3.
- Lemon RN, Muir RB, Mantel GW (1987) The effects upon the activity of hand and forearm muscles of intracortical stimulation in the vicinity of corticomotor neurones in the conscious monkey. *Exp Brain Res* 66(3):621-37.
- Macpherson JM, Marangoz C, Miles TS, Wiesendanger M (1982) Microstimulation of the supplementary motor area (SMA) in the awake monkey. *Exp Brain Res* 45(3):410-6.
- McIntyre CC, Grill WM (2002) Extracellular stimulation of central neurons: influence of stimulus waveform and frequency on neuronal output. *J Neurophysiol* 88(4):1592-604.
- McIntyre CC, Grill WM (2000) Selective microstimulation of central nervous system neurons. *Ann Biomed Eng* 28(3):219-33.
- McKiernan BJ, Marcario JK, Hill Karrer J, Cheney PD (1998) Corticomotoneuronal postspike effects in shoulder, elbow, wrist, digit, and intrinsic hand muscles during a reach and prehension task. *J Neurophysiol* 80(4): 1961-1980.

- Mewes K, Cheney PD (1991) Facilitation and suppression of wrist and digit muscles from single rubromotoneuronal cells in the awake monkey. *J Neurophysiol* 66(6): 1965-77.
- Mewes K, Cheney PD (1994) Primate rubromotoneuronal cells: parametric relations and contribution to wrist movement. *J Neurophysiol* 72: 14-30.
- Mori A, Waters RS, Asanuma H (1983) Low threshold motor effects produced by stimulation of area preinsularis (2 pr.i) of the secondary sensory cortex in the cat; input-output relationship. *Exp Brain Res* 51(1):108-16.
- Naito E, Kinomura S, Geyer S, Kawashima R, Roland PE, Zilles K (2000) Fast reaction to different sensory modalities activates common fields in the motor areas, but the anterior cingulate cortex is involved in the speed of reaction. *J Neurophysiol* 83(3): 1701-9.
- Nakamura H., Kitagawa, H., Kawaguchi, Y. & Tsuji, H (1997) Intracortical facilitation and inhibition after transcranial magnetic stimulation in conscious humans. *J Physiol* 498, 817-823.
- Nelson RJ, McCandlish CA, Douglas VD (1990) Reaction times for hand movements made in response to visual versus vibratory cues. *Somatosens Mot Res* 7(3): 337-52.
- Nowak LG, Bullier J (1998a) Axons, but not cell bodies, are activated by electrical stimulation in cortical gray matter. I. Evidence from chronaxie measurements. *Exp Brain Res* 118(4):477-88.
- Nowak LG, Bullier J (1998b) Axons, but not cell bodies, are activated by electrical stimulation in cortical gray matter. II. Evidence from selective inactivation of cell bodies and axon initial segments. *Exp Brain Res* 118(4):489-500.

- Park MC, Belhaj-Saïf A, Cheney PD (2000) Chronic recording of EMG activity from large numbers of forelimb muscles in awake macaque monkeys. *J Neurosci Methods* 15;96(2): 153-60.
- Park MC, Belhaj-Saïf A, Gordon M, Cheney PD (2001) Consistent features in the forelimb representation of primary motor cortex in rhesus macaques. *J Neurosci* 21(8):2784-92.
- Porter R (1963) Focal Stimulation of Hypoglossal Neurones in the cat. *J Physiol* 169:630-40.
- Ramanathan D, Conner JM, Tuszynski MH (2006) A form of motor cortical plasticity that correlates with recovery of function after brain injury. *Proc Natl Acad Sci U S A*. 103(30):11370-5.
- Rattay F (1999) The basic mechanism for the electrical stimulation of the nervous system. *Neurosci* 89(2):335-46.
- Sanger TD, Garg RR, Chen R (2001) Interactions between two different inhibitory systems in the human motor cortex. *J Physiol* 530(Pt 2):307-17.
- Sato KC, Tanji J. (1989) Digit-muscle responses evoked from multiple intracortical foci in monkey precentral motor cortex. *J Neurophysiol* 62(4):959-70.
- Schieber MH, Deuel RK (1997) Primary motor cortex reorganization in a long-term monkey amputee. *Somatosens Mot Res* 14(3): 157-67.
- Schmidlin E, Wannier T, Bloch J, Rouiller EM (2004) Progressive plastic changes in the hand representation of the primary motor cortex parallel incomplete recovery from a unilateral section of the corticospinal tract at cervical level in monkeys. *Brain Res* 1017(1-2):172-83
- Schmidt EM, McIntosh JS (1990) Microstimulation mapping in precentral cortex during trained movements. *J Neurophysiol*. 64(6): 1668-82.

- Swadlow HA (1992) Monitoring the excitability of neocortical efferent neurons to direct activation by extracellular current pulses. *J Neurophysiol* 68(2):605-19.
- Tandon S, Kambi N, Jain N (2008) Overlapping representations of the neck and whiskers in the rat motor cortex revealed by mapping at different anaesthetic depths. *Eur J Neurosci* 27(1):228-37.
- Thompson FJ, Fernandex JJ (1975) Patterns of cortical projections to hindlimb muscle motoneurone pools. *Brain Res* 97(1): 33-46.
- Waters RS, Asanuma H (1983) Movement of facial muscles following intracortical microstimulation (ICMS) along the lateral branch of the posterior bank of the ansate sulcus, areas 5a and 5b, in the cat. *Exp Brain Res* 50(2-3):459-63.
- Weinrich M, Wise SP (1982) The premotor cortex of the monkey. *J Neurosci* 2(9):1329-45.

CHAPTER SIX

COMPARISON OF OUTPUT EFFECTS ON EMG ACTIVITY

OBTAINED WITH DIFFERENT METHODS OF

MICROSTIMULATION

ABSTRACT

Intracortical microstimulation (ICMS) methods are widely used to study the organization and function of motor cortex. However, few studies have documented how measures of motor output change with different ICMS stimulus parameters. The primary objective of this study was to compare output effects from primary motor cortex (M1) elicited by three forms of ICMS: stimulus triggered averaging of EMG activity (StTA), repetitive short duration ICMS (RS-ICMS, 10 pulses @ 330 Hz) and repetitive long duration ICMS (RL-ICMS, 100 pulses @ 200 Hz). Averages of EMG activity from 24 forelimb muscles were collected from a male rhesus macaque during an isometric push-pull task and a forelimb reaching task. Twenty-two layer V sites were identified and microstimuli were applied at a low rate (15 Hz) to obtain output effects with StTA and at a high rate to obtain output effects with RS-ICMS and RL-ICMS. Across ICMS methods, percent of matching effects was defined as number of muscles with the same sign of effect (excitation, inhibition) regardless of magnitude. Muscles with no post-stimulus effect in either average being compared were not included. At 15 μ A, effects in StTAs matched 58% of the effects elicited with RS-ICMS and 46% of effects elicited with RL-ICMS at the same sites. At higher stimulus intensities, the percent of muscles with matching effects in StTAs improved. The extent of matching effects across stimulation methods improved substantially when only distal muscles were considered. This is probably attributable to the fact that distal

muscles also had the strongest stimulus evoked effects. While significant disparities exist between effects obtained with StTA and short or long duration ICMS, overall the output effects obtained with different methods was surprisingly consistent given the potential for physiological spread and expansion of effects with repetitive stimulation methods.

INTRODUCTION

Intracortical microstimulation (ICMS) approaches have historically been used to reveal basic features of somatotopic organization of motor cortex. Since the original findings with ICMS (Stoney et al., 1968), different variations of this method have been used to map and investigate motor cortex output properties (Baker et al., 1998; Boudrias et al., 2006; Cerri et al., 2003; Davidson and Buford 2006; Godschalk et al., 1995; Hatanaka et al., 2001; Hummelsheim et al., 1986; Lemon et al., 2002; Luppino et al., 1991; Mitz and Wise 1987; Moritz et al., 2007; Park et al., 2001, 2004; Perlmutter et al., 1998; Raos et al., 2003; Schieber 2001) and to characterize the plasticity of motor cortex following injury (Frost et al., 2003; Nudo and Milliken 1996; Schmidlin et al., 2004) or motor skill learning (Kleim et al., 2004; Martin et al., 2005; Nudo et al., 1996).

One common method of ICMS is stimulus triggered averaging (StTA) of electromyographic (EMG) activity which involves applying microstimuli at low frequencies (15 Hz) to avoid temporal summation of excitatory postsynaptic potentials at the motoneuron. The effects from this method are below threshold for overt muscle activation so averaging of EMG activity is required (Cheney and Fetz, 1985). By averaging muscle activity with reference to the stimulus; this method provides a highly sensitive and quantifiable method of revealing both excitatory and inhibitory output effects on motoneurons. Another method is repetitive short duration ICMS (RS-

ICMS), which consists of applying short trains of 10 symmetrical biphasic stimulus pulses at high frequency, typically 330 Hz (Asanuma and Rosén 1972). This is a supra-threshold method and easily produces muscle twitches and twitch-like movements. A new approach termed long duration repetitive ICMS (RL-ICMS) involves the application of high frequency ICMS for relatively long durations (typically 500 ms) matching the duration of typical voluntary movements (Graziano et al., 2002). This method yields natural appearing arm movements ending with the hand positioned in different parts of the animals work space depending on cortical area stimulated. The movements are described as being similar to natural movements involved in visually guided object manipulation. An important feature of movements evoked with RL-ICMS is stimulation of a single cortical site produces movements to a specific end-point location in the monkey's work space, independent of starting hand position.

Although ICMS methods are used extensively, there is a fundamental deficiency of data on the extent to which the relative strength and distribution of output effects across muscles obtained with different methods are comparable. There is also a need for documentation of relationships between motor output effects and stimulus parameters (frequency, duration, and magnitude). Therefore, the purpose of this study was to compare the output effects on forelimb muscle activity from StTA, RS-ICMS and RL-ICMS.

MATERIALS AND METHODS

Behavioral tasks

Data were collected from a male rhesus monkey (*Macaca mulatta*; ~10kg, 9 years old) trained to perform an isometric whole arm push-pull task (Figure 3.1 B) and a reach-to-grasp task (Figure 3.1C). During each data collection session, the monkey was seated in a custom built primate chair inside a sound-attenuating chamber. The left forearm was restrained during task performance. All tasks were performed with the right arm.

For the isometric whole arm push-pull task (Figure 3.1B), the monkeys were required to grip a handle fixed to a force transducer (Grass Medical Instruments, West Warwick, RI) on a linear XYZ positioning system. Monkeys were required to generate ramp and hold trajectories of torque alternately between push (arm extension) and pull (arm flexion) target zones. The inner and outer boundaries of the torque window were 1 N and 2 N respectively. Delivery of an applesauce reward was contingent upon the monkey holding within each zone for one second. The handle was locked into place at position D (Figure 3.1B a).

The reach-to-grasp task (Figure 3.1C) has been described previously (Belhaj-Saïf et al., 1998; McKiernan et al., 1998). The task was initiated when the monkey placed its right hand, palm down, on a pressure detecting plate (home plate). The home plate was located at waist level in front and to the right of the monkey. Holding the plate down for a preprogrammed length of

time (2-3 seconds) triggered the release of a food reward into a cylindrical well at arms length from the monkey. The monkey then grasped and brought the food reward to its mouth. The task was completed by returning the hand to the pressure plate.

Surgical procedures

After training, a 30-mm inside diameter titanium chamber was stereotaxically centered over the forelimb area of M1 on the left hemisphere of the monkey and anchored to the skull with 12 titanium screws (Stryker Leibinger, Germany) and dental acrylic (Lux-it Inc., Blue Springs, MO). Threaded titanium nuts (Titanium Unlimited, Houston, TX) were also attached over the occipital aspect of the skull using 12 additional titanium screws and dental acrylic. These nuts provided a point of attachment for a flexible head restraint system during data collection sessions. The chamber was centered at anterior 16 mm, lateral 22 mm, at a 30° angle to the sagittal plane.

EMG activity was recorded from 24 muscles of the forelimb with pairs of insulated, multi-stranded stainless steel wires (Cooner Wire, Chatsworth, CA) implanted during an aseptic surgical procedure (Park et al., 2000). Pairs of wires for each muscle were tunneled subcutaneously from an opening above the elbow to their target muscles. The wires of each pair were bared of insulation for ~ 2 - 3 mm at the tip and inserted into the muscle belly with a separation of ~ 5 mm. Implant locations were confirmed by stimulation through the wire pair and observation of appropriate muscle twitches. EMG

connector terminals (ITT Cannon, White Plains, NY) were affixed to the upper arm using medical adhesive tape. Following surgery, the monkeys wore a Kevlar jacket (Lomir Biomedical Inc., Malone, NY) reinforced with fine stainless steel mesh (Sperian Protection Americas Inc., Attleboro Falls, MA) to protect the implant. EMG activity was recorded from five shoulder muscles: pectoralis major (PEC), anterior deltoid (ADE), posterior deltoid (PDE), teres major (TMAJ), and latissimus dorsi (LAT); seven elbow muscles: biceps short head (BIS), biceps long head (BIL), brachialis (BRA), brachioradialis (BR), triceps long head (TLON), triceps lateral head (TLAT) and dorso-epitrochlearis (DE); five wrist muscles: extensor carpi radialis (ECR), extensor carpi ulnaris (ECU), flexor carpi radialis (FCR), flexor carpi ulnaris (FCU), and Palmaris longus (PL); five digit muscles: extensor digitorum communis (EDC), extensor digitorum 2 and 3 (ED2,3) extensor digitorum 4 and 5 (ED4,5), flexor digitorum superficialis (FDS), and flexor digitorum profundus (FDP); and two intrinsic hand muscles: abductor pollicis brevis (APB) and first dorsal interosseus (FDI).

All surgeries were performed under deep general anesthesia and aseptic conditions. Postoperatively, monkeys were given an analgesic (Buprenorphine 0.5 mg/kg every 12h for 3-4 days) and antibiotics (Penicillin G, Benzathine / Procaine combination, 40,000 IU/kg every 3 days). All procedures were in accordance with the Association for Assessment and Accreditation of Laboratory Animal Care (AAALAC) and the Guide for the

Care and Use of Laboratory Animals, published by the US Department of Health and Human Services and the National Institutes of Health.

Data collection

Sites in M1 were stimulated using glass and mylar insulated platinum-iridium electrodes with impedances ranging from 0.5 to 1.5 M Ω (Frederick Haer & Co., Bowdoinham, ME). The electrode was positioned within the chamber using an X-Y coordinate manipulator and was advanced at approximately a right angle into the cortex with a manual hydraulic microdrive (Frederick Haer & Co., Bowdoinham, ME). Rigid support for the electrode was provided by a 22 gage cannula (Small Parts Inc., Miami Lakes, FL) inside of a 25 mm long, 3 mm diameter stainless steel post which served to guide the electrode to the surface of the dura.

First cortical unit activity was noted and the electrode was lowered 1.5 mm below this point to layer V. In order to distinguish layer V from more superficial layers, particularly in the bank of the precentral gyrus, neuronal activity was evaluated for the presence of large action potentials that were often modulated with the task and StTAs for the presence of both clear and robust effects at 15 μ A. Individual stimuli were symmetrical bi-phasic pulses: a 0.2 ms negative pulse followed by a 0.2 ms positive pulse. EMG activity was generally filtered from 30 Hz to 1 KHz, digitized at a rate of 4 kHz and

full-wave rectified. Stimuli (15, 30, 60 and 120 μ A) were applied throughout all phases of the task.

- Stimulus triggered averages

Layer V sites in forelimb M1 were identified and microstimuli were applied at 15 Hz. The assessment of single pulse ICMS effects was based on averages of at least 500 trigger events. Segments of EMG activity associated with each stimulus were evaluated and accepted for averaging only when the mean of all EMG data points over the entire 60msec epoch was \geq 5% of full-scale input. This prevented averaging segments in which EMG activity was minimal or absent (McKiernan et al., 1998).

- Repetitive ICMS triggered averages

Layer V sites with clear post-stimulus effects (PStEs) in StTAs of forelimb muscles were identified and selected for data collection with RS-ICMS and RL-ICMS. RS-ICMS consisted of a train of 10 symmetrical biphasic stimulus pulses at 330 Hz (Asanuma and Rosen, 1972). The assessment of effects was based on averages of 30 – 40 trigger events. RL-ICMS consisted of a train of 100 symmetrical biphasic stimulus pulses at 200 Hz (500 ms). The assessment of effects was based on averages of 8 - 12 trigger events.

Data analysis

At each stimulation site, averages were obtained for all 24 muscles using three methods of ICMS (StTA, RS-ICMS and RL-ICMS). The onset latency of the post-stimulus effect was based on visual inspection of the record and was marked where the activity inflected relative to the pre-trigger baseline of EMG. Baseline EMG level was measured from the pre-trigger period in all stimulus triggered averages.

- Stimulus triggered averages

Averages were compiled over a 60 ms epoch, including 20 ms before the trigger to 40 ms after the trigger. Post-stimulus facilitation (PStF) and post-stimulus suppression (PStS) effects were computer-measured as described in detail by Mewes and Cheney (1991, 1994). Nonstationary, ramping baseline activity was subtracted from StTAs using custom analysis software. Mean baseline activity and the standard deviation (SD) of baseline EMG activity was measured from the pre-trigger period typically consisting of the first 12.5 ms of each average. StTAs were considered to have a significant post-stimulus effect (PStF or PStS) if the points of the record crossed a level equivalent to 2 SD of the mean of the baseline EMG for a period ≥ 0.75 ms or more (Park et al., 2001).

- Repetitive ICMS triggered averages

RS-ICMS triggered averages were compiled over a 60 ms epoch, including 10 ms before the trigger to 50 ms after the trigger. RL-ICMS triggered averages were compiled over a 1.2 s epoch, including 200 ms before the trigger to 1,000 ms after the trigger. Mean baseline activity was measured from the pre-trigger period typically consisting of the first 10 ms of each RS-ICMS average and the first 100 ms of each RL-ICMS average. The first pulse of each train was used as a trigger to compute averages of EMG activity. The magnitude of the EMG response was expressed as the mean EMG level present after the first RL-ICMS pulse and throughout the stimulus train.

Quantitative measurement of post-stimulus effect magnitude

The strength of post-stimulus effects was quantified in two ways for StTA. The magnitude of PStF and PStS was expressed as the mean percent increase (+ mpi) and peak percent increase (+ppi) or mean percent decrease (- mpi) and peak percent decrease (-ppi) in EMG activity above (PStF) or below (PStS) baseline EMG activity (Cheney and Fetz, 1985; Kasser and Cheney, 1985; Cheney et al., 1991). The strength of muscle activation with RS-ICMS and RL-ICMS was expressed as + mpi or – mpi. Mean baseline was the average of all bin values in the baseline interval. Mean peak height was the average value between peak onset and offset. Peak values were

measured as the highest point in the peak of facilitation or lowest point in the trough of suppression.

Quantification of matching post-stimulus effects

The percentage of matching output effects to 24 forelimb muscles by three forms of ICMS was determined for 22 layer V sites included in this study. The distribution of effects present in averages of EMG activity was determined at each site for three different forms of ICMS (StTA, RS-ICMS, RL-ICMS). Effects were classified as excitatory (post-stimulus facilitation, PStF), inhibitory (post-stimulus suppression, PStS) or no effect. The percent match of effects from different ICMS methods was defined as the number of muscles with the same sign of effect (excitation, inhibition) regardless of magnitude. Muscles with no effect in either average were excluded. The number of matching effects was divided by the total number of muscles with effects at the same layer V site and with the same stimulus intensity. Comparisons of matches were calculated for: StTA versus RS-ICMS, StTA versus RL-ICMS and RS-ICMS versus RL-ICMS.

Cross-Talk analysis

EMG recordings were tested for cross-talk by computing EMG-triggered averages (Cheney and Fetz, 1980). This procedure involved using the EMG peaks from one muscle as triggers for compiling averages of

rectified EMG activity of all other muscles. To be accepted as a valid post-stimulus effect; the ratio of PStF between test and trigger muscle needed to exceed the ratio of their cross-talk peaks by a factor of two or more (Buys et al., 1986). Based on this criterion, none of the effects obtained in this study needed to be eliminated.

Imaging

Structural MRIs were obtained from a 3 Tesla Siemens Allegra system. Images were obtained with the monkey's head mounted in an MRI compatible stereotaxic apparatus so the orientation and location of the cortical recording chamber and electrode track penetrations could be determined. A two-dimensional rendering of experimental sites was constructed for each monkey. The method for flattening and unfolding cortical layer V in the anterior bank of the central sulcus has been previously described in detail (Park et al., 2001). Briefly, the cortex was unfolded and the location of experimental sites were mapped onto a two dimensional cortical sheet based on the electrode's depth and X-Y coordinate, known architectural landmarks, MRI images, and observations noted during the cortical implant surgeries.

Statistical data analysis

In all tests, statistical significance was based on a P value ≤ 0.05 .

RESULTS

Output effects to 24 forelimb muscles were characterized using three different stimulus parameters (StTA, RS-ICMS, RL-ICMS) applied to 22, layer V sites (Figure 6.1) in the forelimb representation of M1. All sites were characterized using low intensity (15 μ A) microstimuli. For 18 sites, a range of stimulus intensities included 15, 30, 60 and 120 μ A. All four stimulus intensities were applied to 13 sites. The effects from high frequency ICMS methods (RS- and RL-ICMS) were compared to effects obtained with StTA because, at low intensity, it provides a sensitive measure of cortical output that also has high spatial resolution. In fact, it is known that effects in stimulus triggered averages closely match the effects obtained with spike triggered averages from single corticomotoneuronal cells recorded at the same site (Cheney and Fetz, 1985).

Matching Effects from Stimulus Triggered Averages

The distribution of output effects to 24 forelimb muscles was determined for 22 layer V sites with three different forms of ICMS (StTA, RS-ICMS, RL-ICMS). Effects were classified as excitatory (post-stimulus facilitation, PStF), inhibitory (post-stimulus suppression, PStS) or no effect. The percent of matching effects was defined as the number of muscles with the same sign of effect (excitation, inhibition) regardless of magnitude. Muscles with no effect in either compared average were excluded. RL-ICMS

elicited suppression effects were verified as true suppression by comparing EMG activation patterns elicited at different starting hand positions or different segments of the push-pull task (push triggers separated from pull triggers). If any of the resultant RL-ICMS triggered averages yielded increased activity from baseline in one average and decreased activity from baseline in another, the effect was classified as stimulus evoked substitution (see chapter 5 for details). Since stimulus evoked substitution can not be classified as facilitation or suppression alone, it was classified as both. This resulted in a match between stimulus evoked substitution effects and both facilitation and suppression effects elicited with StTA and RS-ICMS. The number of matching effects was divided by the total number of muscles with effects at the same layer V site and with the same stimulus intensity. Comparisons of matches were calculated for: StTA versus RS-ICMS, StTA versus RL-ICMS and RS-ICMS versus RL-ICMS.

At 15 μ A, effects in StTAs matched 58% of the effects elicited with RS-ICMS and 46% of effects elicited with RL-ICMS at the same sites. Effects across the two repetitive ICMS methods showed a 53% match at the same sites. Figure 6.2 shows the effects elicited at a single site with all ICMS methods at 15 μ A. The red boxes outline the matching effects across all three methods. Muscles with effects in StTAs matched 100% of the effects elicited with RS-ICMS and 50% of effects elicited with RL-ICMS. Ten muscles displaying effects with RL-ICMS were not present in the StTA or RS-

ICMS averages (denoted by asterisks). This also reflects the fact that RL-ICMS consistently activates the most muscles. On average, RL-ICMS produced post-stimulus effects in 5.2 more muscles than did StTA at 15 μ A as compared to RS-ICMS which produced effects in 1.9 more muscles. These results are not surprising and suggest that with longer durations of stimulation, effective current spread expands due to temporal summation to an increasing number of neurons. The role of temporal summation with RL-ICMS was also observed in some muscles that showed robust activation but only at relatively long latencies; typically > 200 ms (Fig. 6.3). Robust long latency activation with RL-ICMS was present at all stimulus intensities.

Figure 6.4A shows the overall percent match between ICMS methods at all sites tested with four stimulus intensities. As stimulus intensities increased, the percent of muscles with matching effects steadily improved. Effects were classified as weak post-stimulus effects if the peak, present in the StTA, was less than 20% of the baseline EMG level. This allowed us to eliminate the weak effects and evaluate only the moderate and strong effects produced at each site. However, limiting the analysis to moderate and strong effects did not change the overall results (Figure 6.3B). At 15 μ A, StTA and RS-ICMS consistently produced the best match. At 120 μ A, the two repetitive ICMS methods produced the best match. StTA and RL-ICMS consistently produced the worst match at all four stimulus intensities tested.

Figure 6.5 shows the population data for all sites tested using the three ICMS methods after eliminating effects that were classified as weak. The disparity in matches at individual sites is the highest at the two lower intensities (15, 30 μA). At the two higher intensities (60, 120 μA) all the sites tested show high levels of matching effects. Since the box plot identifies outlier observations (dots above and below each box) and shows the median of all observations (middle line within the box), this type of plot provides an overall representation of results from individual sites. The median percent of matching effects were very similar at all stimulus intensities. The mean percentages of matching effects were not statistically different across the three methods (One Way ANOVA).

The extent of matching effects across stimulation methods improved when only the distal muscles were considered. Figure 6.6A shows the overall percent match between ICMS methods comparing only distal muscles. At 15 μA , effects in StTAs matched 71% of the effects elicited with RS-ICMS and 64% of effects elicited with RL-ICMS at the same sites. Effects across the two repetitive ICMS methods showed a 67% match at the same sites. Again, the differences in the mean percentages of matching effects across all three groups were not great enough to achieve statistical significance (One Way ANOVA). Limiting the analysis to moderate and strong effects alone yielded similar results (Figure 6.6B). The population data shows the level of improvement at individual sites after limiting the data to distal muscles which

were classified as moderate or strong (Figure 6.7). The disparity in matches at individual sites is still highest at lower intensities (15, 30 μ A) compared to higher intensities (60, 120 μ A). However, there are more sights producing 100% matching effects and the sites producing low levels of matching effects are typically the outlier effects.

Evaluating match based on strongest effect

Another way to assess similarity in the distribution of output effects obtained with different ICMS methods is to determine if the same muscle shows the strongest effect independent of the method used. Sites were categorized as matching if muscles with the highest absolute magnitude were the same across ICMS methods being compared. Effects within 5% of the highest magnitude were considered equal to account for slight variations in the order of magnitudes. For example, if at 15 μ A StTA produced the strongest PStF in EDC (mpi = 75) and the second strongest PStF in ED45 (mpi = 72), either were considered a match if the compared average also showed EDC or ED45 as the strongest stimulus elicited effect. Figure 6.8 shows the percentage of sites where the strongest facilitation effects (6.8A) and suppression effects (6.8B) matched. StTA and RS-ICMS produced the highest percent match between strongest facilitation effects elicited. The same was true of suppression with the exception of 15 μ A. Interestingly, the strongest effects elicited by StTA and RS-ICMS match at a number of sites

which remains consistent at higher stimulus intensities. Unlike the comparison between RL-ICMS and StTA which shows a decrease in matching effects as stimulus intensities increase. This comparison reveals a striking departure in the data between comparisons with StTA.

Properties of output effects with different microstimulation methods

Table 6.1 and 6.2 present the characteristics of output effects elicited with different ICMS methods at all sites tested. At 15 μ A, StTA and RS-ICMS produced roughly one third the numbers of effects produced by RL-ICMS. StTA produced 217 post-stimulus effects, RS-ICMS produced 234 and RL-ICMS produced 320 (facilitation and suppression effects together). The gap between the numbers of effects elicited decreased with increasing stimulus intensity. This is due to the fact that with increasing stimulus intensity levels, the number of muscles showing effects increased with StTA and RS-ICMS but stayed somewhat stable for effects elicited with RL-ICMS. This may reflect the fact that physiological spread of current is primarily due to the duration of the stimulus as opposed to the frequency or stimulus intensity. Although the number of post-stimulus facilitation effects generally increased as stimulus intensity increased, the number of suppression effects decreased. This is probably due to the fact that suppression effects are typically weaker than facilitation effects and are easily masked by strong facilitation as stimulus intensity is increased.

Mean onset latencies of EMG effects were identified for all facilitation and suppression effects elicited with all three ICMS methods (Table 6.1 and 6.2, Column 4). At 15 μ A, mean onset latencies for StTAs were comparable to values previously reported (Park et al., 2004). Mean onset latencies for muscles with PStF in StTAs were 9.6 ± 1.7 ms. Facilitation onset latencies found with RS-ICMS and RL-ICMS were 7.7 and 58.4 ms longer than those found with StTA respectively. RS-ICMS mean onset latencies show it takes on average 5 stimulus pulses before a response is elicited in the muscle's activity. Why then do the mean onset latencies with RL-ICMS show an average of 13 stimulus pulses before a response is elicited in the muscles activity? One explanation could be that lower stimulus frequency with RL-ICMS requires more stimulus pulses to elicit muscle responses. However, median onset latency values (Column 5) with RL-ICMS show that half of onset latencies reflect earlier muscle responses, within 7 stimulus pulses. Figure 6.9 shows the distribution of onset latencies observed for the population of effects elicited with RL-ICMS. Outliers with long onset latencies are clearly responsible for the skewed distribution.

Mean onset latencies for muscles with PStS in StTAs were 11.5 ± 2.6 ms. Suppression onset latencies with RS-ICMS and RL-ICMS were 6.6 and 71.4 ms longer than those with StTA respectively. There was a general tendency for onset latencies to shorten as stimulus intensity increased for all ICMS methods. Clearly peak onset latencies are closer for StTA and RS-

ICMS as opposed to those found with RL-ICMS. This is most likely due to additional long latency effects mediated with RL-ICMS and not the other methods of microstimulation. The length of time that the effect remained above or below the 2 standard deviation level of the baseline was measured as the duration of the effect. The average duration of facilitation effects (Table 6.1 and 6.2, Column 7) were close to the length of the stimulus train for both RS-ICMS and RL-ICMS. Durations of facilitation effects for RS-ICMS and RL-ICMS were 25.1 and 443.6 ms respectively.

The magnitude of effects from ICMS methods were calculated using the percent change in the EMG activity level above or below the baseline EMG activity level. Mean percent increase (mpi) and peak percent increase (ppi) were calculated. Mean magnitudes of effects elicited with all three ICMS methods are displayed in Table 6.1 and 6.2 (Columns 8 and 9). Mean facilitation magnitudes (mpi) increased with each higher stimulation level for effects with the exception of RL-ICMS effects at 120 μ A. A comparison of magnitudes reveals that 15 μ A mpi values are 72 and 69 percent greater for RS-ICMS and RL-ICMS respectively compared to StTAs. Figure 6.10 shows the distribution of median mpi values for all ICMS methods and median ppi values for StTA at four stimulus intensities. This comparison reveals a striking separation of magnitudes with repetitive ICMS methods and StTA.

Effects elicited with StTA may be the result of direct activation of the soma of CM cells in the vicinity of the electrode tip or trans-synaptic activation

of those same CM cells. However, they are not likely mediated by trans-synaptic activation of cells outside of M1. Conversely, it has been shown that repetitive ICMS excites interconnected premotor areas and the contralateral hemisphere (Slovin et al., 2003). RL-ICMS effects with long onset latencies likely reflect physiological spread of current and subsequent activation of motoneurons through a less direct route to the spinal cord. Since many effects elicited with RL-ICMS have short onset latencies, it would be a reasonable assumption that effects elicited with RL-ICMS can be separated into two categories; effects elicited through direct corticospinal projections and those elicited through indirect projections to the spinal cord. We used the presence of PStF effects in StTAs as a means to detect activation of motoneurons through a direct corticospinal projection. We separated RL-ICMS and RS-ICMS effects with respect to the presence or absence of PStF effects in StTAs at the same site. One group was comprised of the effects elicited when there was an effect present in the StTA at the same site (direct projection population) and the other group no effect present in the StTA (indirect projection population). Our results show that at 15 μ A, RL-ICMS facilitation effects in the indirect projection population have peak onset latencies which average 84 ms longer than those in the direct projection population. When considering RS-ICMS facilitation effects, the indirect projection population has on average 5.2 ms longer peak onset latencies than those in the direct projection population. Based on these results, RL-ICMS

likely involves a much larger physiological spread of current than does RS-ICMS.

DISCUSSION

The present study represents the first systematic comparison of output effects from StTA, RS-ICMS and RL-ICMS from the same cortical sites. To make a complete comparison of the three forms of stimulation, we evaluated the output effects elicited from the same primary motor cortex sites using several stimulus intensities. The output effects evoked with each of the ICMS methods were assessed and compared for the distribution, temporal characteristics and strength of EMG activity.

Matching output effects with different microstimulation methods

Since StTA of EMG activity involves applying microstimuli at low frequencies (15 Hz) and extensive signal averaging, it can reveal sub-threshold effects in muscles which are functionally connected to the cortical site of stimulation. StTA of EMG activity is therefore a corollary technique to spike triggered averaging (SpTA) of EMG activity. Previous studies have shown a 95% agreement between output effects obtained using StTA and SpTA of EMG activity at single corticomotoneuronal sites in primary motor cortex (Cheney and Fetz 1985). Since repetitive ICMS methods rely on temporal summation of excitatory postsynaptic potentials to evoke overt muscle contraction, there is a possibility that output effects obtained with RS-ICMS and RL-ICMS may show relatively poor agreement with the output effects obtained with StTA. The percentage of matching output effects

elicited with different ICMS methods at low stimulus intensities was considerably poorer (< 58%) than values previously reported for StTA and SpTA. It is reasonable to suspect physiological spread of current for discrepancies in matching effects found in this study. Still, considerably high levels of matching effects (71%) occurred at 15 μ A between StTA and RS-ICMS when only the distal muscle effects were evaluated.

Motor maps with different microstimulation methods

One of the strengths of StTA is the high spatial resolution which allows mapping to individual muscles represented by a small cluster of neurons surrounding the electrode. Motor maps with StTA have revealed a small area of M1 which projects only to distal muscles of the forelimb (Park et al., 2001, 2004). The area is small and there is a possibility that the current spread with repetitive forms of ICMS lose the ability to distinguish this area. At 15 μ A, none of the sites in this study yielded distal only effects with RL-ICMS. Out of the five sites showing only distal effects with StTA, one also had only distal muscle effects with RS-ICMS. As might be expected, that site was the farthest from the border of sites which also yielded effects in proximal muscles. Two of the five sites continued to show distal only effects with StTA at 30 μ A stimulus intensity. The single site showing distal only muscle effects with RS-ICMS also remained consistent at 30 μ A. Although we did not test intensities below 15 μ A, with very low stimulus intensities the distal only

muscle representation may be detectable with RL-ICMS. Regardless, with both repetitive ICMS methods the area of M1 which produces effects in only distal muscles is greatly reduced at stimulus intensities as low as 15 μ A.

These results show that the high spatial resolution obtained with StTA is substantially degraded with high frequency ICMS methods, particularly RL-ICMS and when using stimulus intensities greater than 30 μ A. Since at 15 μ A, individual sites in the distal only muscle representation of M1 are not typically more than 2 mm away from sites which also evoke effects in proximal muscles, it is sensitive to methods which promote physiological spread of current. This is reflected in the fact that RL-ICMS produced effects in both proximal and distal muscles at all the experimental sites which produced effects in only the distal muscles when using StTA. Even RS-ICMS produced effects in both proximal and distal muscles at the majority of sites which produced effects in only the distal muscles using StTA. However, we did not delineate the low threshold relationship between StTA effects and stimulus evoked effects with either repetitive ICMS method. Since movements and muscle twitches can be evoked with repetitive stimulus as low as 3 – 5 μ A (Huntley and Jones 1991; Sato and Tanji 1989) there is an increased likelihood of improvements in resolution with lower stimulus intensities.

Since StTA preferentially activates local neurons directly (Stoney et al., 1968, Jankowska et al., 1975) and repetitive ICMS preferentially elicits its

effects by trans-synaptic activation of neurons (Asanuma and Rosen, 1973; Jankowska et al., 1975) it may be surprising that effects match as well as they do. At higher stimulus intensities, the percent of muscles with matching effects in StTAs showed modest improvement. Eventually reaching relatively good agreement at 120 μ A (range = 76% - 80%). Expansion of effects with higher stimulus intensities was most evident with StTA and RS-ICMS. Less prominent expansion was observed with RL-ICMS and suggests that RL-ICMS is capable of exciting both low and high threshold local neurons and remote neurons with stimulus intensities as low as 15 μ A. Also supporting this notion is the presence of robust long latency activation of muscles with RL-ICMS at 15 μ A. These data likely reflect the importance of stimulus duration for physiological spread of current.

Properties of output effects with different microstimulation methods

Since effects elicited with ICMS likely have both a direct and indirect component (Jankowska et al., 1975; Marcus et al., 1979) the temporal and magnitude characteristics may further elucidate the mechanisms mediating these effects. Our results support those of Jankowska and colleagues (1975) who reported that proportions of direct input increase as the stimulus intensity increases. We observed an overall mean decrease in peak onset latencies as stimulus intensity increased for all ICMS methods. Measures of output effect latencies from repetitive ICMS methods reflect short and long latency

activation of muscles. These effects can be divided into two groups relative to the presence or absence of effects in StTAs at the same site. We used the presence of PStF in StTAs as a means of identifying effects elicited by direct projections to muscles conversely; no effect in StTAs reflects a less direct projection to muscles. RL-ICMS facilitation effects presumably produced by indirect projections had peak onset latencies which averaged 84 ms longer than those presumably produced by more direct projections. In some instances, RL-ICMS could produce onset muscle activity by 5 – 6 ms. RS-ICMS facilitation effects, presumably produced by more indirect projections were on average 5.2 ms longer than those presumably produced by the most direct projections. Based on these results, RL-ICMS likely contributes to a much larger physiological spread of current than does RS-ICMS. This is likely the mechanism behind the production of robust long latency effects to muscles with RL-ICMS.

Further, the increased physiological spread of current with RL-ICMS may be responsible for the pronounced differences when comparing matches between the strongest effects elicited with each ICMS technique. The percentage of matching output effects elicited with StTA and RS-ICMS remained stable as stimulus intensity increased. However the percentage of matching output effects elicited with RL-ICMS compared to the other two methods degraded as stimulus intensity increased. Another pronounced difference with RL-ICMS was the dramatic shift away from increasing

magnitudes with 120 μA . The average magnitudes of effects elicited with StTA and RS-ICMS continued to strengthen as stimulus intensity increased, however with RL-ICMS, magnitudes at 120 μA dropped below the average magnitude with 30 μA (Figure 6.10). These results might suggest that high frequency stimulation of the cortex, at least at high stimulus intensities for long durations, can activate the cortical GABA network which, in turn, inactivates local corticospinal output neurons.

To conclude, our results suggest that motor maps obtained with RS-ICMS can show relatively good matches with StTA and would likely improve at threshold intensities. Output effects with repetitive stimulation methods likely contain direct and indirect components. However, since effects with these methods are usually characterized by visualization of a movement or muscle twitch, as opposed to EMG recordings, our results may be approaching the upper limits of detectable mismatch. Physiological spread of current is most prominent in RL-ICMS suggesting that stimulus duration largely contributes to the division of data between StTA, RS-ICMS and RLICMS.

Table 6.1. Properties of Post-Stimulus Facilitation (PSfF) Output Effects

	# Sites	# PSfF	Mean Onset Latency	Median Onset Latency	Peak Latency	Effect Duration	Magnitude (+mpi)	Magnitude (+ppi)
StTA								
15 μ A	22	174	9.6 \pm 1.7 ms	9.3 ms	12.0 \pm 1.6 ms	4.6 \pm 2.3 ms	26.1 \pm 22.0	44.8 \pm 44.7
30 μ A	17	194	9.2 \pm 1.6 ms	8.5 ms	11.8 \pm 1.7 ms	5.3 \pm 2.7 ms	35.2 \pm 31.5	61.8 \pm 64.1
60 μ A	15	220	8.8 \pm 1.4 ms	8.3 ms	11.6 \pm 1.6 ms	6.0 \pm 2.7 ms	55.1 \pm 54.5	103.2 \pm 117.2
120 μ A	14	228	8.5 \pm 1.5 ms	8.0 ms	11.7 \pm 1.7 ms	7.4 \pm 3.9 ms	80.3 \pm 72.6	152.8 \pm 154.8
RS-ICMS								
15 μ A	22	188	17.3 \pm 6.6 ms	17.3 ms	34.5 \pm 8.9 ms	25.1 \pm 9.6 ms	275.7 \pm 333.2	
30 μ A	17	204	17.4 \pm 6.8 .s	16.5 ms	33.9 \pm 7.7 ms	24.9 \pm 10.4 ms	448.2 \pm 657.7	
60 μ A	15	216	14.6 \pm 6.3 ms	12.6 ms	30.4 \pm 9.2 ms	26.7 \pm 11.2 ms	589.3 \pm 830.7	
120 μ A	14	231	12.5 \pm 5.7 ms	10.8 ms	27.7 \pm 9.8 ms	29.4 \pm 10.5 ms	637.5 \pm 861.2	
RL-ICMS								
15 μ A	22	274	68.0 \pm 74.7 ms	39.0 ms	313.7 \pm 143.9 ms	443.6 \pm 108.3 ms	212.4 \pm 402.1	
30 μ A	17	270	48.2 \pm 51.0 ms	27.9 ms	294.6 \pm 152.0 ms	483.5 \pm 80.8 ms	351.6 \pm 512.9	
60 μ A	15	283	33.5 \pm 37.9 ms	17.8 ms	247.1 \pm 154.4 ms	497.7 \pm 61.4 ms	448.7 \pm 791.5	
120 μ A	14	267	30.4 \pm 45.3 ms	14.0 ms	243.5 \pm 162.8 ms	493.8 \pm 78.5 ms	387.3 \pm 604.3	

Table 6.2. Properties of Post-Stimulus Suppression (PStS) Output Effects

	# Sites	#PStS	Mean Onset Latency	Median Onset Latency	Peak Latency	Effect Duration	Magnitude (-mpi)	Magnitude (-ppi)
StTA								
15 μ A	22	43	11.5 \pm 2.6 ms	12.0 ms	14.0 \pm 3.3	6.8 \pm 5.3 ms	- 15.9 \pm 6.5	- 23.6 \pm 10.5
30 μ A	17	27	12.1 \pm 2.7 ms	12.8 ms	14.3 \pm 2.5 ms	5.3 \pm 3.0 ms	- 14.7 \pm 7.0	- 22.4 \pm 11.9
60 μ A	15	18	11.6 - 2.8 ms	11.8 ms	13.6 \pm 3.0 ms	5.6 \pm 4.0 ms	- 27.0 \pm 20.8	- 38.4 \pm 30.6
120 μ A	14	16	11.4 \pm 2.7 ms	12.0 ms	13.8 \pm 3.8 ms	5.8 \pm 2.5 ms	- 22.1 \pm 7.9	- 31.5 \pm 11.0
RS-								
ICMS								
15 μ A	22	46	18.1 \pm 5.5 ms	16.6 ms	31.7 \pm 9.3 ms	21.6 \pm 8.2 ms	- 50.7 \pm 19.1	
30 μ A	17	42	18.4 \pm 4.8 ms	17.6 ms	31.0 \pm 8.5 ms	20.5 \pm 8.6 ms	- 51.4 \pm 19.7	
60 μ A	15	31	16.6 \pm 4.0 ms	15.6 ms	31.5 \pm 9.0 ms	21.5 \pm 8.3 ms	- 54.4 \pm 19.4	
120 μ A	14	24	15.6 \pm 2.9 ms	16.0 ms	23.6 \pm 8.6 ms	28.3 \pm 6.7 ms	- 64.6 \pm 15.8	
RL-								
ICMS								
15 μ A	22	46	82.9 \pm 60.5	67.8 ms	357.5 \pm 171.2 ms	503.2 \pm 107.9 ms	- 56.3 \pm 23.6	
30 μ A	17	36	46.6 \pm 41.3 ms	34.5 ms	288.5 \pm 169.3 ms	504.3 \pm 75.1 ms	- 42.6 \pm 24.2	
60 μ A	15	17	59.3 \pm 74.2 ms	30.8 ms	368.7 \pm 201.4 ms	502.8 \pm 56.9 ms	- 51.9 \pm 26.3	
120 μ A	14	21	22.0 \pm 11.2 ms	17.8 ms	421.8 \pm 160.5 ms	555.0 \pm 63.1 ms	- 54.3 \pm 25.6	

Figure 6.1. Sites used to compare output effects with different ICMS methods. White circles represent the location of experimental sites in two-dimensional coordinates after unfolding the precentral gyrus. Experimental sites are overlaid on the monkey's respective muscle map.

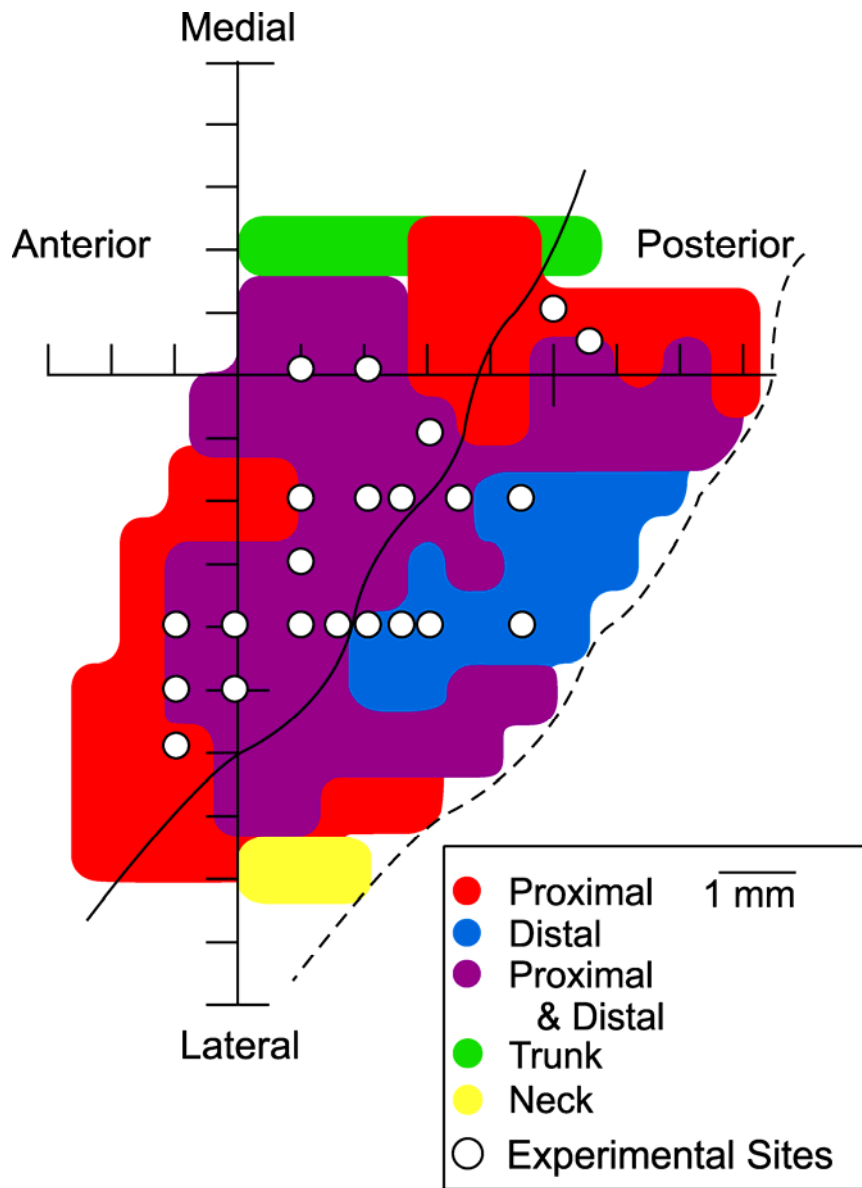


Figure 6.2 Effects produced with different microstimulation methods. A. stimulus triggered averaging (StTA) of EMG activity B. repetitive short duration ICMS (RS-ICMS) and C. repetitive long duration ICMS (RL-ICMS) at a single layer V site in primary motor cortex. Effects were elicited at 15 μ A. Red rectangles outline matching effects with all three methods. Additional effects produced with RL-ICMS are marked with asterisks.

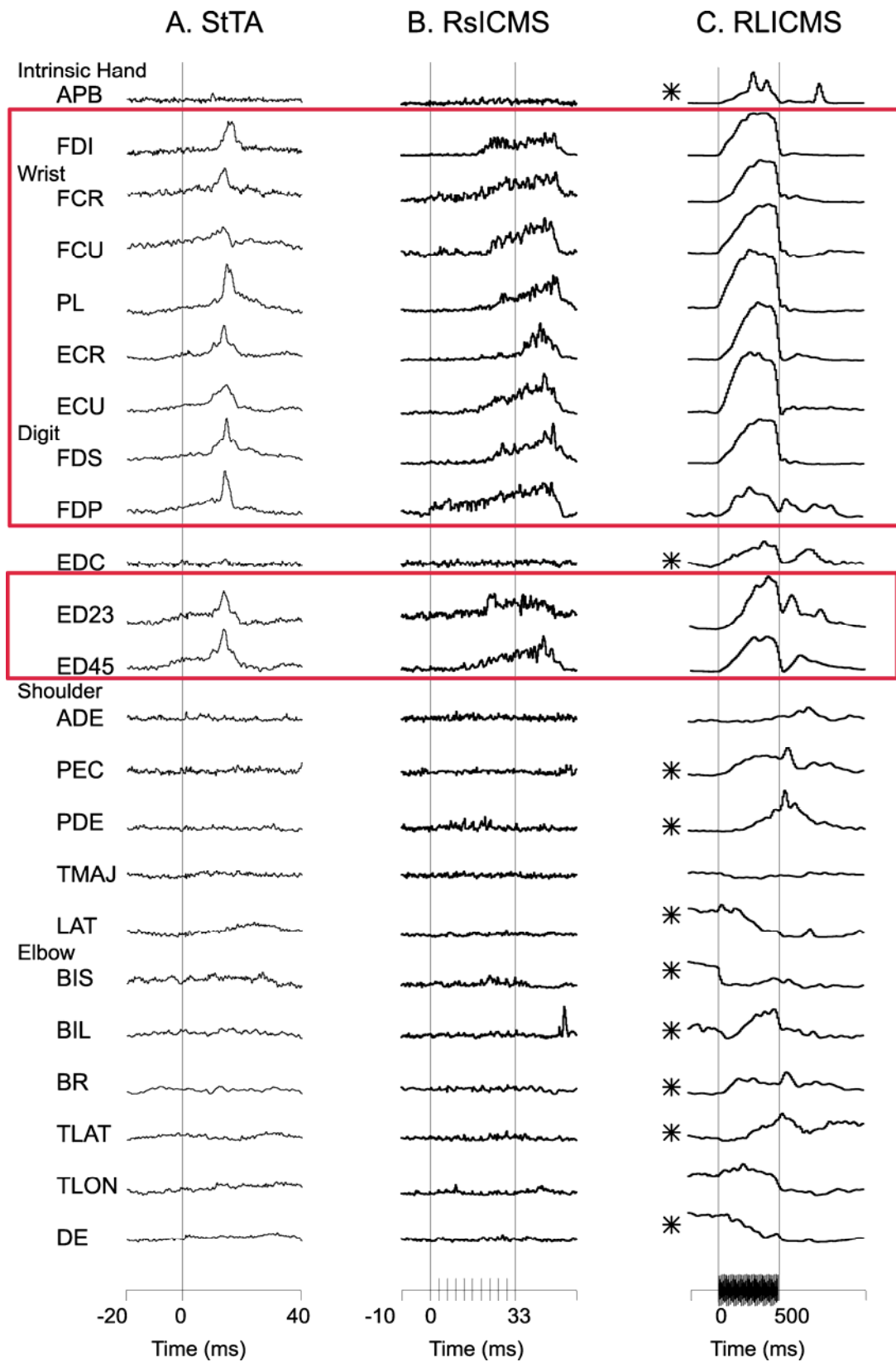


Figure 6.3. Examples of RL-ICMS elicited long latency onset activity. Grey bar represents 500 ms stimulus train. Individual averages are scaled to fit the window.

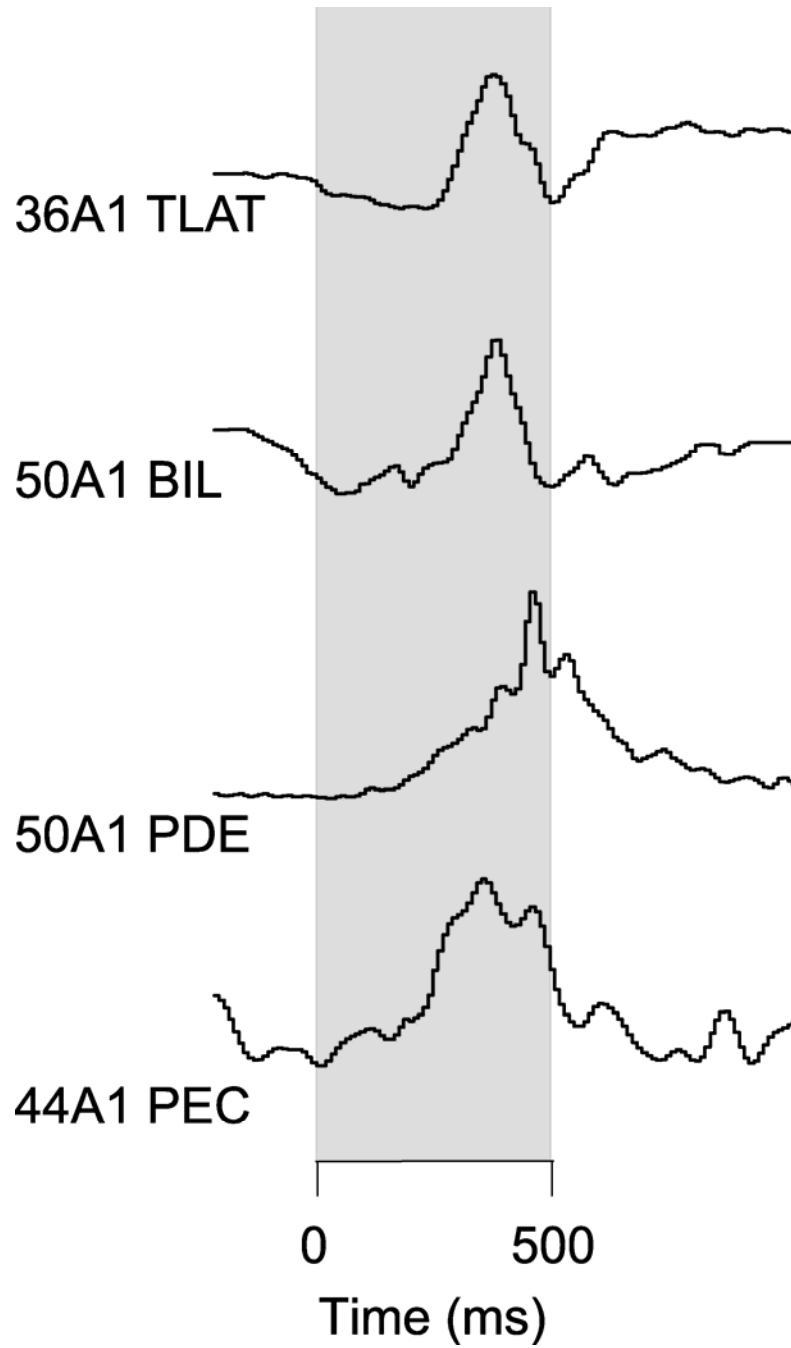


Figure 6.4. Percent of matching output effects across ICMS methods. A. Data based on weak, moderate and strong effects. B. Data based on moderate and strong effects only. Stimulus intensity is plotted along the x-axis. Percent match between effects elicited with two ICMS methods is plotted along the y-axis. Closed circles represent the percent match between stimulus-triggered averages (StTA) and repetitive short duration ICMS (RS-ICMS) output effects. Open circles represent the percent match between StTA and repetitive long duration ICMS (RL-ICMS) output effects. Open triangles represent the percent match between RS-ICMS and RL-ICMS output effects.

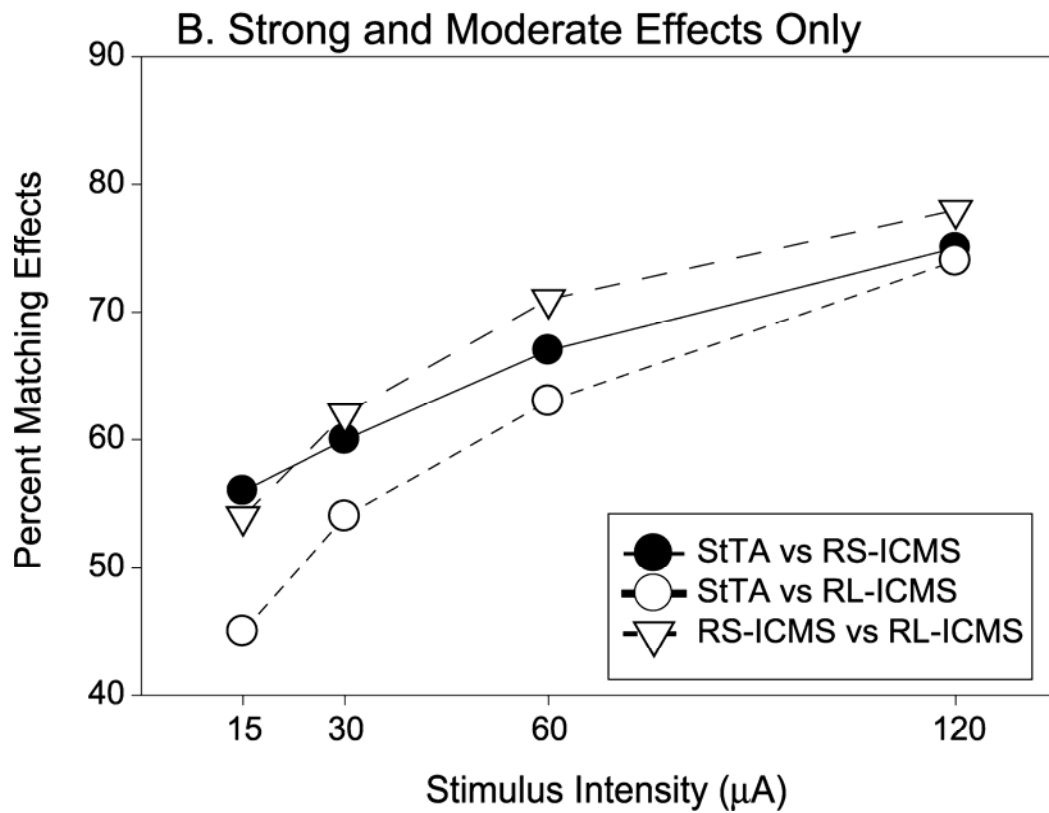
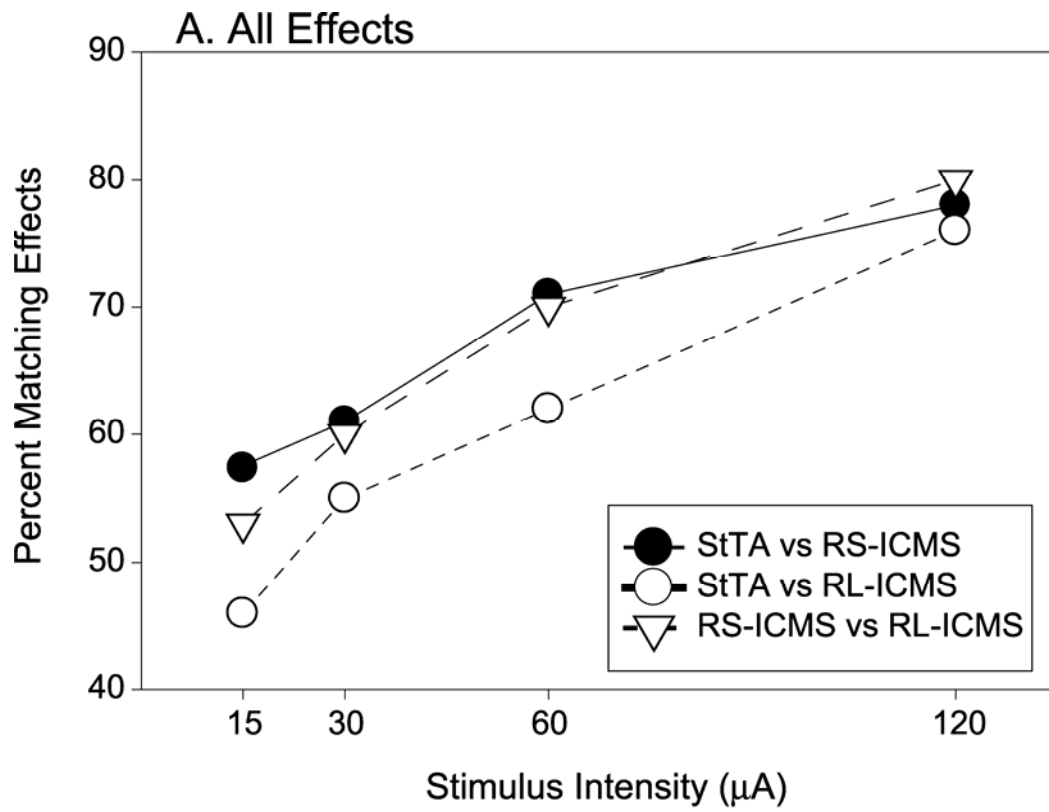


Figure 6.5. Distribution of matching output effects across ICMS methods at individual experimental sites. Box plot data represent moderate and strong effects only. Upper whiskers represent the highest values observed; center lines the population medians and lower whiskers the smallest values. The spacing between different parts of each box indicates the degree of dispersion and skewness in the data. Closed circles represent outliers. Green boxes represent the distribution of match between StTA and RS-ICMS output effects. Yellow boxes represent the distribution of match between StTA and RL-ICMS output effects. Red boxes represent the distribution of match between RS-ICMS and RL-ICMS output effects.

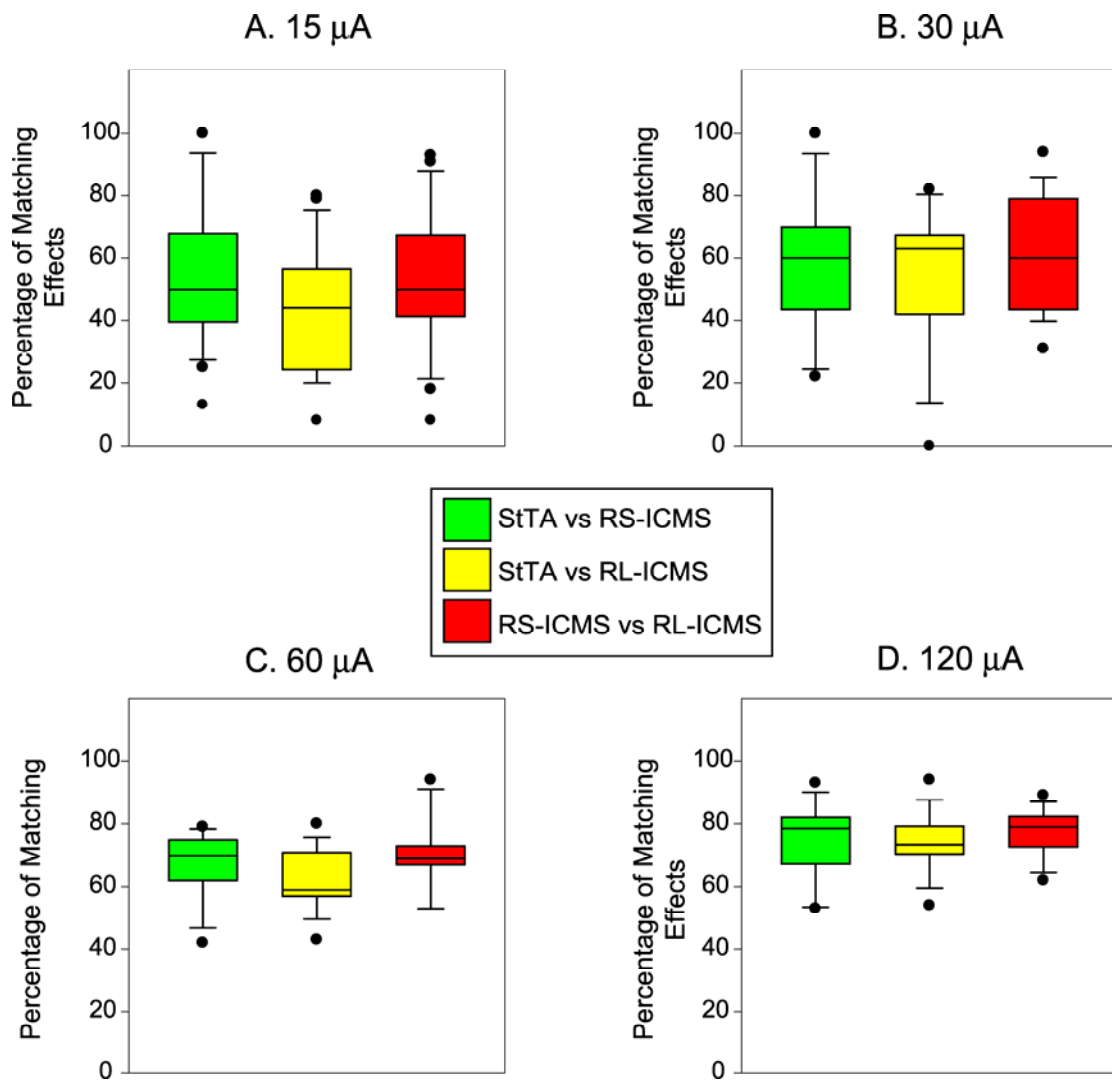


Figure 6.6. Percent of matching distal muscle output effects across ICMS methods. A. Data based on weak, moderate and strong effects. B. Data based on moderate and strong effects only. Stimulus intensity is plotted along the x-axis. Percent match between effects elicited with two ICMS methods is plotted along the y-axis. Closed circles represent the percent match between StTA and RS-ICMS output effects. Open circles represent the percent match between StTA and RL-ICMS output effects. Open triangles represent the percent match between RS-ICMS and RL-ICMS output effects.

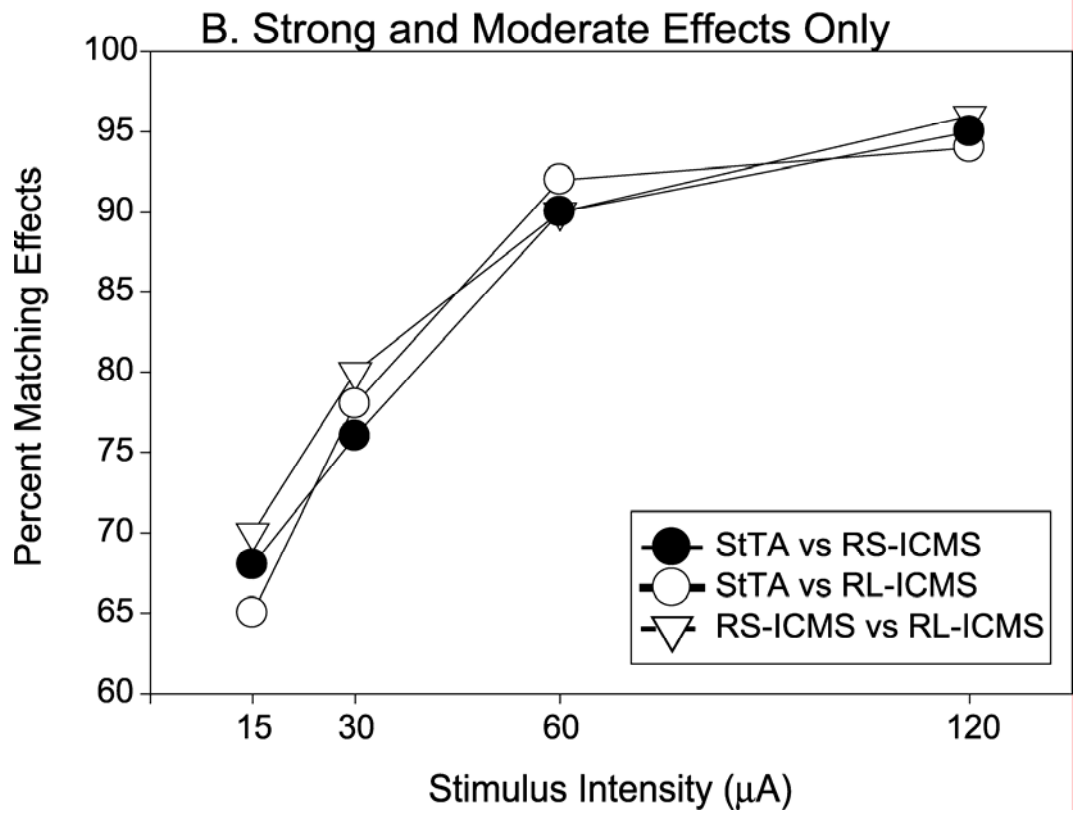
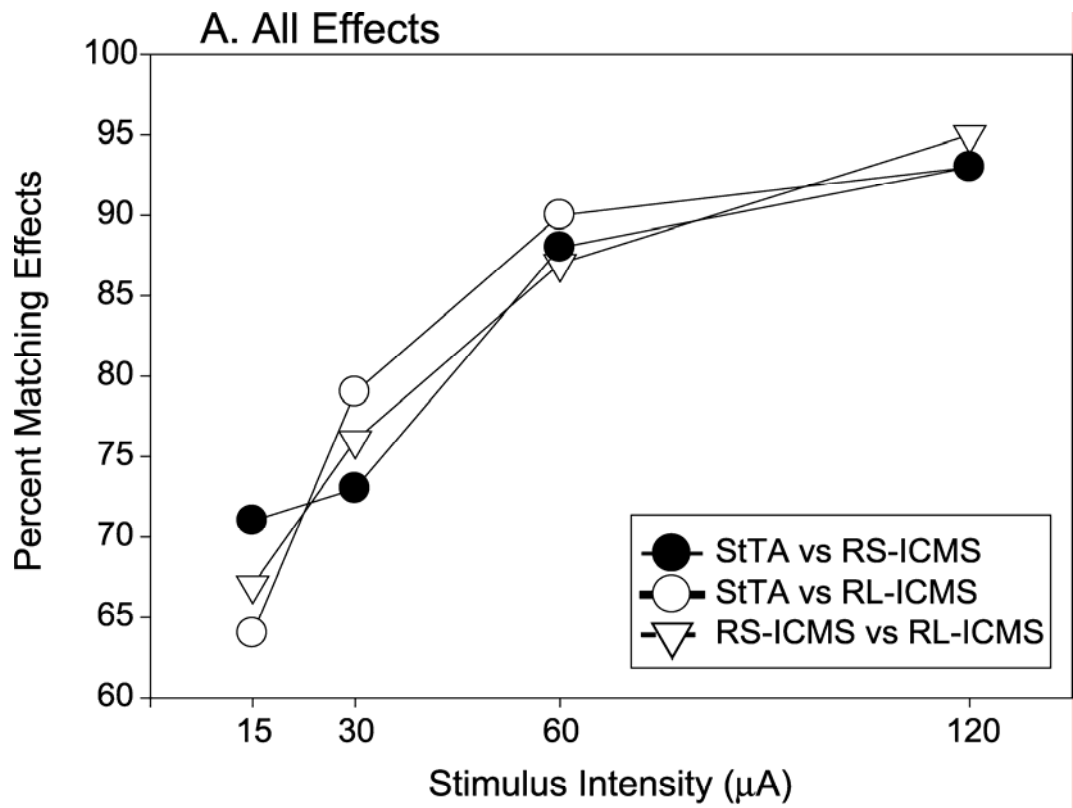


Figure 6.7 Distribution of matching distal muscle output effects across ICMS methods at individual experimental sites. Box plot data represent moderate and strong effects only. Green boxes represent the distribution of match between StTA and RS-ICMS output effects. Yellow boxes represent the distribution of match between StTA and RL-ICMS output effects. Red boxes represent the distribution of match between RS-ICMS and RL-ICMS output effects.

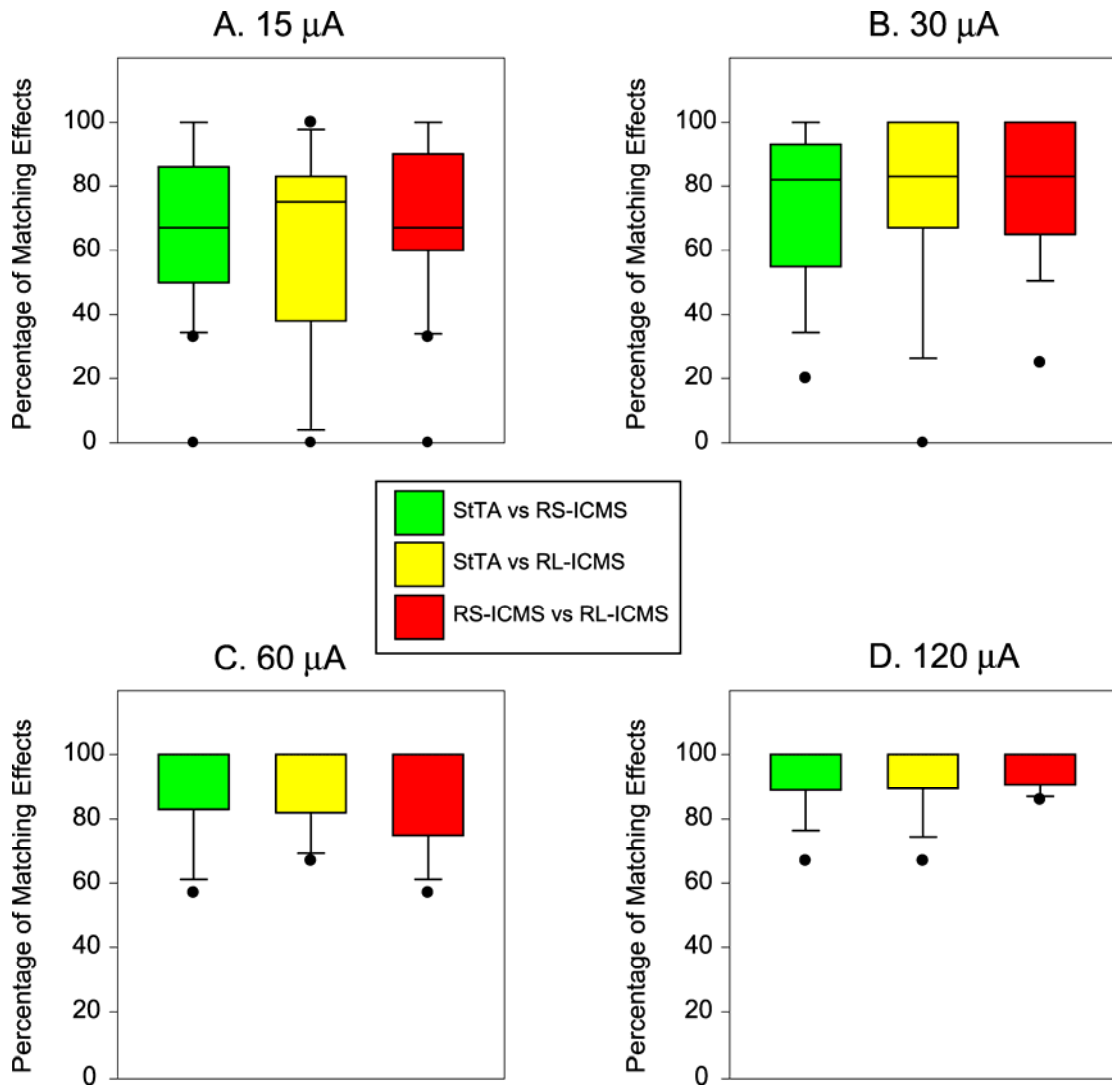


Figure 6.8. Percent of matching output magnitudes across ICMS methods. A. Data based on percent match of the strongest facilitation effects. B. Data based on percent match of the strongest suppression effects. Stimulus intensity is plotted along the x-axis. Percent match between effects elicited with two ICMS methods is plotted along the y-axis. Closed circles represent the percent match between StTA and RS-ICMS output effects. Open circles represent the percent match between StTA and RL-ICMS output effects. Open triangles represent the percent match between RS-ICMS and RL-ICMS output effects.

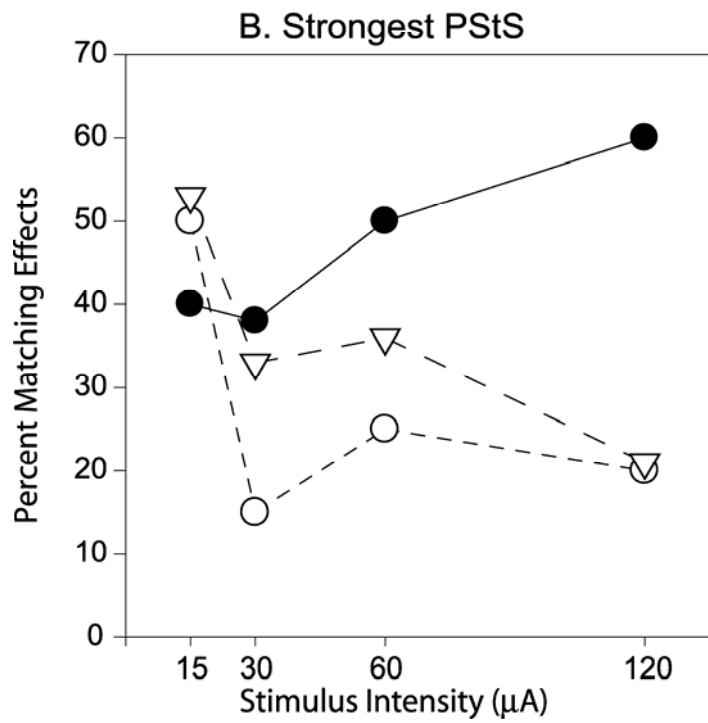
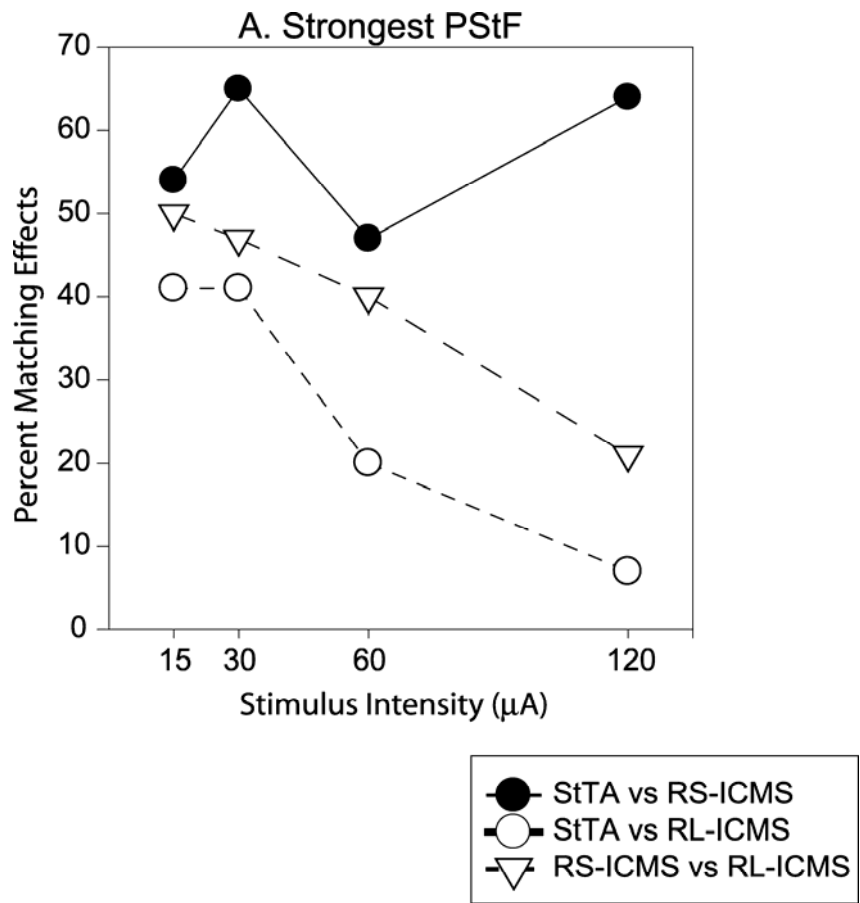


Figure 6.9. Distribution of onset latencies with RL-ICMS. Box plot data represent the population of effects elicited with RL-ICMS which includes all effects.

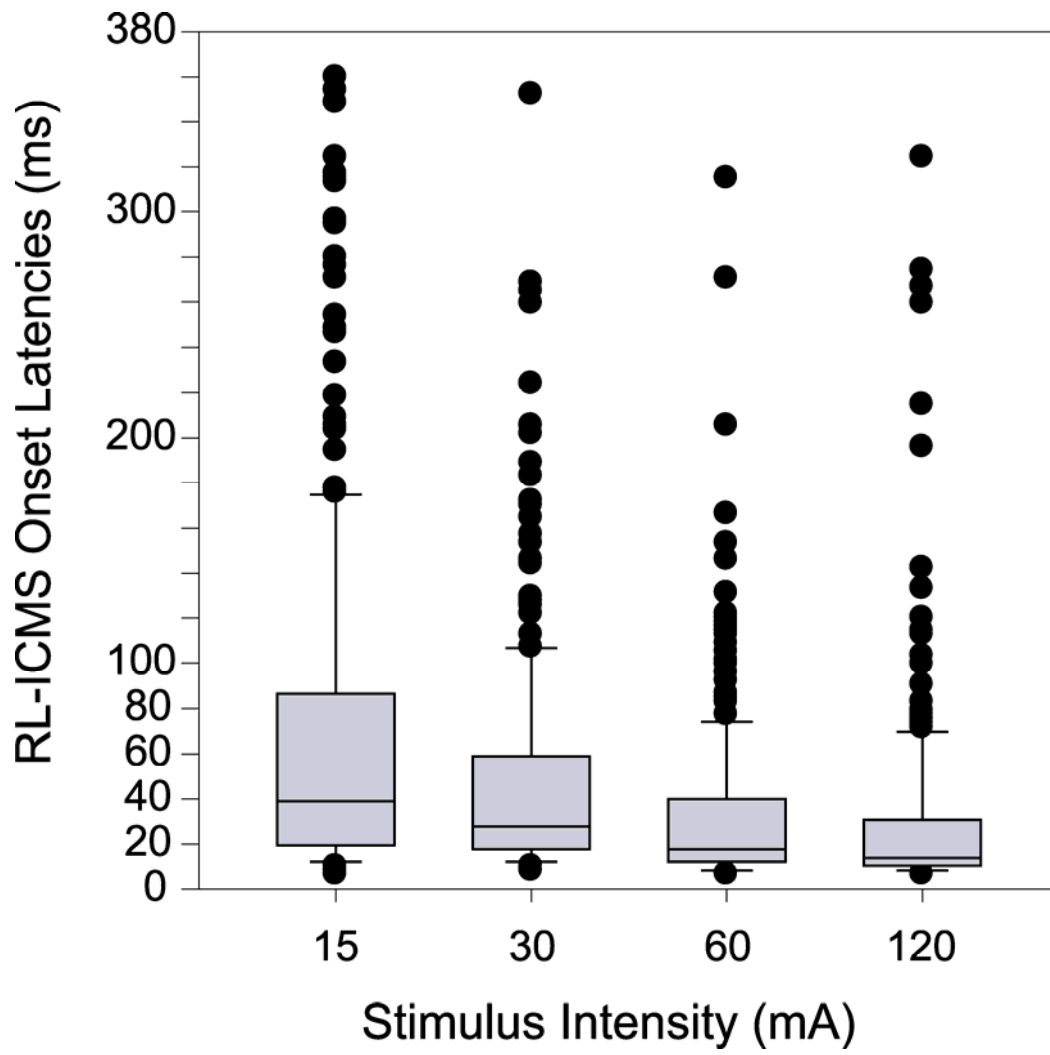
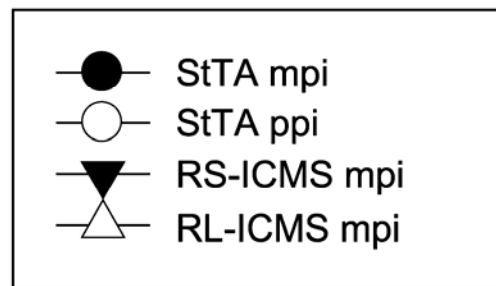
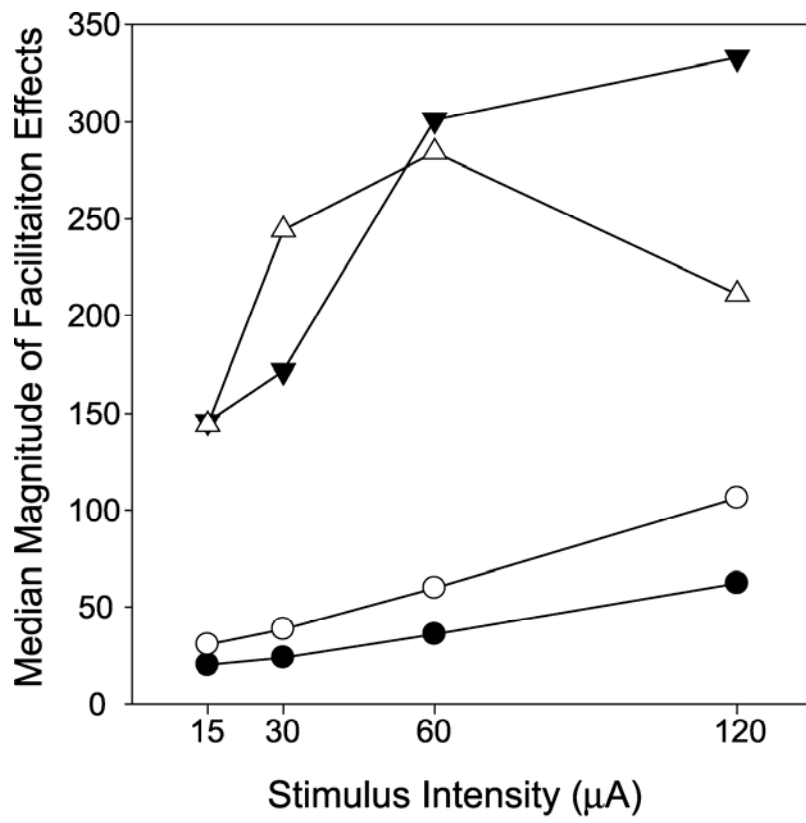


Figure 6.10. Distribution of median magnitude (mpi) values for all ICMS methods including the median magnitude as ppi values for StTA at four stimulus intensities. Closed circles represent median mpi values with StTA. Open circles represent median ppi values with StTA. Closed triangles represent median mpi values with RS-ICMS. Open circles represent median mpi values with RL-ICMS.



REFERENCES

- Asanuma H, Rosén I (1973) Spread of mono- and polysynaptic connections within cat's motor cortex. *Exp Brain Res* 16(5):507-20.
- Asanuma H, Rosén I (1972) Topographical organization of cortical efferent zones projecting to distal forelimb muscles in the monkey. *Exp Brain Res* 14(3): 243-56.
- Baker SN, Olivier E, Lemon RN (1998) An investigation of the intrinsic circuitry of the motor cortex of the monkey using intra-cortical microstimulation. *Exp Brain Res* 123(4):397-411.
- Belhaj-Saïf A, Hill Karrer J, Cheney PD (1998) Distribution and characteristics of post-stimulus effects in proximal and distal forelimb muscles from red nucleus in the monkey. *J Neurophysiol* 79: 1777-1789.
- Boudrias MH, Belhaj-Saïf A, Park MC, Cheney PD (2006) Contrasting properties of motor output from the supplementary motor area and primary motor cortex in rhesus macaques. *Cereb Cortex* 16(5): 632-8.
- Buys EJ, Lemon RN, Mantel GW, Muir RB (1986) Selective facilitation of different hand muscles by single corticospinal neurons in the conscious monkey. *J Physiol* 381: 529-49.
- Cerri G, Shimazu H, Maier MA, Lemon RN (2003) Facilitation from ventral premotor cortex of primary motor cortex outputs to macaque hand muscles. *J Neurophysiol* 90(2):832-42.
- Cheney PD, Fetz EE (1985) Comparable patterns of muscle facilitation evoked by individual corticomotoneuronal (CM) cells and by single intracortical microstimuli in primates: evidence for functional groups of CM cells. *J Neurophysiol* 53(3): 786-804.
- Cheney PD, Fetz EE (1980) Functional classes of primate corticomotoneuronal cells and their relation to active force. *J Neurophysiol* 44(4): 773-91.

- Cheney PD, Mewes K, Widener G (1991) Effects on wrist and digit muscle activity from microstimuli applied at the sites of rubromotoneuronal cells in primates. *J Neurophysiol* 66(6): 1978-92.
- Davidson AG, Buford JA (2006) Bilateral actions of the reticulospinal tract on arm and shoulder muscles in the monkey: stimulus triggered averaging. *Exp Brain Res* 173(1): 25-39.
- Frost SB, Barbay S, Friel KM, Plautz EJ, Nudo RJ (2003) Reorganization of remote cortical regions after ischemic brain injury: a potential substrate for stroke recovery. *J Neurophysiol* 89(6):3205-14.
- Graziano MSA, Taylor CSR, Moore T (2002) Complex movements evoked by microstimulation of precentral cortex. *Neuron* 34: 841-851.
- Godschalk M, Mitz AR, van Duin B, van der Burg H (1995) Somatotopy of monkey premotor cortex examined with microstimulation. *Neurosci Res* 23(3):269-79.
- Hatanaka N, Nambu A, Yamashita A, Takada M, Tokuno H (2001) Somatotopic arrangement and corticocortical inputs of the hindlimb region of the primary motor cortex in the macaque monkey. *Neurosci Res* 40(1):9-22.
- Hummelsheim H, Wiesendanger M, Bianchetti M, Wiesendanger R, Macpherson J (1986) Further investigations of the efferent linkage of the supplementary motor area (SMA) with the spinal cord in the monkey. *Exp Brain Res* 65(1): 75-82.
- Huntley GW, Jones EG (1991) Relationship of intrinsic connections to forelimb movement representations in monkey motor cortex: a correlative anatomic and physiological study. *J Neurophysiol* 66(2): 390-413.
- Jankowska E, Padel Y, Tanaka R (1975) The mode of activation of pyramidal tract cells by intracortical stimuli. *J Physiol* 249(3): 617-36.

- Kasser RJ, Cheney PD (1985) Characteristics of corticomotoneuronal postspike facilitation and reciprocal suppression of EMG activity in the monkey. *J Neurophysiol* 53(4): 959-78.
- Kleim JA, Hogg TM, VandenBerg PM, Cooper NR, Bruneau R, Remple M (2004) Cortical synaptogenesis and motor map reorganization occur during late, but not early, phase of motor skill learning. *J Neurosci* 24(3):628-33.
- Lemon RN, Maier MA, Armand J, Kirkwood PA, Yang HW (2002) Functional differences in corticospinal projections from macaque primary motor cortex and supplementary motor area. *Adv Exp Med Biol* 508:425-34. Review.
- Luppino G, Matelli M, Camarda RM, Gallese V, Rizzolatti G (1991) Multiple representations of body movements in mesial area 6 and the adjacent cingulate cortex: an intracortical microstimulation study in the macaque monkey. *J Comp Neurol* 311(4):463-82.
- Marcus S, Zarzecki P, and Asanuma H (1979) An estimate of effective current spread of stimulation current (Appendix). *Exp Brain Res* 34: 68–72.
- Martin JH, Engber D, Meng Z (2005) Effect of forelimb use on postnatal development of the forelimb motor representation in primary motor cortex of the cat. *J Neurophysiol* 93(5):2822-31.
- McKiernan BJ, Marcario JK, Hill Karrer J, Cheney PD (1998) Corticomotoneuronal postspike effects in shoulder, elbow, wrist, digit, and intrinsic hand muscles during a reach and prehension task. *J Neurophysiol* 80(4): 1961-1980.
- Mewes K, Cheney PD (1991) Facilitation and suppression of wrist and digit muscles from single rubromotoneuronal cells in the awake monkey. *J Neurophysiol* 66(6): 1965-77.

- Mewes K, Cheney PD (1994) Primate rubromotoneuronal cells: parametric relations and contribution to wrist movement. *J Neurophysiol* 72: 14-30.
- Mitz AR, Wise SP (1987) The somatotopic organization of the supplementary motor area: intracortical microstimulation mapping. *J Neurosci* 7(4):1010-21.
- Moritz CT, Lucas TH, Perlmutter SI, Fetz EE (2007) Forelimb movements and muscle responses evoked by microstimulation of cervical spinal cord in sedated monkeys. *J Neurophysiol* 97(1): 110-20.
- Nudo RJ, Milliken GW, Jenkins WM, Merzenich MM (1996) Use-dependent alterations of movement representations in primary motor cortex of adult squirrel monkeys. *J Neurosci* 16(2):785-807.
- Nudo RJ, Milliken GW (1996) Reorganization of movement representations in primary motor cortex following focal ischemic infarcts in adult squirrel monkeys. *J Neurophysiol* 75(5):2144-9.
- Park MC, Belhaj-Saïf A, Cheney PD (2000) Chronic recording of EMG activity from large numbers of forelimb muscles in awake macaque monkeys. *J Neurosci Methods* 15;96(2): 153-60.
- Park MC, Belhaj-Saïf A, Cheney PD (2004) Properties of primary motor cortex output to forelimb muscles in rhesus macaques. *J Neurophysiol* 92(5): 2968-2984.
- Park MC, Belhaj-Saïf A, Gordon M, Cheney PD (2001) Consistent features in the forelimb representation of primary motor cortex in rhesus macaques. *J Neurosci* 21(8):2784-92.
- Perlmutter SI, Iwamoto Y, Baker JF, Peterson BW (1998) Interdependence of spatial properties and projection patterns of medial vestibulospinal tract neurons in the cat. *J Neurophysiol* 79(1): 270-84.

- Raos V, Franchi G, Gallese V, Fogassi L (2003) Somatotopic organization of the lateral part of area F2 (dorsal premotor cortex) of the macaque monkey. *J Neurophysiol* 89(3):1503-18.
- Sato KC, Tanji J (1989) Digit-muscle responses evoked from multiple intracortical foci in monkey precentral motor cortex. *J Neurophysiol* 62(4): 959-70.
- Schieber MH (2001) Constraints on somatotopic organization in the primary motor cortex. *J Neurophysiol* 86(5): 2125-43. Review.
- Schmidlin E, Wannier T, Bloch J, Rouiller EM (2004) Progressive plastic changes in the hand representation of the primary motor cortex parallel incomplete recovery from a unilateral section of the corticospinal tract at cervical level in monkeys. *Brain Res* 1017(1-2):172-83
- Slovin H, Strick P, Hildesheim R, Girnvald A (2003) Voltage sensitive dye imaging in the motor cortex I. Intra- and intercortical connectivity revealed by microstimulation in the awake monkey. Program No. 554.8 *Abstract Viewer/Itinerary Planner*. Washington, DC: Society for Neuroscience, Online.
- Stoney SD Jr, Thompson WD, Asanuma H (1968) Excitation of pyramidal tract cells by intracortical microstimulation: effective extent of stimulating current. *J Neurophysiol* 31(5): 659-69.

CHAPTER SEVEN
CONCLUSIONS

Neurophysiological studies on non-human primates have provided much of our knowledge of the structural organization and function of the primary motor cortex (M1). This knowledge is useful in the treatment of motor disorders and loss of function post traumatic injury. However, many details still elude certainty. First, what is encoded in the firing of M1 neurons? The answer will be necessary for building realistic neuroprosthetics controllable by M1 neurons. M1 neurons have a physical synaptic connection to motoneurons, which is assumed to be fixed, however with the constant barrage of descending input to the region there may be a loss in our ability to reproduce findings with sensitive output detecting measures such as stimulus triggered averaging (StTA) of electromyographic (EMG) activity. It is important to verify that the methods we use to study M1 show a fixed mapping from M1 to muscles of the limbs. Many labs use different variations of intracortical microstimulation (ICMS) to study motor cortex and map its output to muscles. There is a need to document the relationships between motor output effects and the different stimulus parameters of ICMS. Can the findings with ICMS methods be used to determine the function of M1 and other motor regions?

This work was designed to answer these questions by investigating the output of M1 to 24 muscles of the primate forelimb using both neural recording and stimulation methods. A total of four male rhesus macaques were used to obtain the results reported here. All subjects underwent a

cortical chamber implant surgery as well as one or more chronic EMG implantation surgeries. The cortical chamber implant allowed daily access to M1 and specifically the area which contains neurons which project to forelimb muscles. The EMG implants allowed the chronic daily recording of 24 muscles; including both proximal and distal forelimb muscles. The monkeys were trained on three tasks which preferentially activated proximal muscles (push-pull task), preferentially activated distal muscles (wrist task) or activated both proximal and distal muscles (reach-to-grasp task). These three tasks allowed us to study each distinctive representation of M1.

Spike triggered averaging (SpTA) of EMG activity was used to identify M1 neurons which produced post-spike facilitation effects in EMG activity. The effects detectable with SpTA are likely mediated by a synaptic connection to motoneurons, or the corticomotoneuronal (CM) connection (Fetz and Cheney, 1980; Lemon et al., 1986; Mantel and Lemon, 1987). The temporal patterns of spike trains from identified CM neurons were then compared to the activity of the muscles they were determined to project to; their target muscles.

Our results demonstrate that CM cells can predict the EMG activity of their target muscles. Ninety Five percent of CM cells had an activity peak in the same task segment as at least one of their target muscles. These matching activity peaks further showed a functionally relevant timing reflective of the timing required for the CM cell signal to travel from the cell to the

muscle. When individual CM cell-target muscle activity was compared across the entire duration of the task, relationships were rather weak, but they strengthened with each additional neuron that was selectively added into the population. These results support the argument that CM neuronal populations, as defined by a common synaptic target, encode muscle based parameters. Particularly those reflected in EMG activity.

Since SpTA of EMG activity is both labor and time intensive, a faster approach to studying the output of motor cortical regions is the use of StTA of EMG activity. StTA is a corollary technique to SpTA except that instead of revealing the output of a single neuron, it reveals the output of a few neurons surrounding the electrode tip (Cheney 2002). The output effects elicited with StTA include both post-stimulus facilitation (PStF) and suppression (PStS) effects. PStF reflects a CM connection and it has therefore long been assumed that these output effects are relatively fixed even under different task conditions. However, the results of a modification of ICMS which involves the application of high frequency repetitive ICMS for relatively long train durations (RL-ICMS), typically 500ms (Graziano et al., 2002), suggest that M1 output to muscles is not fixed but changes as a function of task conditions. Not only does this call into question the fixed nature of motor maps obtained with ICMS methods but also raises concerns about the use of StTA and high frequency repetitive ICMS methods to interpret motor function.

The stability of M1 output effects to forelimb muscles with StTA and RL-ICMS were investigated under different task conditions. StTA of EMG activity was used to map the cortical forelimb representation of the 24 forelimb muscles being recorded, to delineate between the distal only, proximal only and the proximal-distal representation of M1. Since the effects with StTA are sub-threshold, they can only be detected in muscles where background activity is present and from the accumulation of large numbers of trigger events. Relative to the placement of the microelectrode within M1, the monkeys performed several tasks to preferentially activate the appropriate muscle group, using either the isometric wrist (distal muscle group) or push-pull (proximal, proximal-distal muscle group) tasks. The effect of joint position and muscle stretch feedback to M1 on output effects in StTA of EMG activity was investigated by performance of the tasks at different wrist angles (isometric wrist task), or elbow and shoulder angles (isometric push-pull task). We also investigated the output effects with dynamic movement compared to isometric force.

Our results demonstrate that M1 output effects obtained with StTA of EMG activity are highly stable in both sign and magnitude across widely varying joints angles and motor tasks. Changes in the sign of effects across joint angles were typically only observed in weak effects. These results validate the use of StTA for mapping and other studies of cortical motor output.

RL-ICMS was applied to the left M1 in two rhesus monkeys which resulted in whole limb movements ending with the hand at a consistent placement relative to the monkey's body. The consistent end-point of the hand was, as previously reported (Graziano et al., 2002), independent of initial starting hand position. In order to determine if these movements were the result of functional muscle activation patterns, RL-ICMS was applied to the left M1 of two rhesus monkeys while they reached with their right hand for a food reward placed in various positions around their work space. The first pulse of each train was used as a trigger to compute averages of EMG activity. The effect of starting hand position on output effects in RL-ICMS triggered averages of EMG activity was investigated.

The most common temporal profile evoked by RL-ICMS was tonic activation of muscles, which was maintained throughout the stimulus train. The sign of the effect on muscle activity was stable (facilitation, suppression or no effect) and independent of the starting hand position. Although the temporal activation profiles could be categorized as different, the magnitude of EMG activated by the stimulus was very stable independent of starting hand position. Our results support a model in which RL-ICMS produces sustained co-activation of multiple antagonist muscles, which then generate limb movement according to the length-tension properties of muscles.

Several RL-ICMS effects provided further evidence that the stimulus pulse is arbitrarily activating surrounding neural elements and creating a

stimulus evoked descending input to the motoneuron pools which creates a movement due to tonic activation of muscles. First, it was observed that RL-ICMS could only generate whole limb movements at stimulus intensities of 60 μ A or higher. This suggests that the weight of the arm and inertia must be overcome by the stimulus to generate movements. Second, at several sites it was observed that after the low intensity application of RL-ICMS, the arm simply fell to the monkey's side. This suggests that RL-ICMS interrupted the monkey's voluntary movement. RL-ICMS evoked EMG activity did not sum with the existing level of EMG activity; rather it forced a new EMG level that was independent of existing voluntary background. These results taken together support evidence that the movements evoked by RL-ICMS occur due to the "hijacking" of cortical output by the stimulus. The natural supply of input to M1 is blocked and replaced with a stimulus evoked input. These results should caution investigators against extending the interpretation of findings with ICMS beyond a method which is capable of revealing synaptic connectivity between cortical sites and motoneurons.

The post-stimulus effects mediated by StTA likely reflect the projections of a small group of neurons surrounding the electrode tip. Since StTA is applied at low frequencies, which avoid temporal summation of the post synaptic potential, its output reflects the most direct route to muscles; the CM connection. It is unknown how well output effects elicited with repetitive ICMS compare to those elicited with StTA of EMG activity. Therefore, we

characterized and compared the output effects mediated by StTA, RS-ICMS and RL-ICMS. At 15 μ A, effects in StTAs matched 57% of the effects elicited with RS-ICMS and 46% of effects elicited with RL-ICMS at the same sites. Effects across the two repetitive ICMS methods showed a 53% match at the same sites. The percentage of matching output effects elicited with different ICMS methods at low stimulus intensities was somewhat lower (< 58%) than the 95% match previously reported between StTA and SpTA (Cheney and Fetz 1985). At higher stimulus intensities, the percent of muscles with matching effects in StTAs showed modest improvement in most cases. Eventually reaching somewhat high levels of agreement at 120 μ A (range = 76% - 80%). The extent of matching effects across stimulation methods improved when only the distal muscles were considered. This is probably attributable to the fact that distal muscles also had the strongest stimulus evoked effects.

In conclusion, the role of M1 in the control of muscle activity is important for understanding recovery of function following injury and ultimately enhancing the quality of patient's lives. As our understanding improves, so will the therapeutic approaches used for motor recovery. Our results confirm previous suggestions (Cheney et al., 2002) that the neuronal signals from M1 are the most optimal for controlling neuroprosthetic devices. Further, StTA of EMG activity is a stable and therefore suitable means of characterizing output from the motor areas of the brain.

REFERENCES

- Cheney PD, Fetz EE (1985) Comparable patterns of muscle facilitation evoked by individual corticomotoneuronal (CM) cells and by single intracortical microstimuli in primates: evidence for functional groups of CM cells. *J Neurophysiol* 53(3): 786-804.
- Cheney PD (2002) Electrophysiological Methods for Mapping Brain Motor and Sensory Circuits. In: *Brain Mapping: The Methods, Second Edition* (A. W. Toga, J. C. Mazziotta, eds), pp189-226. New York, NY: Academic Press.
- Fetz EE, Cheney PD (1980) Postspike facilitation of forelimb muscle activity by primate corticomotoneuronal cells. *J Neurophysiol* 44(4): 751-72.
- Graziano MSA, Taylor CSR, Moore T (2002) Complex movements evoked by microstimulation of precentral cortex. *Neuron* 34: 841-851.
- Lemon RN, Mantel GW, Muir RB (1986) Corticospinal facilitation of hand muscles during voluntary movement in the conscious monkey. *J Physiol* 381: 497-527.
- Mantel GW, Lemon RN (1987) Cross-correlation reveals facilitation of single motor units in thenar muscles by single corticospinal neurones in the conscious monkey. *Neurosci Lett* 77(1): 113-8.